

The University of Hull

**Liquid Crystals with Novel Terminal Chains
as Ferroelectric Hosts**

**Being a Thesis submitted for the degree of Doctor of
Philosophy**

in the University of Hull

by

Guirec Yann Cosquer B.Sc. (Hons)

February 2000

Abstract

Changes to the molecular structure of liquid crystals can have a significant effect upon their mesomorphism and ferroelectric properties. Most of the research in liquid crystal for display applications concentrates on the design and synthesis of novel mesogenic cores to which straight terminal alkyl or alkoxy chains are attached. However, little is known about the effects upon the mesomorphism and ferroelectric properties of varying the terminal chains. The compounds prepared in this work have a common core – a 2,3-difluoroterphenyl unit with a nine-atom alkyl (nonyl) or alkoxy (octyloxy) chain at the 4-position, but with an unusual chain at the 4''-position. In some cases the terminal chain contains hetero atoms such as silicon, oxygen, chlorine and bromine or has a bulky end group. In total 46 final materials were synthesised in an attempt to understand the effect of an unusual terminal chains on mesomorphism and for some of these compounds the effect upon the switching times when added to a standard ferroelectric mixture were investigated. It was found that most compounds containing a bulky end group only displayed a smectic C phase, compounds with a halogen substituent as an end unit displayed a smectic A phase and that increasing the chain flexibility by introducing an oxygen atom in the chain reduces the melting and clearing points. The electro-optical measurements carried out on ferroelectric mixtures containing a bulky end group compound showed that shorter switching times were produced than for the ferroelectric mixture containing a straight chain compound. It is suggested that a bulky end group diminishes the extent of inter-layer mixing in the chiral smectic C phase and therefore the molecules move more easily with ferroelectric switching.

Acknowledgements

I would like to express my sincere gratitude towards my supervisor Professor K. J. Toyne for his kindness, patience, expertise and time throughout the course of my work. I would also like to thank Professor J. W. Goodby and Dr M. Hird for their encouragement and useful discussions.

My gratitude also goes to my friends Dr N. Fahmi, Dr E. Murray, Miss A. Coue, P. Hill, my coffee breaks partners (Chris and Alexey), all the members of the Liquid crystal group both past and present, especially, Miss J. H. Wild, S, Sharma, Dr C. Artal and Miss S. Chang. Special thanks must be extended to Dr S. Cowling and Dr R. Lewis for their technical help and members of the lab. C 307 for "putting up" with me.

Thanks must also go to the University of Hull for giving me the Scholarship and D.E.R.A. (Malvern) for giving me a Case Award for the final year of my work, and to the Centre for Organic and Biological Chemistry, Department of Chemistry (especially Mrs B. Worthington and Mrs A. Partanen).

Finally I thank my parents, my sister and Charlotte's family for their encouragement and support.

"Mon p'tit gars travaille, creuse, prend de la peine car c'est le fond qui manque le moins "

Victor Carbon (1907-1995)

To Charlotte

1 Introduction

1.1 History of liquid crystals	p 1
1.2 Types of liquid crystal mesogens	p 3
1.2.1 Thermotropic Liquid Crystals	p 4
1.2.2 Discotic liquid crystals	p 5
1.2.3 Calamitic liquid crystals	p 5
1.3 The nematic and chiral nematic mesophases	p 8
1.4 The smectic mesophases	p 9
1.4.1 Non-tilted smectic mesophases	p 10
1.4.1.1 Smectic A phase	p 10
1.4.1.2 Hexatic smectic B phase	p 11
1.4.1.3 Crystal B phase	p 12
1.4.1.4 Crystal E phase	p 12
1.4.2 Tilted smectic phases	p 12
1.4.2.1 Smectic C phase	p 12
1.4.2.2 Smectic C_{alt} phase	p 17
1.4.2.3 Smectic I phase	p 18
1.4.2.4 Smectic F phase	p 18
1.4.2.5 Crystal J, G, K, H phases	p 18
1.5 Physical properties of liquid crystals	p 20
1.5.1 Physical properties of the nematic phase	p 20
1.5.1.1 Viscosity	p 20
1.5.1.2 Optical anisotropy; birefringence	p 21
1.5.1.3 Dielectric anisotropy	p 21
1.5.1.4 Elastic constants	p 22

1.6 Display devices using chiral nematic materials - twisted and super-twisted nematic devices	p 23
1.7 Characteristics and physical properties of ferroelectric liquid crystals	p 26
1.7.1 Ferroelectricity	p 26
1.7.2 Surface stabilised ferroelectric liquid crystal display	p 29
1.7.3 Physical properties of ferroelectric liquid crystal materials	p 31
1.7.3.1 Role of the dielectric biaxiality	p 32
1.8 Ferroelectric liquid crystal materials	p 35
1.8.1 The "all chiral" approach	p 36
1.8.2 Ferroelectric liquid crystals mixtures	p 37
1.8.3 Achiral host materials	p 38
1.9 Aim of the research	p 42
1.9.1 Bibliography (Section 1)	p 46

2 Experimental section

2.1 Techniques, methods of analyses and general procedures	p 50
2.1.1 Purification and purity of materials	p 50
2.1.2 Purification and drying techniques of starting materials and solvents	p 50
2.1.3 Purity of the compounds	p 51
2.1.3.1 High Performance Liquid Chromatography (HPLC)	p 51
2.1.3.2 Thin Layer Chromatography (TLC)	p 51
2.1.3.3 Gas Liquid Chromatography (GLC)	p 51
2.1.4 Purification of products	p 51
2.1.5 Structural Analysis	p 52
2.1.5.1 ¹H Nuclear Magnetic Resonance Spectroscopy (¹H NMR)	p 52
2.1.5.2 Infrared (IR) Spectroscopy	p 52
2.1.5.3 Mass Spectrometry (MS)	p 52
2.1.5.4 Optical Rotation	p 53
2.1.6 Characterisation of Final Products	p 53
2.1.6.1 Optical Microscopy	p 53
2.1.6.2 Differential Scanning Calorimetry (DSC)	p 53
2.1.7 Nomenclature and abbreviations	p 53
2.1.8 Source of materials	p 55

2.2 Experimental procedures

Scheme 1

p 73

- 2,3-Difluorophenylboronic acid (2)
- 2,3-Difluorophenol (3)
- 1,2-Difluoro-3-octyloxybenzene (4)
- 2,3-Difluoro-4-octyloxyphenylboronic acid (5)

Scheme 2

p 75

- (2,3-Difluorophenyl)nonan-1-ol (6)
- 1,2-Difluoro-3-nonylbenzene (7)
- 2,3-Difluoro-4-nonylphenylboronic acid (8)

Scheme 3

p 77

- 4-Bromo-4'-(1,4-dioxapentyl)biphenyl (13)
- 4-Bromo-4'-(1,4,7-trioxaoctyl)biphenyl (14)
- 4-Bromo-4'-(1,4,7,10-tetraoxaundecyl)biphenyl (15)
- 2,3-Difluoro-4-octyloxy-4''-(1,4-dioxapentyl)terphenyl (16)
- 2,3-Difluoro-4-octyloxy-4''-(1,4,7-trioxaoctyl)terphenyl (17)
- 2,3-Difluoro-4-octyloxy-4''-(1,4,7,10-tetraoxaundecyl)terphenyl (18)
- 2,3-Difluoro-4-nonyl-4''-(1,4-dioxapentyl)terphenyl (19)
- 2,3-Difluoro-4-nonyl-4''-(1,4,7-trioxaoctyl)terphenyl (20)
- 2,3-Difluoro-4-nonyl-4''-(1,4,7,10-tetraoxaundecyl)terphenyl (21)
- 4-Bromo-4'-(1,4-dioxaoctyl)biphenyl (24)
- 4-Bromo-4'-(1,4,7-trioxaundecyl)biphenyl (25)
- 2,3-Difluoro-4-octyloxy-4''-(1,4-dioxaoctyl)terphenyl (26)
- 2,3-Difluoro-4-octyloxy-4''-(1,4,7-trioxaundecyl)terphenyl (27)

Scheme 4

p 82

- 6-Bromohexan-1-ol (29)
- 4-Bromo-4'-(6-hydroxyhexyloxy)biphenyl (30)
- 2,3-Difluoro-4-octyloxy-4''-(6-hydroxyhexyloxy)terphenyl (31)
- 4''-(9,9-Dimethyl-1,8-dioxadecyl)-2,3-difluoro-4-octyloxyterphenyl (32)

Scheme 5

p 84

- 4-Trimethylsilylbutan-1-ol (42)
 5-Trimethylsilylpentan-1-ol (43)
 6-Trimethylsilylhexan-1-ol (44)
 4-Bromo-4'-[2-(trimethylsilyl)ethoxy]biphenyl (45)
 4-Bromo-4'-[3-(trimethylsilyl)propyloxy]biphenyl (46)
 4-Bromo-4'-[4-(trimethylsilyl)butyloxy]biphenyl (47)
 4-Bromo-4'-[5-(trimethylsilyl)pentyloxy]biphenyl (48)
 4-Bromo-4'-[6-(trimethylsilyl)hexyloxy]biphenyl (49)
 2,3-Difluoro-4-octyloxy-4''-[2-(trimethylsilyl)ethoxy]terphenyl (50)
 2,3-Difluoro-4-octyloxy-4''-[3-(trimethylsilyl)propyloxy]terphenyl (51)
 2,3-Difluoro-4-octyloxy-4''-[4-(trimethylsilyl)butyloxy]terphenyl (52)
 2,3-Difluoro-4-octyloxy-4''-[5-(trimethylsilyl)pentyloxy]terphenyl (53)
 2,3-Difluoro-4-octyloxy-4''-[6-(trimethylsilyl)hexyloxy]terphenyl (54)
 2,3-Difluoro-4-nonyl-4''-[2-(trimethylsilyl)ethoxy]terphenyl (55)
 2,3-Difluoro-4-nonyl-4''-[3-(trimethylsilyl)propyloxy]terphenyl (56)
 2,3-Difluoro-4-nonyl-4''-[4-(trimethylsilyl)butyloxy]terphenyl (57)
 2,3-Difluoro-4-nonyl-4''-[5-(trimethylsilyl)pentyloxy]terphenyl (58)
 2,3-Difluoro-4-nonyl-4''-[6-(trimethylsilyl)hexyloxy]terphenyl (59)

Scheme 6

p 91

- 6-Triethylsilylhexan-1-ol (62)
 4-Bromo-4'-[6-(triethylsilyl)hexyloxy]biphenyl (63)
 2,3-Difluoro-4-octyloxy-4''-[6-(triethylsilyl)hexyloxy]terphenyl (64)

Scheme 7

p 93

- 4-Bromo-4'-(3,7-dimethyloctyloxy)biphenyl (66)
 4''-(3,7-Dimethyloctyloxy)-2,3-difluoro-4-octyloxyterphenyl (67)
 4-Bromo-4'-octyloxybiphenyl (69)
 2,3-Difluoro-4,4''-dioctyloxyterphenyl (70)
 2,3-Difluoro-4-nonyl-4''-octyloxyterphenyl (71)

Scheme 8

p 96

- 6-Chlorohexyl toluene-*p*-sulphonate (72)
 1-Chloro-7,7-dimethyloctane (73)
 4-Bromo-4'-(7,7-dimethyloctyloxy)biphenyl (74)
 4''-(7,7-Dimethyloctyloxy)-2,3-difluoro-4-octyloxyterphenyl (75)
 4''-(7,7-Dimethyloctyloxy)-2,3-difluoro-4-nonylterphenyl (76)

Scheme 9

p 99

- 6-(4'-Bromobiphenyl-4-yl)hexyl toluene-*p*-sulphonate (77)
 4-Bromo-4'-[6-(cyclobutylmethoxy)hexyloxy]biphenyl (78)
 4''-[6-(Cyclobutylmethoxy)hexyloxy]-2,3-difluoro-4-octyloxyterphenyl
 (79)

Scheme 10

p 101

- 4-Bromo-4'-(6-bromohexyloxy)biphenyl (80)
 4''-(6-Bromohexyloxy)-2,3-difluoro-4-octyloxyterphenyl (81)
 2,3-Difluoro-4''-[6-(3-methyloxetan-3-ylmethoxy)hexyloxy]-4-
 octyloxyterphenyl (82)

Scheme 11

p 103

- 1-Bromo-4-propyloxybutane (87)
 1-Bromo-4-(1,2-dimethylpropyloxy)butane (88)
 1-Bromo-4-(1,2,2-trimethylpropyloxy)butane (89)
 4-Bromo-4'-(4-propyloxybutyloxy)biphenyl (90)
 4-Bromo-4'-[4-(1,2-dimethylpropyloxy)butyloxy]biphenyl (91)
 4-Bromo-4'-[4-(1,2,2-trimethylpropyloxy)butyloxy]biphenyl (92)

Scheme 12

p 106

- 2-(1-Methylpropyloxy)tetrahydrofuran (98)
 2-(2-Methylpropyloxy)tetrahydrofuran (99)
 2-(1,1-Dimethylpropyloxy)tetrahydrofuran (100)
 2-(2,2-dimethylpropyloxy)tetrahydrofuran (101)
 4-(1-Methylpropyloxy)butan-1-ol (102)
 4-(2-Methylpropyloxy)butanol (103)
 4-(1,1-Dimethylpropyloxy)butanol (104)
 4-(2,2-Dimethylpropyloxy)butanol (105)
 4-Bromo-4'-[4-(1-methylpropyloxy)butyloxy]biphenyl (106)
 4-Bromo-4'-[4-(2-methylpropyloxy)butyloxy]biphenyl (107)
 4-Bromo-4'-[4-(1,1-dimethylpropyloxy)butyloxy]biphenyl (108)
 4-Bromo-4'-[4-(2,2-dimethylpropyloxy)butyloxy]biphenyl (109)

Scheme 13

p 111

2,3-Difluoro-4-octyloxy-4''-(4-propyloxybutyloxy)terphenyl (110)

4''-[4-(1,2-Dimethylpropyloxy)butyloxy]-2,3-difluoro-4-octyloxyterphenyl (111)

2,3-Difluoro-4-octyloxy-4''-[4-(1,2,2-trimethylpropyloxy)butyloxy]-terphenyl (112)

2,3-Difluoro-4''-[4-(1-methylpropyloxy)butyloxy]-4-octyloxy-terphenyl (113)

2,3-Difluoro-4''-[4-(2-methylpropyloxy)butyloxy]-4-octyloxy-terphenyl (114)

4''-[4-(1,1-Dimethylpropyloxy)butyloxy]-2,3-difluoro-4-octyloxy-terphenyl (115)

4''-[4-(2,2-Dimethylpropyloxy)butyloxy]-2,3-difluoro-4-octyloxy-terphenyl (116)

4''-[4-(1,2-Dimethylpropyloxy)butyloxy]-2,3-difluoro-4-nonyl-terphenyl (117)

2,3-Difluoro-4''-[4-(1-methylpropyloxy)butyloxy]-4-nonyl-terphenyl (118)

4''-[4-(1,1-Dimethylpropyloxy)butyloxy]-2,3-difluoro-4-nonyl-terphenyl (119)

4''-[4-(2,2-Dimethylpropyloxy)butyloxy]-2,3-difluoro-4-nonyl-terphenyl (120)

Scheme 14

p 116

3,7-Dimethyloctanoic acid (122)

3,7-Dimethyloctanoyl chloride (123)

4-Bromo-4'-(3,5,5-trimethylhexyl)biphenyl (126)

4-Bromo-4'-(3,7-dimethyloctyl)biphenyl (127)

2,3-Difluoro-4-octyloxy-4''-(3,5,5-trimethylhexyl)terphenyl (128)

4''-(3,7-Dimethyloctyl)-2,3-difluoro-4-octyloxyterphenyl (129)

2,3-Difluoro-4-nonyl-4''-(3,5,5-trimethylhexyl)terphenyl (130)

4''-(3,7-Dimethyloctyl)-2,3-difluoro-4-nonylterphenyl (131)

Scheme 15

p 120

4-Bromo-4'-(3-chloropropyl)biphenyl (135)

4-Bromo-4'-(4-chlorobutyl)biphenyl (136)

4-Bromo-4'-(5-chloropentyl)biphenyl (137)

4''-(3-Chloropropyl)-2,3-difluoro-4-octyloxyterphenyl (138)

4''-(4-Chlorobutyl)-2,3-difluoro-4-octyloxyterphenyl (139)

4''-(5-Chloropentyl)-2,3-difluoro-4-octyloxyterphenyl (140)

Scheme 16

p 123

2-Iodoethyl methyl ether (142)

Ethyl 2-(4'-bromobiphenyl-4-oxy)propionate (144)

2-(4'-Bromobiphenyl-4-oxy)propan-1-ol (145)

(R)-(+)-4-Bromo-4'-[2-(2-methoxyethoxy)-1-methylethoxy]biphenyl (146)*(R)*-(+)-2,3-Difluoro-4''-[2-(2-methoxyethoxy)-1-methylethoxy]-4-octyloxyterphenyl (147)**Scheme 17**

p 126

(R)-(+)-4-Bromo-4'-(2-methoxy-1-methylethoxy)biphenyl (148)*(R)*-(+)-2,3-Difluoro-4''-(2-methoxy-1-methylethoxy)-4-octyloxyterphenyl (149)**2.3 Experimental discussion**

p 127

2.3.1 Discussion of the general synthesis routes

p 127

2.3.1.1 Strategies for the synthesis of the cores

p 127

2.3.2 Specific synthetic strategy for the terminal chains

p 133

2.3.2.1 Mitsunobu ether synthesis (Schemes 3 and 7)

p 133

2.3.2.2 Synthesis of the *tert*-butyloxy end group (Scheme 4)

p 134

2.3.2.3 Synthesis of the trimethylsilyl end group series (Schemes 5 and 6)

p 135

2.3.2.4 Synthesis of *t*-butyl end group (Scheme 8)

p 136

2.3.2.5 Synthesis of the cyclobutyl end group (Scheme 9)

p 137

2.3.2.6 Synthesis of the oxetane end group (Scheme 10)	p 137
2.3.2.7 Synthesis of the branched end groups (Schemes 11, 12 and 13)	p 138
2.3.2.8 Synthesis of chloro end groups (Scheme 15)	p 144
2.3.2.9 Synthesis of the chiral ethylenoxy compounds (Schemes 16 and 17)	p 146

3 Results and discussion

3.1 Mesomorphic studies	p 148
3.1.1 The effect of oxygen atoms at various positions along the terminal chain	p 148
3.1.1.1 Terminal chains with oxygen substituents	p 148
3.1.1.2 Chiral terminal chains with oxygen substituents	p 152
3.1.2 Terminal chain with silicon substituents	p 153
3.1.2.1 Dialkoxy systems with silicon substituents	p 153
3.1.2.2 Alkoxy-alkyl systems with silicon substituents	p 157
3.1.2.3 Dialkoxy systems with nine atoms chains but different end groups	p 159
3.1.2.4 Alkoxy-alkyl systems with nine atoms chains and different end groups	p 161
3.1.3 <i>t</i>-Butyloxy end group	p 163
3.1.4 Effects of a four membered ring end group	p 166
3.1.5 Terminal chains with constant length but varying steric end groups	p 167

3.1.6	Branched alkoxy-alkyl and dialkyl terminal chains	p 172
3.1.7	Chloro end group	p 174
3.1.8	Photomicrographs of the mesophases for end group compound	p 176
3.2	Mixture studies on compounds containing a bulky end group	p 179
3.3	Electro-optical studies of bulky end groups in a standard Mixture	p 184
3.3.1	Experimental techniques	p 184
3.3.2	Theory of Ps measurements – Triangular Wave Studies	p 187
3.3.3	Procedure for measuring Ps values	p 188
3.3.4	Tilt angle measurements	p 189
3.3.5	Response time measurements	p 189
3.3.6	τ/V_{min} measurements	p 195
3.4	Conclusions	p 199
3.5	Bibliography (Section 3)	p 201

Introduction

Section 1

1 Introduction

1.1 History of liquid crystals

Liquid crystals have for a long time been the subject of scientific interest since they constitute a fourth state of matter in addition to the established states of solid, liquid, and gas. When Reinitzer¹ in 1888 and Lehman² in 1889 reported the first examples of unusual melting behaviour of an ester of cholesterol, they knew that they had discovered one of the most exciting properties arising from a wide family of synthetic and natural compounds.

Since that time there has been intensive research in the study of the relationship between molecular structure and mesomorphism, as well as in the applications for such compounds³.

A simple definition of *mesogen* or *liquid crystal-forming material* is that when a liquid crystal melts from a solid it exhibits one or more thermodynamically stable intermediate states called mesophases, and it then finally becomes an isotropic liquid. In the overall change from solid to isotropic solid, there is a stepwise breakdown of the mesogenic molecules' ordering, the molecules can rotate and oscillate rapidly about one or more axes⁴; and there is a gradual collapse of their long range positional ordering, and finally disruption in the short-range order but the orientational order remains⁵. A liquid crystal mesophase could be defined as an elastic fluid-like ordered state. There are only about defined 25 liquid crystal phases so far compared to the 230 crystalline space groups.

Molecules in a liquid crystalline state are free to move around as in an isotropic liquid, however they tend to orient in a preferred direction with one another, breaking the isotropy of the physical properties of the system. Liquid crystals are anisotropic - their physical properties are not identical in all directions, and the anisotropy of the optical, electric, elastic and magnetic properties has led to the use of liquid crystal materials in display devices and as sensors^{6,7}.

These liquid crystalline phases are usually identified using an optical polarising microscope in conjunction with Differential Scanning Calorimetry (DSC) and X-ray diffraction studies.

The identification of liquid crystalline phases is usually done by using a polarising microscope in conjunction with DSC and X-ray diffraction studies. The identification of liquid crystalline phases is usually done by using a polarising microscope in conjunction with DSC and X-ray diffraction studies.

The identification of liquid crystalline phases is usually done by using a polarising microscope in conjunction with DSC and X-ray diffraction studies. The identification of liquid crystalline phases is usually done by using a polarising microscope in conjunction with DSC and X-ray diffraction studies.



Figure 1: A graph showing the relationship between two variables, likely related to the liquid crystalline phase transition.

Figure 2: A graph showing the relationship between two variables, likely related to the liquid crystalline phase transition.

Figure 3: A graph showing the relationship between two variables, likely related to the liquid crystalline phase transition.

The identification of liquid crystalline phases is usually done by using a polarising microscope in conjunction with DSC and X-ray diffraction studies. The identification of liquid crystalline phases is usually done by using a polarising microscope in conjunction with DSC and X-ray diffraction studies.

1.2 Types of liquid crystal mesogens

There are two main families of liquid crystals: thermotropic⁸ and lyotropic⁹ liquid crystals (figure 1.1). The thermotropic liquid crystals exhibit liquid crystalline mesophases on melting from the crystal phase or cooling from the isotropic liquid, whereas the lyotropic materials exhibit liquid crystalline mesophases when mixed with a particular solvent.

Lyotropic liquid crystals are formed by amphiphilic mixtures and the mesophases are thermodynamically stable at defined temperatures pressures and concentrations. The types of mesophase depend upon their concentration and the degree of curvature produced by the packing arrangements of the amphiphilic molecules. There are three main types of lyotropic mesophase, namely lamellar, hexagonal and cubic phases, with increasing curvature in their packing arrangements. The structure and properties of liquid crystal polymers will not be discussed in this work.

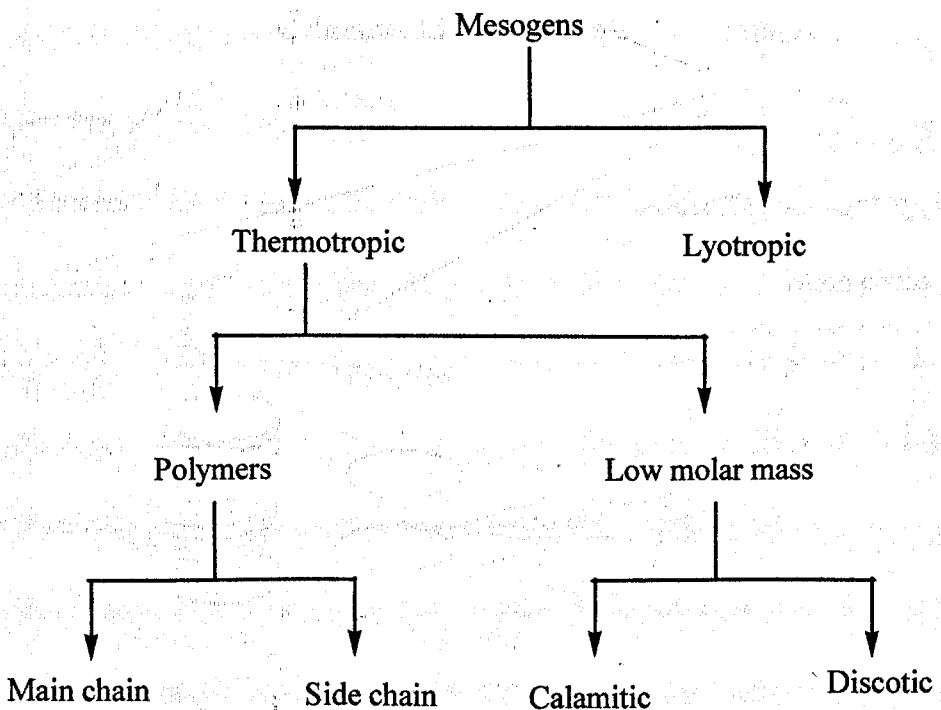


Figure 1.1 The different classes of liquid crystals

Thermotropic mesogens exhibit liquid crystal mesophases on heating or cooling, and the temperature range over which the mesophases are exhibited varies from material to material. When a material displays a mesophase both on cooling and heating the

mesophase is called an *enantiotropic* mesophase. However when the mesophase is solely displayed on cooling from the isotropic liquid, and below the melting point of the material, the phase is called a *monotropic* phase.

1.2.1 Thermotropic Liquid Crystals

The thermotropic liquid crystal family can be divided into two groups: the low mass materials and the polymeric materials^{10,11}. The low mass materials can be further divided into the calamitic, discotic liquid crystals¹², phasmidic¹³, biforked¹⁴ and board-like molecules¹⁵. The liquid crystal polymers can be separated into the main chain and side chain polymers (figure 1.2). The structure and properties of liquid crystal polymers will not be discussed in this work.

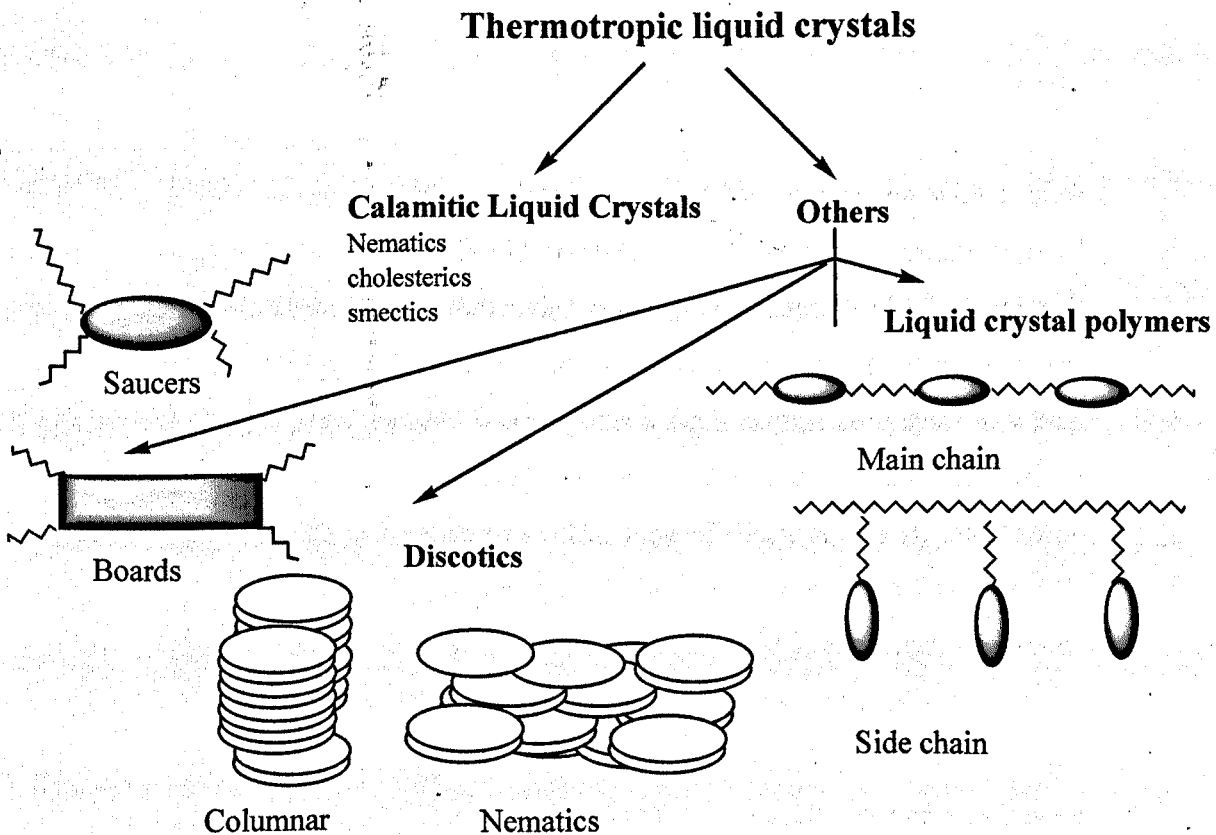


Figure 1.2 The different types of thermotropic liquid crystals

1.2.2 Discotic liquid crystals

Discotic liquid crystal molecules are usually disc shaped¹² molecules composed of a core based on benzene, triphenylene¹⁶ or truxene¹⁷ to which several peripheral groups are attached. Discotic liquid crystals have two basic types of mesophase: columnar and nematic. Columnar mesophase are polymorphic (similar to smectic phases). The polymorphism occurs because of the different symmetry classes of the two-dimensional lattice of the columns as follows :

Symmetry group	Molecular arrangement within the column
Hexagonal	Ordered
Rectangular	Disordered
Oblique	

1.2.3 Calamitic liquid crystals

The term calamitic means that the molecules are rod-like molecules with a high length to breadth ratio. Calamitic liquid crystals^{18,19} are the most common type of thermotropic liquid crystals. The molecules are generally composed of a core unit with two terminal alkyl or alkoxy chains and in some cases lateral substituents are present (figure 1.3)²⁰. The material incorporates a rigid central core system, which maintains the rod-like shape of the molecule and encourages the ordering of the molecules necessary to form mesophases. The type of rings, A and B, that can be incorporated into this core system are varied, from aromatic rings (usually 1,4-disubstituted-phenyl rings) with or without heteroatoms, to alicyclic rings, *e.g.* *trans*-cyclohexyl rings, bicyclo[2.2.2]-octanes and cyclobutyl rings (see figure 1.3).

The rings within the core may either be directly attached to each other or may have a rigid linking group, C, which is usually an ester, ether or acetylenic groups (see figure 1.3). These different types of rings greatly affect both the mesomorphism and the mesophase stability.

Lateral substituents²¹, M and N, may also affect both the mesomorphism and mesophase stability (see figure 1.3). The most common lateral substituents used are

relatively small units such as F, Cl, NO₂, CN and CH₃. The head and tail groups, R and R' are usually straight alkyl or alkoxy chains but they may also be branched²². These terminal chains are flexible and generally help to reduce the melting point of the material. The head and tail group may be directly linked to the core system or they may also be linked through ether or ester linkages, X and Y.

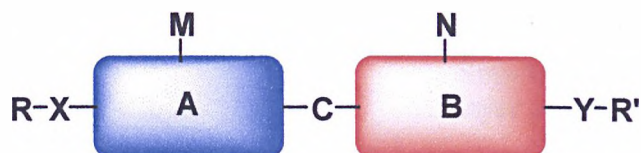


Figure 1.3 The different types of calamitic liquid crystals

The melting process of a calamitic liquid crystal can be summarised as shown in figure 1.4. T_6 is the melting point of a non-mesogenic material, T_1 and T_4 are crystal-to-liquid crystal mesophase transition temperatures *i.e.* temperatures, T_2 , T_3 and T_5 are transition temperatures between liquid crystal mesophases or between a liquid crystal mesophase and the isotropic liquid and are reversible (indicated as half-headed arrows).

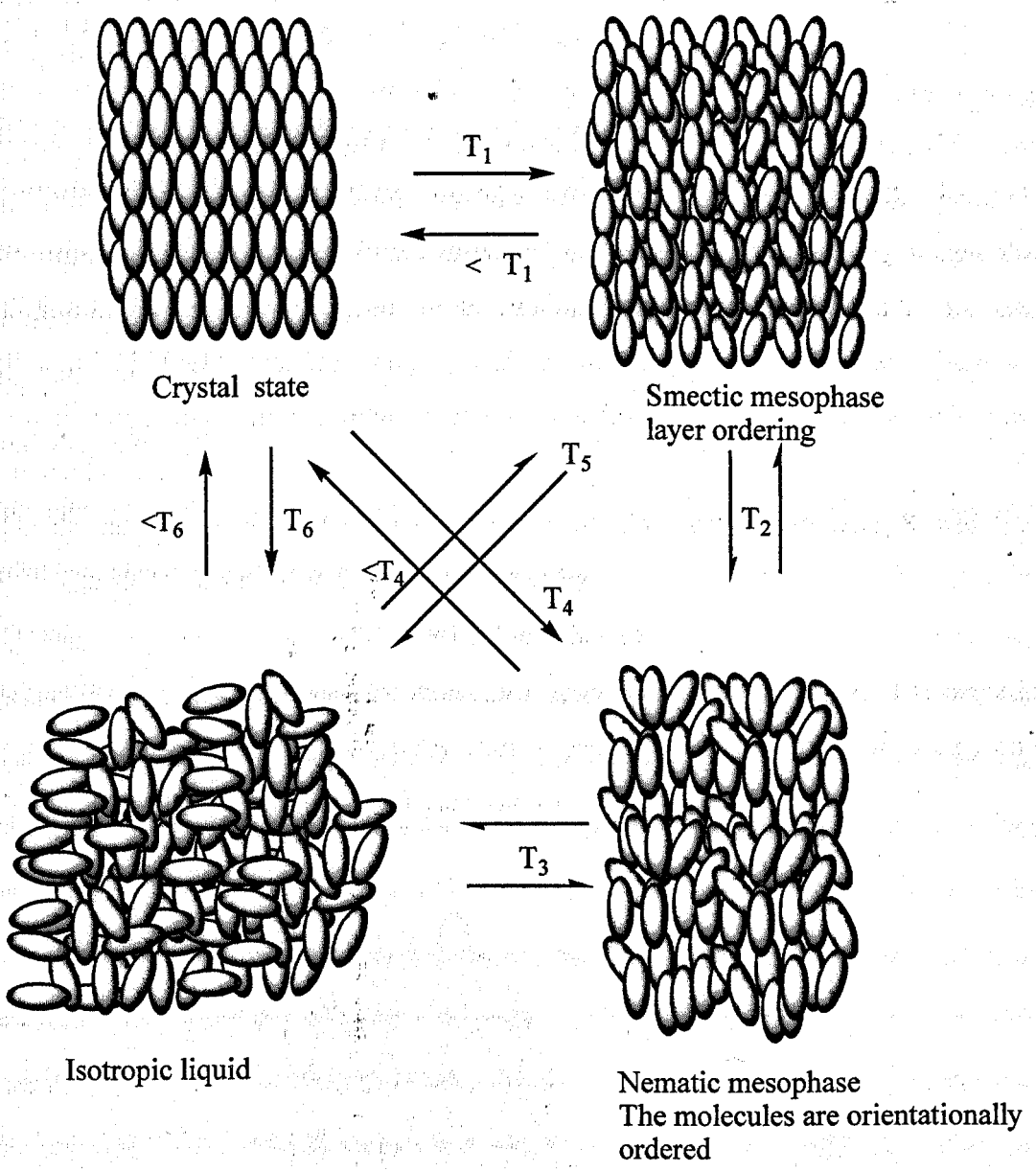


Figure 1.4 Melting process of a calamitic liquid crystal

1.3 The nematic and chiral nematic mesophases

The nematic mesophase^{23,24} differs from the isotropic liquid by the presence of long range orientational ordering of the long molecular axis. However the nematic phase is the least ordered of all the liquid crystal mesophases. The molecules align parallel, or nearly parallel, to a preferred direction called the director, along which the molecules are preferably aligned but are randomly arranged in a head to tail manner (figure 1.5). There is no long range positional ordering of the molecules, which are free to rotate about their long molecular axes and, to some degree, about their short molecular axes.

The degree of alignment along the director is called the order parameter, S , which is typically in the range 0.4 to 0.7 and is defined by

$$|S| = 1/2 (3\cos^2\theta - 1)$$

where θ is the angle between the molecules' long axis and the director. The nematic phase also has a rotational symmetry with respect to the director. There is only one type of nematic mesophase for achiral systems.

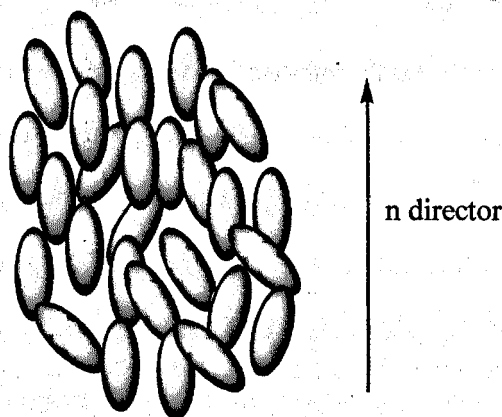


Figure 1.5 Representation of the nematic phase

The cholesteric mesophase, which was first observed for chiral derivatives² of cholesterol, should in fact be called the chiral nematic mesophase, N^* . It is not only exhibited by cholesterol derivatives but also by a wide range of non-steroid calamitic liquid crystals. In this mesophase the molecules are still arranged in the same fashion as in the nematic phase, however the introduction of chirality forces the director to form a helical distortion (figure 1.6). This helical formation is commonly known as a single-twist structure⁴. The helical structure has a temperature dependent pitch (the

pitch is defined as the distance required to rotate the average direction of the molecules through 360° - the full turn of the helix) and gives the material two unique properties, namely form chirality and the ability to selectively reflect light. As the molecules in the chiral nematic phase are rotationally and orientationally disordered with respect to their short axes, the phase is uniaxial. However if their breadth is increased, their rotation about their long molecular axis is restricted and therefore the phase is biaxial.

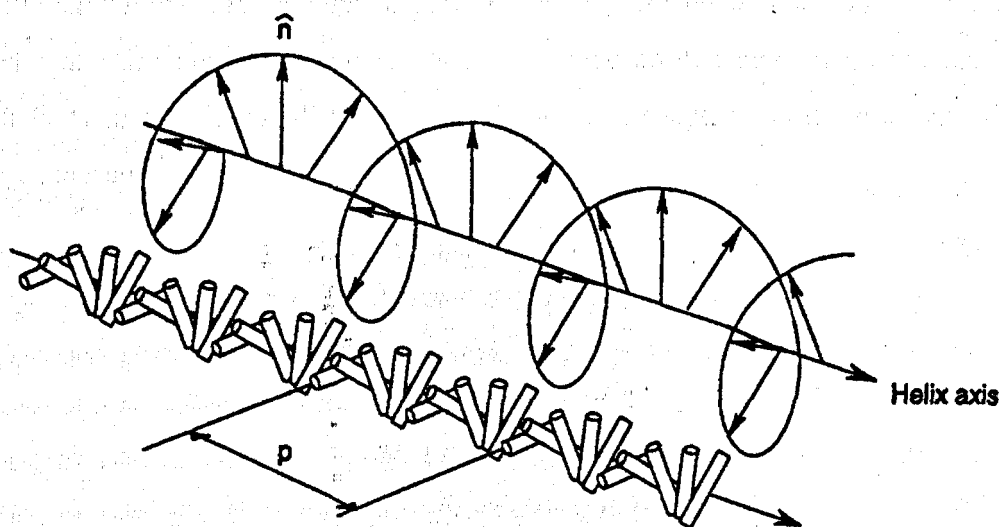


Figure 1.6 A representation of the chiral nematic phase.

1.4 The smectic mesophases

Smectic phases, are more ordered than the nematic mesophase and can appear directly on cooling from the isotropic liquid or from the nematic mesophase. Smectic phases have lamellar structures which enable various alignments within and between the layers to occur and so smectic phases exhibit polymorphism. There are five smectic liquid crystal mesophases (in increasing order of stability: SmA, SmC, SmB, SmI, SmF)²⁵ and six quasi-smectic disordered crystals phases (crystal B, J, G, crystal E, K, H) which are not regarded as liquid crystals since they possess long range positional order. The smectic mesophases are classified on the basis of the degree of local positional order and upon whether the molecules are tilted with respect to the layer normal.

1.4.1 Non-tilted smectic mesophases

1.4.1.1 Smectic A phase

The smectic A phase^{26,27,28} is the least ordered smectic phase, where the molecules are arranged in diffuse layers so that their long molecular axes are on average perpendicular to the layer planes and give a one-dimensional density wave for the centre of molecular mass (see figure 1.7). The molecules are subjected to rapid re-orientational motion about their long molecular axes as well as relaxations about their short molecular axes. The molecules are arranged so that there is no translational periodicity in the planes of the layers or between the layers and there is only short range ordering²⁹.

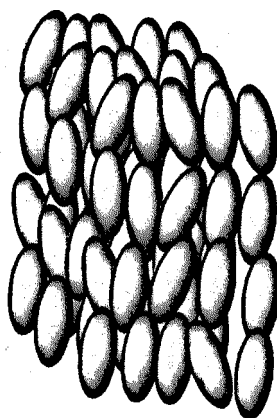


Figure 1.7 Representation of the smectic A phase

However, the smectic A phase is more complicated than this simple arrangement of molecules in single orthogonal layers and there are four subclasses of the smectic A phase.

The SmA_1 phase has head-to-tail orientation (figure 1.8), the SmA_2 is a bilayer phase with anti-ferroelectric ordering (figure 1.8), the SmA_d is a semi-bilayer phase with partial molecular overlapping due to associations (figure 1.8), and the $Sm\tilde{A}$ is a phase with a modulated ordering of the molecules within the layers giving a ribbon-like structure (figure 1.9).

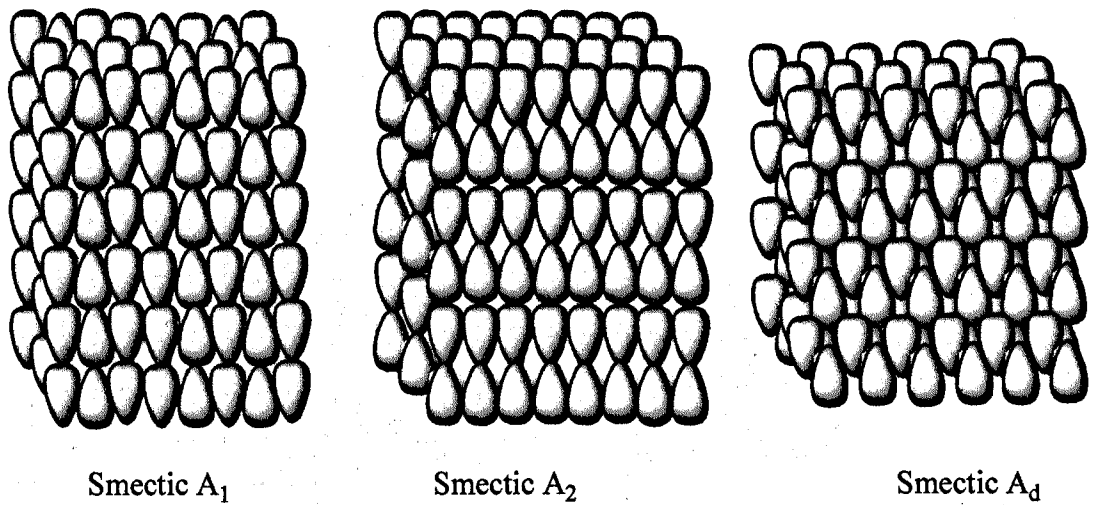


Figure 1.8 Representation of the different types of smectic A phases

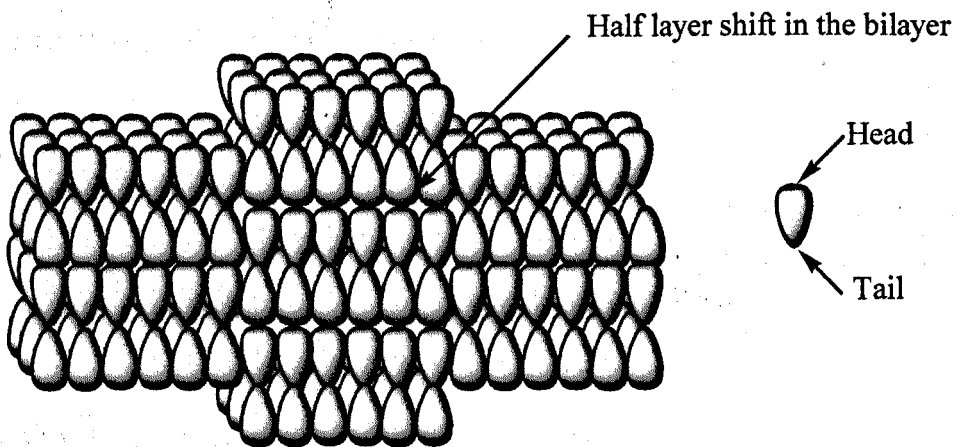


Figure 1.9 Representation of the smectic \tilde{A} phase

1.4.1.2 Hexatic smectic B phase

As in the smectic A phase, the molecules in the hexatic smectic B phase are arranged in layers so that their long axes are orthogonal to the layered planes. Locally the molecules are essentially hexagonally close packed and they are undergoing rapid re-orientational motion about their long molecular axes as in the smectic A phase. The hexagonal close-packing extends over a short distance (figure 1.10).

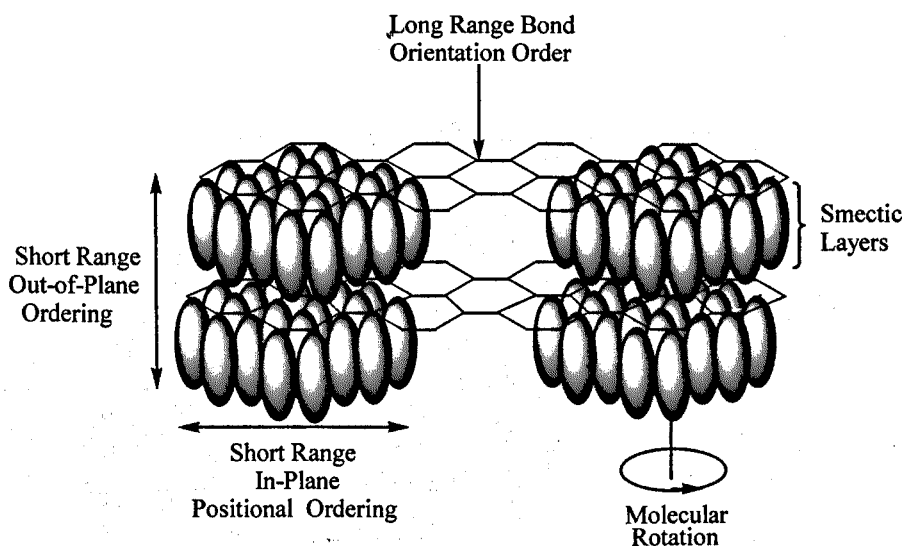


Figure 1.10 Representation of the hexatic smectic B phase

1.4.1.3 Crystal B phase²⁸

The crystal B phase has a similar structure to that of the hexatic smectic B phase, the difference being the greater long-range translational order of the molecules in three directions.

1.4.1.4 Crystal E phase

The crystal E phase develops from a contraction of the hexagonal lattice of the crystal B phase and the molecules have restricted rotation along their long molecular axes and this phase is therefore biaxial.

1.4.2 Tilted smectic phases

The tilted smectic phases are arguably the most interesting and fascinating of the smectic phases both from the view of their academic interest and for their technical applications. The smectic C phase in particular, in its different arrangements and its chiral versions has recently triggered as much interest as the nematic phase did in the early 1970's for their use in solid state devices.

1.4.2.1 Smectic C phase⁴

In the smectic C phase, the molecules are arranged in diffused layers as in the smectic A phase, but their long molecular axis is tilted from the layer normal through an average temperature-dependent angle θ (figure 1.11).

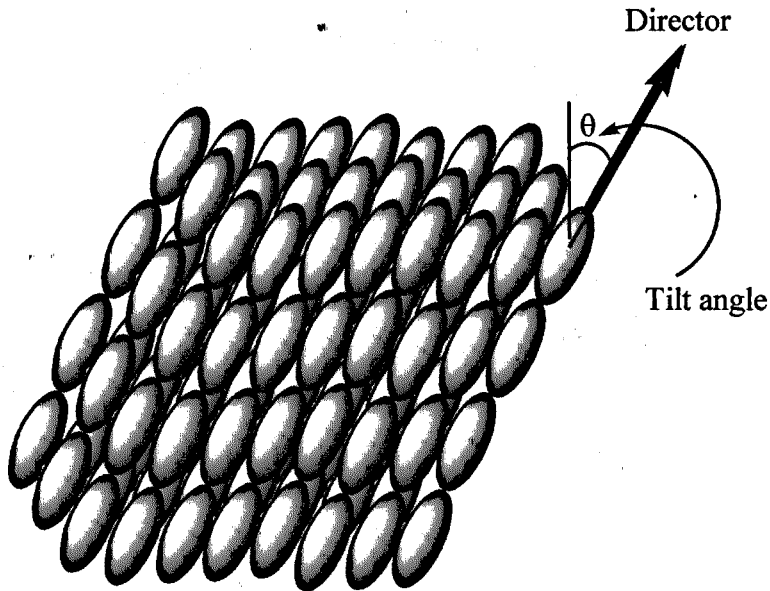


Figure 1.11 Representation of the tilted smectic C phase

The tilt angle, θ , varies with temperature, T , as described by equation 1.4.2.1

$$(\theta)_T = \theta_0(T_c - T)^\alpha \quad 1.4.2.1$$

where θ_0 is a constant, T_c is the SmA to SmC transition (Curie point), and $\alpha \approx 0.5$ so that the angle saturates as T decreases. The molecules have short range ordering within and between the layers. The order parameter of the smectic C phase, ξ , is not as simple as the order parameter of the nematic phase (see section 1.3) since it has two components which reflect the magnitude of the tilt angle and its direction in space ψ and is as follows³⁰ (figure 1.12):

$$\xi = \theta e^{i\psi}$$

There have been a number of attempts to describe the structure of the smectic C phase and the mechanism and reason for its formation. The first model by McMillan³¹ in 1973 was based on dipolar molecular interactions (figure 1.13). The rotation of the molecules about their long molecular axes is “frozen out” in the nematic or in the smectic A phases at the transition to the smectic C phase. The dipole moments align creating a torque parallel to the layer planes, which forces the molecules to tilt.

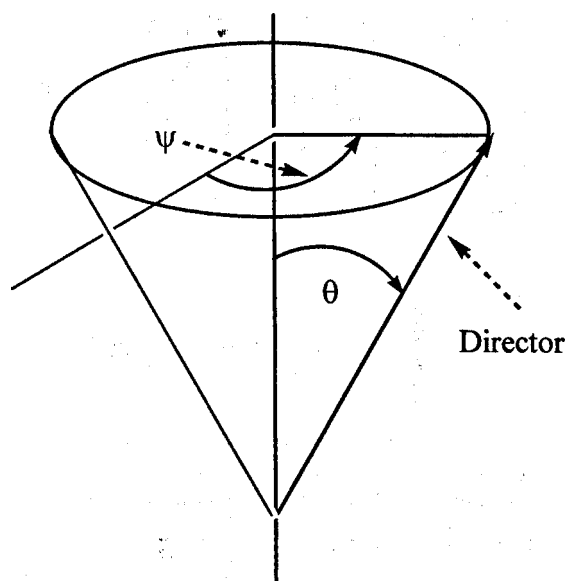


Figure 1.12 A diagram to illustrate the two component order parameter describing the SmA/SmC transition.

The second model by Wulf³², 1975 was based purely on the steric factors on the packing of zig-zag shaped molecules (figure 1.14). Neither of these models are fully satisfactory or explain experimental observations, as the formation of the smectic C phase was shown to be dependent on the number and length of the terminal aliphatic chains³³. More complex models and theories based on induced-dipole-permanent-dipole interactions have been developed, however they became more abstract in terms of the molecules that had been synthesised and characterised. These models predicted several possible molecular arrangements for one layer to the next and, as for the smectic A, the smectic C phase has four subclasses. The SmC or SmC₁ is a conventional smectic C phase where the molecules have random head to tail orientations (figure 1.11), the SmC₂ is a bilayer phase with antiferroelectric ordering of the constituent molecules, the SmC_d is a semi-bilayer phase with a partially formed molecular associations (figure 1.15) and the SmĊ is a phase with modulated antiferroelectric character of the molecules within the layers, giving a ribbon-like structure (figure 1.15).

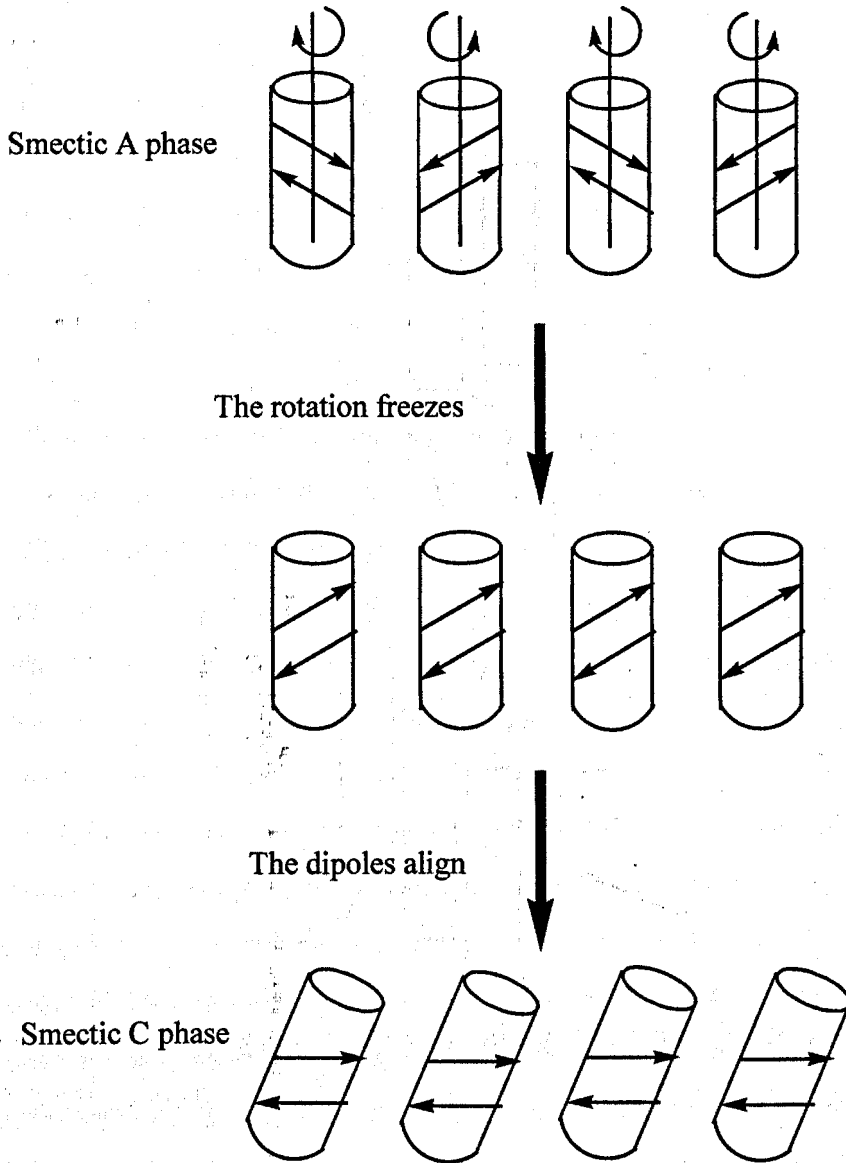


Figure 1.13 McMillan's model for the formation of the smectic C phase

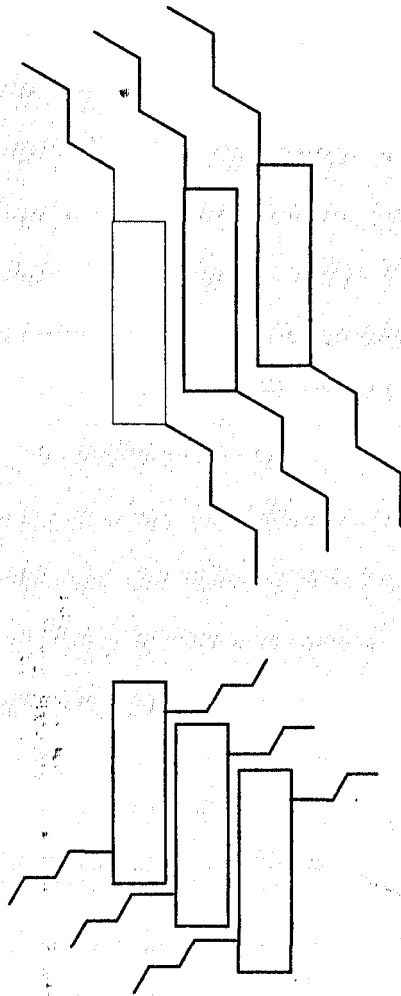


Figure 1.14 Wulf's packing model of hypothetical zig-zag shaped molecules to produce a smectic C phase

There are several basic molecular features which are required for mesogenic molecules to favour the formation of the smectic C phase, and these include, aromaticity in the central rigid core, long terminal aliphatic chains³⁴, polarity in the central linkage, linearity of the central linkage, staggering of the aromatic units and terminal dipolar functionalities in the core²⁵.

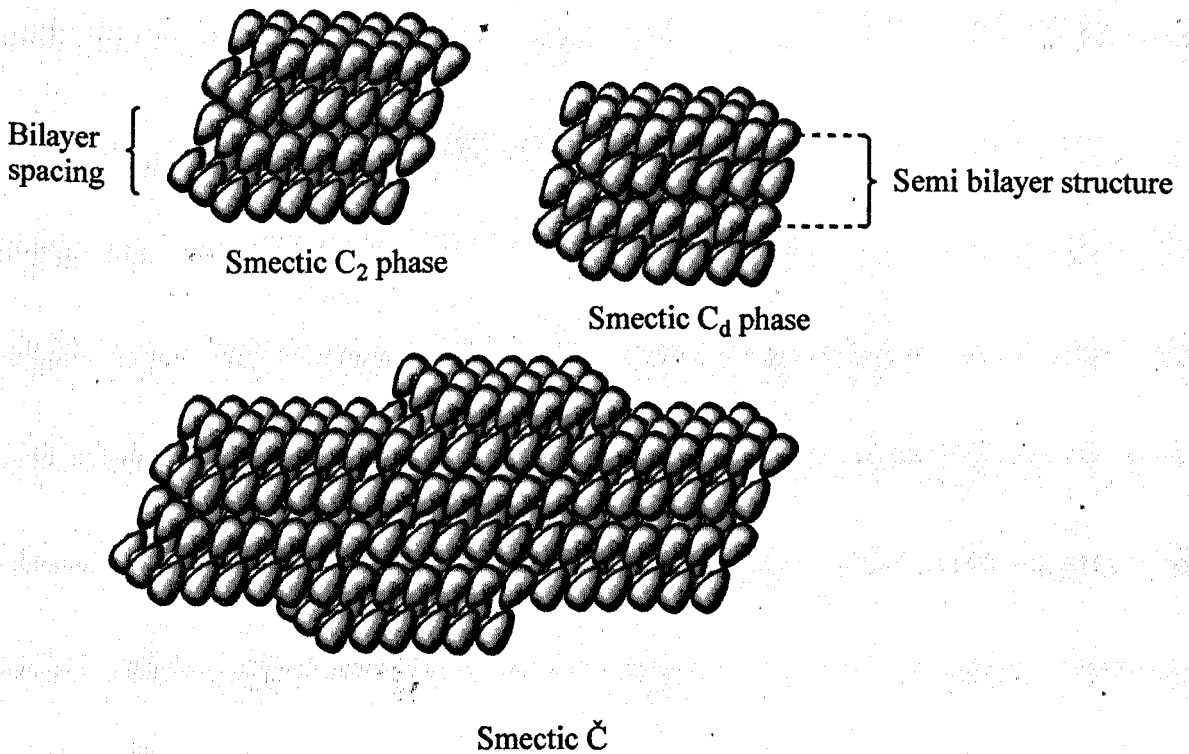


Figure 1.15 Bilayer structures of the smectic C phase

1.4.2.2 Smectic C_{alt} phase

In the smectic C_{alt} ³⁵ phase the molecules are arranged as in the smectic C phase with the major difference being that the tilt direction is rotated through 180° in successive layers (figure 1.16). The smectic C_{alt} is apparently more ordered than the smectic C phase as it has only been found below the smectic C phase on cooling. The chiral version of the alternating-tilt smectic C phase can be exploited in display devices³⁶.

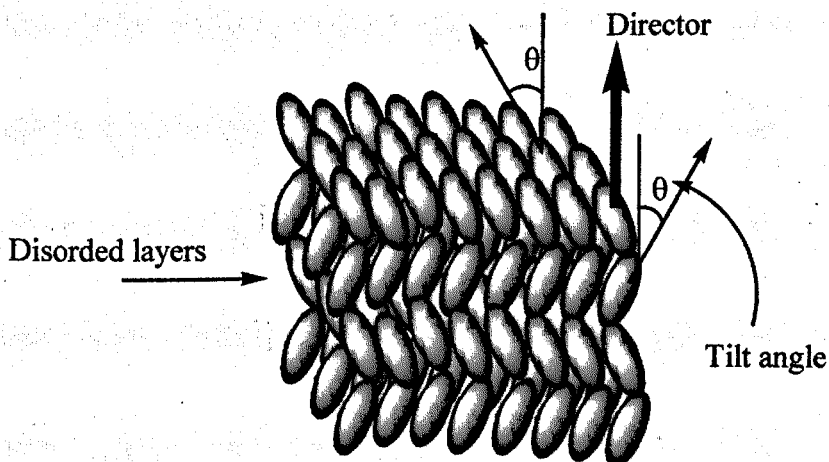


Figure 1.16 Structure of the alternating-tilt smectic C_{alt} phase

1.4.2.3 Smectic I phase

The smectic I^{37,38} phase is a tilted version of the hexatic smectic B phase with the tilt towards the point of the apex of the hexagon (figure 1.17).

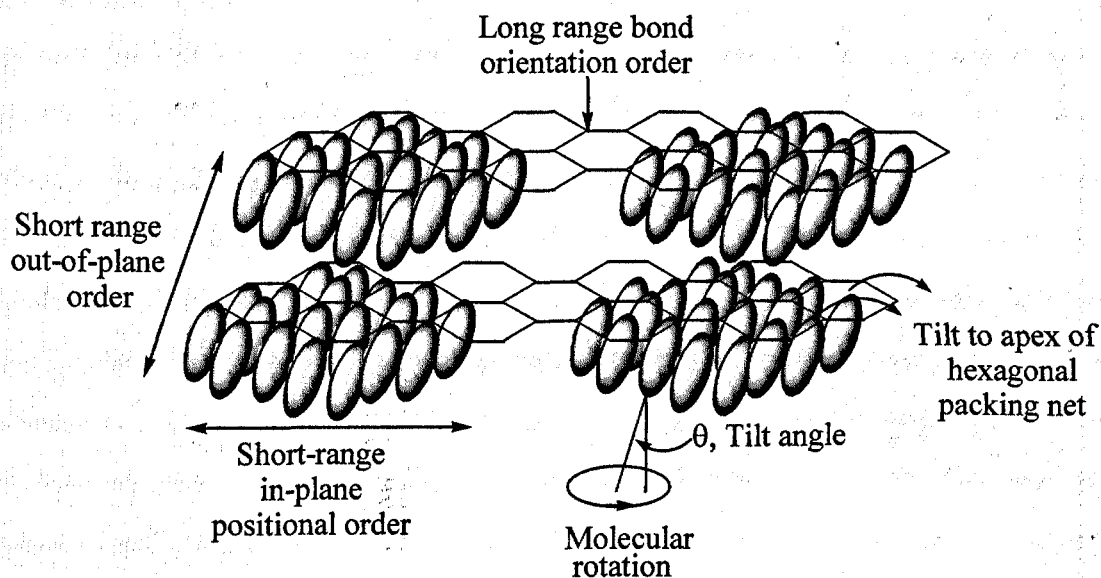


Figure 1.17 Structure of the smectic I phase.

1.4.2.4 Smectic F phase³⁹

As in the smectic I phase, the molecules of the smectic F phase are hexagonally close packed with respect to the director. The molecules have short range positioning within the layers but the difference lies in the tilt direction, in the smectic F phase, the molecules tilt towards the side of the hexagon, in contrast to the smectic I phase (see section 1.4.2.3).

1.4.2.5 Crystal J, G, K, H phases²⁹

Crystal J and G phases are tilted versions of the crystal B phase, and crystal K and H phases are tilted analogues³⁹ of the crystal E phase. The molecules in the crystal J and K phases tilt towards the apex of the distorted hexagonal lattice and for the crystals G and H phases the molecules are tilted towards the edge of the distorted hexagonal lattice. In summary, the smectic and quasi-smectic phases are represented in figure 1.18.

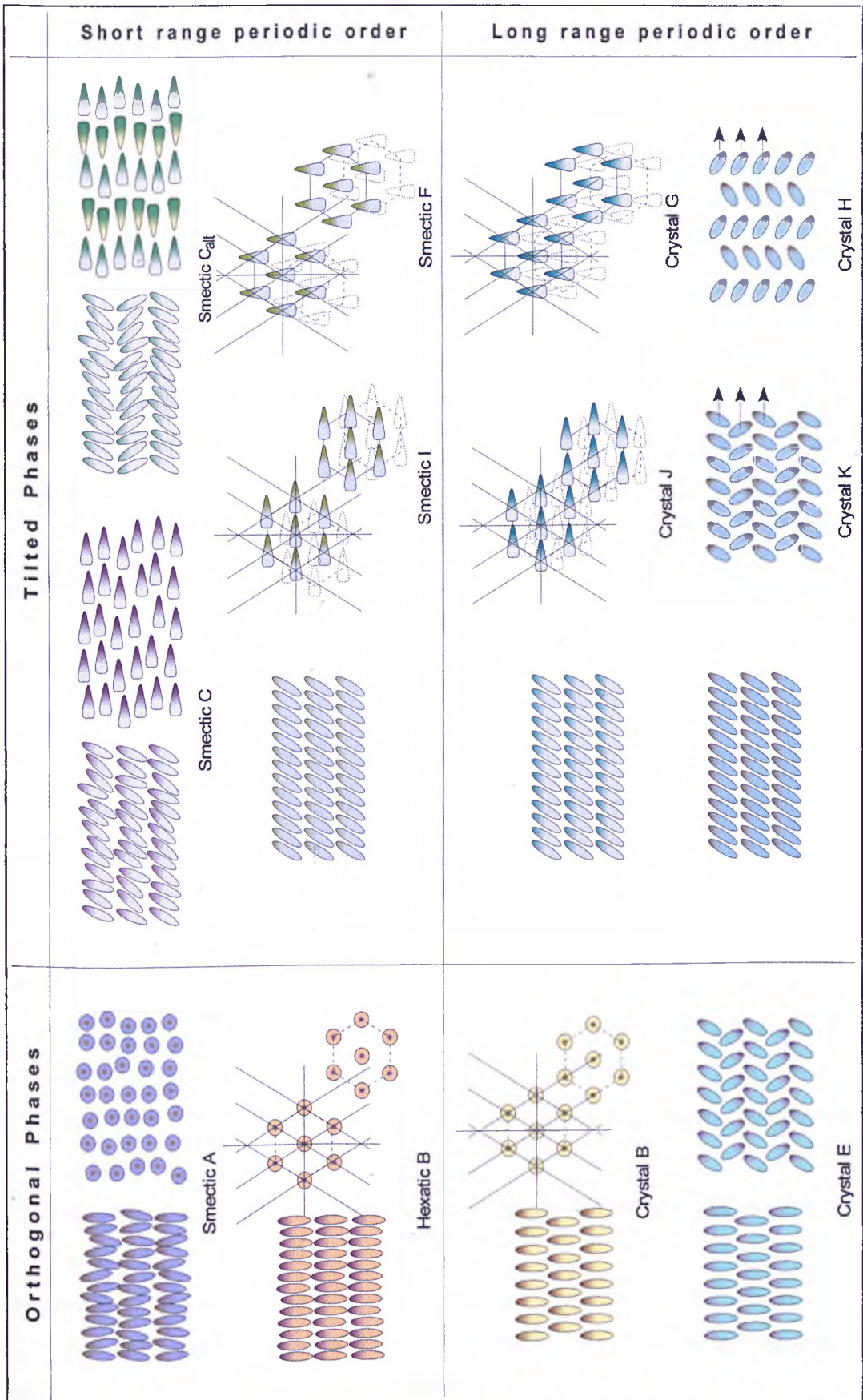


Figure 1.18 Representation of the smectic and quasi-smectic phases (courtesy of D. Parghi)

1.5 Physical properties of liquid crystals³

The main interest in the physical properties of liquid crystals arises because of the anisotropic nature of the properties which are not identical in all directions. Each mesophase has specific properties. These properties are particularly important for using that mesophase in distinctive applications. The main physical properties relevant to the nematic and smectic C mesophases will be discussed here.

1.5.1 Physical properties of the nematic phase⁴⁰

The nematic phase is characterised by long range orientational ordering of the long molecular axis which tends to be parallel to the director. As a result of this ordering the nematic mesophase exhibits anisotropy in many of its properties which can be used for electro-optical applications. The properties mainly of concern for such applications are viscosity, refractive indices, dielectric constants and elastic constants.

1.5.1.1 Viscosity

For the nematic phase as indeed for every liquid crystalline mesophase the viscosity is related to the order *i.e.* the order parameter. The nematic phase is the least ordered of all liquid crystalline mesophases and therefore the least viscous or the most fluid-like-phase. The nematic phase possesses three flow viscosities and a rotation viscosity namely,

η_1 where the director is perpendicular to the flow pattern but parallel to the velocity gradient,

η_2 where the director is parallel to the flow pattern but perpendicular to the velocity gradient,

η_3 where the director is perpendicular to both the flow pattern and the velocity gradient.

The rotational viscosity, γ_1 , is a very important property for the electro-optic application of the nematic phase and arises from the motion of the molecules from a planar orientation to the homeotropic orientation.

1.5.1.2 Optical anisotropy; birefringence

Birefringence (Δn) is a basic property of all liquid crystals and is intrinsic to their geometric anisotropy. The nematic phase is optically anisotropic. When a ray of light enters the nematic material, it is split into two unequally refracted rays in mutually perpendicular planes. The two rays of polarised light are the ordinary ray and the extraordinary ray. For the ordinary ray the electric vector is perpendicular to the optic axis. For the extraordinary ray the electric vector is parallel to the optic axis. If the direction of propagation is not parallel to the optical axis, then both rays on travelling through the medium will experience different refractive indices and therefore have different velocities. The difference between these refractive indices at their maximum value is the birefringence, *i.e.*, the maximum value of the optical anisotropy: $\Delta n = n_e - n_o$

The two refractive indices are temperature dependent and Δn decreases when the nematic mesophase transforms to the isotropic liquid state. The birefringence is a very important property for display applications and the appropriate value for Δn can be designed by molecular engineering. Materials containing electron-rich mesogenic cores and terminal chains give high Δn values.

1.5.1.3 Dielectric anisotropy

The nematic phase is also electrically anisotropic and its permittivity (the measure of its ability to transmit an electric field) is not constant in all directions. The dielectric anisotropy $\Delta\epsilon$ is the difference between the permittivity parallel to the molecular director ϵ_{\parallel} and the permittivity perpendicular to the director ϵ_{\perp} , $\Delta\epsilon = \epsilon_{\parallel} - \epsilon_{\perp}$, when $\epsilon_{\parallel} > \epsilon_{\perp}$ the dielectric anisotropy is positive. The dielectric anisotropy is frequency and temperature dependent and it decreases as the clearing point is approached, as is the case for the optical anisotropy. The dielectric anisotropy plays a very important role in twisted nematic display applications as it determines the threshold voltage required for the molecular motion from the planar orientation to the homeotropic orientation which destroys the wave-guide effect in the off-state.

1.5.1.4 Elastic constants

When a solid is torn or stressed in the limit of its elasticity, restoring forces act to retain the original shape of the solid. For the case of a liquid crystalline mesophase and in particular for the nematic mesophase, there are three possible deformations. Though these elastic forces are not as great as for the case of a solid, they play a vital role for display applications. The elastic constants drive the relaxation *e.g.* the motion from the homeotropic alignment of the molecules back to their planar configuration in a twisted nematic display. There are three possible deformations: splay, twist and bend (figure 1.19) and more important than their individual values is the ratio of bend/splay (k_{33}/k_{11}), which needs to be low for optimum electro-optical characteristics with typical values in the range 0.6 to 0.8. The values and ratio of the elastic constants are more difficult to obtain by molecular engineering than are the viscosities, and the optical and dielectric anisotropies.

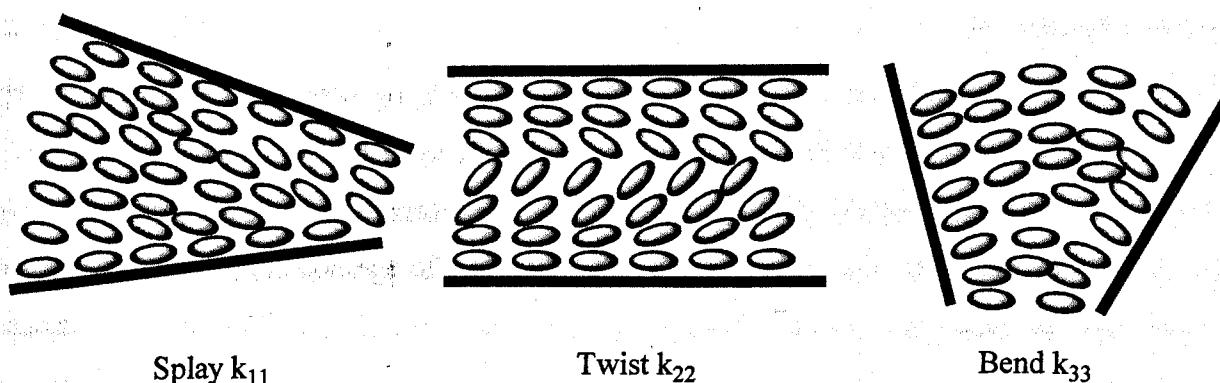


Figure 1.19 Representations of elastic deformations for a nematic material

1.6 Display devices using chiral nematic materials - twisted and super-twisted nematic devices⁴¹

All of the physical properties described above, especially the property of birefringence, can be exploited for the purposes of creating flat-panel displays. Usually a thin film of a liquid crystal is placed between two plates of glass which have been treated with surface alignment materials. These plates are manufactured with transparent electrodes that make it possible to apply an electric field across small areas of the film of liquid crystal. Polarising filters are placed on one or both sides of the glass to polarise the light entering and leaving the cell. Usually the polarisers are crossed, which means that light would not be able to pass through the empty display. The liquid crystal, however, will modify the polarisation of the light in some way that is dependent on the electric field being applied to it. Therefore, it is possible to dynamically create regions where light will get through and regions where it will not.

There are many issues that must be addressed when designing and analysing the performance of a flat-panel display, *e.g.*, the amount of voltage necessary to turn on a pixel in the display, the switching times of the pixels, the brightness/darkness response direction, the contrast of a liquid crystal display between its 'on' and 'off' states.

In a twisted nematic device, the molecules are sandwiched between two glass plates treated with surface alignment material so that they align parallel to the rubbed direction and are inclined at a pre-tilt angle of 1-3° to the glass plates. The rubbed directions are at right angles to each other so that the molecules perform a 90° twist across the cell (figure 1.20).

In the twisted state (when no field is applied), the entering light is polarised by the first polariser. The polarisation of the light then twists with the director of the nematic medium and its polarisation state is rotated through 90°. If the two polarisers are at right angles to each other, light is transmitted and the cell appears bright. However, when an electric field is applied across the cell, the director will want to align with the field (assuming that the material has a positive dielectric

anisotropy). Consequently the liquid crystal material will lose its twisted structure and therefore the linearly polarised light entering the liquid crystal material will not have its polarisation state rotated through 90° so light cannot pass through the other polariser and the cell appears dark. In some displays, the polarisers are parallel to each other, thus reversing the contrast in the 'on' and 'off' states.

This type of device has many limitations, such as a slow response and long relaxation times and also the difference between its 'on' and 'off' voltages is too large to address many pixels in a complex display. Furthermore, the effective viewing angle of the display can be very small and the polarisers work best on light that is propagating perpendicular to the display. When this type of device is used for portable computers, the screen can only be clearly seen when the operator is directly in front of it, and therefore this limits the application of these devices to small display areas.

The problem of a limited field of view was overcome when a greater twist of 270° (or 210° to obtain greyscale) was introduced using a greater amount of chiral dopant in the nematic mixture to give what are called super-twisted nematic devices. Twisted and super-twisted liquid crystal devices offer numerous advantages over other displays, for examples their low cost, their lightness, and their relatively high resistance to shock. However, they also have a number of limitations, a major one being their slow response time, which prevents their wider use, for example, in video imaging flat display panels.

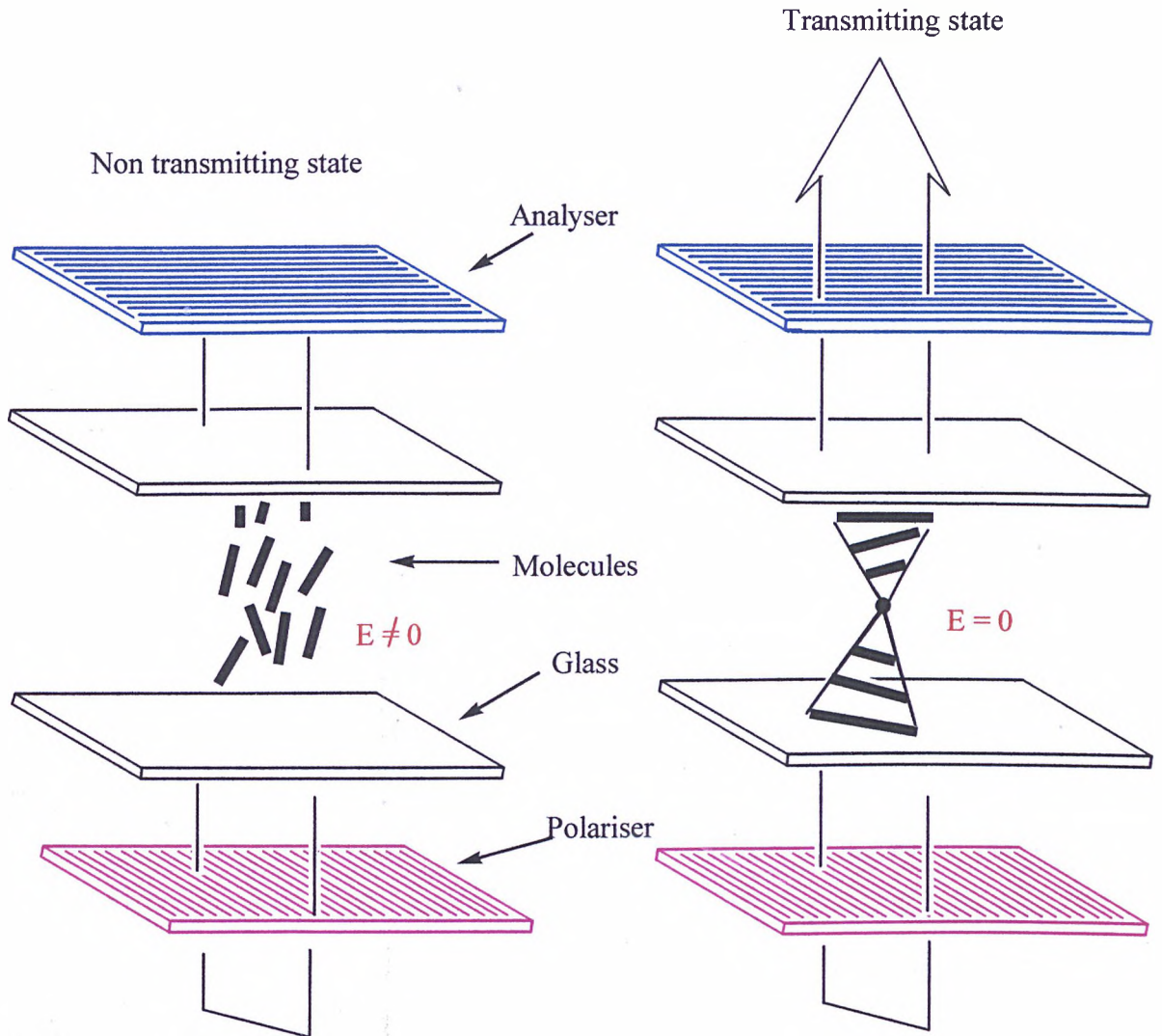


Figure 1.20 Representation of a twisted nematic display

1.7 Characteristics and physical properties of Ferroelectric Liquid Crystals

1.7.1 Ferroelectricity

In 1975, Meyer *et al.*⁴² using symmetry arguments demonstrated that chiral tilted smectic phases were ferroelectric *i.e.* displayed a spontaneous polarisation.

When the molecules are achiral the environmental symmetry of the smectic C phase consists of a centre of symmetry, a two-fold axis and a mirror plane containing the molecular tilt and perpendicular to the layers. The group symmetry of the plane is C_{2h} (figure 1.21).

When the molecules of the smectic C phase are chiral the symmetry is reduced to a two-fold axis⁴³ of rotation and the group symmetry is now C_2 . The dipoles associated with the environment about the chiral centres align because of molecular interactions, and this results in a spontaneous polarisation, P_s , that develops along the C_2 axis of the phase (figure 1.21).

However, in the bulk mesophase (not considering a single layer or a few layers) there is a slight and gradual change in the direction of the molecular tilt caused by the molecular chirality, which describes a helix (figure 1.22). The pitch of the helix is temperature dependent (as for chiral nematic N^*).

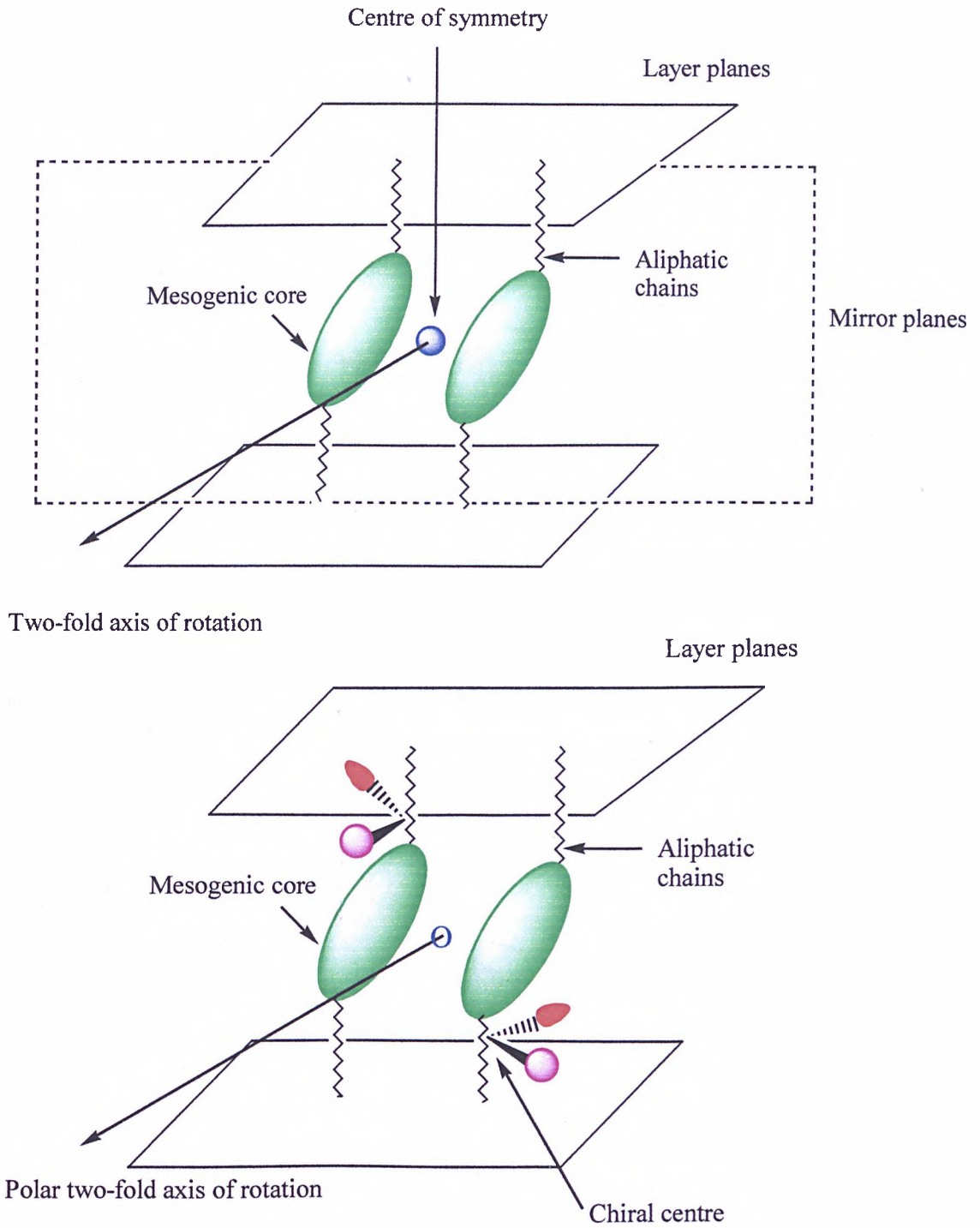


Figure 1.21 Representation of the C_{2h} symmetry of the smectic C phase and (above) of the C_2 symmetry of the chiral smectic C phase (below).

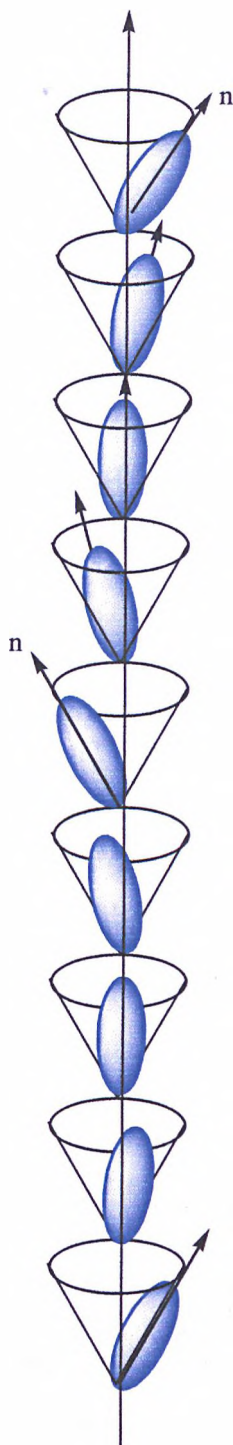


Figure 1.22 Representation of the helical structure of the chiral smectic C phase.

A single layer of SmC^* material shows spontaneous polarisation in the absence of an external electrical field, therefore it can be classified as ferroelectric and its polarisation can be re-orientated by an applied field. In the bulk mesophase, the molecular tilt spirals about an axis perpendicular to the layers, and the layer polarisation also rotates relative to the helical ordering of the tilt and therefore is zero

for the bulk of the phase. The phase has therefore been described as being helielectric⁴⁵ or chiroelectric. In order for the bulk of mesophase to exhibit a spontaneous polarisation, the helix needs to be unwound.

1.7.2 Surface Stabilised Ferroelectric Liquid Crystal Display

The Surface Stabilised Ferroelectric Liquid Crystal (SSFLC) display invented by Clark and Lagerwall⁴⁶ consists of a thin cell, with a spacing less than the pitch of the helix. The chiral smectic C material is sandwiched between two glass sheets whose surfaces have been treated so that the smectic layers lie perpendicular to the glass surface ('bookshelf geometry')^{7, 41}. The mode of operation of the SSFLC device is based on the switching of the optic axis of the molecules between two degenerate states. As the molecules lie parallel to the glass plates the spontaneous polarisation points either up or down. When an external DC field is applied, the P_s direction can be reversed to align with the field, and the change in the P_s direction causes the molecules to switch from one tilted state to the other around a cone of angle 2θ . Once the ferroelectric material has been switched by an appropriate external field, it will retain its orientation until a field of opposite direction is applied, hence the name bistable device.

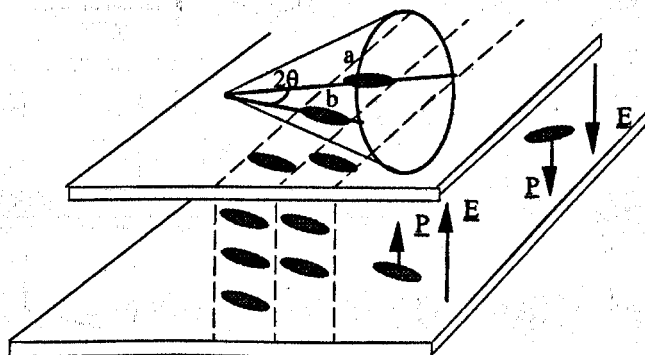


Figure 1.23 Representation of the switching mode of a typical SSFLC cell with its molecules homogeneously aligned state a and state b⁴⁷.

Ideally, the smectic C layers are perpendicular to the plane of the cell in the so called bookshelf configuration. The polarisers are crossed (90°) with one polariser parallel to the optic axis of one bistable state⁴⁸ (figure 1.24). When the molecular optical axis is aligned parallel to the plane of polarisation, the light passes through the liquid crystal material and is absorbed by the analyser and so the cell appears dark. On the

other hand, when an external DC field is applied, the inversion of the direction of the spontaneous polarisation occurs and forces the long molecular axis to rotate around the smectic C cone (ideally 45°) with respect to the polarisers and in effect the material becomes a half wave plate which rotates the plane of incident light through 90° and therefore the cell appears bright.

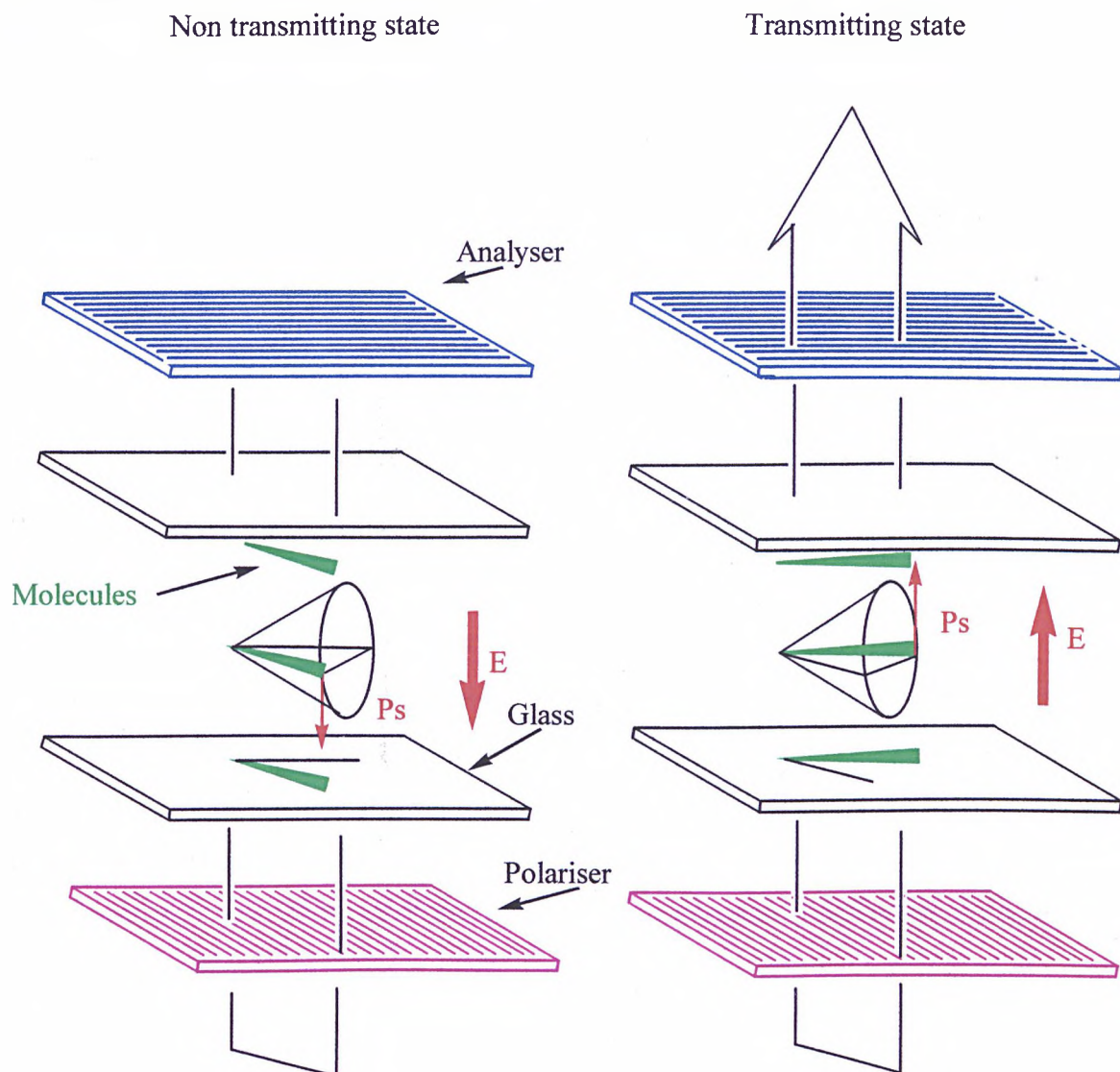


Figure 1.24 Representation of the dark and bright states of a SSFLC cell.

1.7.3 Physical properties of ferroelectric liquid crystal materials^{47,48,49}

The physical properties of ferroelectric liquid which directly influence the performance in a SSFLC cell are birefringence, tilt angle, spontaneous polarisation, rotational viscosity and dielectric biaxiality.

The intensity of the light transmitted, I , through the cell is expressed as follows⁵⁰

$$I = I_0 \sin^2 4\theta \sin^2 (\pi\Delta n d)/\lambda$$

where I_0 is the intensity of the incident light of wavelength λ , Δn is the birefringence of the medium and d is the cell gap. It follows that in order to obtain maximum transmittance, the tilt angle θ must be equal to 22.5° . The cell gap, birefringence and wavelength are related:

at maximum transmittance, $I = I_0$, $\theta = 22.5^\circ$, and therefore $\sin^2 (\pi\Delta n d)/\lambda = 1$,

$$\text{and so } (\pi\Delta n d)/\lambda = \pi/2,$$

$$\text{and } \Delta n d = \lambda/2.$$

As was the case for the tilt angle, the P_s is temperature dependent as shown by the equation below:

$$P_s = P_0(T_c - T)^\beta$$

where P_0 is a constant dependent upon the nature of each dopant, T_c is the Curie point (the SmA* to SmC* transition temperature), T is the actual temperature and β has a value theoretically equal to 0.5. As the temperature decreases, the value of the P_s increases to an almost constant value.

Goodby *et al.*⁵¹ have shown that the sign of the spontaneous polarisation depends upon the direction of the polarity of the two-fold axis and they have produced the following rules:

$$\text{Sed P (-) + I} \quad \text{Sol P (+) + I} \quad \text{Sod P (-) - I} \quad \text{Sel P (+) - I}$$

$$\text{Red P (-) - I} \quad \text{Rol P (+) - I} \quad \text{Rod P (-) + I} \quad \text{Rel P (+) + I}$$

Where S or R is the absolute configuration, o or e is the parity, l or d is the screw direction of the helix, P (+) or P (-) is the polarisation direction and - I or + I is the inductive effect of the off-axis substituent at the chiral centre.

The switching time τ is expressed as follows⁵²,

$$\tau \approx \gamma_{\text{eff}}/PsE$$

where γ_{eff} is the effective viscosity and E is the intensity of the applied electric field.

γ_{eff} is related to θ by the expression

$$\gamma_{\text{eff}} = \gamma_0 \sin^2 \theta$$

where γ_0 is the hypothetical rotational viscosity for a smectic C structure with a tilt angle of 90° and therefore the switching time can be expressed as.

$$\tau \approx \gamma_0 \sin^2 \theta / PsE$$

Therefore, short switching times can be obtained with a low rotational viscosity, applying a high electrical field and using a material with a high Ps . However, applying a high electrical field is not a suitable solution for several reasons, including the possibility of conductivity problems, shorting the cell and the disadvantage of using high power supplies.

1.7.3.1 Role of the dielectric biaxiality

In the case of nematic devices, the dielectric anisotropy alone determines the electro-optic effect since it is related to the root mean square (rms) of the AC field by $\Delta\epsilon E^2$. In ferroelectric devices, the response is characterised by the Ps and the dielectric anisotropy of the material, and when a field is applied the molecules experience a dielectric force ($\Delta\epsilon E^2$) and a ferroelectric torque proportional to PsE . At low fields the ferroelectric torque prevails over the dielectric torque, but at high electric field the dielectric torque dominates⁵³. It follows that the value of Ps , $\Delta\epsilon$ and E must be balanced appropriately to prevent any loss of contrast as the director will experience opposite forces.

Ferroelectric liquid crystals lack full biaxiality⁵⁴ and therefore the contrast in a display is reduced. The chiral smectic C phase is biaxial and the physical properties perpendicular to the director are different from those in directions parallel and perpendicular to the plane of the tilt.

The optical biaxiality of the chiral smectic C phase is less important than the dielectric biaxiality and the chiral smectic C can be considered optically uniaxial⁴⁷.

By convention ϵ_3 is the permittivity in the long axis of the molecule, ϵ_2 is in the direction of the spontaneous polarisation and finally ϵ_1 is perpendicular to ϵ_3 and ϵ_2 (figure 1.25).

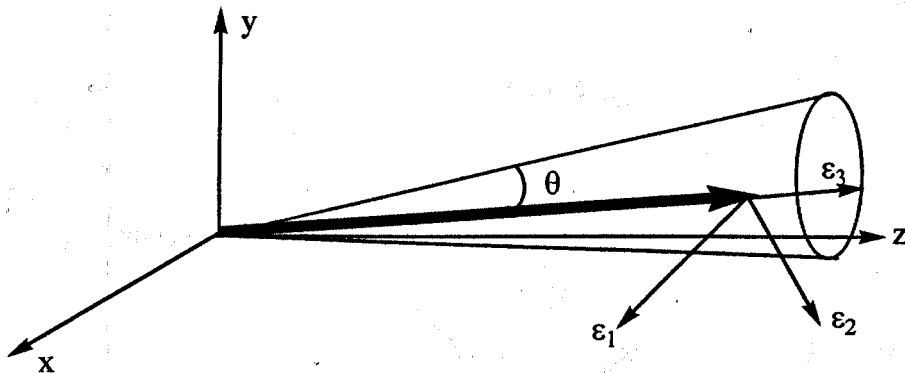


Figure 1.25 Dielectric permittivities of a molecule in a SSFLC cell

The uniaxial dielectric anisotropy is $\Delta\epsilon = \epsilon_3 - \epsilon_1$, the dielectric biaxiality is $\delta\epsilon = \epsilon_2 - \epsilon_1$, and $\delta\epsilon$ is large and often dominates $\Delta\epsilon$. The largest permittivity ϵ_2 is usually along the direction parallel to the direction of the Ps, and thus an effective way of overcoming the lack of full bistability is to apply an AC field. The AC field only couples to the dielectric tensor and not to the Ps as its frequency is too high to stabilise the fully switched state⁵⁵. The dielectric biaxiality also plays an important role in the electro-optic DC switching of the ferroelectric liquid crystal material as shown in the equation below for a material with a positive dielectric biaxiality⁵⁶,

$$|V_{\min}| \propto |(Ps d)/(\delta\epsilon)|$$

where V_{\min} is the voltage at which the minimum switching time is obtained. This type of behaviour is usually seen only for materials with low Ps ($<10 \text{ nC cm}^{-2}$) because high Ps systems require a higher electric field, which would damage the smectic layers⁷.

The switching time of a material can be expressed as a function of its rotational viscosity, γ , and its dielectric biaxiality, $\delta\epsilon$, as shown by the following expression,

$$\tau \propto \gamma/\delta\epsilon.$$

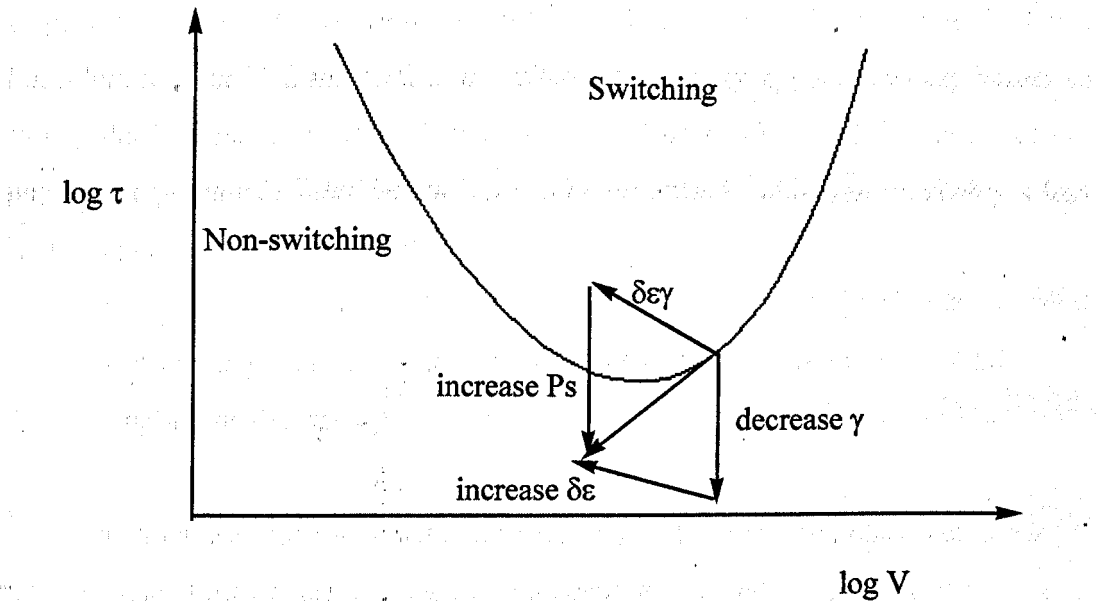


Figure 1.26 Method to reduce V_{\min} and τ_{\min} .

Figure 1.26 shows^{53,57} two possible methods to improve the devices' performance; V_{\min} is decreased by increasing the dielectric biaxiality while τ_{\min} is lowered by increasing the Ps or lowering the viscosity. As in practice the operating voltage of a device is chosen according to the drive circuitry, the Ps of the material is adjusted to yield a suitable V_{\min} . FLC materials operating in the τV_{\min} mode require a low viscosity and a high dielectric biaxiality.

1.8 Ferroelectric Liquid crystal materials^{30,48,49}

Displays using ferroelectric smectic C liquid crystals offer numerous advantages over nematic based displays. Ferroelectric liquid crystal devices are faster switching than nematic based displays devices, they can also provide higher resolution over a large display area and a better viewing angle⁵⁸. However the physical criteria for a ferroelectric smectic C material to be suitable for display applications are harder to satisfy than for nematic materials used in twisted or supertwisted devices. All the physical requirements listed below have to be optimised⁵⁹ although inevitably a less ideal property has to be accepted.

- A cooling phase sequence $N^* \rightarrow SmA^* \rightarrow SmC^*$ is required to obtain optimum alignment.
- A wide SmC^* range with no underlying ordered smectic phases to allow use of the device over the normal ambient temperature range *i.e.* below room temperature to over 60 °C.
- A high spontaneous polarisation. The response time is determined by the magnitude of the spontaneous polarisation of the material.
- The pitch of the helix of the chiral nematic phase must be greater than four times the cell gap to prevent the tendency to form a helical chiral smectic C phase and to permit good alignment.
- The pitch of the helix of the chiral smectic C phase must be greater than the cell gap so that it can be suppressed in order to get a spontaneous polarisation.
- An optical anisotropy of value 0.14 for a 2 μm cell such that maximum contrast and colour density are obtained.
- A low rotational viscosity to obtain fast switching times.
- A high dielectric positive biaxiality to retain good alignment as it couples

to an AC external field in the direction of the Ps.

1.8.1.1.2.3. Ferroelectric liquid crystal mixtures

- A tilt angle of 22.5° to give optimum transmission.
- No absorption of visible light for optimum colour operation.
- The material must be chemically and photochemically stable.

1.8.1 The “all-chiral” approach

There are different approaches to the development of FLC materials. In principle, a single component system can be designed, however the properties required are so numerous and variable that a single chiral component cannot meet them all, and therefore mixtures of materials are used.

Furthermore, with all chiral materials the process is more expensive and the synthesis of chiral materials is more complicated than the synthesis of achiral materials. The chiral functionality is usually provided by the starting material and chiral materials are often expensive or if they are synthesised, they are harder to purify. It is important that the nature of the chirality is retained or inverted through the synthesis in a controlled way - the optical purity has to be unchanged. When an optical inversion occurs in the synthesis (as for an S_N2 process) a 100% optical inversion should occur. The enantiomeric excess of the product system has to be constant if the properties of the mixtures are to be reproducible. Goodby and co-workers⁶⁰ witnessed that mesophase stability, and especially spontaneous polarisation, depended on the optical purity of the material used. This casts doubts on the reproducibility of measurements on chiral material mixtures over a period of time when different sources of material and different synthetic routes are used.

The method most often chosen to produce ferroelectric mixtures is to use mixtures of achiral materials doped with a chiral compound to provide the possibility of spontaneous polarisation when the helical structure is suppressed. This method offers the possibility of cutting costs and also minimises the importance of the chiral compound to simply providing the spontaneous polarisation in the mixture.

1.8.2 Ferroelectric liquid crystals mixtures

The chiral dopant does not need to be mesogenic, but it needs to have a very good compatibility with the achiral host material and also to give a long helical pitch. These requirements are more easily achieved when the chiral dopant has a structure similar to the structure of the constituents of the achiral host mixture, so that the transition temperatures are not decreased too severely. The synthesis of the chiral dopant should preferably not involve optical resolution (which is frequently an inefficient and laborious process), both (*R*)- and (*S*)- enantiomeric forms should be available if possible and the chiral dopant should be stable to racemisation. The chiral dopant should have a high spontaneous polarisation, so that only a small amount needs to be added, to minimise its effect on the mesophase stabilities of the mixture.

A high spontaneous polarisation is obtained when the chiral centre is close to the core so that the free rotation of the chiral centre is restricted and the direction of its dipole is confined. The nature of the chiral centre also plays a vital role, and it should possess a high degree of polarity; this is best achieved when the chiral centre possesses either a CN, F or Cl substituent. Typical chiral dopants⁶¹ used in ferroelectric mixtures are shown in figure 1.27.

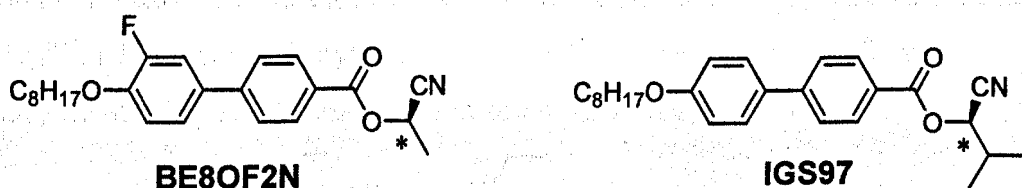


Figure 1.27 Typical chiral dopants used in ferroelectric mixtures

For **BE8OF2N** and **IGS97** the spontaneous polarisation is amplified by the coupling of the dipole of the cyano moiety with the dipole of the carbonyl group.

1.8.3 Achiral host materials

Ferroelectric liquid crystals have the basic structure of the other calamitic liquid crystals (see figure 1.28). The molecules are generally composed of a core unit with two terminal (alkyl or alkoxy) chains and in some cases lateral substituents.

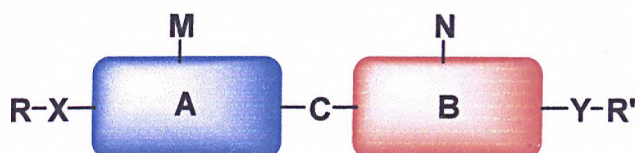


Figure 1.28 The general structure of calamitic ferroelectric liquid crystals

There has been extensive research into the design and synthesis of novel ferroelectric host materials^{62, 63, 64} and the quality of the host will depend upon several criteria such as:

- A low melting point.
- A wide smectic C range.
- A low viscosity.
- A negative dielectric anisotropy.
- A high dielectric biaxiality.
- A high chemical and photochemical stability.

Most ferroelectric host materials contain at least two rings and phenyl rings are most common since they have a greater tendency to form smectic C phases than cyclohexyl rings⁶⁵ or bicyclo[2,2,2]octyl rings (figure 1.29) however heterocyclic rings (figure 1.30) are also important components in some ferroelectric systems.

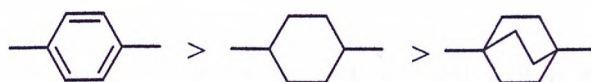


Figure 1.29 The order of tendency to form the smectic C phase

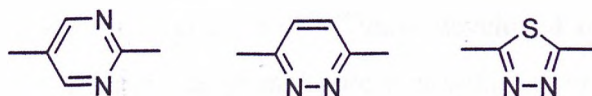


Figure 1.30 Types of heterocyclic rings used in ferroelectric host materials

The ring systems might be linked directly **1.1** or by an ester group **1.2**, but compounds of type **1.1** tend to have high melting points and compounds of type **1.2**

tend to have a high viscosity, both these properties being undesirable for compounds used in mixtures (see figure 1.31).

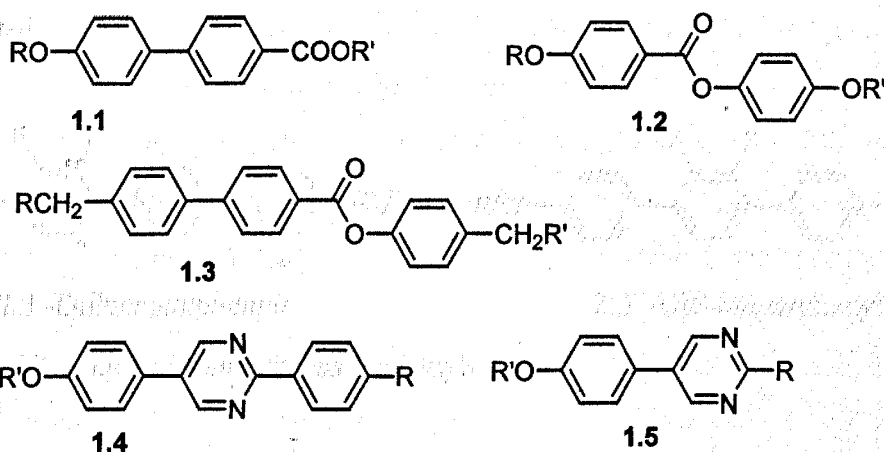


Figure 1.31 Different types of smectogens

Compounds of the type 1.3 can show smectic C_{alt} phases when the chain on the phenyl ring is branched⁶⁶; compounds of the type 1.4 tend to have a fairly low viscosity but their melting points are too high. Compounds 1.5 with 7 or more carbon atoms in the chain also give a smectic C phase⁶⁷. The phenylpyrimidines offer advantages over other systems in that they have low viscosities and low melting points but their smectic C range is too narrow. The smectic C range can be increased by using two alkoxy terminal chains but this causes an increase in viscosity. It therefore appears that in order to generate a smectic C phase with acceptable properties, aromaticity is required in the central rigid core region with dipolar functionalities near one end and long terminal chain terminal.

The best materials are obtained when no link is used within the core, so that the viscosity is not too great, and when three rings are present to provide wide smectic C stability. Based on these ideas, Gray *et al.*^{68,69} have developed achiral host materials for ferroelectric systems using a terphenyl core unit with one or more lateral fluoro substituents to modify the core. The fluoro substituent was used to modify the transition temperatures and mesophase behaviour because of its small size and its high electronegativity. Fluoro substitution usually reduces the melting point, suppresses underlying smectic phases and introduces the tendency for the molecules to tilt. When two fluoro substituents are in an *ortho*-relationship, the effect is even

greater; the 2,3- or 2',3'-difluoroterphenyls (see figure 1.32) are no broader than the mono-fluoro substituted terphenyls, the ordered smectic phases are eliminated, the dielectric anisotropy becomes negative and neither the melting point nor the viscosity is affected.

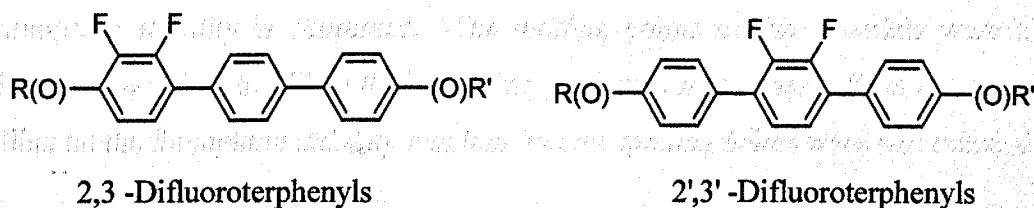


Figure 1.32 *o*-Difluoro substituted terphenyls

The position of the *ortho*-difluoro substituents has an effect on the mesophase mesomorphism as well as on the melting and clearing points. The 2',3'-difluoroterphenyls^{70,71,72} have a lower melting point and lower smectic C mesophase stability as well as a greater nematic tendency than the 2,3-difluoroterphenyls. The smectic C phase is enhanced when the difluoro substituent is on an outer ring and gives the lateral dipole near one end of the molecule. Both cores show smectic C phases when fairly long terminal chains are attached; the compounds have high negative dielectric anisotropies, high clearing points and usually have the desired cooling phase sequence of $N \rightarrow \text{SmA} \rightarrow \text{SmC}$.

A simplistic view of how mesogenicity arises in molecules is that the core provides the anisotropy necessary to give mesomorphic behaviour and the terminal chains serve to reduce the melting point so that mesophases can be observed. Most liquid crystal research has been concentrated on the design and synthesis of novel cores, and the flexible part of the calamitic liquid crystal molecule has been alkoxy or alkyl terminal chains.

The effect of changing the nature of the terminal chains on the mesomorphism and transition temperatures has only been studied in detail with respect to their length. Only recently have researchers started to study the influence of the chain structure on the mesophase morphology and transition temperature^{73,74}. Kelly has studied the effect of the position of a double bond along a chain⁷⁵ and Goulding and co-

workers⁷⁶ have studied the effect of an oxygen atom at varying positions along a chain. Each of these investigations has shown that the length and the nature of the terminal chain can influence the mesomorphic properties of the material. Coates^{77,78} studied the effect of a methyl-branching at various positions along the chain and showed that the closer the branching point was to the core the more severely the mesophase stability is depressed. The melting points of the materials were also significantly reduced. When the branching point was further away from the core, its effect on the mesophase stability was less, but the melting points were still reduced.

... of the liquid crystal phase in these systems. The terminal chain length and the nature of the terminal chain can influence the mesomorphic properties of the material. Coates^{77,78} studied the effect of a methyl-branching at various positions along the chain and showed that the closer the branching point was to the core the more severely the mesophase stability is depressed. The melting points of the materials were also significantly reduced. When the branching point was further away from the core, its effect on the mesophase stability was less, but the melting points were still reduced.

... of the liquid crystal phase in these systems. The terminal chain length and the nature of the terminal chain can influence the mesomorphic properties of the material. Coates^{77,78} studied the effect of a methyl-branching at various positions along the chain and showed that the closer the branching point was to the core the more severely the mesophase stability is depressed. The melting points of the materials were also significantly reduced. When the branching point was further away from the core, its effect on the mesophase stability was less, but the melting points were still reduced.

... of the liquid crystal phase in these systems. The terminal chain length and the nature of the terminal chain can influence the mesomorphic properties of the material. Coates^{77,78} studied the effect of a methyl-branching at various positions along the chain and showed that the closer the branching point was to the core the more severely the mesophase stability is depressed. The melting points of the materials were also significantly reduced. When the branching point was further away from the core, its effect on the mesophase stability was less, but the melting points were still reduced.

1.9 Aims of the research

Most of the research on liquid crystals has focussed on the synthesis of novel mesogenic cores, which are attached to simple alkyl or alkoxy terminal chains. Very little is known about the influence of different types of terminal chains on a chosen core and much more information is needed in order to understand the effect of the terminal chains on the mesomorphology of mesogens and on the electro-optic effects in a typical SSFLC cell or other devices.

Gray⁷⁹ suggested that terminal groups fill the space remaining when the mesogenic cores in the liquid crystal phase are in close contact. The terminal chains can act as spacers and regulate the intermolecular spacing, thus controlling the molecular forces which cause the liquid crystalline state. From the hydrodynamic point of view, the terminal chain determines the length of the molecule and thus the radius of gyration, which is important for viscosity. S. Kazuyuki and co-workers⁸⁰ synthesised ferroelectric materials containing siloxy chain end groups, because this group, which is believed to be more flexible than an alkyl chain, decreases the viscosity and lowers melting points. Coles *et al.*⁸¹ also synthesised a series of low molar mass ferroelectric materials containing organosiloxane end groups and these materials showed subzero crystallisation temperatures, short switching times^{82,83}, and high tilt angles (see figure 1.33).

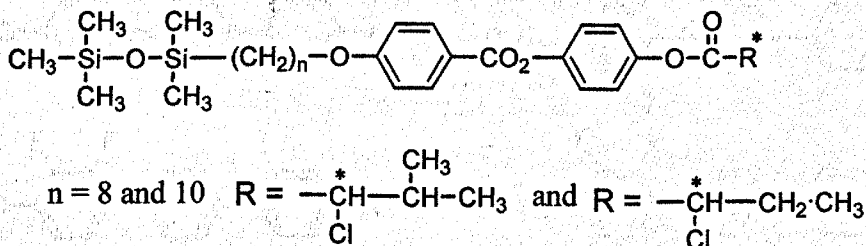


Figure 1.33 A series of low molar mass ferroelectric materials containing organosiloxane end groups synthesised by Coles and co-workers⁸¹

The reason for the short switching times of these compounds could either be the nature of the silicon-oxygen bonds which allows easier rotation of the molecule and so the greater flexibility of the group reduces the viscosity, or the bulkiness of the group, which interferes with the inter-layer mixing and therefore allows faster switching around the cone angle from one bistable state to the other.

In order to study whether and how the switching is affected by the nature of the end group on the terminal chain, the synthesis of several series of compounds containing different end groups of different sizes and polarity was planned.

For this research, a 2,3-difluoroterphenyl core was chosen because compounds derived from this core have reasonably low melting points, low viscosities and, most importantly wide smectic C ranges⁶⁹. Many 2,3-difluoroterphenyls also show the cooling phase sequence $N \rightarrow \text{SmA} \rightarrow \text{SmC}$ required for optimum alignment of the material in a cell for electro-optical measurements, and host mixtures based on difluoroterphenyls are the preferred materials used in the DERA ferroelectric programme.

A nine-atom chain at the 4-position (figure 1.34) was chosen for compounds in this work since it has been established that a significant chain length is required for the mesogenic core to exhibit the smectic C phase. Compounds 1.6–1.9 have approximately the same chain length at the 4-position and allow a study of the alkoxy / alkyl effect on mesomorphism and transition temperatures.

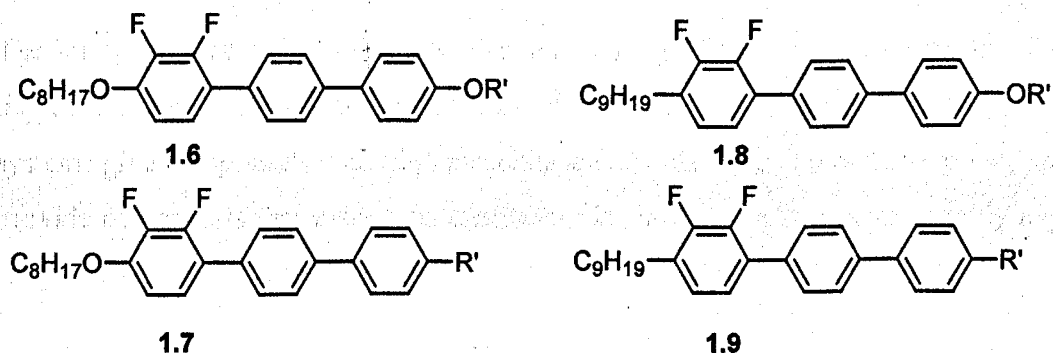


Figure 1.34 Core systems used in this work

The chain at the 4-position was fixed as an octyloxy or as a nonyl chain, and the terminal chain at the 4''-position was varied. The chain at the 4''-position was altered in several ways; examples were targeted which were branched, with or without heteroatoms such as oxygen, silicon or halogens (chlorine or bromine).

A series of compounds containing a trimethylsilyl end group on a chain of varying length was targeted. Analogues of this compound were synthesised: one containing

no bulky end group, one where the silicon atom was replaced by a carbon atom, and finally one with a *t*-butyloxy end group (see figure 1.36).

Although the terms “terminal” and “end group” are sometimes used synonymously, they are used with distinct meanings in the present case: ‘terminal’ chains are chains which lie along the long molecular axis and the end group is the region at the end of the terminal chain (and they differ from lateral chains which are attached ‘perpendicular’ to the long molecular axis) (see figure 1.35).

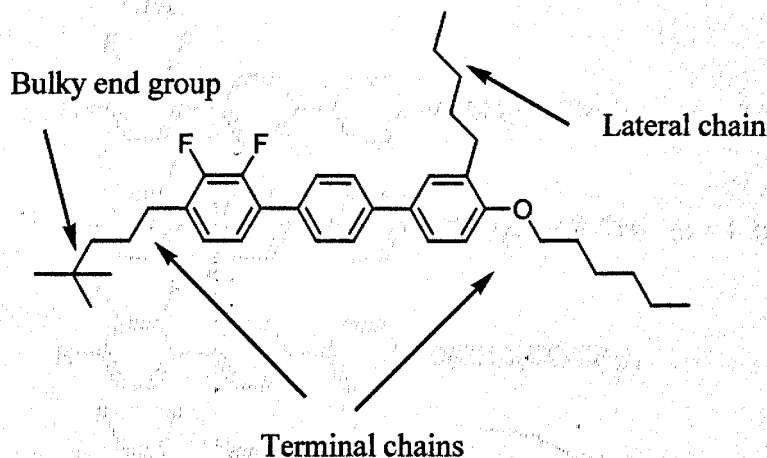
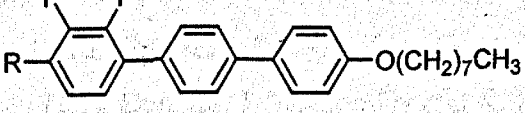
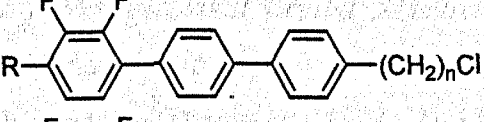
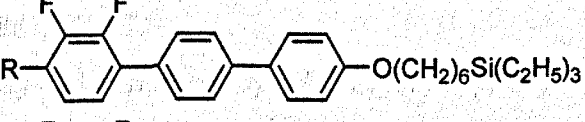
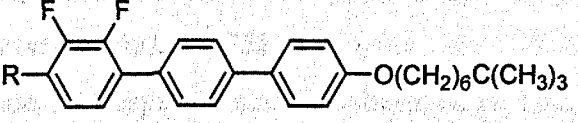
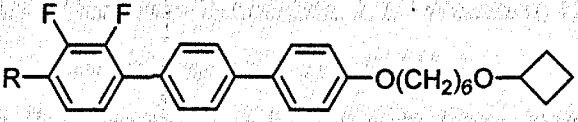
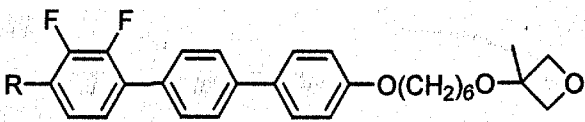
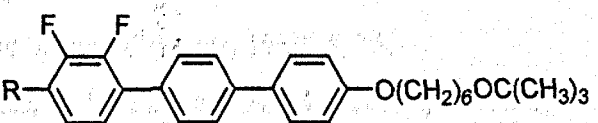
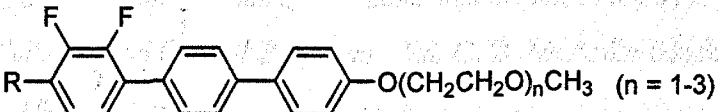
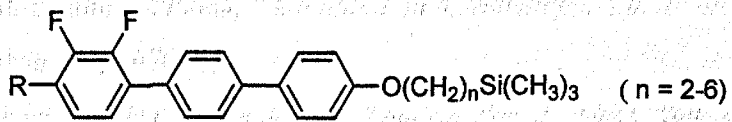
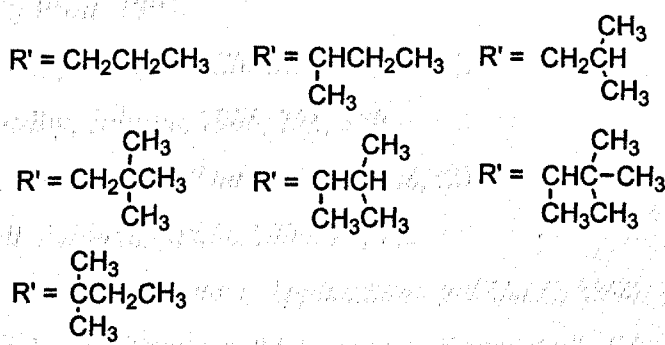
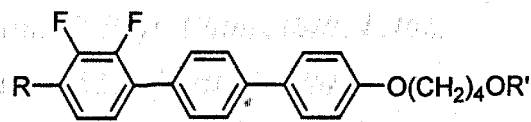


Figure 1.35 Representation of a terminal chain with a bulky end group

The bulky end group is likely to hinder the packing of the molecules and therefore decrease the melting points and the mesophase stabilities. Because terphenyl core systems give compounds with high mesophase stabilities, a bulky end group may still provide compounds that exhibit an enantiotropic smectic C phase at reasonably high temperatures.

The intention was to study the effect of the bulky end group on the melting point and mesophase morphology of the compounds and also to assess how these compounds affect the switching times of mixtures in which they are included. Other variations to the end group which were planned included a series of compounds with the same chain length but with varying steric sizes, a series of compounds containing chloro end groups, and a series of compounds containing varying ethylenoxy units. The complete set of compounds prepared in this work is summarised in figure 1.36 with the parent compounds.



$R = \text{C}_8\text{H}_{17}\text{O}$ and $R = \text{C}_9\text{H}_{19}$ (not all combinations of substituents were prepared)

Figure 1.36 The range of compounds with different end groups prepared in this work

1.9.1 Bibliography Section 1

1 F. Reinitzer, *Montash*, 1888, 9, 421.

- 2 O. Lehmann, *Z. Phys. Chem.*, 1889, **4**, 462.
- 3 P. Collings and J. S. Patel, *Handbook of Liquid Crystal Research*, Oxford University Press, 1997.
- 4 J. W. Goodby, *J. Mater. Chem.*, 1991, **1**, 307.
- 5 J. W. Goodby, *Science*, 1986, **231**, 350.
- 6 D. Erdmann, *Kontakte (Darmstadt)*, 1988, (2), 3.
- 7 M. Schadt, *Liquid Crystals*, 1993, **14**, 73.
- 8 D. Demus, "Liquid Crystals; Applications and Uses", 1990, 1.
- 9 Lyotropic Liquid Crystals, "Advances in Chemistry", Ed. S. Friberg, ACS Washington DC, 1976, 152.
- 10 H. Fikelman, *Philos. Trans. R. Soc. London, Ser. A.*, 1983, **309**, 35.
- 11 , 'Side Chain Liquid Crystal Polymers', Ed. C. B. McArdle Blackie, Glasgow, 1989.
- 12 D. Demus, *Liquid Crystals*, 1989, **5**, 75.
- 13 J. Malthete, N. H. Tinh and A. M. Levelut, *J. Chem. Soc., Chem. Commun.*, 1987, 1548.
- 14 Y. Feng, A. M. Levelut and C. Destrade, *Liquid Crystals.*, 1990, **7**, 265.
- 15 M. Edent, O. Herrmann-Schoenhen, J. H. Wendorff, H. Ringsdorf and P. Tschierner, *Makromol. Chem.*, 1988, **9**, 445.
- 16 N. Boden, R. C. Borner, R. J. Bushy, A. N. Cammidge and M. V. Jesudness, *Liquid Crystals*, 1993, **15**, 851.
- 17 C. Destrade, H. Gasparoux and A. Babeau, N. H. Tinh, *Mol. Cryst. Liq. Cryst.*, 1981, **67**, 37.
- 18 G. W. Gray and J. W. Goodby, *Mol. Cryst., Liq., Cryst.*, 1976, **37**, 157.
- 19 "Selected Topics in Liquid Crystal Research", Ed. Hano-Dieter Koswig, Akademie-Verlag, Berlin, 1990.
- 20 E. Poetsch, *Kontakte (Darmstadt)*, 1988, (2), 15.
- 21 M. Hird and K. J. Toyne, *Mol. Cryst., Liq., Cryst.*, 1998, **323**, 1.
- 22 C. J. Booth, D. A. Dunmur, J. W. Goodby and K. J. Toyne, *Liquid Crystals*, 1994, **20**, 815.
- 23 P. G. de Gennes, "The Physics of Liquid Crystals", Clarendon Press, Oxford, 1974.
- 24 G. Friedel, *Ann. Physique*, 1922, **18**, 273.

- 25 J. W. Goodby and T. M. Leslie, *Mol. Cryst. Liq. Cryst.*, 1984, **110**, 175.
- 26 A. J. Leadbetter, J. L. A. Durrant and M. Rugman. *Mol. Cryst. Liq. Cryst. Lett.*, 1977, **34**, 231.
- 27 A. J. Leadbetter, *Phys. Bulletin*, 1977, **28** 127.
- 28 F. Grandjean, *Cr. Hebd. Acad. Sci.*, 1917, **166**, 165.
- 29 G. W. Gray and J. W. Goodby, 'Smectic Liquid Crystals', "Textures and Structures", Leonard Hill, Philadelphia, 1984.
- 30 N. A. Clark and S. T. Lagerwall in *Ferroelectric Liquid Crystals, Principles, Properties and Applications, Ferroelectricity and Related Phenomena* Vol. 7, 1991, 6, Ed. J. W. Goodby, R. Blinc, N. A. Clark, S. T. Lagerwall, M. A. Osipov, S. A. Pikin, T. Sakurai, K. Yoshino and B. Žekš, Gordon and Breach Scientific Publishers.
- 31 W. L. McMillan, *Physical Review A*, 1973, **8**, 1921.
- 32 A. Wulf, *Physical Review A*, 1975, **11**, 365.
- 33 J. W. Goodby, G. W. Gray and D. G. McDonnell, *Mol. Cryst. Liq. Cryst. Lett.*, 1977, **34**, 138.
- 34 D. M. Walba, S. C. Slater, W. N. Thurmes, N. A. Clark, M. A. Handshy and F. Supon, *J. Am. Chem. Soc.*, 1986, **108**, 5210.
- 35 J. W. Goodby, *Mol. Cryst. Liq. Cryst.*, 1997, **292**, 99.
- 36 J. W. Goodby, *Journal of The Korean Physical Society*, 1998, **32**, S1052.
- 37 P. Gane, A. J. Leadbetter and P. G. Wrighton, *Mol. Cryst. Liq. Cryst.*, 1981, **66**, 247.
- 38 J. W. Goodby and G. W. Gray, *J. Phys. (Paris)*, 1979, **40**, 247.
- 39 A Leadbetter, J.P. Goughan, B. A. Kelly, G. W. Gray and J. W. Goodby, *J. Phys. (Paris) Lett.*, 1980, **40**, 178.
- 40 U. Finkenzeller, *Kontakte (Darmstadt)*, 1988, (2), 7.
- 41 B. S Scheuble, *Kontakte (Darmstadt)*, 1989, (1), 34.
- 42 R. B. Meyer, L. Liebert, L. Strzele and P. Keller, *J. Phys. Lett.*, 1975, **36**, L69.
- 43 R. B. Meyer, *Mol. Cryst. Liq. Cryst.*, 1977, **40**, 33.
- 44 C. Escher, *Kontakte (Darmstadt)*, 1986 (2), 3.
- 45 H. B. Brand, P. E. Cladis and P. L. Finn, *Phys. Rev.,A.*, 1985, **36**, 373.
- 46 N. A. Clark and S. T. Lagerwall, *Appl. Phys. Lett.*, 1980, **36**, 899.

- 47 U Finkenzeller, A. E. Pausch, E. Poetsch and J. Suermann, *Kontakte (Darmstadt)*, 1993 (2), 3.
- 48 *Handbook of Liquid Crystals* (Vol 2A, Low molecular weight liquid crystals I) Eds. D. Demus, J. W. Goodby, G. W. Gray, H.-W. Speiss and V. Vill, Wiley-VCH, Weinheim, 1998.
- 49 P. J. Collins and M. Hird, *Introduction to Liquid Crystals*, Taylor and Francis, Glasgow and London, 1997.
- 50 M. Born, *Optik*, Springer Verlag, Berlin-Heidelberg-New York, 1972.
- 51 J. W. Goodby and E. Chin, *J. Am. Chem. Soc.*, 1986, **108**, 4736.
- 52 M. A. Handsby and N. A. Clark, *Appl. Phys. Lett.*, 1982, **41**, 39.
- 53 J. C. Jones, M. J. Towler and J. R. Hughes, *Displays*, 1993, **14**, 87.
- 54 K. Kondo, H. Takezoe, A. Fukuda, E. Kuze, K. Flatischler and K. Sharp, *Jap. J. Appl. Phys.*, 1983, **22**, 294.
- 55 J. P Lepasent., J. N. Perbet, B. Mourey, M. Hareng, G. Decoberg and J. C. Dubois, *Mol. Cryst. Liq. Cryst.*, 1985, **129**, 161.
- 56 J. C. Jones, M. J. Towler and E. P. Raynes, *Ferroelectrics*, 1991, **121**, 91.
- 57 M. Glendenning, *Ph D Thesis*, University of Hull, 1998, England.
- 58 D. M. Walba, D. J. Dyer, X. H. Chen, U. Muller, P. Cobben, R. Shao and N. A. Clark, *Mol. Cryst. Liq. Cryst.*, 1996, **228**, 83.
- 59 D. Coates, *Thermotropic Liquid Crystals*, Ed. G. W. Gray, J. Wiley & Sons 1987, p 99.
- 60 J. W. Goodby, Proc. 17th ILCC, Strasbourg, France, 1998.
- 61 L. K. M. Chan, G. W. Gray, D. Lacey, R. M. Scrowston, I. G. Shenouda and K. J. Toyne, *Mol. Cryst. Liq. Cryst.*, 1989, **172**, 125.
- 62 D. Demus and H. Zasche, *Mol. Cryst. Liq. Cryst.*, 1981, **63**, 129.
- 63 D. Demus, B Krucke, F. Kushel, H. U. Nothnick, G. Pelze and H. Zasche, *Mol. Cryst. Liq. Cryst. Lett.*, 1979, **56**, 115.
- 64 M. E. Neubert and L. T. Carlino, *Mol. Cryst. Liq. Cryst.*, 1980, **59**, 253.
- 65 G. W. Gray and S. M. Kelly, *Mol. Cryst. Liq. Cryst.*, 1981, **75**, 95.
- 66 I. Nishiyama and J. W. Goodby, *J. Mater. Chem.*, 1992, **2**, 1015.
- 67 R. Hopf, B. S. Scheuble, R. Hittich, J. Krause, V. Reiffenrath and E. Poetsch, patent No WO 86/06401.

- 68 L. K. Chan, G. W. Gray, D. Lacey and K. J. Toyne, *Mol. Cryst. Liq. Cryst.*, 1988, **158**, 209.
- 69 G. W. Gray, M. Hird, D. Lacey and K. J. Toyne, *Mol. Cryst. Liq. Cryst.*, 1989, **172**, 165.
- 70 G. W. Gray, M. Hird and K. J. Toyne, *Mol. Cryst. Liq. Cryst.*, 1991, **204**, 43.
- 71 M. Hird and K. J. Toyne, *Liquid Crystals*, 1994, **16**, 625.
- 72 G. W. Gray, M. Hird, D. Lacey and K. J. Toyne, *J. Chem. Soc. Perkin Trans II*, 1989, 2041.
- 73 C. C. Dong, M. Hird, J. W. Goodby, P. Styring and K. J. Toyne, *Ferroelectrics*, 1996, **180**, 245.
- 74 M. Hird, K. J. Toyne, G. W. Gray, D. G. McDonnell and I. Sage, *Liquid Crystals*, 1995, **18**, 1.
- 75 S. M Kelly, *Liquid Crystals*, 1996, **20**, 493.
- 76 M. J. Goulding and S. Greenfield, *Liquid Crystals*, 1993, **13**, 345.
- 77 D. Coates, *Liquid Crystals*, 1987, **2**, 63.
- 78 D. Coates, *Liquid Crystals*, 1987, **2**, 423.
- 79 G. W Gray, *The Molecular Physics of Liquid Crystals* (Academic Press) 1979.
- 80 S. Kazuyuki, K. Takatoh and M. Sakamoto, *Liquid Crystals*, 1993, **13**, 283.
- 81 J. Newton, H. Coles and H. Owen, *Ferroelectrics*, 1993, **148**, 379.
- 82 J. Newton, H. Coles and H. Owen, *Liquid Crystals*, 1993, **15**, 5, 739.
- 83 M. Ibn-Elhaj, H. J. Coles, D. Guillon and A. Skoulios, *J. Phys. II France*, 1993, **3**, 1807.

The authors are indebted to the National Science Foundation for the support of this work. The authors also wish to thank the following individuals for their assistance in the preparation of the manuscript: J. H. ...

The authors are indebted to the National Science Foundation for the support of this work. The authors also wish to thank the following individuals for their assistance in the preparation of the manuscript: J. H. ...

Experimental

Section 2

The authors are indebted to the National Science Foundation for the support of this work. The authors also wish to thank the following individuals for their assistance in the preparation of the manuscript: J. H. ...

The authors are indebted to the National Science Foundation for the support of this work. The authors also wish to thank the following individuals for their assistance in the preparation of the manuscript: J. H. ...

The authors are indebted to the National Science Foundation for the support of this work. The authors also wish to thank the following individuals for their assistance in the preparation of the manuscript: J. H. ...

The authors are indebted to the National Science Foundation for the support of this work. The authors also wish to thank the following individuals for their assistance in the preparation of the manuscript: J. H. ...

The authors are indebted to the National Science Foundation for the support of this work. The authors also wish to thank the following individuals for their assistance in the preparation of the manuscript: J. H. ...

2.1 Techniques, methods of analysis and general procedures

A number of techniques have been used for the synthesis and characterisation of the materials reported in this thesis and descriptions of these procedures and specifications are given below.

2.1.1 Purification and purity of materials

Since impurities in liquid crystal materials can drastically influence their mesomorphic properties, the compounds were synthesised from starting materials, which were as pure as possible. Unreacted material was frequently detected by thin layer chromatography and GC and subsequently removed by column chromatography on silica gel or by recrystallisation (see below).

2.1.2 Purification and drying techniques of starting materials and solvents

Unless stated otherwise in the text, starting materials were obtained from Aldrich, Avocado, Fluka or Lancaster Synthesis. The starting materials were used without further purification. All solvents were used as bought unless stated below.

- (i) Dry tetrahydrofuran (THF) was obtained by distillation over sodium metal under a dry nitrogen atmosphere using benzophenone as an indicator to detect the absence of moisture.
- (ii) Dry dichloromethane (DCM) was obtained by distillation from calcium hydride under a dry nitrogen atmosphere.
- (iii) Diethyl ether was dried over sodium wire.
- (iv) Tetrakis(triphenylphosphine)palladium(0) was synthesised as described by Coulson¹.

All apparatus used for air sensitive reactions or reagents was dried in an oven (250 °C), assembled whilst hot and allowed to cool whilst being purged with a constant stream of dry nitrogen before use.

2.1.3 Purity of the compounds

2.1.3.1 High Performance Liquid Chromatography

The purity of all final compound was checked by GC, thin layer chromatography and normal and reversed phase high performance liquid chromatography (HPLC) using Merck Microsorb C18 or Si columns and acetonitrile (May and Chromonorm) as mobile phase. The purity of all intermediates was found to be greater than 98% unless stated otherwise, and the purity of final compounds was found to be greater than 99%.

2.1.3.2 Thin Layer Chromatography (TLC)

The plates used were aluminium backed TLC plates coated with silica gel, [Kieselgel 60 F254], supplied by Merck (Darmstadt). If the products contained conjugated regions they were viewed using an ultraviolet lamp ($\lambda = 254$ and 365 nm). In other situations, the plates were stained with iodine.

2.1.3.3 Gas Liquid Chromatography (GLC)

GC analyses were performed using a Chrompack 9001 capillary gas chromatograph equipped with a WCOT fused silica column (CP-Sil 5 CB $0.12 \mu\text{m}$, 10 m long \times 0.25 mm internal diameter), using nitrogen as the carrier gas. The purity of all intermediates was checked by gas chromatography (GC) [Chrompack 9001 capillary gas chromatograph equipped with a WCOT fused silica (CP-Sil 5 CB $0.12 \mu\text{m}$, 10 m long \times 0.25 mm internal diameter).

2.1.4 Purification of products

The purification of the synthesised products was carried out by either column chromatography, distillation and recrystallisation or a combination of these techniques as described below.

Column Chromatography:

Gravity column chromatography was carried out using Kieselgel 60 (230-400 mesh) silica gel obtained from Merck (Darmstadt); the eluents were as detailed in the experimental procedure.

Distillation

Many distillations were carried out using a standard distillation process and the temperatures and pressures are as quoted in the text. However, where approximate boiling points are quoted the materials were purified by Kugelrohr distillation, using a Büchi GKR-51 apparatus.

Percentage yields

All percentage yields quoted are after recrystallisation.

2.1.5 Structural Analysis

Confirmation of the structures of intermediates and products was obtained by the following techniques.

2.1.5.1 ^1H Nuclear Magnetic Resonance Spectroscopy (^1H NMR)

The structures of all compounds were confirmed by ^1H NMR spectroscopy using a JEOL Lambda 400 (400 MHz) or a JEOL JNM-GX270 (270 MHz) spectrometer as stated in the experimental procedure. Tetramethylsilane (TMS) was used as the internal standard for all samples and deuteriated chloroform (CDCl_3) as the solvent for all samples.

The value, J , for the coupling constants were found to be 6.5-8.5 Hz in the aromatic region, and are not reported in this work.

2.1.5.2 Infrared (IR) Spectroscopy

IR spectroscopy was carried out using either a Perkin-Elmer 783 spectrophotometer or a Perkin-Elmer 1000 Fourier transform (FT-IR) spectrophotometer.

2.1.5.3 Mass Spectrometry (MS)

The mass spectra of all compounds were obtained using a Finnigan-MAT 1020 GC/MS spectrometer.

2.1.5.4 Optical Rotation

The optical activity of certain products was carried out using an Optical Activity Ltd. AA-10 automatic polarimeter.

2.1.6 Characterisation of Final Products

2.1.6.1 Optical Microscopy

All phase transitions were observed using an Olympus BH2 polarising microscope in conjunction with a Mettler FP52 heating stage and FP5 control unit.

2.1.6.2 Differential Scanning Calorimetry (DSC)

DSC analyses were carried out on all the liquid crystalline materials using a Perkin-Elmer 7 Series / Unix DSC with a gold pan-indium standard (melting point onset 156.547 °C, enthalpy ΔH (28.392 J g⁻¹).

2.1.7 Nomenclature and Abbreviations

Throughout this thesis the IUPAC system of nomenclature has been used as a guide.

The meanings of the abbreviations used are listed below:

mp	=	melting point
bp	=	boiling point
Cr	=	crystal
I	=	isotropic liquid
N	=	nematic
SmA	=	smectic A
SmC	=	smectic C
SmC _{alt}	=	smectic C alt
N*	=	chiral nematic
SmA*	=	chiral smectic A

¹H NMR nomenclature

br = broad

s = singlet

d = doublet

t = triplet

q = quartet

m = multiplet

Solvent and catalystsCDCl₃ = deuterated chloroform

DEAD = diethyl azodicarboxylate

DCM = dichloromethane

DME = 1,2-dimethoxyethane

DMSO = dimethylsulphoxide

THF = tetrahydrofuran

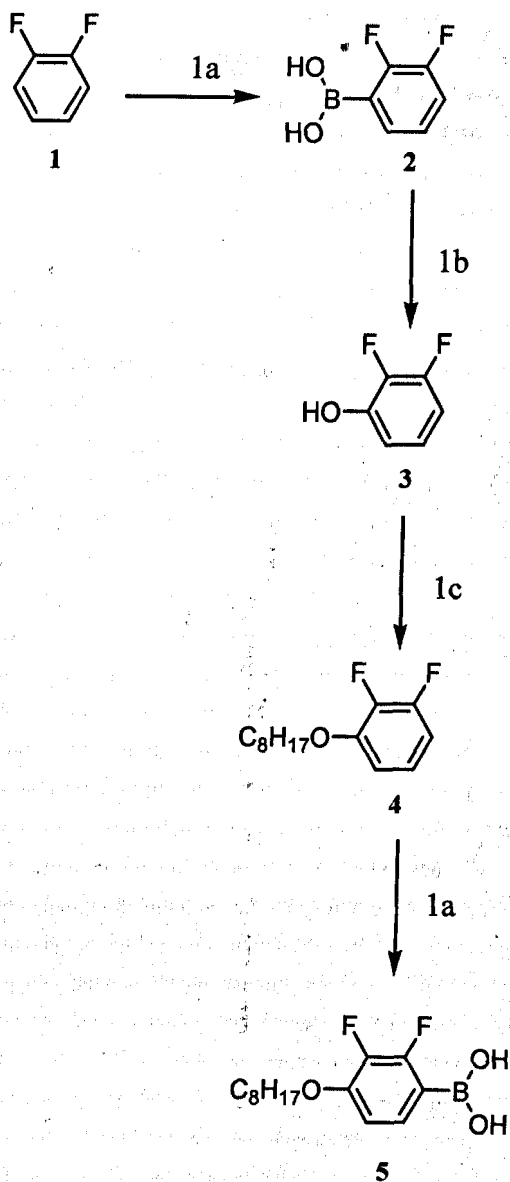
TBAB = *tert*-butylammonium bromideTBME = *tert*-butyl methyl ether

Terphenyl: for ease terphenyl stands for [1,1':4',1''] terphenyls unless stated otherwise.

2.1.8 Source of materials

The list of starting materials supplied by Avocado, Aldrich, Lancaster or Fluka are given below.

Difluorobenzene (1), 2-methoxyethanol (9), di(ethylene glycol) methyl ether (10), tri(ethylene glycol) methyl vinyl ether (11), 4-bromo-4'-hydroxybiphenyl (12), 2-butoxyethanol (22), di(ethylene glycol) butyl ether (23), hexan-1,6-diol (28), 4-chlorobutan-1-ol (36), 5-chloropentan-1-ol (37), 6-chlorohexan-1-ol (38), triethylchlorosilane (60), 3,7-dimethyloctan-1-ol (65), octan-1-ol (68), 3,7,7-trimethylhexanoylchloride (124), 4-bromobiphenyl (125), chloromethyl ethyl ether (141), ethyl (*S*)-(-)-lactate (143).



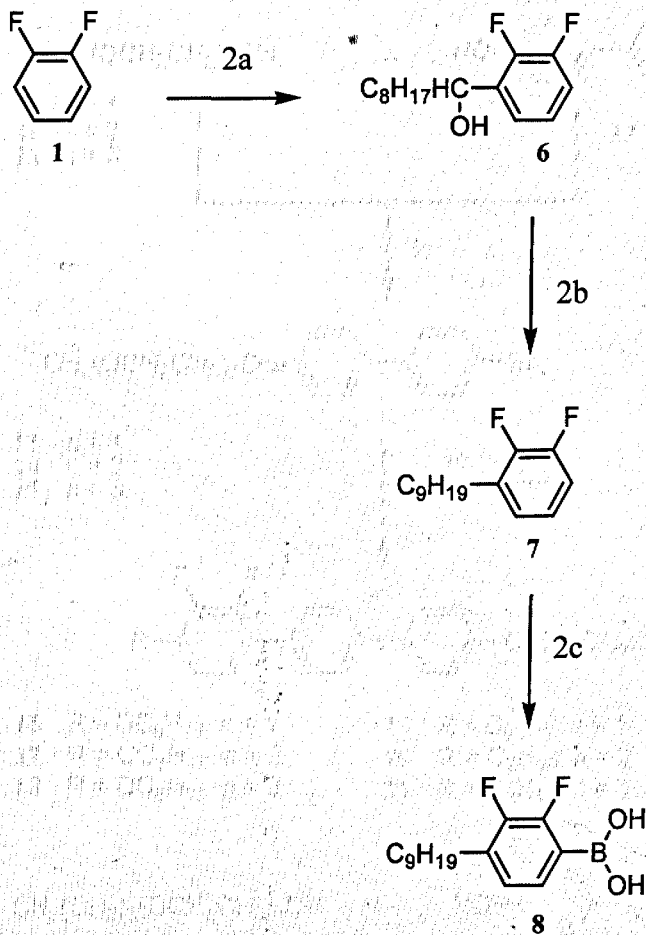
Reagents

1a...BuLi, $-78\text{ }^{\circ}\text{C}$, THF; $\text{B}(\text{OMe})_3$; aq HCl

1b... H_2O_2

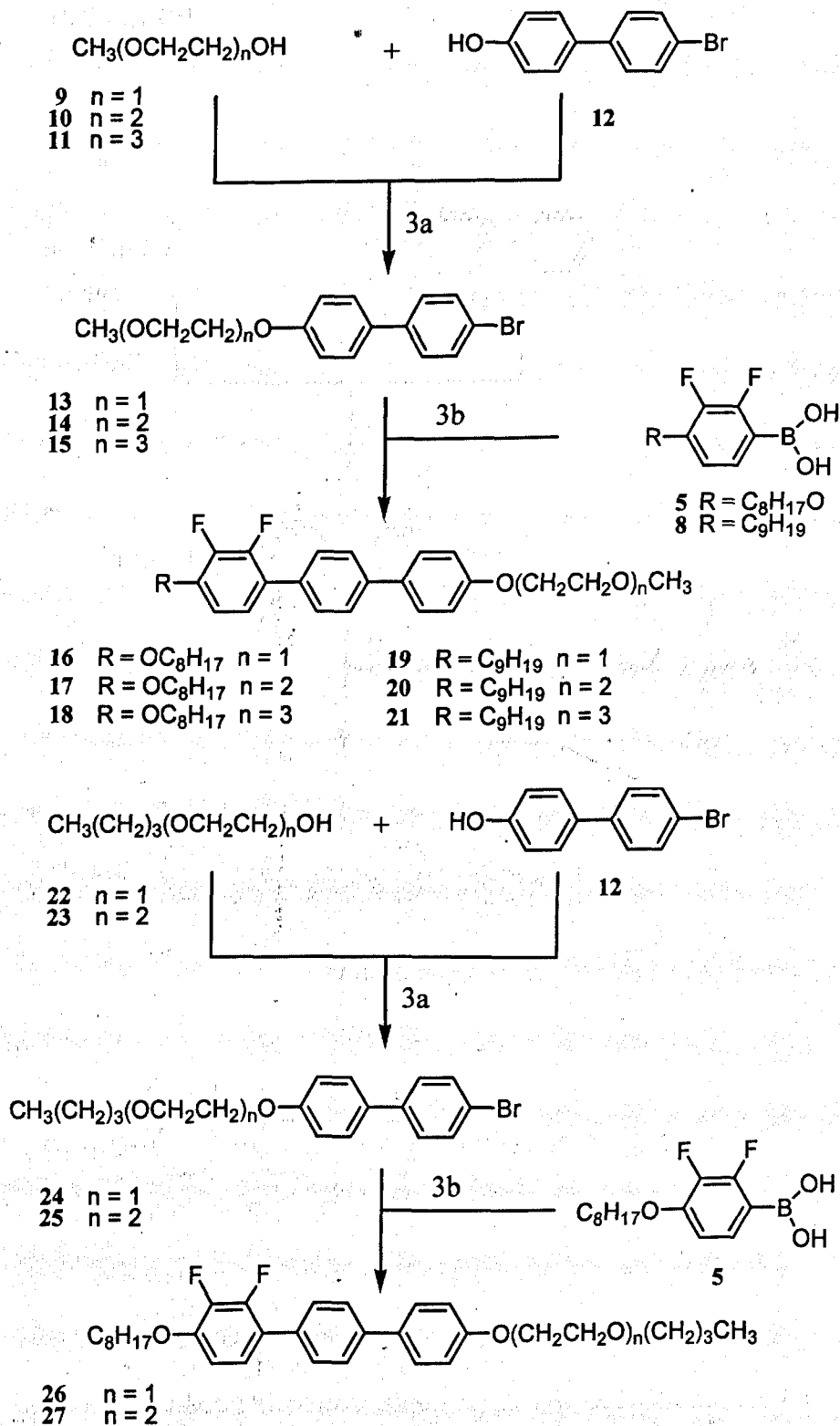
1c...1-bromooctane, K_2CO_3 , butanone

Scheme 1

**Reagents**

2a...BuLi, - 78 °C THF; nonanal

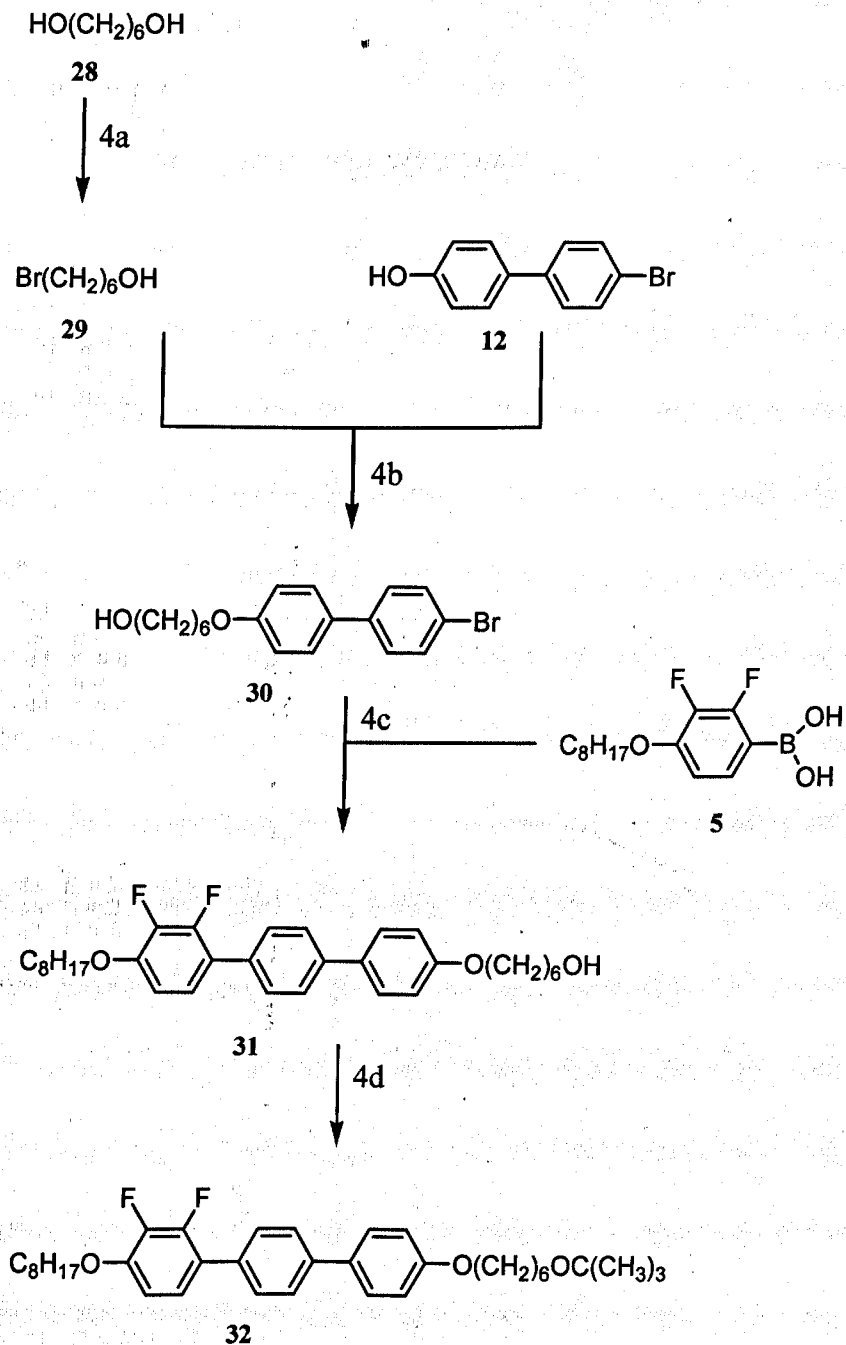
2b...P₂O₅, H₂/Pd2c...BuLi, - 78 °C THF; B(OMe)₃; aq HCl**Scheme 2**



Reagents

3a...PPh₃, DEAD, THF3b...DME, Pd(PPh₃)₄, 2M Na₂CO₃

Scheme 3



Reagents

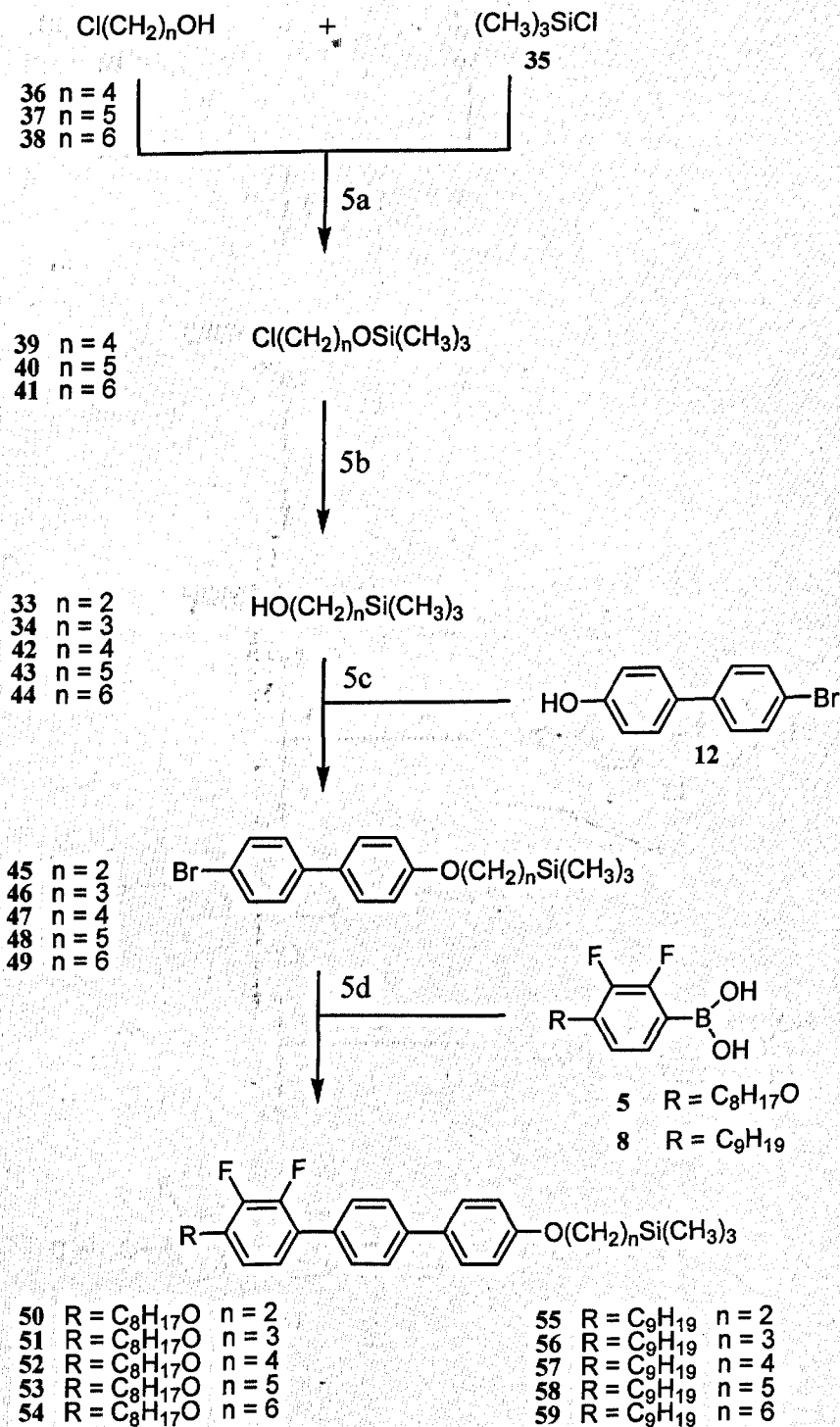
4a...HBr, benzene

4b...K₂CO₃, butanone

4c...DME, Pd(PPh₃)₄, 2M Na₂CO₃

4d...*t*-butyl trichloroacetimidate, BF₃.Et₂O, DCM/hexane 1:1

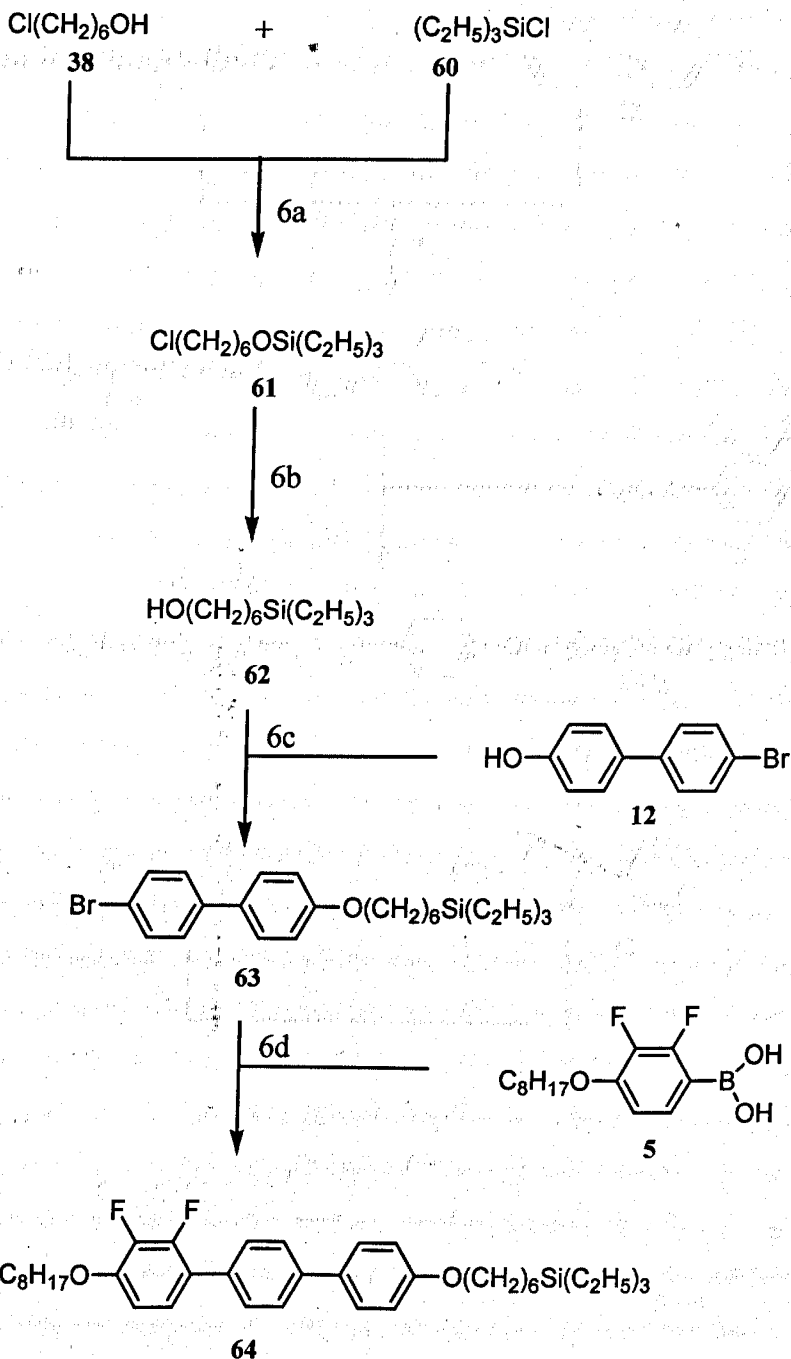
Scheme 4



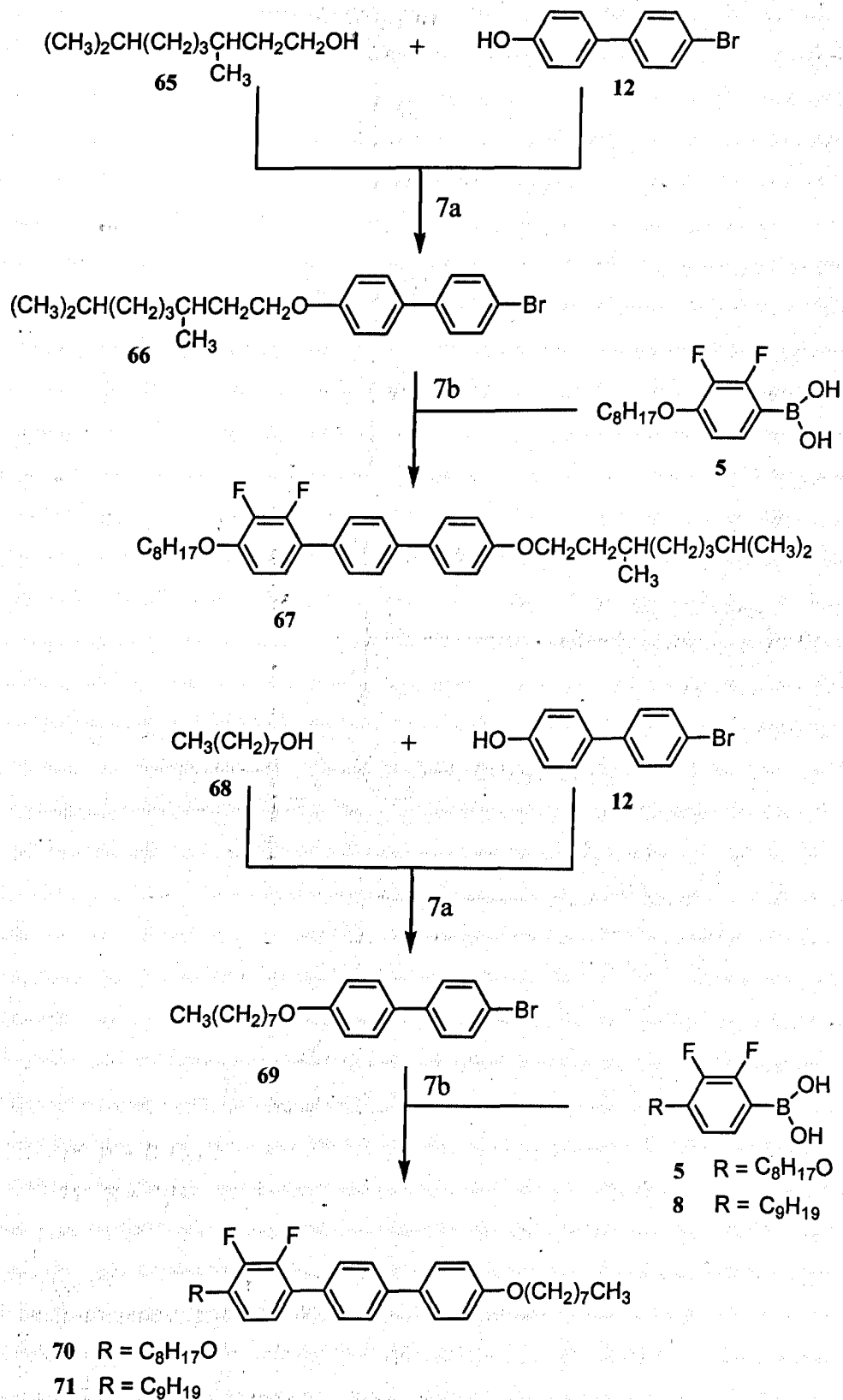
Reagents

5a...NH₃, benzene5b...Li, Et₂O, THF5c...PPh₃, DEAD, THF5d...DME, Pd(PPh₃)₄, 2M Na₂CO₃

Scheme 5



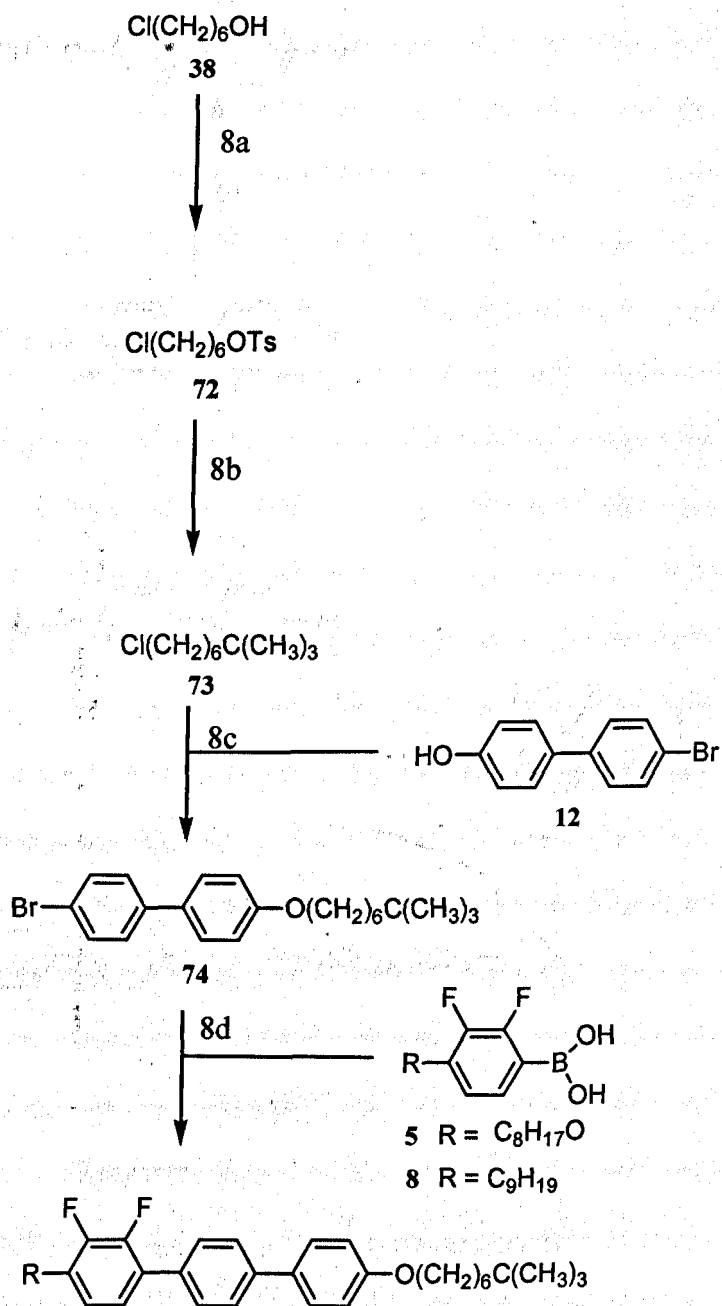
Scheme 6



Reagents

7a... PPh_3 , DEAD, THF7b...DME, $\text{Pd}(\text{PPh}_3)_4$, 2M Na_2CO_3

Scheme 7



Reagents

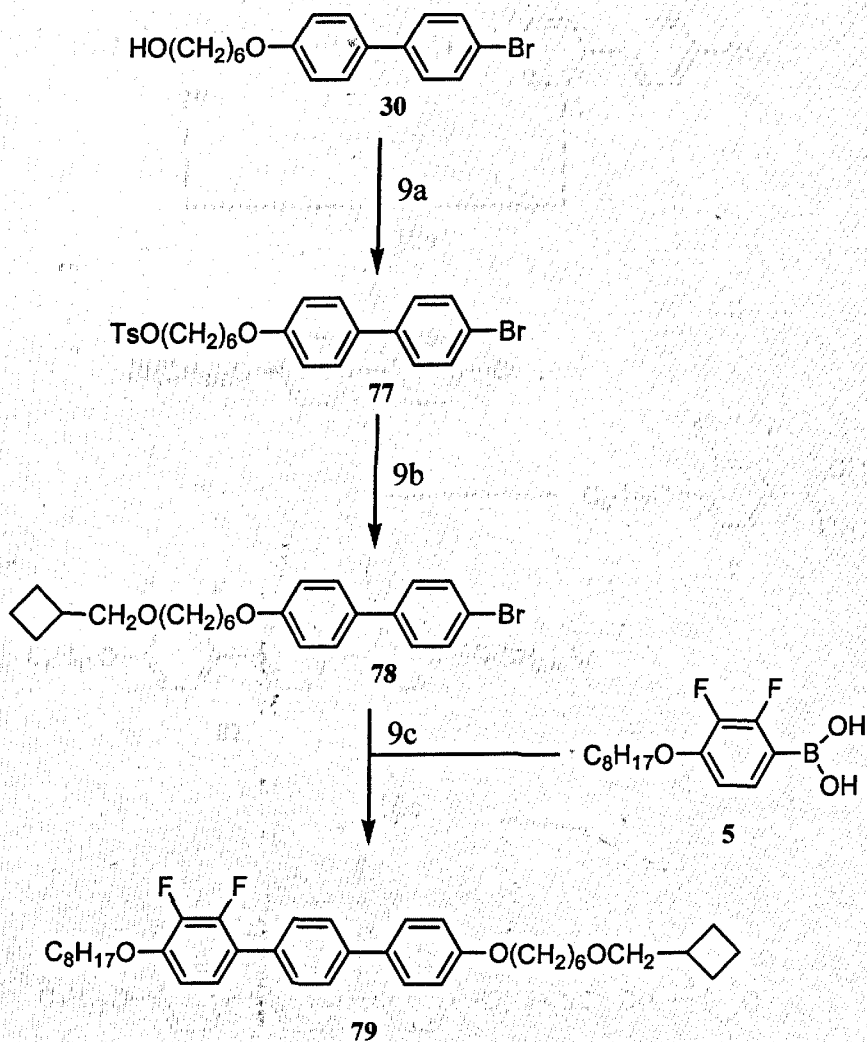
8a...*p*-toluenesulphonyl chloride, DCM, pyridine

8b...*t*-butylmagnesium chloride, LiBr, CuCl₂, lithium thiophenolate

8c...K₂CO₃, butanone

8d...DME, Pd(PPh₃)₄, 2M Na₂CO₃

Scheme 8



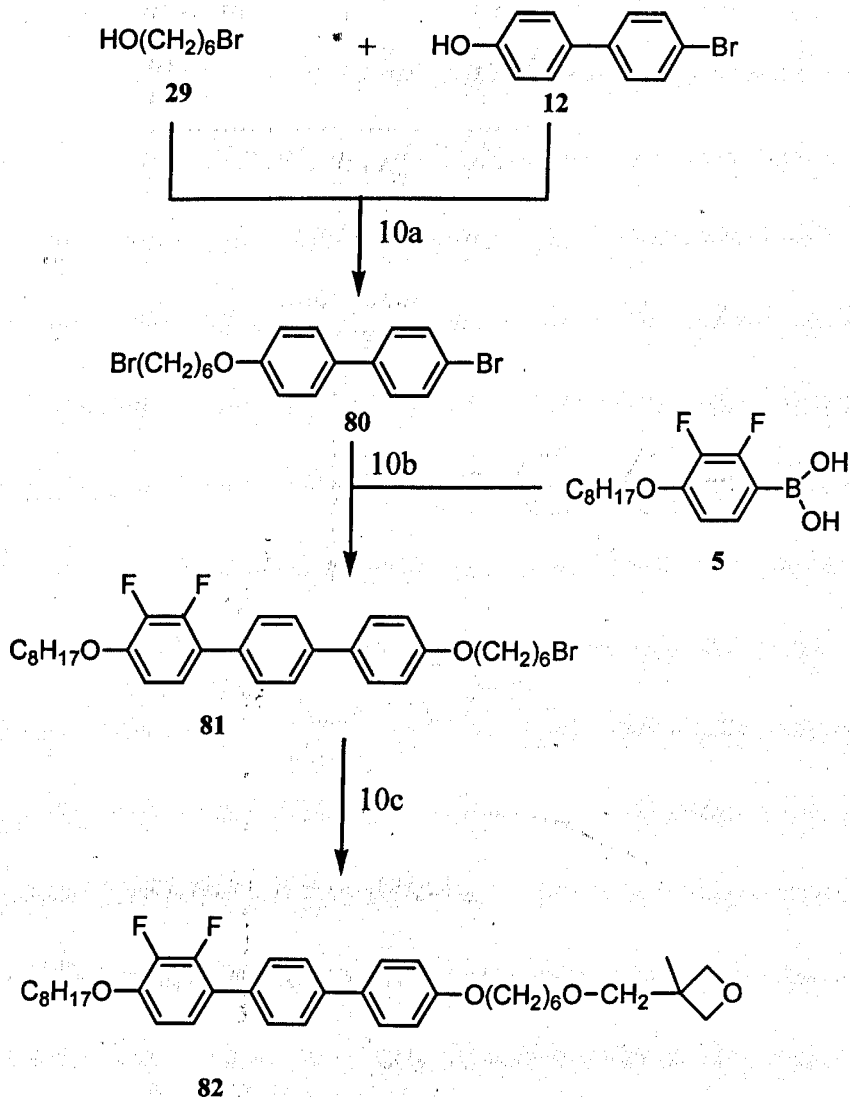
Reagents

9a...*p*-toluenesulphonyl chloride, DCM, pyridine

9b...cyclobutylmethanol, DMSO, KOH

9c...DME, Pd(PPh₃)₄, 2M Na₂CO₃

Scheme 9



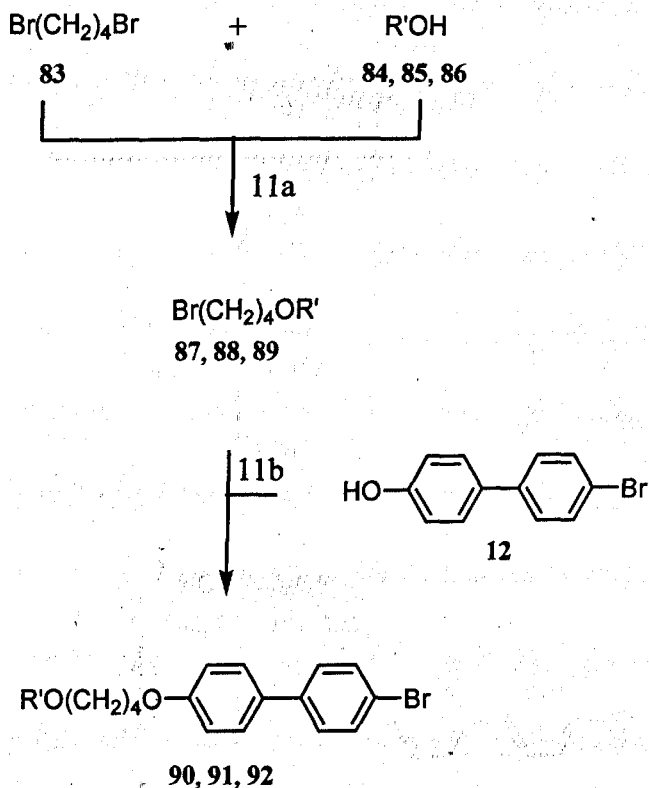
Reagents

10a...PPh₃, DEAD, THF

10b...DME, Pd(PPh₃)₄, 2M Na₂CO₃

10c...3-(hydroxymethyl)-3-methyloxetane,
hexane-50% aq NaOH (1:1), TBAB

Scheme 10



84, 87, 90 $\text{R}' = \text{CH}_2\text{CH}_2\text{CH}_3$

85, 88, 91 $\text{R}' = \begin{matrix} \text{CH}_3 \\ | \\ \text{CHCH} \\ | \quad | \\ \text{CH}_3 \quad \text{CH}_3 \end{matrix}$

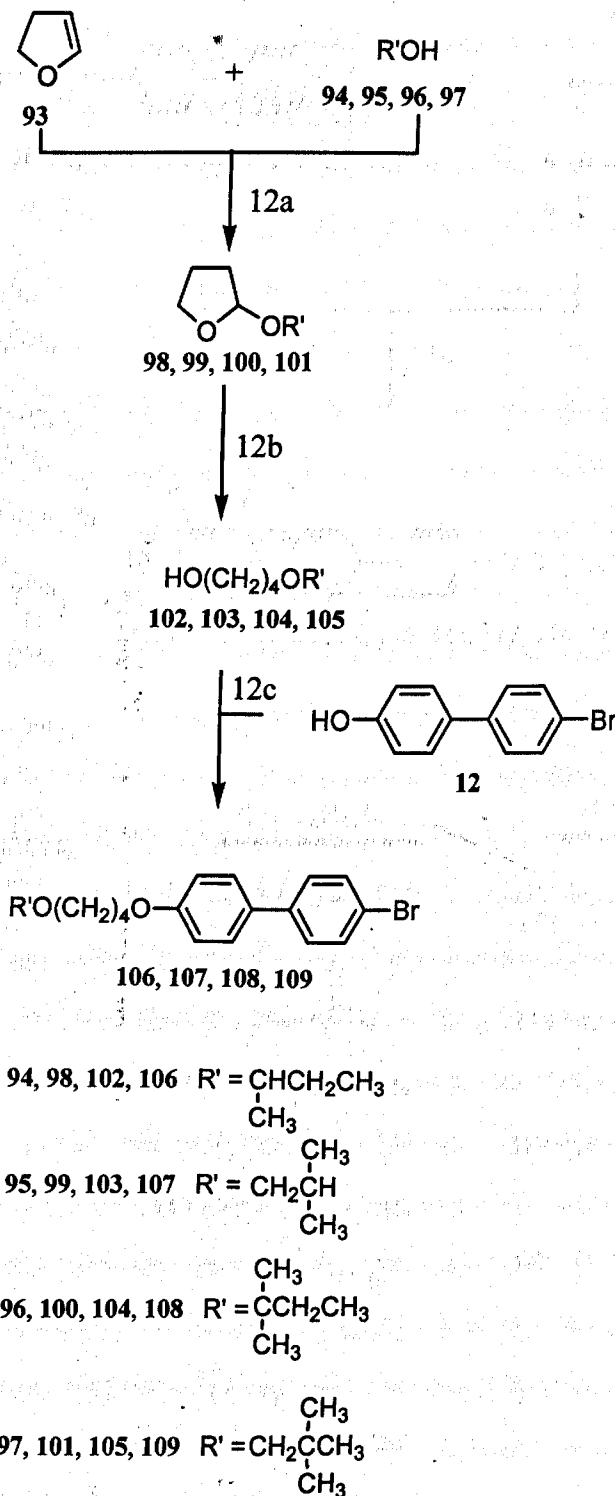
86, 89, 92 $\text{R}' = \begin{matrix} \text{CH}_3 \\ | \\ \text{CHC}-\text{CH}_3 \\ | \quad | \\ \text{CH}_3 \quad \text{CH}_3 \end{matrix}$

Reagents

11a...TBAB, hexane, 50% aq NaOH

11b...K₂CO₃, butanone

Scheme 11



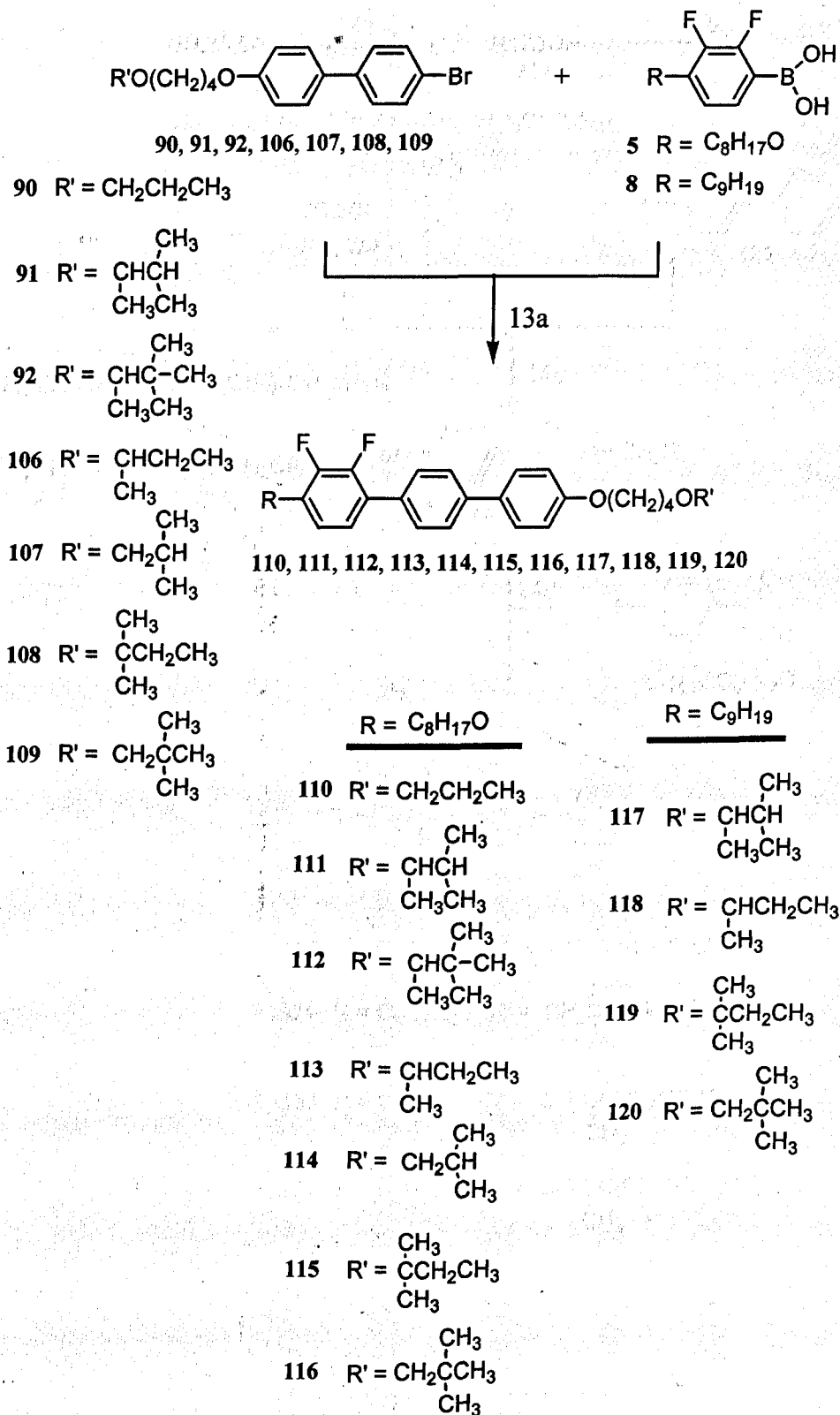
Reagents

12a...*p*-toluenesulphonic acid, THF

12b...AlCl₃, LiAlH₄, diethyl ether

12c...PPh₃, DEAD, THF

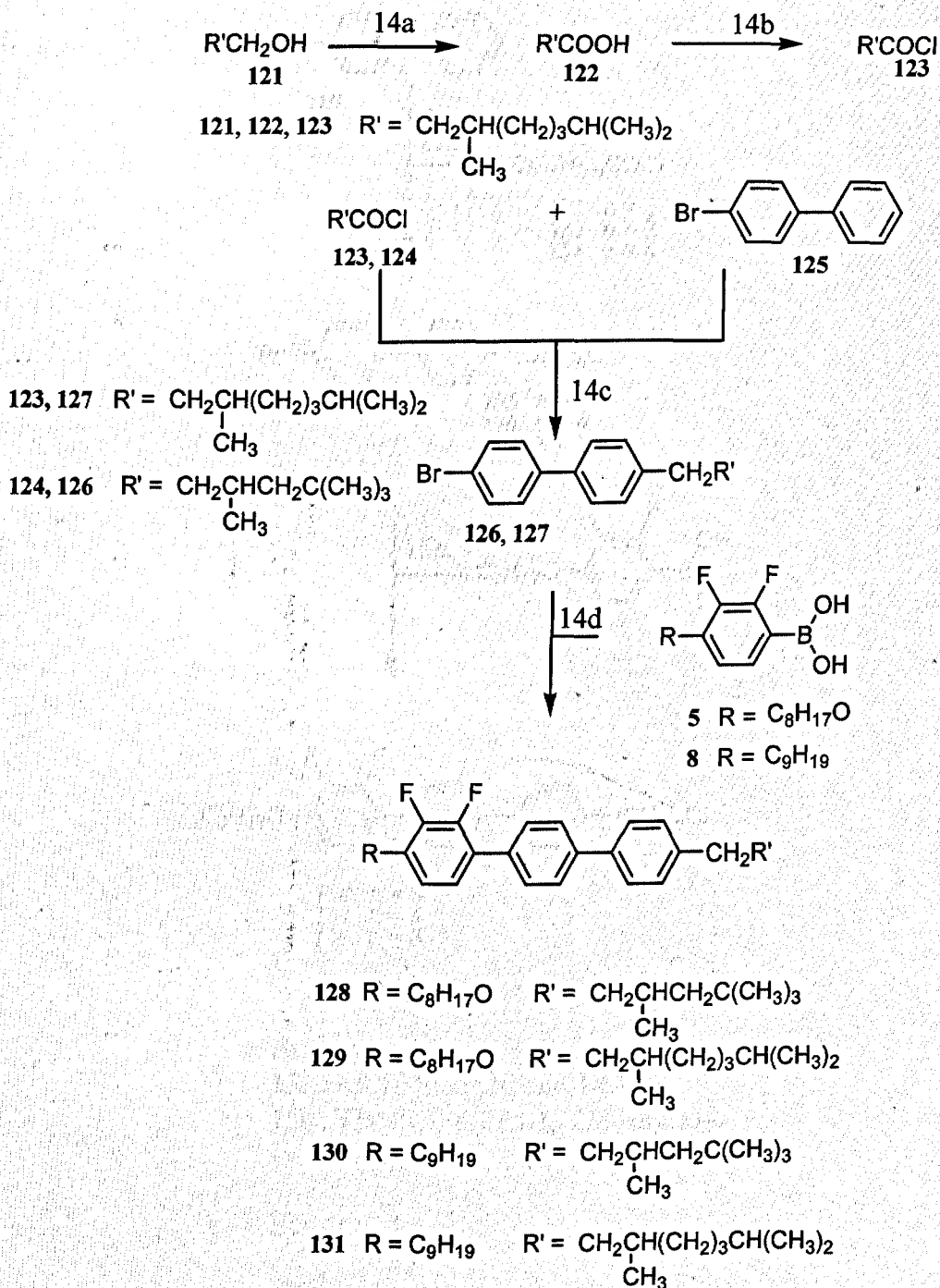
Scheme 12



Reagents

13a...TBME, Pd(PPh₃)₄, 2M Na₂CO₃

Scheme 13



Reagents

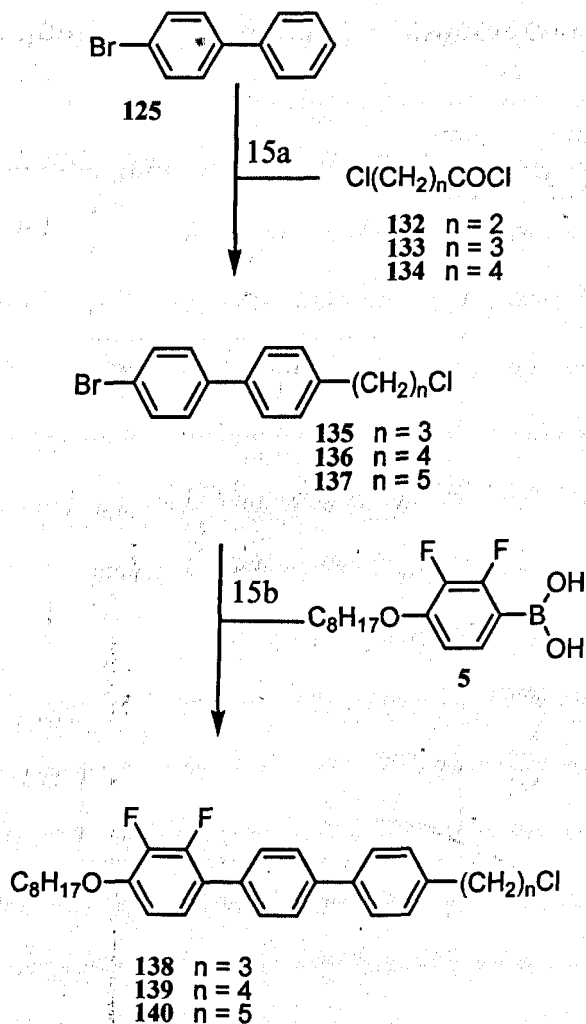
14a...CrO₃, H₂SO₄, acetone

14b...thionyl chloride

14c...AlCl₃, triethylsilane, DCM

14d...TBME, Pd(PPh₃)₄, 2M Na₂CO₃

Scheme 14

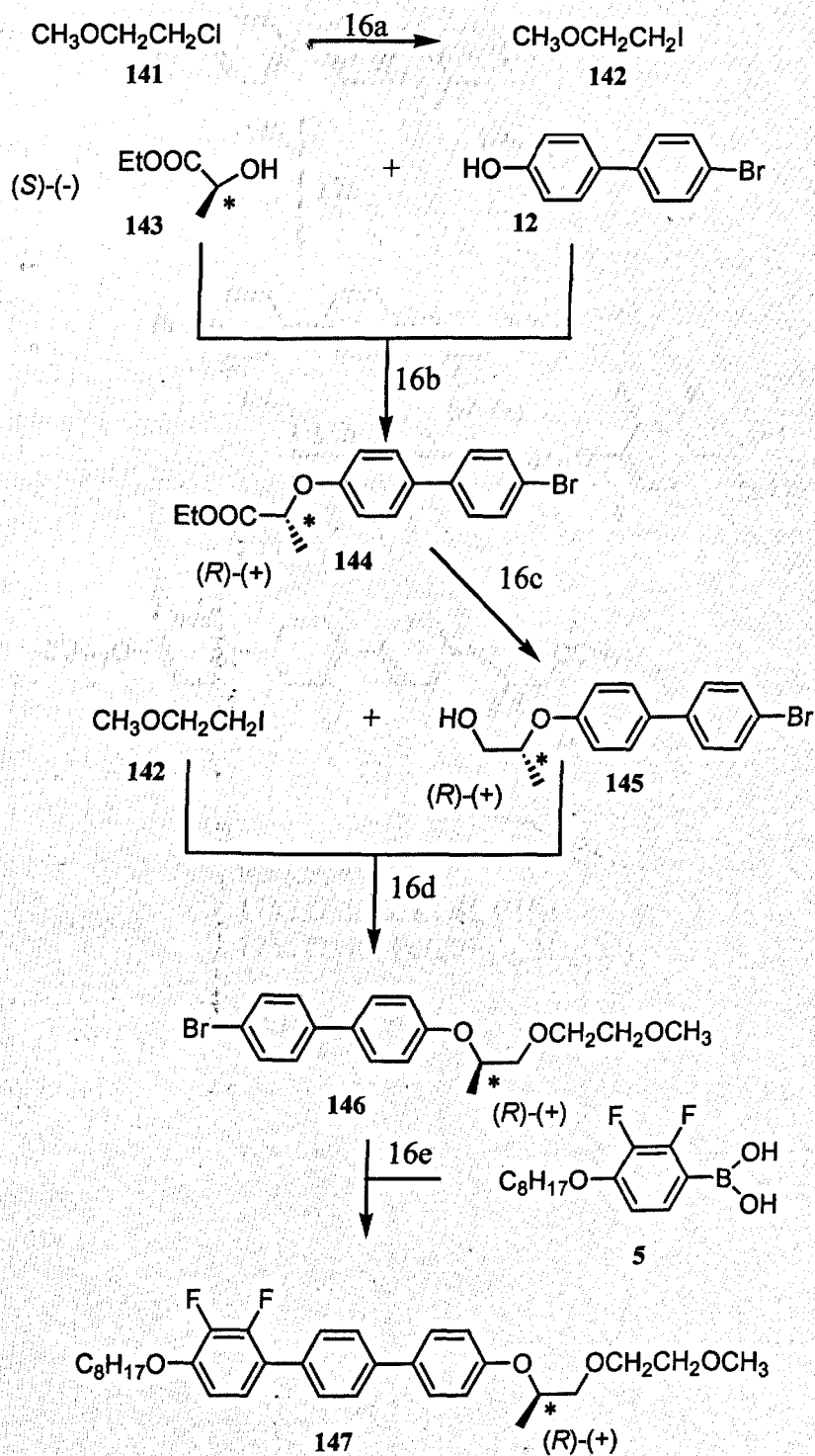


Reagents

15a... AlCl_3 , triethylsilane, DCM

15b...TBME, $\text{Pd}(\text{PPh}_3)_4$, $2\text{M Na}_2\text{CO}_3$

Scheme 15



Reagents

16a...NaI, acetone

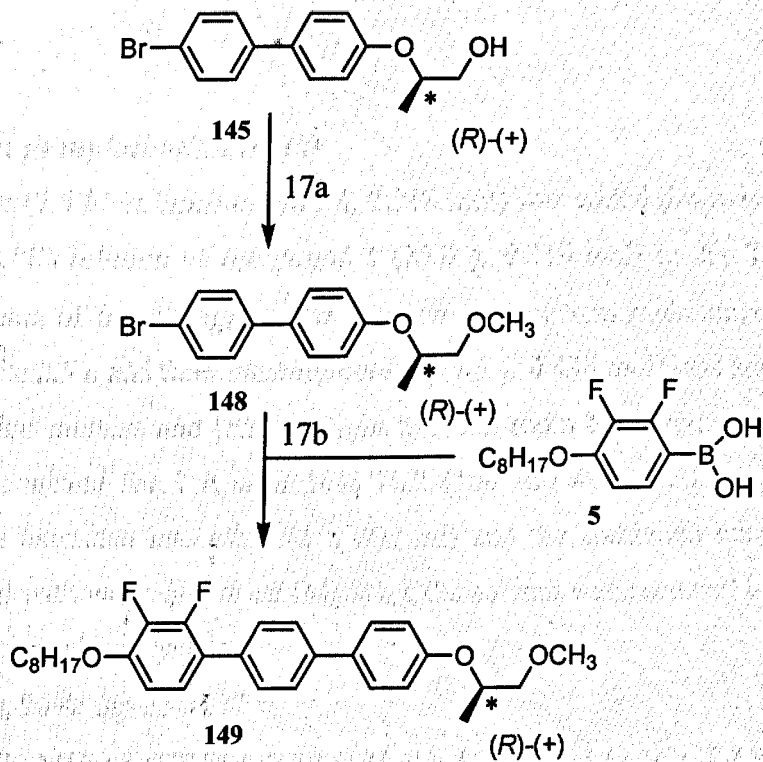
16b...PPh₃, DEAD, THF

16c...LiAlH₄, dry diethyl ether

16d...KOH, DMSO

16e...DME, Pd(PPh₃)₄, 2M Na₂CO₃

Scheme 16



Reagents

17a...DMSO, KOH, CH₃I

17b...DME, Pd(PPh₃)₄, Na₂CO₃

Scheme 17

Scheme 1

2,3-Difluorophenylboronic acid (2)

Butyllithium (2.5 M in hexanes, 88 ml, 0.219 mol) was added dropwise to a stirred, cooled (-78 °C) solution of compound 1 (25.0 g, 0.219 mol) in dry THF (400 ml) under a stream of dry nitrogen. The reaction mixture was maintained under these conditions for 2.5 h and then trimethylborate (45.5 g, 0.438 mol) was added dropwise to the reaction mixture and left overnight to reach room temperature. The reaction mixture was stirred for 1 h with 10% HCl (100 ml) at room temperature. The product was extracted into ether (2 x 200 ml) and the combined ethereal extracts were washed with water and dried (MgSO₄), the solvent was removed under reduced pressure to give white crystals.

Yield 31.1 g, 90%; mp 234-237 °C.

¹H NMR (270 MHz) δ (CDCl₃): 7.10 (1 H, dd, J 7.8), 7.15 (1 H, t, J 7.8), 7.50 (1 H, br s), 7.65 (1 H, t, J 7.8), one proton signal was not detected.

ν_{\max} (KCl): 3700-3000, 1625, 1470, 1360, 1270, 1045, 900 cm⁻¹.

m/z: 158 (M⁺), 140, 125, 114.

2,3-Difluorophenol (3)

10% Hydrogen peroxide (160 ml of 100 vol. in 240 ml in water) was added dropwise to a solution of compound 2 (31.1 g, 0.202 mol) in ether (100 ml) and heated under reflux overnight. The ether layer was separated and the aqueous layer was washed with ether (100 ml). The combined ethereal layers were washed with 10% sodium hydroxide solution and the separated aqueous layer was acidified with 36% HCl. The product was extracted into ether (2 x 200 ml), and the combined ethereal layers were washed with brine, water and dried (MgSO₄). The solvent was removed *in vacuo* to give a white solid.

Yield 25.4 g, 99%; mp 35-36 °C.

¹H NMR (270 MHz) δ (CDCl₃): 5.30 (1 H, s), 6.65-6.80 (2 H, m), 6.90 (1 H, dd, J 7.8).

ν_{\max} (KCl): 3700-3000, 1625, 1540, 1515, 1490, 1475, 1350, 1310, 1250, 1190, 1020 cm⁻¹.

m/z: 130 (M⁺), 110 and 101.

1,2-Difluoro-3-octyloxybenzene (4)

Potassium carbonate (33.2 g, 0.240 mol) was added to a solution of compound 3 (26.0 g, 0.200 mol) in butanone (200 ml). The mixture was left stirring at room temperature and a solution of 1-bromooctane (37.6 g, 0.019 mol) in butanone (50 ml) was added dropwise. The reaction mixture was heated under reflux for 44 h, filtered and the butanone was removed from the filtrate under reduced pressure. The product was extracted into ether (2 x 150 ml) and the combined ethereal extracts were washed successively with water, 5% sodium hydroxide, water, and dried (MgSO₄). The solvent was removed *in vacuo* and the residue was distilled under reduced pressure to give a colourless oil.

Yield 24.8 g, 53%; bp 164-166 °C at 18 mmHg.

¹H NMR (270 MHz) δ (CDCl₃): 0.85 (3 H, t, J 6.2), 1.15-1.35 (8 H, m), 1.45 (2 H, quintet, J 6.2), 1.80 (2 H, quintet, J 6.4), 4.00 (2 H, t, J 6.4), 6.75 (2 H, m), 6.95 (1 H, m).

ν_{\max} (KCl): 2950, 2880, 1635, 1525, 1490, 1480, 1325, 1300, 1265, 1090 cm⁻¹.

m/z: 242 (M⁺), 171, 156, 130.

2,3-Difluoro-4-octyloxyphenylboronic acid (5)

Quantities: compound 4 (24.0 g, 0.106 mol), butyllithium (2.5 M in hexanes 42.3 ml, 0.106 mol), trimethyl borate (21.9 g, 0.212 mol). The experimental procedure was as described for the preparation of compound 2.

Yield 30.2 g, 100%.

¹H NMR (270 MHz) δ (CDCl₃): 0.90 (3 H, t, J 5.9), 1.25-1.35 (8 H, m), 1.45 (2 H, quintet, J 5.9), 1.80 (2 H, quintet, J 6.2), 4.05 (2 H, t, J 6.3), 6.80 (1 H, m), 7.80 (1 H, m), the OH protons were not detected.

ν_{\max} (KCl): 3600-3100, 2980, 2940, 2880, 1635, 1530, 1475, 1365, 1310, 1225, 1090 cm⁻¹.

m/z: 286 (M⁺), 271, 258, 241(100%).

Scheme 2

(2,3-Difluorophenyl)nonan-1-ol (6)

Butyllithium (2.5 M in hexanes 52.5 ml, 0.131 mol) was added dropwise to a stirred, cooled (-78 °C) solution of compound 1 (12.0 g, 0.105 mol) in dry THF (400ml) under a stream of dry nitrogen. The reaction mixture was maintained under these conditions for 2.5 h and a solution of nonanal (14.9 g, 0.105 mol) in dry THF (50 ml) was added dropwise at - 78 °C. The mixture was allowed to slowly reach room temperature overnight. Ammonium chloride solution (2M, 200 ml) was added and the product was extracted into ether (2 x 150 ml), the combined ethereal extracts were washed with water and dried (MgSO₄). The solvent was removed *in vacuo* and the residue was distilled under reduced pressure to give a colourless oil.

Yield 19.5 g, 70%; bp 120-126 °C at 0.1 mmHg.

¹H NMR (270 MHz) δ (CDCl₃): 0.85 (3 H, t, J 5.7), 1.15-1.40 (12 H, m), 1.70-1.80 (2 H, m), 2.95 (1 H, s), 5.00 (1 H, t, J 6.2), 7.00- 7.10 (2 H, m), 7.12-7.20 (1 H, m).

ν_{\max} (KCl): 3600-3100, 2940, 2860, 1630, 1600, 1485, 1270, 1210, 1060, 820 cm⁻¹.

m/z: 256 (M⁺), 238, 216, 203.

1,2-Difluoro-3-nonylbenzene (7)

Phosphorous pentoxide (34.1 g, 0.240 mol) was added to a stirred solution of compound 6 (19.5 g, 0.095 mol) in pentane (150 ml). The mixture was stirred at room temperature overnight and the mixture was filtered. 5% Palladium-on-charcoal (1.85 g) was added to the filtrate and the stirred mixture was hydrogenated at room temperature overnight. The mixture was filtered and pentane was removed *in vacuo* and the product was distilled to give a colourless oil.

Yield 12.1 g, 65%; bp 150-156 °C at 15 mmHg .

¹H NMR (270 MHz) δ (CDCl₃): 0.90 (3 H, t, J 6.1), 1.50-1.65 (12 H, m), 1.68 (2 H, quintet, J 6.3), 1.72 (2 H, t, J 6.3), 6.91-7.01 (3 H, m).

ν_{\max} (KCl): 2980, 2960, 2860, 1630, 1600, 1490, 1285, 1210, 1040, 995, 825, 780, 730 cm⁻¹.

m/z: 240 (M⁺), 197, 182.

2,3-Difluoro-4-nonylphenylboronic acid (8)

Butyllithium (2.5 M in hexanes, 20.0 ml, 0.050 mol) was added dropwise to a stirred, cooled (-78 °C) solution of compound 7 (12.0 g, 0.050 mol) in dry THF (250 ml) under a stream of dry nitrogen. The reaction mixture was maintained under these conditions for 2.5 h and then trimethyl borate (10.4 g, 0.100 mol) was added dropwise and the reaction mixture was left overnight to reach room temperature.

The reaction mixture was stirred for 1 h with 10% HCl (100 ml) at room temperature. The product was extracted into ether (2 x 200 ml) and the combined ethereal extracts were washed with water and dried (MgSO₄); the solvent was removed under reduced pressure to give white crystals.

Yield 14.2 g, 95% (mp not recorded).

¹H NMR (270 MHz) δ (CDCl₃): 0.90 (3 H, t, J 5.7), 1.25-1.35 (12 H, m), 1.60 (2 H, m), 2.67 (2 H, t, J 6.3), 7.00-7.05 (1 H, m), 7.35-7.42 (1 H, m), the OH protons were not detected.

ν_{max} (KCl): 3600-3100, 2960, 2940, 2850, 1640, 1460, 1435, 1250, 1220, 1135, 670 cm⁻¹.

m/z: 267, 256, 213, 199, 184.

Scheme 3

4-Bromo-4'-(1,4-dioxapentyl)biphenyl (13)

Compound **12** (4.00 g, 0.016 mol) and compound **9** (1.22 g, 0.016 mol) were mixed in dry THF (75 ml) and left stirring at room temperature for 10 min; then a solution of triphenylphosphine (4.20 g, 0.016 mol) and DEAD (2.80 g, 0.0161 mol) in dry cold THF (60 ml) was added dropwise at room temperature over 10 min. The reaction mixture was left stirring overnight. The reaction product was extracted into ether (2 x 200 ml), and the combined ethereal solutions were washed with water and dried (MgSO₄). The crude product was adsorbed onto silica gel and purified by column chromatography [ethyl acetate-petroleum fraction (bp 40-60 °C), 1:5] to give white crystals.

Yield 2.95 g, 60%; mp 102-103 °C.

¹H NMR (270 MHz) δ (CDCl₃): 3.44 (3 H, s), 3.76-3.82 (2 H, m), 4.13-4.19 (2 H, m), 7.00 (2 H, d), 7.37-7.56 (3 x 2 H, d).

ν_{\max} (KCl): 2880, 1610, 1465, 1305, 1090, 840, 515 cm⁻¹.

m/z: 308/306 (M⁺), 250/248 (100%), 152, 139.

Compounds **14** and **15** were prepared following a similar procedure to that described for the preparation of compound **13**.

4-Bromo-4'-(1,4,7-trioxaoctyl)biphenyl (14)

Quantities: compound **10** (1.93 g, 0.016 mol), compound **12** (4.00 g, 0.016 mol) triphenylphosphine (4.19 g, 0.016 mol) and DEAD (2.80 g, 0.016 mol).

Yield 3.90 g, 66%; mp 91-92 °C (white powder).

¹H NMR (270 MHz) δ (CDCl₃): 3.44 (3 H, s), 3.62-3.70 (2 H, m), 3.70-3.78 (2 H, m), 3.80-3.86 (2 H, m), 4.20-4.27 (2 H, m), 7.04 (2 H, d), 7.40-7.59 (3 x 2 H, d).

ν_{\max} (KCl): 2880, 1605, 1460, 1305, 1080, 840, 500 cm⁻¹.

m/z: 352/350 (M⁺), 250/248, 152, 139, 59 (100%).

4-Bromo-4'-(1,4,7,10-tetraoxaundecyl)biphenyl (15)

Quantities: compound **11** (5.27 g, 0.032 mol), compound **12** (8.00 g, 0.032 mol) triphenylphosphine (8.44 g, 0.032 mol), and DEAD (5.60 g, 0.032 mol).

Yield 8.85 g 70%; mp 65-66 °C (white powder).

$^1\text{H NMR}$ (270 MHz) δ (CDCl_3): 3.48 (3 H, s), 3.62-3.69 (2 H, m), 3.72-3.90 (6 H, m), 3.95-4.20 (2 H, m), 4.24-4.31 (2 H, m), 7.08 (2 H, d), 7.47-7.66 (3 x 2 H, d).

ν_{max} (KCl) 2880, 1605, 1460, 1300, 1100, 805, 510 cm^{-1} .

m/z 396/394, 250/248, 152, 139, 103, 59 (100%).

2,3-Difluoro-4-octyloxy-4''-(1,4-dioxapentyl)terphenyl (16)

Compound **13** (1.23 g, 4.0 mmol), an aqueous 2M-solution of sodium carbonate (40 ml) and tetrakis(triphenylphosphine)palladium(0) (0.12 g, 0.12 mmol) were mixed in DME (60 ml) under dry nitrogen at room temperature and compound **5** (1.37 g, 4.8 mmol) was added. The stirred reaction mixture was heated overnight under reflux under dry nitrogen until g.l.c. and t.l.c. revealed a complete reaction. The product was extracted into DCM (2 x 150 ml) and washed with brine, water and dried (MgSO_4). The solvent was removed under reduced pressure and the residue was purified by column chromatography [diethyl ether-hexane, 3:1] and recrystallised from acetonitrile-hexane (1:1) to give white crystals.

Yield 1.0 g, 50%.

Transition temperatures ($^{\circ}\text{C}$): Cr 133.8 SmC 158.5 SmA 165.3 N 178.9 I.

$^1\text{H NMR}$ (270 MHz) δ (CDCl_3): 0.90 (3 H, t, J 5.2), 1.20-1.53 (10 H, m), 1.85 (2 H, quintet, J 5.9), 3.40 (3 H, s), 3.57-3.63 (2 H, m), 4.08 (2 H, t, J 6.3), 4.20 (2 H, t, 6.4), 6.76-6.84 (1 H, m), 7.00 (2 H, d), 7.08-7.18 (1 H, m), 7.52-7.58 (2 x 2 H, d), 7.62 (2 H, d).

ν_{max} (KCl): 2920, 1610, 1500, 1440, 1080, 800 cm^{-1} .

m/z : 468 (M^+), 356, 298 (100%), 468, 410.

Compounds **17**, **18**, **19**, **20** and **21** were prepared following a similar procedure to that described for the preparation of compound **16**.

2,3-Difluoro-4-octyloxy-4''-(1,4,7-trioxaoctyl)terphenyl (17)

Quantities: compound **14** (1.40 g, 4.0 mmol), tetrakis(triphenylphosphine)-palladium(0) (0.12 g, 0.12 mmol), and compound **5** (1.34 g, 4.7 mmol).

Yield 1.2 g, 60% (white crystals).

Transition temperatures ($^{\circ}\text{C}$): Cr 120.5 SmC 130.5 SmA 135.5 N 140.8 I.

$^1\text{H NMR}$ (270 MHz) δ (CDCl_3): 0.84-0.95 (3 H, m), 1.20-1.53 (10 H, m), 1.78-1.92 (2 H, m), 3.40 (3 H, s), 3.57-3.63 (2 H, m), 3.72-3.78 (2 H, m), 3.90 (2 H, t, J 6.4),

4.08 (2 H, t, J 6.4), 4.20 (2 H, t, J 6.4), 6.76-6.84 (1 H, m), 7.02 (2 H, d), 7.08-7.18 (1 H, m), 7.52-7.58 (2 x 2 H, d), 7.62 (2 H, d).

$\nu_{\max}(\text{KCl})$: 2920, 1610, 1500, 1440, 1080, 800 cm^{-1} .

m/z : 512 (M^+), 400, 298 (100%), 269.

2,3-Difluoro-4-octyloxy-4''-(1,4,7,10-tetraoxaundecyl)terphenyl (18)

Quantities: compound 15 (1.58 g, 4.0 mmol), tetrakis(triphenylphosphine)-palladium(0) (0.12 g, 0.12 mmol), and compound 5 (1.37 g, 4.8 mmol).

Yield 1.2 g, 58% (white powder).

Transition temperatures ($^{\circ}\text{C}$): Cr 106.0 SmC 117.5 SmA 121.8 N 126.5 I.

$^1\text{H NMR } \delta$ (CDCl_3): 0.84-0.95 (3 H, m), 1.19-1.55 (10 H, m), 1.78-1.92 (2 H, m), 3.40 (3 H, s), 3.52-3.59 (2 H, m), 3.64-3.72 (2 H, m), 3.73-3.80 (4 H, m), 3.90 (2 H, t, J 5.2), 4.08 (2 H, t, 5.8), 4.20 (2 H, t, J 5.9), 6.76-6.84 (1 H, m), 7.02 (2 H, d), 7.08-7.18 (1 H, m), 7.51-7.57 (2 x 2 H, d), 7.61 (2 H, d).

$\nu_{\max}(\text{KCl})$ 2920, 1610, 1500, 1440, 1080, 800 cm^{-1} .

m/z : 566 (M^+ , 100%), 297, 251, 147, 103.

2,3-Difluoro-4-nonyl-4''-(1,4-dioxapenty)terphenyl (19)

Quantities: compound 13 (1.23 g, 4.0 mmol), tetrakis(triphenylphosphine)-palladium(0) (0.12 g, 0.12 mmol), and compound 8 (1.37 g, 4.8 mmol).

Yield 0.96 g, 50% (white crystals).

Transition temperatures ($^{\circ}\text{C}$): Cr 101.3 SmC 125.5 SmA 154.9 N 158.5 I.

$^1\text{H NMR } \delta$ (CDCl_3): 0.84-0.93 (3 H, m), 1.20-1.43 (12 H, m), 1.58-1.70 (2 H, m), 2.65-2.73 (2 H, m), 3.45 (3 H, s), 3.75-3.82 (2 H, m), 4.14-4.22 (2 H, m), 6.96-7.05 (3 H, m), 7.11-7.18 (1 H, m), 7.53-7.68 (3 x 2 H, d).

$\nu_{\max}(\text{KCl})$: 2925, 1620, 1455, 1250, 1125, 825 cm^{-1} .

m/z : 466 (M^+ , 100%), 408, 295, 266.

2,3-Difluoro-4-nonyl-4''-(1,4,7-trioxaoctyl)terphenyl (20)

Quantities: compound 14 (1.40 g, 4.0 mmol), tetrakis(triphenylphosphine)-palladium(0) (0.12 g, 0.12 mmol), and compound 8 (1.37 g, 4.8 mmol).

Yield 1.04 g, 52% (white powder).

Transition temperatures ($^{\circ}\text{C}$): Cr 84.8 SmC 102.9 SmA 107.6 N 115.0 I.

$^1\text{H NMR } \delta$ (CDCl_3): 0.83-0.93 (3 H, m), 1.20-1.45 (12 H, m), 1.57-1.72 (2 H, m), 2.67 (2 H, t, J 5.6), 3.40 (3 H, s), 3.56-3.62 (2 H, m), 3.72-3.78 (2 H, m), 3.90 (2 H, t, J 5.9), 4.20 (2H, t, J 6.0), 6.95-7.05 (3 H, m), 7.11-7.18 (1 H, m), 7.52-7.68 (3 x 2 H, d).

$\nu_{\text{max}}(\text{KCl})$: 2920, 1605, 1430, 1252, 1110, 805 cm^{-1} .

m/z : 510 (M^+), 408, 295, 266.

2,3-Difluoro-4-nonyl-4''-(1,4,7,10-tetraoxaundecyl)terphenyl (21)

Quantities: compound **15** (1.58 g, 4.0 mmol), tetrakis(triphenylphosphine)palladium (0) (0.12 g, 0.12 mmol), and compound **8** (1.37 g, 4.8 mmol).

Yield 1.04 g, 50% (white crystals).

Transition temperatures ($^{\circ}\text{C}$): Cr 82.9 SmC 89.8 N 92.6 I.

$^1\text{H NMR } \delta$ (CDCl_3): 0.83-0.93 (3 H, m), 1.20-1.46 (12 H, m), 1.57-1.72 (2 H, m), 2.67 (2 H, t, J 5.8), 3.40 (3 H, s), 3.52-3.60 (2 H, m), 3.62-3.70 (6H, m), 3.88 (2 H, t, J 5.9), 4.19 (2 H, t, J 6.0), 6.95-7.05 (3 H, m), 7.09-7.19 (1 H, m), 7.53-7.68 (3 x 2 H, d).

$\nu_{\text{max}}(\text{KCl})$ 2925, 1605, 1465, 1252, 1100, 805 cm^{-1} .

m/z 554 (M^+ , 100%), 408, 295, 266.

Compounds **24**, and **25** were prepared following a similar procedure to that described for the preparation of compound **13**.

4-Bromo-4'-(1,4-dioxaoctyl)biphenyl (24)

Quantities: compound **22** (3.80 g, 0.032 mol), compound **12** (8.00 g, 0.032 mol) triphenylphosphine (8.44 g, 0.032 mol), and DEAD (5.60 g, 0.032 mol).

Yield 7.82 g, 70%; mp 104-105 $^{\circ}\text{C}$ (white powder).

$^1\text{H NMR}$ (270 MHz) δ (CDCl_3): 0.91-0.96 (3 H, m), 1.33-1.44 (2 H, m), 1.56-1.64 (2 H, m), 3.54 (2 H, t, J 6.2), 3.80 (2 H, t, J 6.4), 4.15 (2 H, t, J 6.0), 6.98 (2 H, d), 7.37-7.53 (3 x 2 H, d).

$\nu_{\text{max}}(\text{KCl})$: 2935, 1610, 1460, 1290, 1190, 820, 500 cm^{-1} .

m/z : 350/348 (M^+), 250/248 (100%), 139, 110.

4-Bromo-4'-(1,4,7-trioxaundecyl)biphenyl (25)

Quantities: compound **23** (5.20 g, 0.032 mol), compound **12** (8.00 g, 0.032 mol) triphenylphosphine (8.44 g, 0.032 mol), and DEAD (5.60 g, 0.032 mol).

Yield 8.17 g (65%), (the melting point was not recorded); (white powder).

$^1\text{H NMR}$ (270 MHz) δ (CDCl_3): 0.89-0.93 (3 H, m), 1.32-1.42 (2 H, m), 1.57 (2 H, quintet, J 5.4), 3.48 (2 H, t, J 5.7), 3.61-3.64 (2 H, m), 3.72-3.74 (2 H, m), 3.90 (2 H, t, J 5.7), 4.16 (2 H, t, J 6.1), 6.98 (2 H, d), 7.38-7.54 (3 x 2 H, d).

$\nu_{\text{max}}(\text{KCl})$: 2935, 1610, 1480, 1305, 820, 500 cm^{-1} .

m/z : 394/392 (M^+), 250/248 (100%), 152, 139.

Compounds **26** and **27** were prepared following a similar procedure to that described for the preparation of compound **16**.

2,3-Difluoro-4-octyloxy-4''-(1,4-dioxaoctyl)terphenyl (26)

Quantities: compound **24** (1.53 g, 4.0 mmol), tetrakis(triphenylphosphine)-palladium(0) (0.12 g, 0.12 mmol), and compound **5** (1.37 g, 4.8 mmol).

Yield 1.34 g, 60% (white powder).

Transition temperatures ($^{\circ}\text{C}$): Cr 108.0 SmC 146.5 I.

$^1\text{H NMR}$ δ (CDCl_3): 0.85-0.97 (6 H, m), 1.23-1.53 (12 H, m), 1.57-1.66 (2 H, m), 1.80-1.90 (2 H, quintet, J 5.2), 3.55 (2 H, t, J, 5.2), 3.82 (2 H, t, J 5.4), 4.08 (2 H, t, J 5.9), 4.17 (2 H, t, J 6.0), 6.78-6.85 (1 H, m), 7.00 (2H, d), 7.10-7.16 (1 H, m), 7.50-7.56 (2 x 2 H, d), 7.62 (2 H, d).

$\nu_{\text{max}}(\text{KCl})$: 2980, 2880, 1640, 1610, 1500, 1480, 1305, 1260, 1080, 800 cm^{-1} .

m/z : 510 (M^+ , 100%), 397, 298, 251, 57.

2,3-Difluoro-4-octyloxy-4''-(1,4,7-trioxaundecyl)terphenyl (27)

Quantities: compound **25** (1.42 g, 3.5 mmol), tetrakis(triphenylphosphine)-palladium(0) (0.12 g, 0.12 mmol), and compound **5** (1.20 g, 4.2 mmol).

Yield 1.21 g, 63% (white powder).

Transition temperatures ($^{\circ}\text{C}$): Cr 72.8 SmC 119.5 I.

$^1\text{H NMR}$ δ (CDCl_3): 0.85-0.97 (6 H, m), 1.23-1.53 (14 H, m), 1.85 (2 H, quintet, J 6.2), 3.49 (2 H, t, J 6.4), 3.63 (2 H, t, J 6.2), 3.72-3.77 (2 H, m), 3.90 (2 H, t, J 6.4), 4.09 (2 H, t, J 6.4), 4.20 (2 H, t, J 6.4), 6.78-6.85 (1 H, m), 7.00 (2 H, d), 7.10-7.16 (1 H, m), 7.52-7.58 (2 x 2 H, d), 7.62 (2 H, d).

$\nu_{\text{max}}(\text{KCl})$: 2960, 2880, 1650, 1620, 1500, 1480, 1300, 1260, 1120, 1080, 800 cm^{-1} .

m/z : 554 (M^+ , 100%), 323, 297, 89, 57.

Scheme 4

6-Bromohexan-1-ol (29)

Hydrobromic acid (48.5%, 36 ml, 0.221 mol), was added to a solution of compound 28 (25.0 g, 0.221 mol) in benzene (200 ml). The mixture was heated under reflux for 26 h and the water formed was removed using a Dean-Stark water separator. Benzene was removed *in vacuo*, the residue was dissolved in diethyl ether (300 ml), washed with 6N sodium hydroxide solution (250 ml) and water (250 ml). The ethereal solution was then dried (MgSO₄) and the solvent was removed *in vacuo*; the residue was purified by column chromatography [DCM] to give a colourless oil.

Yield 19.9 g, 50%; bp 108-110 °C at 5 mmHg.

¹H NMR (270 MHz) δ (CDCl₃): 1.35-1.52 (4 H, m), 1.60 (2 H, quintet, J 5.8), 1.80 (2 H, quintet, J 6.0), 3.42 (2 H, t, J 5.8), 3.70 (2 H, t, J 6.0) the OH proton was not detected.

ν_{\max} (KCl): 3600, 2900, 2800, 1440, 1280, 1250, 720, 500 cm⁻¹.

m/z: 182/180 (M⁺), 102/100 (100%).

4-Bromo-4'-(6-hydroxyhexyloxy)biphenyl (30)

A solution of compound 29 (3.64 g, 0.020 mol) in butanone (80 ml) was added at room temperature to a stirred mixture of compound 12 (5.00 g, 0.020 mol) and potassium carbonate (5.50 g, 0.040 mol) in butanone (70 ml). The reaction mixture was heated under reflux for 48 h. The potassium carbonate was filtered off and the solvent was removed *in vacuo*, the residue was dissolved in diethyl ether (250 ml) and washed with water (2 x 150 ml) and dried (MgSO₄). The solvent was removed *in vacuo* and the crude solid was then recrystallised from ethanol to give white crystals.

Yield 3.60 g, 49%; mp 140-141 °C.

¹H NMR (270 MHz) δ (CDCl₃): 1.36-1.64 (6 H, m), 1.81 (2 H, quintet, J 5.8), 2.81 (1 H, s), 3.52 (2 H, t, J 5.0), 4.00 (2 H, t, J 6.0), 6.95 (2 H, d), 7.38-7.56 (3 x 2 H, d).

ν_{\max} (KCl): 3360, 2980, 2890, 1610, 1480, 1390, 1260, 1080, 1005, 810, 500 cm⁻¹.

m/z: 350/348 (M⁺), 250/248 (100%), 244, 218, 192, 138, 114, 58 (100%).

2,3-Difluoro-4-octyloxy-4''-(6-hydroxyhexyloxy)terphenyl (31)

A solution of compound 30 (3.30 g, 9.5 mmol), a 2M-aqueous solution of sodium carbonate (40ml) and tetrakis(triphenylphosphine)palladium(0) (0.28 g, 0.28 mmol) were mixed in DME (60 ml) under dry nitrogen at room temperature and compound 5 (3.25 g, 11.4 mmol) was added. The stirred reaction mixture was heated under reflux under dry nitrogen overnight until g.l.c. and t.l.c. revealed a complete reaction. The product was extracted into DCM (2 x 150 ml) and washed with brine, water and dried (MgSO₄). The solvent was removed under reduced pressure and the residue was purified by column chromatography [DCM-hexane, 1:1] and recrystallised from ethanol-hexane (1:4) to give a white powder.

Yield 1.20 g, 30%.

Transition temperatures (°C): Cr 158.3 SmC 168.9 SmA 179.5 N 185.0 I.

¹H NMR (270 MHz) δ (CDCl₃): 0.90 (3 H, t, J 6.3), 1.24 (1 H, s), 1.22-1.40 (16 H, m), 1.80-1.88 (4 H, m), 3.67 (2 H, t, J 6.1), 4.02 (2 H, t, J 5.9), 4.08 (2 H, t, J 6.1), 6.78-6.83 (1 H, m), 6.88 (2 H, d), 7.08-7.13 (1 H, m), 7.52-7.58 (2 x 2 H, d), 7.67 (2 H, d).

ν_{\max} (KCl): 3600-3300, 2930, 2850, 1600, 1495, 1390, 1300, 1250, 1070, 800 cm⁻¹.

m/z: 510 (M⁺), 493, 298, 87 (100%).

4''-(9,9-Dimethyl-1,8-dioxadecyl)-2,3-difluoro-4-octyloxyterphenyl (32)

A solution of compound 31 (1.10 g, 2.1 mmol) in a minimum volume of DCM (100 ml of hexane was added to reduce the polarity of the solvent) was prepared and *t*-butyl trichloroacetimidate (0.91 g, 4.2 mmol), and a catalytic amount of boron trifluoride etherate (20 μl) were added at room temperature. The reaction mixture was left stirring until g.l.c. and t.l.c. analyses revealed a complete reaction. The solvent was removed *in vacuo* and the product was purified by column chromatography [DCM] and recrystallised from ethanol to give a white powder.

Yield 0.80 g, 67%.

Transition temperatures (°C): Cr 99.1 SmC_{alt} 119.8 SmC 151.8 I.

¹H NMR (270 Mhz) δ (CDCl₃): 0.85-0.97 (3 H, m), 1.20 (9 H, s), 1.24-1.26 (16 H, m), 1.77-1.90 (4 H, m), 3.35 (2 H, t, J 5.6), 4.01 (2 H, t, J 5.5), 4.08 (2 H, t, 5.3), 6.78-6.85 (1 H, m), 7.00 (2 H, d), 7.10-7.16 (1 H, m), 7.52-7.66 (3 x 2 H, d).

ν_{\max} (KCl): 2980, 1640, 1500, 1480, 1300, 1080, 800 cm⁻¹.

m/z: 566 (M⁺), 423, 298, 83, 57.

Scheme 5

4-Trimethylsilylbutan-1-ol (42)

A solution of compound 36 (15.9 g, 0.146 mol) and chlorotrimethylsilane (15.8 g, 0.146 mol) in benzene (80 ml) was cooled to 0 °C with a strong flow of ammonia bubbling through for 1 h. The resulting ammonium chloride was filtered off and the solvent was removed *in vacuo*. The silyl ether (39) produced was used in the next step without purification.

A solution of the silyl ether (16.3 g, 0.091 mol) in dry diethyl ether (100 ml) was reacted with finely chipped lithium (1.66 g, 0.240 mol) under reflux for 1 h. Dry THF (100 ml) was added and the diethyl ether was distilled off and the reaction mixture was then heated under reflux for 1 h. The reaction mixture was allowed to cool to room temperature, ice was added to destroy unreacted lithium metal and the product was extracted into diethyl ether (2 x 150 ml), washed with brine, water and dried (MgSO₄). The solvent was removed and the product was distilled under reduced pressure to give a colourless oil.

Yield 13.4 g, 85%; bp 77-80 °C at 15 mmHg.

¹H NMR (270 MHz) δ (CDCl₃): 0.05 (9 H, s), 0.48-0.52 (2 H, m), 1.50-1.58 (4 H, m), 2.25 (1 H, s), 3.51 (2 H, t, J 6.5).

ν_{\max} (KCl): 3300, 2950, 1240, 1040, 850, 820, 760, 690 cm⁻¹.

m/z: 146 (M⁺), 129, 73.

Compounds 43 and 44 were prepared following a similar procedure to that described for the preparation of compound 42. Compounds 40 and 41 were used in the next step without purification.

5-Trimethylsilylpentan-1-ol (43)

Quantities: compounds 37 (10.0 g, 0.088 mol), chlorotrimethylsilane (10.6 g, 0.098 mol), and lithium (1.14 g, 0.162 mol).

Yield 6.80 g, 72%; bp 82-86 °C at 15 mmHg (colourless oil).

¹H NMR (270 MHz) δ (CDCl₃): 0.08 (9 H, s), 0.42-0.53 (2 H, m), 1.23-1.42 (4 H, m), 1.43-1.57 (2 H, m), 3.57 (2 H, t, J 6.4), the OH proton was not detected.

ν_{\max} (KCl): 3330, 2950, 1420, 1240, 1180, 1040, 820, 750, 690 cm⁻¹.

m/z: 160(M⁺), 143 (100%).

6-Trimethylsilylhexan-1-ol (44)

Quantities: compound **38** (12.0 g, 0.088 mol), chlorotrimethylsilane (10.6 g, 0.098 mol), and lithium (1.14 g, 0.162 mol) (colourless oil).

Yield 11.6 g, 76%; bp 96-98 °C at 15 mmHg.

¹H NMR (270 MHz) δ (CDCl₃): 0.08 (9 H, s), 0.42-0.53 (2 H, m), 1.21-1.48 (6 H, m), 1.43-1.57 (2 H, m), 3.57 (2 H, t, J 6.3), the OH proton was not detected.

ν_{\max} (KCl): 3300, 2960, 1420, 1250, 1190, 1040, 850, 750, 690 cm⁻¹.

m/z: 174 (M⁺), 157, 101 (100%).

4-Bromo-4'-[2-(trimethylsilyl)ethoxy]biphenyl (45)

A solution of triphenylphosphine (5.55 g, 0.021 mol) and DEAD (3.72 g, 0.021 mol) in dry cold THF (100 ml) was added dropwise at room temperature over ten min to a stirred solution of compound **12** (5.25 g, 0.021 mol) and compound **33** (2.50 g, 0.021 mol) in dry THF (75 ml). The reaction mixture was left stirring overnight. The reaction product was extracted into diethyl ether (2 x 200 ml), and the combined ethereal solutions were washed with water and dried (MgSO₄). The crude product was adsorbed onto silica gel and purified by column chromatography [DCM-petroleum fraction (bp 40-60 °C), 1:4] and recrystallised from hexane to give a white powder.

Yield 3.76 g, 51%; mp 120-121 °C.

¹H NMR (270 MHz) δ (CDCl₃): 0.09 (9 H, s), 1.12 (2 H, t, J 6.5), 4.09 (2 H, t, J 6.3), 6.93 (2 H, d), 7.38-7.55 (3 x 2 H, d).

ν_{\max} (KCl): 2970, 1605, 1475, 1305, 1050, 965, 820 cm⁻¹.

m/z: 350/348 (M⁺), 308/306, 307/305, 245 (100%), 101.

Compounds **46**, **47**, **48** and **49** were prepared following a similar procedure to that described for the preparation of compound **45**.

4-Bromo-4'-[3-(trimethylsilyl)propyloxy]biphenyl (46)

Quantities: triphenylphosphine (4.45 g, 0.019 mol), DEAD (3.72 g, 0.019 mol), compound **12** (4.68 g, 0.019 mol), and compound **34** (2.50 g, 0.019 mol).

Yield 4.76 g, 70%; mp 119-120 °C (white powder).

¹H NMR (270 MHz) δ (CDCl₃): 0.01 (9 H, s) 0.60 (2 H, t, J 6.2), 1.70-1.82 (2 H, m), 3.90 (2 H, t, J 6.4), 6.90 (2 H, d), 7.34-7.50 (3 x 2 H, d).

ν_{\max} (KCl): 2960, 1605, 1480, 1300, 815, 545 cm⁻¹.

m/z : 364/362 (M^+), 250/248, 245 (100%), 165.

4-Bromo-4'-[4-(trimethylsilyl)butyloxy]biphenyl (47)

Quantities: triphenylphosphine (3.17 g, 0.012 mol), DEAD (2.11 g, 0.012 mol), compound **12** (3.00 g, 0.012 mol), and compound **42** (1.67 g, 0.012 mol).

Yield 3.00 g, 65%; mp 122-123 °C (white powder).

$^1\text{H NMR}$ (400 MHz) δ (CDCl_3): 0.01 (9 H, s), 0.54-0.58 (2 H, m), 1.44-1.52 (2 H, m), 1.80 (2 H, quintet, J 7.2), 3.98 (2 H, t, J 9.3), 6.94 (2 H, d), 7.42-7.52 (3 x 2 H, d).

$\nu_{\text{max}}(\text{KCl})$: 2980, 2880, 1615, 1495, 1400, 1300, 1260, 1205, 870, 820, 810, 500 cm^{-1} .

m/z : 378/376 (M^+), 308/306, 250/248, 226 (100%), 139, 73.

4-Bromo-4'-[5-(trimethylsilyl)pentyloxy]biphenyl (48)

Quantities: triphenylphosphine (4.22 g, 0.016 mol), DEAD (2.81 g, 0.016 mol), compound **12** (4.00 g, 0.016 mol), and compound **43** (2.58 g, 0.016 mol).

Yield 4.10 g, 65%; mp 129-130 °C (white powder).

$^1\text{H NMR}$ (400 MHz) δ (CDCl_3): 0.01 (9 H, s), 0.52 (2 H, t, J 6.5), 1.33-1.53 (4 H, m), 1.77 (2 H, quintet, J 4.2), 3.96 (2 H, t, J 4.2), 6.94 (2 H, d, J 5.5), 7.42-7.52 (3 x 2 H, d).

$\nu_{\text{max}}(\text{KCl})$: 2980, 2940, 2880, 1605, 1480, 1280, 1250, 1180, 1010, 880, 850, 820, 500 cm^{-1} .

m/z : 392/390 (M^+), 307, 250/248, 211, 152 (100%), 73.

4-Bromo-4'-[6-(trimethylsilyl)hexyloxy]biphenyl (49)

Quantities: triphenylphosphine (3.17 g, 0.012 mol), DEAD (2.10 g, 0.012 mol), compound **12** (3.00 g, 0.012 mol), and compound **44** (2.10 g, 0.012 mol).

Yield 3.33 g, 68%; mp 127-128 °C (white powder).

$^1\text{H NMR}$ (270 MHz) δ (CDCl_3): 0.15 (9 H, s), 0.47-0.53 (2 H, m), 1.24-1.53 (6 H, m), 1.81 (2 H, quintet, J 4.6), 4.02 (2 H, t, J 5.5), 6.96 (2 H, d), 7.42-7.52 (3 x 2 H, d).

$\nu_{\text{max}}(\text{KCl})$: 2980, 2940, 2880, 1605, 1480, 1310, 1280, 1250, 1180, 880, 850, 820, 500 cm^{-1} .

m/z : 406/404 (M^+), 250/248, 211, 152 (100%), 73.

2,3-Difluoro-4-octyloxy-4''-[2-(trimethylsilyl)ethoxy]terphenyl (50)

Compound 45 (1.40 g, 4.0 mmol), an aqueous solution of 2M-sodium carbonate (40 ml) and tetrakis(triphenylphosphine)palladium(0) (0.12 g, 0.12 mmol) were mixed in DME (50 ml) under dry nitrogen at room temperature and compound 5 (1.37 g, 4.8 mmol) was added. The stirred reaction mixture was heated overnight under reflux under dry nitrogen until g.l.c. and t.l.c. revealed a complete reaction. The product was extracted into DCM (2 x 150 ml) and washed with brine, water and dried (MgSO₄). The solvent was removed under reduced pressure and the residue was purified by column chromatography [DCM-hexane, 1:4] and recrystallised from ethanol-hexane (1:10) to give a white powder.

Yield 1.12 g, 55%.

Transition temperatures (°C): Cr 72.8 SmC 119.1 N 130.7 I.

¹H NMR (270 MHz) δ (CDCl₃): 0.00 (9 H, s), 0.80 (2 H, t, J 6.2), 1.07 (3 H, t, J 6.1), 1.15-1.37 (10 H, m), 1.75 (2 H, quintet, J 6.2), 3.95-4.07 (4 H, m), 6.67-6.74 (1 H, m), 6.87 (2 H, d), 7.00-7.08 (1 H, m), 7.42-7.60 (3 x 2 H, d).

ν_{\max} (KCl): 2920, 1610, 1500, 1300, 1080, 800 cm⁻¹.

m/z: 510 (M⁺), 482, 371, 255, 247.

Compounds 51, 52, 53, 54, 55, 56, 57, 58 and 59 were prepared following a similar procedure as that described for compound 50.

2,3-Difluoro-4-octyloxy-4''-[3-(trimethylsilyl)propyloxy]terphenyl (51)

Quantities: compound 46 (1.45 g, 4.0 mmol), tetrakis(triphenylphosphine)-palladium(0) (0.12 g, 0.12 mmol), and compound 5 (1.34 g, 4.7 mmol).

Yield 1.2 g, 60% (white powder).

Transition temperatures (°C): Cr 95.0 SmC 149.5 I.

¹H NMR (270 MHz) δ (CDCl₃): 0.00 (9 H, s), 0.56-0.68 (2 H, t, J 5.8), 0.82-0.94 (3 H, m), 1.20-1.55 (10 H, m), 1.72-1.90 (4 H, m), 3.95-4.00 (2 H, t, J 6.1), 4.10 (2 H, t, J 6.0), 6.78-6.89 (1 H, m), 6.97 (2 H, d), 7.11-7.21 (1 H, m), 7.48-7.68 (3 x 2 H, d).

ν_{\max} (KCl): 2980, 2880, 1610, 1505, 1480, 1300, 1260, 1110, 1080, 840, 800 cm⁻¹.

m/z: 524 (M⁺), 370, 298 (100%), 266, 73, 58.

2,3-Difluoro-4-octyloxy-4''-[4-(trimethylsilyl)butyloxy]terphenyl (52)

Quantities: compound 47 (1.00 g, 2.6 mmol), tetrakis(triphenylphosphine)-palladium(0) (0.12 g, 0.12 mmol), and compound 5 (0.91 g, 3.2 mmol).

Yield 0.81 g, 58% (white powder).

Transition temperatures (°C): Cr 80.2 SmC 143.1 I.

¹H NMR (400 MHz) δ (CDCl₃): 0.01 (9 H, s), 0.59 (2 H, t, J 8.5), 0.89 (3 H, t, J 7.1), 1.25-1.44 (8 H, m), 1.46-1.55 (4 H, m), 1.78-1.88 (4 H, m), 4.02 (2 H, t, J 6.5), 4.09 (2 H, t, J 6.5), 6.83-6.89 (1 H, m), 7.02 (2 H, d), 7.12-7.18 (1 H, m), 7.54-7.67 (3 x 2 H, d).

ν_{\max} (KCl): 2980, 2880, 1500, 1470, 1300, 1260, 1080, 860, 840, 800 cm⁻¹.

m/z: 538 (M⁺), 370, 355, 269, 73.

2,3-Difluoro-4-octyloxy-4''-[5-(trimethylsilyl)pentyloxy]terphenyl (53)

Quantities: compound 48 (1.00 g, 2.5 mmol), tetrakis(triphenylphosphine)-palladium(0) (0.12 g, 0.12 mmol), and compound 5 (0.88 g, 3.1 mmol).

Yield 0.57 g, 65% (white powder).

Transition temperatures (°C): Cr 106.0 SmC 159.4 I.

¹H NMR (400 MHz) δ (CDCl₃): 0.01 (9 H, s), 0.55 (2 H, t, J 8.1), 0.91 (3 H, t, J 5.8), 1.29-1.46 (10 H, m), 1.47-1.53 (4 H, m), 1.76-1.89 (4 H, m), 4.01 (2 H, t, J 6.6), 4.09 (2 H, t, J 6.4), 6.82-6.89 (1 H, m), 6.98 (2 H, d), 7.14-7.20 (1 H, m), 7.54-7.66 (3 x 2 H, d).

ν_{\max} (KCl): 2920, 1610, 1500, 1440, 1080, 800 cm⁻¹.

m/z: 552 (M⁺), 408, 370, 355, 298, 258.

2,3-Difluoro-4-octyloxy-4''-[6-(trimethylsilyl)hexyloxy]terphenyl (54)

Quantities: compound 49 (1.00 g, 2.3 mmol), tetrakis(triphenylphosphine)-palladium(0) (0.12 g, 0.12 mmol), and compound 5 (0.84 g, 3.0 mmol).

Yield 0.75 g, 58% (white powder).

Transition temperatures (°C): Cr 93.6 SmC 156.6 I.

¹H NMR (270 MHz) δ (CDCl₃): 0.00 (9 H, s), 0.50 (2 H, t, J 7.8), 0.76 (3 H, t, J 6.5), 1.22-1.52 (16 H, m), 1.72-1.88 (4 H, m), 4.00 (2 H, t, J 6.3), 4.07 (2 H, t, J 6.2), 6.80-6.88 (1 H, m), 6.96 (2 H, d), 7.06-7.14 (1 H, m), 7.52-7.68 (3 x 2 H, d).

ν_{\max} (KCl): 2980, 2880, 1610, 1500, 1470, 1300, 1260, 1080, 870, 840, 800 cm⁻¹.

m/z: 566 (M⁺), 402, 355, 318, 298, 246.

2,3-Difluoro-4-nonyl-4''-[2-(trimethylsilyl)ethoxy]terphenyl (55)

Quantities: compound 45 (0.50 g, 1.4 mmol), tetrakis(triphenylphosphine)-palladium(0) (0.09 g, 0.09 mmol), and compound 8 (0.50 g, 1.7 mmol).

Yield 0.35 g, 50% (white powder).

Transition temperatures (°C): Cr 47.2 SmC 78.6 N 95.3 I.

¹H NMR (400 MHz) δ (CDCl₃): 0.12 (9 H, s), 0.60 (2 H, t, J 4.8), 0.87 (3 H, t, J 7.0), 1.16 (2 H, t, J 7.0), 1.22-1.47 (10 H, m), 1.64 (2 H, quintet, J 6.9), 2.71 (2 H, t, J 6.3), 4.14 (2 H, t, J 6.3), 6.98 (2 H, d, J 9.3), 7.00-7.09 (1 H, m), 7.14-7.23 (1 H, m), 7.52-7.70 (3 x 2 H, d).

ν_{\max} (KCl): 2980, 2940, 2890, 1605, 1470, 1250, 860, 810 cm⁻¹.

m/z: 508 (M⁺), 481, 364, 294, 73.

2,3-Difluoro-4-nonyl-4''-[3-(trimethylsilyl)propyloxy]terphenyl (56)

Quantities: compound 46 (1.00 g, 2.8 mmol), tetrakis(triphenylphosphine)-palladium(0) (0.12 g, 0.12 mmol), and compound 8 (0.94 g, 3.3 mmol).

Yield 0.82 g, 57% (white powder).

Transition temperatures (°C): Cr 80.1 SmC 113.3 I.

¹H NMR (400 MHz) δ (CDCl₃): 0.00 (9 H, s), 0.60 (2 H, t, J 4.3), 0.84 (3 H, t, J 7.0), 1.22-1.34 (12 H, m), 1.61 (2 H, quintet, J 7.4), 1.72-1.82 (2 H, m), 2.66 (2 H, t, J 7.6), 3.93 (2 H, t, J 6.9), 6.92-6.97 (2 H, m), 6.98-7.03 (1 H, m), 7.10-7.16 (1 H, m), 7.52-7.57 (2x2 H, d), 7.61 (2 H, d).

ν_{\max} (KCl): 2980, 2930, 2880, 1605, 1470, 1250, 840, 800 cm⁻¹.

m/z: 522 (M⁺), 481, 408, 364, 295, 73.

2,3-Difluoro-4-nonyl-4''-[4-(trimethylsilyl)butyloxy]terphenyl (57)

Quantities: compound 47 (0.90 g, 2.4 mmol), tetrakis(triphenylphosphine)-palladium(0) (0.12 g, 0.12 mmol), and compound 8 (0.82 g, 2.8 mmol).

Yield 0.64 g, 50%.

Transition temperatures (°C): Cr 54.2 SmC 107.5 I.

¹H NMR (400 MHz) δ (CDCl₃): 0.01 (9 H, s), 0.59 (2 H, t, J 8.5), 0.83 (3 H, t, J 7.1), 1.25-1.44 (10 H, m), 1.46-1.55 (4 H, m), 1.78-1.88 (4 H, m), 2.67 (2 H, t, J 7.6), 3.93 (2 H, t, J 6.9), 6.92-6.97 (2 H, m), 6.98-7.03 (1 H, m), 7.10-7.16 (1 H, m), 7.52-7.57 (2 x 2 H, d), 7.61 (2 H, d).

ν_{\max} (KCl): 2980, 2890, 1500, 1470, 1300, 1260, 1080, 860, 840, 800 cm⁻¹.

m/z : 536 (M^+), 408, 295, 266, 73.

2,3-Difluoro-4-nonyl-4''-[5-(trimethylsilyl)pentyl]oxy]terphenyl (58)

Quantities: compound 48 (0.50 g, 1.3 mmol), tetrakis(triphenylphosphine)-palladium(0) (0.08 g, 0.08 mmol), and compound 8 (0.44 g, 1.5 mmol).

Yield 0.41 g, 57%.

Transition temperatures ($^{\circ}\text{C}$): Cr 72.2 SmC 127.2 I.

$^1\text{H NMR}$ (400 MHz) δ (CDCl_3): 0.02 (9 H, s), 0.50-0.57 (2 H, t, J 4.8), 0.87-0.90 (14 H, m), 1.22-1.45 (2 H, m), 1.47-1.55 (3 H, m), 1.65 (2 H, quintet, J 8.2), 1.82 (2 H, quintet, J 7.1), 2.69 (2 H, t, J 8.2), 4.00 (2 H, t, J 8.0), 6.95-7.03 (3 H, m), 7.12-7.18 (1 H, m), 7.52-7.67 (3 x 2 H, d).

ν_{max} (KCl): 2930, 2850, 1610, 1470, 1250, 820 cm^{-1} .

m/z : 550 (M^+), 480, 407, 295, 266.

2,3-Difluoro-4-nonyl-4''-[6-(trimethylsilyl)hexyl]oxy]terphenyl (59)

Quantities: compound 49 (1.00 g, 2.5 mmol), tetrakis(triphenylphosphine)-palladium(0) (0.12 g, 0.12 mmol), and compound 8 (0.84 g, 3.0 mmol).

Yield 0.67 g, 48%.

Transition temperatures ($^{\circ}\text{C}$): Cr 57.6 SmC 123.0 I.

$^1\text{H NMR}$ (400 MHz) δ (CDCl_3): 0.00 (9 H, s), 0.50 (2 H, t, J 5.8), 0.84 (3 H, t, J 7.0), 1.20-1.52 (18 H, m), 1.63 (2 H, quintet, J 7.2), 1.72-1.82 (2 H, m), 2.66 (2 H, t, J 7.5), 3.93 (2 H, t, J 6.9), 6.96 (2 H, d), 7.00-7.05 (1 H, m), 7.13-7.18 (1 H, m), 7.52-7.66 (3 x 2 H, d).

ν_{max} (KCl): 2960, 2880, 1610, 1490, 1470, 1260, 860, 840, 810 cm^{-1} .

m/z : 564 (M^+), 408, 295, 73.

Scheme 6

6-Triethylsilylhexan-1-ol (62)

A solution of compound **38** (15.0 g, 0.110 mol) and chlorotriethylsilane (**60**) (18.2 g, 0.121 mol) in benzene (120 ml) was cooled to 0 °C with a strong flow of ammonia bubbling through for 1 h. The resulting ammonium chloride was filtered off and the solvent was removed *in vacuo*. The silyl ether (**61**) produced was used in the next step without purification.

A solution of the silyl ether (**61**) (19.3 g, 0.065 mol) in dry diethyl ether (100 ml) was reacted with finely chipped lithium (1.14 g, 0.162 mol) under reflux for 1 h. Dry THF (100 ml) was added and the diethyl ether was distilled off and the reaction mixture was then heated under reflux for 2 h. The reaction mixture was allowed to cool to room temperature, ice was added to destroy unreacted lithium metal and the product was extracted into diethyl ether (2 x 150 ml), washed with brine, water and dried (MgSO₄). The solvent was removed and the product was distilled under reduced pressure to give a colourless oil.

Yield 10.1 g, 72%; bp 135-140 °C at 15 mmHg.

¹H NMR (270 MHz) δ (CDCl₃): 0.01 (9 H, s), 0.40-0.60 (6 H, m), 0.85-1.03 (11 H, m), 1.22-1.42 (6 H, m), 1.46-1.62 (2 H, m), 3.54-3.69 (2 H, m), the OH proton was not detected.

ν_{\max} (KCl): 3500, 2950, 1420, 1240, 1170, 1040, 850, 710, 680 cm⁻¹.

m/z: 216 (M⁺), 199, 101.

4-Bromo-4'-[6-(triethylsilyl)hexyloxy]biphenyl (63)

Quantities: triphenylphosphine (6.34 g, 0.024 mol), DEAD (4.20 g, 0.024 mol), compound **12** (6.00 g, 0.024 mol) and compound **62** (5.22 g, 0.024 mol).

A solution of triphenylphosphine (6.34 g, 0.024 mol) and DEAD (4.20 g, 0.024 mol) in dry cold THF (100 ml) was added dropwise at room temperature over ten min to a stirred solution of compound **12** (6.00 g, 0.024 mol) and compound **62** (5.22 g, 0.024 mol) in dry THF (100 ml). The reaction mixture was left stirring overnight. The reaction product was extracted into diethyl ether (2 x 250 ml), and the combined ethereal solutions were washed with water and dried (MgSO₄). The purification of this compound was unsuccessful, and the compound was used in the next step without further purification.

2,3-Difluoro-4-octyloxy-4''-[6-(triethylsilyl)hexyloxy]terphenyl (64)

Compound **63** (1.00 g, approximately 2.2 mmol), an aqueous solution of 2M-sodium carbonate (40 ml) and tetrakis(triphenylphosphine)palladium(0) (0.12 g, 0.12 mmol) were mixed in DME (50 ml) under dry nitrogen at room temperature and compound **5** (0.84 g, 3.0 mmol) was added. The stirred reaction mixture was heated overnight under reflux and dry nitrogen until g.l.c. and t.l.c. revealed a complete reaction. The product was extracted into DCM (2 x 150 ml) and washed with brine, water and dried (MgSO₄). The solvent was removed under reduced pressure and the residue was purified by column chromatography [DCM-hexane, 1:8] and recrystallised from ethanol-hexane (1:6) to give a white powder.

Yield 0.55 g

Transition temperatures (°C): Cr 54.4 SmC 125.8 I.

¹H NMR (270 MHz) δ (CDCl₃): 0.00 (9 H, t, J 7.1), 0.84-0.98 (6 H, m), 1.22-1.53 (21 H, m), 1.73-1.90 (4 H, m), 4.01 (2 H, t, J 5.4), 4.10 (2 H, t, J 5.4), 6.78-6.86 (1 H, m), 6.96 (2 H, d), 7.06-7.14 (1 H, m), 7.52-7.68 (3 x 2 H, d).

ν_{\max} (KCl): 2980, 2960, 2880, 1500, 1480, 1120, 1080, 810 cm⁻¹.

m/z : 608 (M⁺), 495, 298, 73.

Scheme 7

4-Bromo-4'-(3,7-dimethyloctyloxy)biphenyl (66)

Compound **12** (2.50 g, 0.010 mol) and compound **65** (1.58 g, 0.010 mol) were mixed in dry THF (50 ml) and left stirring at room temperature for 10 min; then a solution of triphenylphosphine (2.60 g, 0.010 mol) and DEAD (1.75 g, 0.010 mol) in dry cold THF (50 ml) was added dropwise at room temperature over 10 min. The reaction mixture was left stirring overnight. The reaction product was extracted in ether (2 x 100 ml), and the combined ethereal solutions were washed with water and dried (MgSO_4). The crude product was adsorbed onto silica gel and purified by column chromatography [ethyl acetate-petroleum fraction (bp 40-60 °C), 1:5] to give a white powder.

Yield 2.92 g, 75%; mp 101-102 °C.

$^1\text{H NMR}$ (270 MHz) δ (CDCl_3): 0.85 (6 H, d, J 6.5), 0.95 (3 H, d, J 6.3), 1.12-1.40 (6 H, m), 1.47-1.74 (3 H, m), 1.78-1.89 (1 H, m), 4.02 (2 H, t, J 5.9), 6.96 (2 H, d), 7.37-7.54 (3 x 2 H, d).

ν_{max} (KCl): 2940, 1610, 1460, 1290, 1190, 820, 500 cm^{-1} .

m/z : 394/392 ($\text{M}+4^+$), 250/248, 152, 101, 89 (100%).

4''-(3,7-Dimethyloctyloxy)-2,3-difluoro-4-octyloxyterphenyl (67)

Compound **66** (0.80 g, 2.0 mmol), an aqueous solution 2M-sodium carbonate (40 ml) and tetrakis(triphenylphosphine)palladium(0) (0.12 g, 0.12 mmol) were mixed in DME (60 ml) under dry nitrogen at room temperature and compound **5** (0.62 g, 2.2 mmol) was added. The stirred reaction mixture was heated overnight under reflux under dry nitrogen until g.l.c. and t.l.c. revealed a complete reaction. The product was extracted into DCM (2 x 150 ml) and washed with brine, water and dried (MgSO_4). The solvent was removed under reduced pressure and the residue was purified by column chromatography [ether-hexane, 3:1] and recrystallised from ethanol to give white crystals.

Yield 0.78 g, 65%.

Transition temperatures (°C): Cr 82.5 SmC 132.2 N 138.0 I.

^1H NMR (270 MHz) δ (CDCl_3): 0.84-0.92 (9 H, m), 0.96 (3 H, d, J 6.0), 1.10-1.42 (18 H, m), 1.44-1.65 (4 H, m), 3.82 (2 H, t, J 5.4), 4.02 (2 H, t, J 5.8), 6.78-6.85 (1 H, m), 7.00 (2 H, d), 7.10-7.16 (1 H, m), 7.52-7.66 (3 x 2 H, d).

ν_{max} (KCl): 2980, 2880, 1610, 1505, 1480, 1305, 1260, 1200, 1080, 800 cm^{-1} .

m/z : 550 (M^+) (100%), 423, 393, 298, 57.

Compound **69** was prepared following a similar procedure to that described for the preparation of compound **66**.

4-Bromo-4'-octyloxybiphenyl (**69**)

Quantities: compound **12** (2.50 g, 0.010 mol), compound **68** (1.30 g, 0.010 mol), triphenylphosphine (2.60 g, 0.010 mol), and DEAD (1.75 g, 0.010 mol).

Yield 2.90 g, 80%; mp 128-129 $^{\circ}\text{C}$ (white powder).

^1H NMR (270 MHz) δ (CDCl_3): 0.89 (3 H, t, J 5.0), 1.22-1.52 (10 H, m), 1.61-1.71 (2 H, quintet, J 5.3), 4.04 (2 H, t, J 5.3), 6.96 (2 H, d), 7.44 (2 H, d), 7.51 (2 H, d), 7.53 (2 H, d).

ν_{max} (KCl): 2980, 1610, 1480, 1370, 1300, 1260, 1180, 1000, 860, 810, 680 cm^{-1} .

m/z : 262/360 (M^+), 250/248, 101, 89, 57.

Compound **70** and **71** were prepared following a similar procedure to that described for the preparation of compound **67**.

2,3-Difluoro-4,4''-dioctyloxyterphenyl (**70**)

Quantities: compound **69** (1.00 g, 2.7 mmol), tetrakis(triphenylphosphine)-palladium(0) (0.12 g, 0.12 mmol), and compound **5** (0.90 g, 3.2 mmol).

Yield 1.12 g, 80% (white powder).

Transition temperatures ($^{\circ}\text{C}$): Cr 114.8 SmC 175.8 N 178.1 I.

^1H NMR (400 MHz) δ (CDCl_3): 0.80-0.98 (6 H, m), 1.19-1.57 (20 H, m), 1.83 (4 H, quintet, J 7.2), 4.00 (2 H, t, J 6.7), 4.08 (2 H, t, J 6.7), 6.76-6.86 (1 H, m), 6.98 (2 H, d), 7.18-7.28 (1 H, m), 7.48-7.68 (3 x 2 H, d).

ν_{max} (KCl): 2960, 2860, 1640, 1610, 1500, 1480, 1310, 1260, 1080, 800 cm^{-1} .

m/z : 522 (M^+), 410, 298 (100%), 143, 57.

2,3-Difluoro-4-nonyl-4''-octyloxyterphenyl (71)

Quantities: compound **69** (1.00 g, 2.7 mmol), tetrakis(triphenylphosphine)-palladium(0) (0.12 g, 0.12 mmol), and compound **8** (0.90 g, 3.2 mmol).

Yield 1.15 g, 83% (white powder).

Transition temperatures (°C): Cr 63.1 CrystJ 68.9 SmI 79.6 SmC 90.2 SmA 148.9 I.

$^1\text{H NMR}$ (270 MHz) δ (CDCl_3): 0.82-0.99 (6 H, m), 1.09-1.54 (22 H, m), 1.60 (2 H, quintet, J 6.9), 1.83 (2 H, quintet, J 6.9), 2.80 (2 H, t, J 6.9), 4.08 (2 H, t, J 6.9), 6.93-7.02 (3 H, m), 6.98 (1 H, m), 7.50-7.65 (3 x 2 H, d).

ν_{max} (KCl): 2980, 2960, 2870, 1605, 1460, 1290, 1260, 1180, 810 cm^{-1} .

m/z : 520 (M^+ , 100%), 408, 391, 296.

Scheme 8

6-Chlorohexyl toluene-*p*-sulphonate (72)

A solution of compound 38 (25.0 g, 0.183 mol) in DCM (166 ml) and pyridine (33 ml) was cooled to $-5\text{ }^{\circ}\text{C}$. Toluene-*p*-sulphonyl chloride (40.1 g, 0.210 mol) was slowly added to the stirred solution and left to react overnight. The reaction mixture was treated with ice (80 g) and left stirring for 1 h. The organic layer was washed with ice cold 2M-sulphuric acid and then dried (MgSO_4). The solvent was removed *in vacuo* and the residue was purified by column chromatography [DCM] to give a white powder 40.20 g, 85%; mp $27\text{-}28\text{ }^{\circ}\text{C}$.

$^1\text{H NMR}$ (400 MHz) δ (CDCl_3): 1.26-1.44 (4 H, m), 1.62-1.78 (4 H, m), 2.45 (3 H, s), 3.49 (2 H, t, J 4.8), 4.03 (2 H, t, J 5.0), 7.34 (2 H, d), 7.79 (2 H, d).

ν_{max} (KCl): 2960, 2880, 1610, 1490, 1290, 1260, 820 cm^{-1} .

1-Chloro-7,7-dimethyloctane (73)

The catalyst used in this reaction was prepared by adding the following reagents to dry THF (12.90 ml), under a stream of dry nitrogen in an ice bath to make a 0.1M solution of catalyst: lithium bromide (0.112 g, 1.29 mmol), lithium thiophenolate (1M in THF 1.29 ml, 1.29 mol) and copper(I) bromide dimethyl sulfide (0.27 g, 1.29 mmol). The catalyst was then added to a solution of compound 72 (7.00 g, 0.025 mol) in dry THF (50 ml) the reaction mixture was left to stir for 15 min at room temperature. *tert*-Butylmagnesium chloride (1M in dry THF, 25.1 ml, 0.025 mol) was added dropwise to the reaction mixture under a stream of dry nitrogen and the reaction mixture was left stirring overnight. The reaction mixture was then washed with DCM and cold water; the chlorinated layer was then dried (MgSO_4). The solvent was removed *in vacuo* and the residue was purified by column chromatography [DCM] to give a colourless oil.

Yield 1.32 g, 30%.

$^1\text{H NMR}$ (270 MHz) δ (CDCl_3): 0.86 (9 H, s), 1.14-1.18 (2 H, m), 1.20-1.38 (4 H, m), 1.50 (2 H, quintet, J 7.5), 1.81 (2 H, quintet, J 7.1), 3.50 (2 H, t, 7.1).

Only $^1\text{H NMR}$ analysis was carried out to characterise compound 73.

4-Bromo-4'-(7,7-dimethyloctyloxy)biphenyl (74)

Potassium carbonate (0.56 g, 4.8 mmol) was added to a solution of compound 12 (0.80 g, 3.2 mmol) in butanone (50 ml) with potassium iodide (0.1 g) as catalyst. This mixture was left stirring at room temperature for 10 min and a solution of compound 73 (0.50 g, 2.8 mmol) in butanone (10 ml) was added dropwise. The reaction mixture was heated under reflux for 44 h. The mixture was filtered and butanone was removed from the filtrate under reduced pressure. The product was extracted into ether (2 x 75 ml) and the combined ethereal extracts were washed successively with water, 5% sodium hydroxide and water, and dried (MgSO₄). The solvent was removed *in vacuo* and the residue was purified by column chromatography [DCM] to give a white powder.

Yield 0.80 g, 80%; mp 123-124 °C.

¹H NMR (270 MHz) δ(CDCl₃): 0.86 (9 H, s), 1.14-1.18 (2 H, m), 1.20-1.38 (4 H, m), 1.50 (2 H, quintet, J 7.5), 1.81 (2 H, quintet, J 7.1), 4.00 (2 H, t, J 7.1), 6.96 (2 H, d), 7.41 (2 H, d), 7.47 (2 H, d), 7.52 (2 H, d).

ν_{\max} (KCl): 2960, 2880, 1610, 1490, 1290, 1260, 820 cm⁻¹.

m/z: 390/388 (M⁺), 250/248 (100%), 141, 57.

4''-(7,7-Dimethyloctyloxy)-2,3-difluoro-4-octyloxyterphenyl (75)

Compound 74 (0.40 g, 1.1 mmol) and a 2M-aqueous solution of sodium carbonate (40 ml) and tetrakis(triphenylphosphine)palladium(0) (0.06 g, 0.06 mmol) were mixed in DME (60 ml) under dry nitrogen at room temperature to which compound 5 (0.37 g, 1.3 mmol) was added. The stirred reaction mixture was heated under reflux under dry nitrogen overnight until g.l.c. and t.l.c. revealed a complete reaction. The product was extracted into DCM (2 x 50 ml) and washed with brine, water and dried (MgSO₄). The solvent was removed under reduced pressure and the residue was purified by column chromatography [DCM-hexane, 1:5] and recrystallised from hexane and a trace of ethanol to give white crystals.

Yield 0.42 g, 70%.

Transition temperatures (°C): Cr 97.3 SmC 160.1 I.

¹H NMR (400 MHz) δ (CDCl₃): 0.86-0.92 (12 H, m), 1.15-1.21 (2 H, m), 1.29-1.37 (12 H, m), 1.44-1.52 (4 H, m), 1.76-1.89 (4 H, m), 3.99 (2 H, t, J 6.4), 4.08 (2 H, t, J 6.6), 6.78-6.84 (1 H, m), 6.99 (2 H, d), 7.10-7.16 (1 H, m), 7.54-7.57 (2 x 2 H, d), 7.62 (2 H, d).

$\nu_{\max}(\text{KCl})$: 2960, 2880, 1500, 1400, 1290, 1260, 1080, 800 cm^{-1} .

m/z : 550 (M^+), 438 (100%), 410, 298, 57.

4''-(7,7-Dimethyloctyloxy)-2,3-difluoro-4-nonylterphenyl (76)

Quantities: compound **74** (0.40 g, 1.1 mmol), tetrakis(triphenylphosphine)-palladium(0) (0.06 g, 0.06 mmol), compound **8** (0.37 g, 1.3 mmol). The reaction procedure was as described for the preparation of compound **75**.

Yield 0.39 g, 65% (white powder).

Transition temperatures ($^{\circ}\text{C}$): Cr 60.4 SmC 126.5 I.

^1H NMR (400 MHz) δ (CDCl_3): 0.87 (9 H, s), 0.89 (3 H, t, J 6.3), 1.15-1.37 (18 H, m), -1.50 (2 H, quintet, J 7.6), 1.65 (2 H, quintet, J 7.4), 1.82 (2 H, quintet, J 6.9), 2.69 (2 H, t, 7.4), 4.00 (2 H, t, J 6.3), 6.98-7.02 (3 H, m), 7.12-7.16 (1 H, m), 7.57-7.65 (3 x 2 H, d).

$\nu_{\max}(\text{KCl})$: 2880, 2865, 1460, 1250, 820 cm^{-1} .

m/z : 548 (M^+), 536, 408 (100%), 295, 73.

Scheme 9

6-(4'-Bromobiphenyl-4-yl)hexyl toluene-*p*-sulphonate (77)

A solution of compound 30 (5.00 g, 0.0143 mol) in DCM (166 ml) and pyridine (33 ml) was cooled to $-5\text{ }^{\circ}\text{C}$. Toluene-*p*-sulphonylchloride (3.00 g, 0.0160 mol) was slowly added to the stirred solution which was left to react overnight. The reaction mixture was treated with ice (10 g) and left stirring for 1 h. The reaction mixture was washed with ice cold sulphuric acid and water and the organic layer was then dried (MgSO_4). The solvent was removed *in vacuo* and the residue was purified by column chromatography [DCM] to give a white powder.

Yield 5.70 g, 80%.

$^1\text{H NMR}$ (400 MHz) δ (CDCl_3): 1.35-1.48 (4 H; m), 1.68 (2 H, quintet, J 6.2), 1.75 (2 H, quintet, J 5.8), 2.44 (3 H, s), 3.95 (2 H, t, J 6.2), 4.04 (2 H, t, J 5.8), 6.93 (2 H, d), 7.33 (2 H, d), 7.40 (2 H, d), 7.48 (2 H, d), 7.52 (2 H, d), 7.79 (2 H, d).

ν_{max} (KCl): 2980, 1605, 1490, 1300, 1260, 1080, 1000, 1060, 820, 680 cm^{-1} .

4-Bromo-4'-[6-(cyclobutylmethoxy)hexyloxy]biphenyl (78)

A solution of compound 77 (2.50 g, 5.0 mmol) in DMSO (50 ml) was cooled to $-5\text{ }^{\circ}\text{C}$ and potassium hydroxide powder (Fluka, 1.03 g, 0.018 mol) was added and the mixture was stirred using a mechanical stirrer, a solution of cyclobutylmethanol (0.80 g, 10.0 mmol) in DMSO (15 ml) was added dropwise. The reaction mixture was kept at $-5\text{ }^{\circ}\text{C}$ for 1 h and then removed from the cooling bath for a further 2 h. The product was extracted in hexane (150 ml) and washed with water in order to remove all traces of DMSO. Hexane was removed under reduced pressure and the residue was purified by column chromatography [DCM-hexane, 1:6] to give a white powder.

Yield 1.55 g, 75%; mp 101-102 $^{\circ}\text{C}$.

$^1\text{H NMR}$ (400 MHz) δ (CDCl_3): 1.37-1.96 (8 H, m), 2.00-2.11 (5 H, m), 2.56 (2 H, m), 3.29 (2 H, d, J 7.6), 3.42 (2 H, t, J 7.6), 4.00 (2 H, t, J 5.7), 6.95 (2 H, d), 7.40 (2 H, d), 7.46 (2 H, d), 7.52 (2 H, d).

ν_{max} (KCl): 2980, 2880, 1605, 1490, 820 cm^{-1} .

m/z : 418/416 (M^+), 348, 337, 250/248, 169.

4''-[6-(Cyclobutylmethoxy)hexyloxy]-2,3-difluoro-4-octyloxyterphenyl (79)

Compound 78 (0.70 g, 1.7 mmol) and a 2M-aqueous solution of sodium carbonate (40 ml) were mixed in DME (60 ml) and with tetrakis(triphenylphosphine)-palladium(0) (0.12 g, 0.12 mmol) under dry nitrogen; to which compound 5 (0.58 g, 2.0 mmol) was added. The stirred reaction mixture was heated under reflux overnight. The product was extracted into DCM and washed with brine, water and dried (MgSO_4). The solvent was removed under reduced pressure and the residue was purified by column chromatography [DCM-hexane, 1:5] and recrystallised from hexane to give white crystals.

Yield 0.70 g, 72%.

Transition temperatures ($^{\circ}\text{C}$): Cr 92.5 SmC 148.1 I.

$^1\text{H NMR}$ (400 MHz) δ (CDCl_3): 0.88 (3 H, t, J 7.1), 1.22-1.52 (14 H, m), 1.57 (2 H, quintet, J 7.1), 1.68-1.91 (8 H, m), 1.96-2.05 (2 H, m), 2.51 (1 H, ht, J 7.3), 3.36 (2 H, d, J 7.3), 3.38 (2 H, t, J 6.8), 4.00 (2 H, t, J 6.2), 4.07 (2 H, t, J 6.2), 6.81-6.86 (1 H, m), 6.96 (2 H, d, J 8.3), 7.13-7.18 (1 H, m), 7.53-7.57 (4 H, m), 7.61-7.64 (2 H, m).

$\nu_{\text{max}}(\text{KCl})$: 2980, 2880, 1500, 1470, 1310, 1260, 1120, 1080, 800 cm^{-1} .

m/z : 578(M^+), 482, 370, 298, 101 (100%).

Scheme 10

4-Bromo-4'-(6-bromohexyloxy)biphenyl (80)

A solution of triphenylphosphine (3.46 g, 0.013 mol) and DEAD (2.30 g, 0.012 mol) in dry cold THF (100 ml) was added dropwise over 10 min to a solution of compound **12** (3.00 g, 0.012 mol) and compound **29** (2.20 g, 0.012 mol) in dry THF (50 ml) stirring at room temperature. The reaction mixture was left stirring overnight. The reaction product was extracted into diethyl ether (2 x 200 ml), and the combined ethereal solutions were washed with water and dried (MgSO₄). The crude product was adsorbed onto silica gel and purified by column chromatography [DCM-petroleum fraction (bp 40-60 °C), 1:6] and recrystallised from ethanol to give white crystals.

Yield 3.25 g, 60%; mp 109-110 °C.

¹H NMR (270 MHz) δ (CDCl₃): 1.47-1.62 (4 H, m), 1.75-2.00 (4 H, m), 3.43 (2 H, t, J 6.3), 4.00 (2 H, t, J 5.9), 6.87-7.01 (2 H, d), 7.37-7.57 (3 x 2 H, d).

ν_{\max} (KCl): 2980, 1605, 1480, 1000, 810 cm⁻¹.

m/z: 414/412/410 (M⁺), 334/332/330, 250/248, 57 (100%).

4''-(6-Bromohexyloxy)-2,3-difluoro-4-octyloxyterphenyl (81)

Compound **80** (1.02 g, 2.5 mmol) and a 2M-aqueous solution of sodium carbonate (40 ml) were mixed in DME (60 ml) with tetrakis(triphenylphosphine)palladium(0) (0.12 g, 0.12 mmol) under dry nitrogen and compound **5** (0.85 g, 3.0 mmol) was added. The stirred reaction mixture was heated under reflux overnight. The product was extracted into DCM (100 ml) and washed with brine and water and dried (MgSO₄). The solvent was removed under reduced pressure and the residue was purified by column chromatography [DCM-hexane, 1:5] and recrystallised from hexane to give a white powder.

Yield 0.80 g, 70%.

Transition temperatures (°C): Cr 100.7 SmA 117.8 I.

¹H NMR (400 MHz) δ (CDCl₃): 0.89 (3 H, t, J 6.8), 1.23-1.42 (8 H, m), 1.44-1.60 (6 H, m), 1.78-1.94 (6 H, m), 3.44 (2 H, t, J 6.8), 4.02 (2 H, t, J 6.7), 4.09 (2 H, t, J 6.7), 6.78-6.84 (1 H, m), 6.98 (2 H, d), 7.10-7.16 (1 H, m), 7.54-7.57 (2 x 2 H, d), 7.63 (2 H, d).

ν_{\max} (KCl): 2970, 2880, 1500, 1470, 1310, 1260, 1080, 800 cm⁻¹.

m/z : 574/572 (M^+), 460, 298, 269, 71.

2,3-Difluoro-4''-[6-(3-methyloxetan-3-ylmethoxy)hexyloxy]-4-octyloxyterphenyl (82)

A solution of compound **81** (0.70 g, 1.7 mmol) in diethyl ether (50 ml) was cooled to 0 °C in an ice bath with a sodium hydroxide aqueous solution (50 ml of solution prepared by mixing 50 g of sodium hydroxide and 100 ml of water) and *t*-butylammonium bromide (0.10 g used as phase transfer catalyst), to which a solution of 3-(hydroxymethyl)-3-methyloxetane (0.50 g, 5.0 mmol) in hexane (70 ml) was added dropwise over 1 h with vigorous mechanical stirring. The reaction mixture was allowed to warm to room temperature and left stirring for 2 h, then the reaction mixture was heated under reflux for 4 h. The organic layer was collected, dried ($MgSO_4$) and the solvent was removed in vacuo. The crude oil was purified by column chromatography [DCM-petroleum fraction (bp 40-60 °C), 1:5] to give a white powder.

Yield 0.66 g, 66%.

Transition temperatures (°C): Cr 97.7 SmC 124.8 N 137.8 I.

1H NMR (400 MHz) δ ($CDCl_3$): 0.93 (3 H, t, J 6.8), 1.22-1.42 (13 H, m), 1.43-1.57 (6 H, m), 1.77-1.90 (4 H, m), 3.47-3.53 (4 H, m), 4.02 (2 H, t, J 7.3), 4.08 (2 H, t, J 7.3), 4.30 (2 H, t, J 6.2), 4.52 (2 H, t, J 6.2), 6.77-6.85 (1 H, m), 6.97 (2 H, d), 7.10-7.16 (1 H, m), 7.52-7.59 (2 x 2 H, d), 7.63 (2 H, d).

$\nu_{max}(KCl)$: 2932, 2854, 1635, 1606, 1500, 1469, 1080, 800 cm^{-1} .

m/z : 594 (M^+), 410, 297, 269, 55.

Scheme 11

1-Bromo-4-propyloxybutane (87)

A solution of compound **83** (10.0 g, 0.043 mol) in hexane (80 ml) was cooled at 0 °C with a sodium hydroxide aqueous solution (150 ml of solution prepared by mixing 75 g of sodium hydroxide and 150 ml of water) and *tert*-butylammonium bromide (4 mol %, 0.35 g, 1.7 mmol used as phase transfer catalyst), and a solution of compound **84** (1.27 g, 0.022 mol) in hexane (70 ml) was added dropwise over 1 h with vigorous mechanical stirring. The reaction mixture was allowed to warm to room temperature and left stirring for 2 h, the reaction mixture was then heated under reflux for 4 h. The organic layer was collected and dried (MgSO₄) and the solvent was removed *in vacuo*. The crude oil was purified by column chromatography [DCM-petroleum fraction (bp 40-60 °C), 1:5] to give a colourless oil.

Yield 2.35 g, 61%.

¹H NMR (270 MHz) δ (CDCl₃): 0.93 (3 H, t, J 4.9), 1.58 (2 H, sextet, J 4.9), 1.66-1.78 (2 H, m), 1.88-2.02 (4 H, m), 3.35 (2 H, t, J 4.2), 3.40-3.49 (2 H, m).

ν_{\max} (KCl): 2980, 2890, 1450, 1260, 1120 cm⁻¹.

m/z: 137, 79, 43 (100%).

Compounds **88** and **89** were prepared following a similar procedure to that described for the preparation of compound **87**.

1-Bromo-4-(1,2-dimethylpropyloxy)butane (88)

Quantities: compound **83** (19.2 g, 0.090 mol), compound **85** (3.93 g, 0.044 mol) and *tert*-butylammonium bromide (0.68 g, 4.4 mmol).

Yield 4.46 g, 45% (colourless oil).

¹H NMR (270 MHz) δ (CDCl₃): 0.86 (3 H, d, J 7.3), 0.89 (3 H, d, J 7.3), 1.06 (3 H, d, J 6.4), 1.60-1.75 (2 H, m), 1.95-2.00 (3 H, m), 3.10 (1 H, quintet, J 6.4), 3.31-3.37 (1 H, m), 3.45 (2 H, t, J 6.4), 3.49-3.55 (1 H, m).

ν_{\max} (KCl): 2980, 2880, 1480, 1460, 1380, 1260, 1110 cm⁻¹.

m/z: 137, 71, 67, 56 (100%).

1-Bromo-4-(1,2,2-trimethylpropyloxy)butane (89)

Quantities: compound **83** (42.4 g, 0.196 mol), compound **86** (9.1 g, 0.090 mol) and *tert*-butylammonium bromide (0.68 g, 4.4 mmol).

Yield 7.40 g, 35% (colourless oil).

$^1\text{H NMR}$ (270 MHz) δ (CDCl_3): 0.85 (9 H, s), 1.10 (3 H, d, J 6.7), 1.63-1.74 (2 H, m), 1.81-1.98 (2 H, m), 3.10 (1 H, q, J 6.7), 3.32 (1 H, dt, J 6.3), 3.44 (1 H, dt, J 6.3), 3.50 (2 H, t, J 4.3).

ν_{max} (KCl): 2980, 2890, 1495, 1460, 1380, 1260, 1110 cm^{-1} .

m/z : 137, 109, 87, 69, 57 (100%).

4-Bromo-4'-(4-propyloxybutyloxy)biphenyl (90)

A solution of compound **12** (2.15 g, 0.011 mol) in butanone (80 ml) was added at room temperature to a stirring mixture of compound **87** (2.50 g, 0.010 mol) and potassium carbonate (3.80 g, 0.020 mol) in butanone (70 ml) and the reaction mixture was heated under reflux for 48 h. Potassium carbonate was filtered off and the solvent was removed *in vacuo*, the residue was dissolved in diethyl ether (250 ml) and washed with water (2 x 150 ml) and dried (MgSO_4). The solvent was removed *in vacuo* and the residue was purified by column chromatography [DCM-hexane, 1:8] and recrystallised from ethanol to give a white powder.

Yield 2.45 g, 67%; mp 116-117 $^{\circ}\text{C}$.

$^1\text{H NMR}$ (270 MHz) δ (CDCl_3): 0.93 (3 H, t, J 7.2), 1.59 (2 H, sextet, J 7.2), 1.73-1.79 (2 H, m), 1.85-1.92 (2 H, m), 3.38 (2 H, t, J 6.4), 3.48 (2 H, t, J 6.4), 4.02 (2 H, t, J 6.4), 6.95 (2 H, d), 7.39 (2 H, d), 7.46 (2 H, d), 7.51 (2 H, d).

ν_{max} (KCl): 2980, 2880, 1610, 1495, 1260, 1120, 820, 500 cm^{-1} .

m/z : 364/362 (M^+), 250/248 (100%), 168, 139, 115.

Compounds **91** and **92** were prepared following a similar procedure to that described for the preparation of compound **90**.

4-Bromo-4'-[4-(1,2-dimethylpropyloxy)butyloxy]biphenyl (91)

Quantities: compound **88** (1.20 g, 5.4 mmol), compound **12** (1.34 g, 5.4 mmol) and potassium carbonate (2.24 g, 0.023 mol).

Yield 1.25 g, 60%; mp 115-116 $^{\circ}\text{C}$ (white crystals).

$^1\text{H NMR}$ (400 MHz) δ (CDCl_3): 0.87 (6 H, d, J 6.5), 0.91 (3 H, d, J 6.5), 1.66-1.81 (3 H, m), 1.82-1.97 (2 H, m), 3.12 (1 H, q, J 4.6), 3.34-3.45 (1 H, m), 3.52-3.63 (1 H, m), 4.05 (2 H, t, J 6.4), 6.95 (2 H, d), 7.40 (2 H, d), 7.52 (2 H, d) 7.60 (2 H, d).

$\nu_{\text{max}}(\text{KCl})$: 2990, 2880, 1610, 1490, 1295, 1260, 1120, 1060, 820, 500 cm^{-1} .

m/z : 392/390 (M^+), 305, 263, 250/248 (100%), 152, 139.

4-Bromo-4'-[4-(1,2,2-trimethylpropyloxy)butyloxy]biphenyl (92)

Quantities: compound **89** (2.00 g, 8.5 mmol), compound **12** (2.10 g, 8.5 mmol), and potassium carbonate (3.51 g, 0.0254 mol).

Yield 2.24 g, 65%; mp 114-115 $^{\circ}\text{C}$ (white powder).

$^1\text{H NMR}$ (400 MHz) δ (CDCl_3): 0.88 (9 H, s), 1.05 (3 H, d, J 5.7), 1.73 (2 H, q, J 6.9), 1.83-1.95 (2 H, m), 2.97 (1 H, q, J 5.7), 3.31 (1 H, dt, J 6.2), 3.64 (1 H, dt, J 6.2), 4.03 (2 H, t, J 6.4), 6.96 (2 H, d), 7.42 (2 H, d), 7.47 (2 H, d) 7.52 (2 H, d).

$\nu_{\text{max}}(\text{KCl})$: 2990, 2880, 1610, 1490, 1295, 1260, 1120, 1060, 820, 500 cm^{-1} .

m/z : 406/404 (M^+), 305, 263, 247, 152 (100%), 85.

Scheme 12

2-(1-Methylpropyloxy)tetrahydrofuran (98)

Toluene-*p*-sulphonic acid (0.1 g) was added to a solution of compound 93 (14.3 g, 0.143 mol) and compound 94 (9.63 g, 0.130 mol) in dry THF (100 ml) and left stirring for ½ h at room temperature. The reaction mixture was then heated under reflux for 1½ h; the solution was cooled and neutralised with methanolic sodium methoxide. The resulting solid was filtered off and THF was removed *in vacuo* from the filtrate. The residue was distilled under reduced pressure to give a colourless oil.

Yield 12.5 g, 66.7%; bp 80 °C at 25 mmHg.

¹H NMR (400 MHz) δ (CDCl₃): 0.85-1.07 (3 H, m), 1.11 (1.5 H, d, J 6.2), 1.17 (1.5 H, d, J 6.2), 1.36-1.58 (2 H, m), 1.77-2.07 (4 H, m), 3.56-3.69 (1 H, m), 3.81-3.95 (2 H, m), 5.19-5.28 (1 H, m).

ν_{\max} (KCl): 2990, 2880, 1460, 1380, 1190, 1110, 920 cm⁻¹.

m/z: 128, 65, 58 (100%).

Compounds 99, 100, and 101 were prepared following a similar procedure to that described for the preparation of compound 98.

2-(2-Methylpropyloxy)tetrahydrofuran (99)

Quantities: compound 93 (10.0 g, 0.143 mol), compound 95 (9.63 g, 0.130 mol), and toluene-*p*-sulphonic acid (0.1 g).

Yield 11.9 g, 64% (colourless oil).

¹H NMR (400 MHz) δ (CDCl₃): 0.88 (3 H, d, J 0.9), 0.90 (3 H, d, J 0.90), 1.76-1.94 (4 H, m), 1.95-2.05 (1 H, m), 3.14 (1 H, dd, J 7.6), 3.41 (1 H, dd, J 7.6), 3.82-3.91 (2 H, m), 5.09 (1 H, dd, J 6.5).

ν_{\max} (KCl): 2990, 2880, 1460, 1380, 1340, 1190, 1110, 1080, 1040, 920 cm⁻¹.

m/z: 128, 65, 58 (100%).

2-(1,1-Dimethylpropyloxy)tetrahydrofuran (100)

Quantities: compound 93 (10.0 g, 0.143 mol), compound 96 (11.4 g, 0.130 mol), and toluene-*p*-sulphonic acid (0.1 g).

Yield 12.7 g, 62%. (colourless oil).

$^1\text{H NMR}$ (400 MHz) δ (CDCl_3): 0.87 (3 H, t, J 7.1), 1.18 (3 H, s), 1.20 (3 H, s), 1.52 (2 H, q, J 7.1), 1.76-2.23 (4 H, m), 3.73-3.83 (1 H, m), 3.88-3.98 (1 H, m), 5.38 (1 H, dd, J 6.1).

ν_{max} (KCl): 2990, 2980, 1480, 1380, 1190, 1040, 910 cm^{-1} .

m/z : 158 (M^+), 141, 72 (100%).

2-(2,2-dimethylpropyloxy)tetrahydrofuran (101)

Quantities: compound **93** (5.43 g, 0.077 mol), compound **97** (5.70 g, 0.065 mol), and toluene-*p*-sulphonic acid (0.1 g).

Yield 7.0 g, 67% (colourless oil).

$^1\text{H NMR}$ (400 MHz) δ (CDCl_3): 0.89 (9 H, s), 1.76-2.23 (4 H, m), 2.99 (1 H, d, J 9.0), 3.45 (1 H, d, J 9.0), 3.81-3.91 (2 H, m), 5.04-5.11 (1 H, m).

ν_{max} (KCl): 2990, 1490, 1390, 1100, 1050 cm^{-1} .

m/z : 158 (M^+), 142, 71 (100%).

4-(1-Methylpropyloxy)butan-1-ol (102)

A solution of aluminium chloride (18.7 g, 0.140 mol) in dry diethyl ether (300 ml) was cooled to 0 °C and lithium aluminium hydride 1M in diethyl ether (35.0 ml, 0.035 mol) was added and stirred for 30 min. A solution of compound **98** (10.0 g, 0.070 mol) in dry diethyl ether (50 ml) was added over 30 min to the reaction mixture which was left stirring to reach room temperature. The reaction mixture was then heated under reflux for 2 h, cooled in an ice bath and water was added to destroy any unreacted hydride; 10% aqueous sulphuric acid was added until two clear layers were obtained. The two layers were separated, the aqueous was washed with diethyl ether (150 ml) and the combined ethereal solutions were then dried (MgSO_4). The solvent was removed *in vacuo* and the residue obtained was distilled to give a colourless oil.

Yield 6.0 g, 60%; bp 208-212 °C.

$^1\text{H NMR}$ (400 MHz) δ (CDCl_3): 0.83 (3 H, t, J 8.0), 1.06 (3 H, d, J 6.4), 1.31-1.51 (2 H, m), 1.56-1.62 (4 H, m), 3.12 (1 H, s), 3.22-3.31 (1 H, m), 3.30-3.35 (1 H, m), 3.40-3.46 (1 H, m), 3.53-3.56 (2 H, m).

ν_{max} (KCl): 3400, 2980, 1450, 1360, 1060 cm^{-1} .

m/z : 146 (M^+), 69, 57 (100%).

Compounds **103**, **104** and **105** were prepared following a similar procedure to that described for the preparation of compound **102**.

4-(2-Methylpropyloxy)butanol (**103**)

Quantities: compound **99** (10.0 g, 0.070), aluminium chloride (18.7 g, 0.1400 mol), and 1M-lithium aluminium hydride in diethyl ether (35.0 ml, 0.035 mol).

Yield 5.80 g, 58%; bp 206-209 °C (colourless oil).

$^1\text{H NMR}$ (400 MHz) $\delta(\text{CDCl}_3)$: 0.89 (6 H, d, J 3.2), 1.64-1.69 (4 H, m), 1.81-1.91 (1 H, m), 3.14 (1 H, s), 3.20 (2 H, d, J 5.6), 3.45 (2 H, t, J 5.6), 3.62 (2 H, t, J 5.6).

$\nu_{\text{max}}(\text{KCl})$: 3400, 3980, 1460, 1380, 1080 cm^{-1} .

m/z : 146 (M^+), 70, 56 (100%).

4-(1,1-Dimethylpropyloxy)butanol (**104**)

Quantities: compound **100** (10.0 g, 0.063 mol), aluminium chloride (16.9 g, 0.127 mol), and 1M-lithium aluminium hydride in diethyl ether (31.6 ml, 0.032 mol).

Yield 5.30 g, 53%; bp 214-218 °C (colourless oil).

$^1\text{H NMR}$ (400 MHz) $\delta(\text{CDCl}_3)$: 0.87 (3 H, t, J 5.6), 1.15 (6 H, s), 1.50 (2 H, quintet, J 5.6), 1.65-1.68 (4 H, m), 3.35-3.38 (3 H, m), 3.60 (2 H, m).

$\nu_{\text{max}}(\text{KCl})$: 3400, 2980, 1480, 1380, 1190, 1090 cm^{-1} .

m/z : 160 (M^+), 143, 86 (100%).

4-(2,2-Dimethylpropyloxy)butanol (**105**)

Quantities: compound **101** (6.00 g, 0.038 mol), aluminium chloride (10.1 g, 0.076 mol), and 1M-lithium aluminium hydride in diethyl ether (19.0 ml, 1.9 mmol).

Yield 4.00 g, 66%; bp 200-205 °C (colourless oil).

$^1\text{H NMR}$ (400 MHz) $\delta(\text{CDCl}_3)$: 0.91 (9 H, s), 1.62-1.74 (4 H, m), 2.82 (1 H, s), 3.10 (2 H, s), 3.46 (2 H, t, J 5.6), 3.65 (2 H, t, J 5.6).

$\nu_{\text{max}}(\text{KCl})$: 3400, 2980, 2890, 1490, 1380, 1120, 1060 cm^{-1} .

m/z : 160 (M^+), 143, 102, 86.

4-Bromo-4'-[4-(1-methylpropyloxy)butyloxy]biphenyl (106)

A solution of triphenylphosphine (3.46 g, 0.013 mol) and DEAD (2.30 g, 0.012 mol) in dry cold THF (100 ml) was added dropwise over ten min to a solution of compound **12** (3.00 g, 0.012 mol) and compound **102** (1.76 g, 0.012 mol) in dry THF (75 ml) stirring at room temperature. The reaction mixture was left stirring overnight. The reaction product was extracted into diethyl ether (2 x 200 ml), and the combined ethereal solutions were washed with water and dried (MgSO_4). The crude product was adsorbed onto silica gel and purified by column chromatography [DCM-petroleum fraction (bp 40-60 °C), 1:3] and recrystallised from ethanol to give white powder.

Yield 2.80 g, 60%; mp 112-113 °C.

$^1\text{H NMR}$ (400 MHz) δ (CDCl_3): 0.91 (3 H, t, J 7.2), 1.12 (3 H, d, J 5.6), 1.38-1.58 (2 H, m), 1.71-1.78 (2 H, m), 1.86-1.93 (2 H, m), 3.31 (1 H, sextet, J 6.4), 3.39-3.45 (1 H, m), 3.52-3.57 (1 H, m), 4.02 (2 H, t, J 6.4), 6.94 (2 H, d), 7.39 (2 H, d), 7.46 (2 H, d), 7.51 (2 H, d).

ν_{max} (KCl): 2980, 2880, 1605, 1490, 1120, 820, 500 cm^{-1} .

m/z : 378/376 (M^+), 304, 250/248, 129, 57 (100%).

Compounds **107**, **108** and **109** were prepared following a similar procedure to that described for the preparation of compound **106**.

4-Bromo-4'-[4-(2-methylpropyloxy)butyloxy]biphenyl (107)

Quantities: triphenylphosphine (3.46 g, 0.013 mol), DEAD (2.30 g, 0.013 mol), compound **12** (3.00 g, 0.012 mol), and compound **103** (1.76 g, 0.012 mol).

Yield 2.91 g, 62%; mp 115-116 °C (white powder).

$^1\text{H NMR}$ (400 MHz) δ (CDCl_3): 0.91 (6 H, d, J 7.0), 1.72-1.93 (5 H, m), 3.18 (2 H, t, J 6.4), 3.48 (2 H, t, J 6.4), 4.03 (2 H, t, J 6.4), 6.96 (2 H, d), 7.40 (2 H, d), 7.46 (2 H, d), 7.52 (2 H, d).

ν_{max} (KCl): 2980, 2880, 1610, 1495, 1290, 1260, 1120, 1110 cm^{-1} .

m/z : 378/376 (M^+), 305, 263, 250/248 (100%), 152, 129.

4-Bromo-4'-[4-(1,1-dimethylpropyloxy)butyloxy]biphenyl (108)

Quantities: triphenylphosphine (3.46 g, 0.013 mol), DEAD (2.30 g, 0.013 mol), compound **12** (3.00 g, 0.012 mol), and compound **104** (1.76 g, 0.012 mol).

Yield 2.91 g, 62%; mp 112-113 °C (white powder).

$^1\text{H NMR}$ (400 MHz) δ (CDCl_3): 0.91 (9 H, s), 1.76 (2 H, quintet, J 5.6), 1.89 (2 H, quintet, J 5.6), 3.07 (2 H, s), 3.48 (2 H, t, J 6.3), 4.03 (2 H, t, J 6.4), 6.96 (2 H, d), 7.41 (2 H, d), 7.47 (2 H, d), 7.53 (2 H, d).

ν_{max} (KCl): 2980, 2880, 1610, 1490, 1400, 1300, 1260, 1120, 820, 500 cm^{-1} .

m/z : 392/390 (M^+), 370, 305/303, 286, 250/248 (100%), 221, 219, 157.

4-Bromo-4'-[4-(2,2-dimethylpropyloxy)butyloxy]biphenyl (109)

Quantities: triphenylphosphine (3.14 g, 0.012 mol), DEAD (2.10 g, 0.012 mol), compound **12** (3.00 g, 0.012 mol), and compound **105** (1.76 g, 0.012 mol).

Yield 2.00 g, 41%; mp 112-113 °C (white powder).

$^1\text{H NMR}$ (400 MHz) δ (CDCl_3): 0.87 (3 H, t, J 7.3), 1.13 (6 H, s), 1.49 (2 H, q, J 7.2), 1.71 (2 H, quintet, J 5.6), 1.89 (2 H, quintet, J 5.6), 3.37 (2 H, t, J 6.4), 4.02 (2 H, t, J 6.4), 6.96 (2 H, d), 7.41 (2 H, d), 7.47 (2 H, d), 7.51 (2 H, d).

ν_{max} (KCl): 2980, 2880, 1610, 1495, 1290, 1260, 1120, 820, 500 cm^{-1} .

m/z : 392/390 (M^+), 305/303, 265/263, 250/248 (100%), 151, 139.

Scheme 13

2,3-Difluoro-4-octyloxy-4''-(4-propyloxybutyloxy)terphenyl (110)

Compound **90** (0.90 g, 2.5 mmol), and a 2M-aqueous solution of sodium carbonate (40 ml), were mixed in TBME (60 ml), and tetrakis(triphenylphosphine)palladium(0) (0.12 g, 0.12 mmol) under dry nitrogen and compound **5** (0.85 g, 3.0 mmol) were added to the reaction mixture. The stirred reaction mixture was heated under reflux overnight. The product was extracted into DCM (100 ml) and washed with brine, water and dried (MgSO₄). The solvent was removed under reduced pressure and the residue was purified by column chromatography [DCM-hexane, 1:5] and recrystallised from hexane to give white powder.

Yield 0.80 g, 60%.

Transition temperatures (°C): Cr 104.5 SmC 158.8 N 162.3 I.

¹H NMR (400 MHz) δ (CDCl₃): 0.87-0.96 (6 H, m), 1.23-1.37 (8 H, m), 1.47 (2 H, quintet, J 6.8), 1.62 (2 H, sextet, J 7.2), 1.73-1.94 (6 H, m), 3.39 (2 H, t, J 6.8), 3.49 (2 H, t, J 6.6), 4.04 (2 H, t, J 6.6), 4.08 (2 H, t, J 6.8), 6.77-6.84 (1 H, m), 6.96 (2 H, d), 7.10-7.17 (1 H, m), 7.51-7.57 (2 x 2 H, d), 7.63 (2 H, d).

ν_{\max} (KCl): 2980, 2960, 2880, 1500, 1480, 1310, 1260, 1120, 1080, 800 cm⁻¹.

m/z: 524 (M⁺), 465, 409, 297 (100%), 115.

Compounds **111**, **112**, **113**, **114**, **115**, **116**, **117**, **118**, **119**, and **120** were prepared following a procedure similar to that described for the preparation of compound **110**.

4''-[4-(1,2-Dimethylpropyloxy)butyloxy]-2,3-difluoro-4-octyloxyterphenyl (111)

Quantities: compound **91** (0.70 g, 1.8 mmol), tetrakis(triphenylphosphine)-palladium(0) (0.12 g, 0.12 mmol), and compound **5** (0.62 g, 2.1 mmol).

Yield 0.52 g, 55% (white powder).

Transition temperatures (°C): Cr 84.5 SmC 142.8 I.

¹H NMR (400 MHz) δ (CDCl₃): 0.84-0.94 (9 H, m), 1.08 (3 H, m), 1.22-1.50 (15 H, m), 1.65-1.96 (2 H, m), 3.14 (1 H, q, J 5.8), 3.36-3.46 (1 H, m), 3.56-3.66 (1 H, m), 4.04 (2 H, t, J 6.4), 4.08 (2 H, t, J 6.4), 6.78-6.86 (1 H, m), 6.98 (2 H, d), 7.08-7.18 (1 H, m), 7.52-7.66 (3 x 2 H, d).

ν_{\max} (KCl): 2980, 2960, 2880, 1500, 1480, 1310, 1260, 1120, 1080, 800 cm⁻¹.

m/z: 552 (M⁺), 465, 410, 352, 298 (100%), 280, 251, 176, 143, 115, 73 (100%).

2,3-Difluoro-4-octyloxy-4''-[4-(1,2,2-trimethylpropyloxy)butyloxy]terphenyl (112)

Quantities: compound **92** (0.60 g, 1.5 mmol), tetrakis(triphenylphosphine)-palladium(0) (0.12 g, 0.12 mmol), and compound **5** (0.52 g, 1.8 mmol).

Yield 0.55 g, 65% (white powder).

Transition temperatures (°C): Cr 88.7 SmC 139.4 I.

¹H NMR (400 MHz) δ (CDCl₃): 0.85-0.95 (12 H, m), 1.05 (3 H, d, J 6.7), 1.24-1.42 (6 H, m), 1.44-1.53 (4 H, m), 1.73 (2 H, quintet, J 6.9), 1.80-1.97 (4 H, m), 2.98 (1 H, q, J 6.1), 3.32 (1 H, dt, J 6.3), 3.64 (1 H, dt, J 6.3), 4.04 (2 H, t, J 6.7), 4.08 (2 H, t, J 6.7), 6.78-6.84 (1 H, m), 6.98 (2 H, d), 7.10-7.16 (1 H, m), 7.51-7.57 (2 x 2 H, d), 7.63 (2 H, d).

ν_{\max} (KCl): 2980, 2960, 2880, 1500, 1470, 1500, 1260, 1115, 1080, 820, 800 cm⁻¹.

m/z: 566 (M⁺), 465, 409, 298 (100%), 157.

2,3-Difluoro-4''-[4-(1-methylpropyloxy)butyloxy]-4-octyloxyterphenyl (113)

Quantities: compound **106** (0.60 g, 1.6 mmol), tetrakis(triphenylphosphine)-palladium(0) (0.12 g, 0.12 mmol), and compound **5** (0.52 g, 1.8 mmol).

Yield 0.49 g, 57% (white powder).

Transition temperatures (°C): Cr 99.7 SmC 155.5 I.

¹H NMR (400 MHz) δ (CDCl₃): 0.87-0.94 (6 H, m), 1.13 (3 H, d, J 6.1), 1.29-1.35 (8 H, m), 1.40-1.60 (4 H, m), 1.75 (2 H, quintet, J 6.1), 1.81-1.93 (4 H, m), 3.31 (1 H, sextet, J 6.1), 3.46 (1 H, dt, J 6.1), 3.56 (1 H, dt, J 6.1), 4.04 (2 H, t, J 6.5), 4.08 (2 H, t, J 6.5), 6.78-6.83 (1 H, m), 6.98 (2 H, d), 7.10-7.16 (1 H, m), 7.54-7.57 (2 x 2 H, d), 7.64 (2 H, d).

ν_{\max} (KCl): 2980, 2880, 1610, 1500, 1480, 1310, 1260, 1080, 810, 800 cm⁻¹.

m/z: 538 (M⁺), 465, 439, 409, 143 (100%).

2,3-Difluoro-4''-[4-(2-methylpropyloxy)butyloxy]-4-octyloxyterphenyl (114)

Quantities: compound **107** (0.60 g, 1.5 mmol), tetrakis(triphenylphosphine)-palladium(0) (0.12 g, 0.12 mmol), and compound **5** (0.52 g, 1.8 mmol).

Yield 0.55 g, 65% (white powder).

Transition temperatures (°C): Cr 92.0 SmC 148.7 I.

¹H NMR (400 MHz) δ (CDCl₃): 0.88 (3 H, d, J 7.3), 0.91 (6 H, d, J 6.4), 1.30-1.54 (10 H, m), 1.73-1.94 (7 H, m), 3.20 (2 H, d, J 6.8), 3.49 (2 H, t, J 6.2), 4.04 (2 H, t, J

6.9), 4.08 (2 H, t, J 6.6), 6.78-6.83 (1 H, m), 6.98 (2 H, d), 7.11-7.16 (1 H, m), 7.52-7.58 (2 x 2 H, d), 7.63 (2 H, d).

$\nu_{\max}(\text{KCl})$: 2980, 2940, 2880, 1500, 1470, 1300, 1260, 1115, 1080, 820, 800 cm^{-1} .

m/z : 538 (M^+), 465, 297, 250, 129, 73 (100%), 57.

4''-[4-(1,1-Dimethylpropyloxy)butyloxy]-2,3-difluoro-4-octyloxyterphenyl (115)

Quantities: compound **108** (0.70 g, 1.8 mmol), tetrakis(triphenylphosphine)-palladium(0) (0.12 g, 0.12 mmol), and compound **5** (0.67 g, 2.3 mol).

Yield 0.55 g, 55% (white powder).

Transition temperatures ($^{\circ}\text{C}$): Cr 82.6 SmC 138.2 I.

$^1\text{H NMR}$ (400 MHz) δ (CDCl_3): 0.84-0.92 (6 H, m), 1.14 (6 H, s), 1.29-1.35 (8 H, m), 1.44-1.56 (4 H, m), 1.71 (2 H, quintet, J 6.1), 1.80-1.93 (4 H, m), 3.38 (2 H, t, J 6.3), 4.03 (2 H, t, J 6.0), 4.08 (2 H, t, J 6.0), 6.78-6.83 (1 H, m), 6.98 (2 H, d), 7.10-7.16 (1 H, m), 7.53-7.57 (2 x 2 H, m), 7.63 (2 H, d).

$\nu_{\max}(\text{KCl})$: 2980, 2860, 1500, 1470, 1300, 1260, 1080, 800 cm^{-1} .

m/z : 552 (M^+), 439 (100%), 409, 143.

4''-[4-(2,2-Dimethylpropyloxy)butyloxy]-2,3-difluoro-4-octyloxyterphenyl (116)

Quantities: compound **109** (0.68 g, 1.7 mmol), tetrakis(triphenylphosphine)-palladium(0) (0.12 g, 0.12 mmol), and compound **5** (0.60 g, 2.1 mmol).

Yield 0.64 g, 68% (white powder).

Transition temperatures ($^{\circ}\text{C}$): Cr 87.6 SmC 148.6 I.

$^1\text{H NMR}$ (400 MHz) δ (CDCl_3): 0.87 (3 H, t, J 6.9), 0.91 (9 H, s), 1.29-1.35 (8 H, m), 1.43-1.52 (2 H, m), 1.76 (2 H, quintet, J 6.1), 1.84 (2 H, quintet, J 6.5), 1.91 (2 H, quintet, J 6.5), 3.07 (2 H, s), 3.49 (2 H, t, J 6.1), 4.05 (2 H, t, J 6.5), 4.08 (2 H, t, J 6.5), 6.78-6.84 (1 H, m), 6.98 (2 H, d), 7.10-7.16 (1 H, m), 7.52-7.59 (2 x 2 H, d), 7.62 (2 H, d).

$\nu_{\max}(\text{KCl})$: 2970, 2880, 1610, 1495, 1475, 1260, 1120, 810 cm^{-1} .

m/z : 552 (M^+), 461, 439, 409, 143 (100%).

4''-[4-(1,2-Dimethylpropyloxy)butyloxy]-2,3-difluoro-4-nonylterphenyl (117)

Quantities: compound **91** (0.70 g, 1.8 mmol), tetrakis(triphenylphosphine)-palladium(0) (0.12 g, 0.12 mmol), and compound **8** (0.67 g, 2.3 mol).

Yield 0.55 g, 55% (white powder).

Transition temperatures (°C): Cr 55.2 SmC 114.3 I.

^1H NMR (400 MHz) δ (CDCl_3): 0.90 (6 H, dd, J 6.5), 1.03-1.11 (3 H, m), 1.21-1.42 (15 H, m), 1.64 (2 H, m), 1.71-1.79 (3 H, d, J 6.3), 1.86-1.96 (2 H, m), 2.69 (2 H, t, J 7.6), 3.13 (1 H, quintet, J 5.8), 3.41 (1 H, dt, J 6.1), 3.58 (1 H, dt, J 6.1), 4.04 (2 H, t, J 5.7), 6.97-7.02 (3 H, m) 7.11-7.16 (1 H, m), 7.52-7.67 (3 x 2 H, d).

ν_{max} (KCl): 2980, 2960, 2860, 1610, 1490, 1470, 1260, 1120, 810 cm^{-1} .

m/z : 550 (M^+), 463, 408, 295 (100%), 143.

2,3-Difluoro-4''-[4-(1-methylpropyloxy)butyloxy]-4-nonylterphenyl (118)

Quantities: compound **106** (0.50 g, 1.3 mmol), tetrakis(triphenylphosphine)-palladium(0) (0.12 g, 0.12 mmol), and compound **8** (0.42 g, 1.5 mmol).

Yield 0.46 g, 65% (white powder).

Transition temperatures (°C): Cr 66.1 SmC 119.0 I.

^1H NMR (400 MHz) δ (CDCl_3): 0.86-0.94 (6 H, m), 1.13 (3 H, d, J 6.4), 1.23-1.60 (14 H, m), 1.65 (2 H, quintet, J 6.4), 1.76 (2 H, quintet, J 6.8), 1.91 (2 H, quintet, J 6.7), 2.69 (2 H, t, J 7.5), 3.32 (1 H, sextet, J 6.0), 3.41-3.47 (1 H, m), 3.53-3.60 (1 H, m), 4.04 (2 H, t, J 6.5), 6.97-7.02 (3 H, m), 7.12-7.17 (1 H, m), 7.54-7.65 (3 x 2 H, d).

ν_{max} (KCl): 2980, 2880, 1610, 1500, 1380, 1260, 1180, 1100, 800 510 cm^{-1} .

m/z : 536 (M^+), 463, 408, 379, 295, 129, 71 (100%).

4''-[4-(1,1-Dimethylpropyloxy)butyloxy]-2,3-difluoro-4-nonylterphenyl (119)

Quantities: compound **108** (0.55 g, 1.4 mmol), tetrakis(triphenylphosphine)-palladium(0) (0.12 g, 0.12 mmol), and compound **8** (0.48 g, 0.0017 mol).

Yield 0.46 g, 60% (white powder).

Transition temperatures (°C): Cr 54.7 SmC 105.7 I.

^1H NMR (400 MHz) δ (CDCl_3): 0.86-0.90 (6 H, m), 1.14 (6 H, s), 1.23-1.42 (12 H, m), 1.49 (2 H, q, J 7.5), 1.66 (2 H, quintet, J 7.4), 1.72 (2 H, quintet, J 7.4), 1.89 (2 H, quintet, J 7.4), 2.69 (2 H, t, J 7.6), 3.38 (2 H, t, 6.3), 4.04 (2 H, t, J 6.3), 6.97-7.02 (3 H, m), 7.12-7.17 (1 H, m), 7.54-7.65 (3 x 2 H, d).

ν_{max} (KCl): 2980, 2880, 1605, 1470, 1400, 1160, 1020, 805, 500 cm^{-1} .

m/z : 550 (M^+), 463, 408 (100%), 295, 57.

4''-[4-(2,2-Dimethylpropyloxy)butyloxy]-2,3-difluoro-4-nonylterphenyl (120)

Quantities: compound **109** (0.50 g, 1.3 mmol), tetrakis(triphenylphosphine)-palladium(0) (0.12 g, 0.12 mmol), and compound **8** (0.42 g, 1.5 mmol).

Yield 0.46 g, 65% (white powder).

Transition temperatures (°C): Cr 54.3 SmC 116.4 I.

$^1\text{H NMR}$ (400 MHz) δ (CDCl_3): 0.81 (3 H, t, J 6.7), 0.84 (9 H, s), 1.15-1.36 (14 H, m), 1.57 (2 H, quintet, J 7.1), 1.69 (2 H, quintet, J 6.6), 1.83 (2 H, quintet, J 6.1), 2.62 (2 H, t, J 7.4), 3.42 (2 H, t, J 6.1), 3.98 (2 H, t, J 6.2), 6.89-6.94 (3 H, m), 7.04-7.10 (1 H, m), 7.47-7.57 (3 x 2 H, d).

$\nu_{\text{max}}(\text{KCl})$: 2980, 2970, 2880, 1610, 1495, 1475, 1260, 1120, 810 cm^{-1} .

m/z : 550 (M^+), 462, 407, 295, 181, 143, 73.

Scheme 14

3,7-Dimethyloctanoic acid (122)

A solution of chromium trioxide (55.5 g, 0.555 mol) in water (68 ml) and 2M-sulphuric acid (12 ml) was added dropwise to a solution of compound 121 (43.7 g, 0.308 mol) in acetone (100 ml), the temperature was maintained at 40-60 °C and the reaction mixture was left stirring overnight. Acetone was carefully removed *in vacuo*, the reaction mixture was diluted in water and washed with diethyl ether (2 x 200 ml). The ethereal solution was washed with 10% sodium hydroxyde solution (200 ml); and the aqueous phase was acidified with 36% HCl (200 ml) and washed once more with diethyl ether (2 x 200 ml). The organic layer was dried (MgSO₄) and the diethyl ether was removed *in vacuo*. The crude product was distilled to give a colourless oil.

Yield 13.60 g, 28%; bp 139-141 °C at 15 mmHg.

¹H NMR (270 MHz) δ (CDCl₃): 0.86 (6 H, d, J 6.7), 0.96 (3 H, d, J 6.8), 1.10-1.40 (6 H, m), 1.50 (1 H, m), 1.90-2.02 (1 H, m), 2.10-2.20 (1 H, s), 2.40-2.50 (2 H, m).

ν_{\max} (KCl): 3300-2850, 1710, 1350, 945 cm⁻¹.

m/z: 172 (M⁺), 113, 97, 87 (100%).

3,7-Dimethyloctanoyl chloride (123)

Compound 122 (13.6 g, 0.077 mol) was heated under reflux for 1 h with thionyl chloride (13.1 g, 0.115 mol), the excess of thionyl chloride was distilled off.

Yield 13.4 g, 90%.

No attempt was made to purify the crude oil and no analyses were carried out, the product was used immediately.

4-Bromo-4'-(3,5,5-trimethylhexyl)biphenyl (126)

A solution of compound 125 (7.00 g, 0.030 mol), aluminium (4.40 g, 0.033 mol) and compound 124 (3.90 g, 0.036 mol), in dry DCM was prepared at room temperature. The stirring reaction mixture was left to react at room temperature until g.l.c. and t.l.c. analyses revealed a complete reaction, the reaction mixture was then treated with triethylsilane (9.30 g, 0.080 mol) and left stirring overnight. The reaction product was extracted into DCM (2 x 100 ml) and the combined organic layers were washed with brine, water and dried (MgSO₄). The product was adsorbed onto silica

gel and purified by column chromatography [DCM] and recrystallised from ethanol to yield a white powder.

Yield 7.00 g, 66%; mp 93-94 °C.

$^1\text{H NMR}$ (270 MHz) δ (CDCl_3): 0.46-0.55 (2 H, m), 0.86-0.97 (9 H, m), 0.99 (2 H, d, J 6.2), 1.06-1.16 (1 H, m), 1.26-1.33 (1 H, m), 1.43-1.68 (2 H, m), 2.50-2.72 (2 H, m), 7.24 (2 H, d), 7.40-7.57 (3 x 2 H, d).

ν_{max} (KCl): 2940, 1480, 1070, 1000, 805, 650 cm^{-1} .

m/z : 360/358 (M^+), 247/245, 165 57 (100%).

4-Bromo-4'-(3,7-dimethyloctyl)biphenyl (127)

Quantities: Compound 123 (6.90 g, 0.036 mol), compound 125 (7.00 g, 0.0300 mol), aluminium chloride (4.40 g, 0.033 mol), and triethylsilane (9.30 g, 0.080 mol).

Yield 6.75 g, 60%; mp 88-89 °C (white powder).

$^1\text{H NMR}$ (270 MHz) δ (CDCl_3): 0.87 (6 H, d, J 6.4), 0.96 (3 H, d, J 6.5), 1.10-1.40 (6 H, m), 1.41-1.72 (4 H, m), 2.52-2.75 (2 H, t, J 6.3), 7.24 (2 H, d), 7.40-7.58 (3 x 2 H, d).

ν_{max} (KCl): 2980, 2940, 1490, 1470, 1080, 1000, 810, 500 cm^{-1} .

m/z : 374/372 (M^+), 258, 250/248, 245, 165, 57 (100%).

2,3-Difluoro-4-octyloxy-4''-(3,5,5-trimethylhexyl)terphenyl (128)

Compound 126 (1.00 g, 2.8 mmol), an aqueous solution of 2M-sodium carbonate (40 ml) and tetrakis(triphenylphosphine)palladium(0) (0.12 g, 0.12 mmol) were mixed in TBME (60 ml) under dry nitrogen at room temperature and compound 5 (1.00 g, 3.5 mmol) was added. The stirred reaction mixture was heated overnight under reflux under dry nitrogen until g.l.c. and t.l.c. revealed a complete reaction. The product was extracted into DCM (2 x 150 ml) and washed with brine, water and dried (MgSO_4). The solvent was removed under reduced pressure and the residue was purified by column chromatography [DCM-hexane, 1:8] and recrystallised from hexane to give a white powder.

Yield 1.02 g, 70%.

Transition temperatures (°C): Cr 55.4 SmC 104.5 I.

$^1\text{H NMR}$ (400 MHz) δ (CDCl_3): 0.85-0.97 (14 H, m), 1.00 (3 H, d, J 6.7), 1.07-1.14 (1 H, m), 1.23-1.43 (8 H, m), 1.44-1.70 (4 H, m), 1.88 (2 H, quintet, J 6.5), 2.57-2.73

(2 H, m), 4.07 (2 H, t, J 6.5), 6.78-6.85 (1 H, m), 6.97-7.03 (1 H, m), 7.25 (2 H, d), 7.52-7.66 (3 x 2 H, d).

$\nu_{\max}(\text{KCl})$: 2980, 2880, 1640, 1500, 1480, 1300, 1080, 800 cm^{-1} .

m/z : 520 (M^+), 408 (100), 295, 57.

Compounds 129, 130 and 131 were prepared following a similar procedure to that described for the preparation of compound 128.

4''-(3,7-Dimethyloctyl)-2,3-difluoro-4-octyloxyterphenyl (129)

Quantities: compound 127 (1.00 g, 2.8 mmol), tetrakis(triphenylphosphine)-palladium(0) (0.12 g, 0.12 mmol), and compound 5 (1.00 g, 3.5 mmol).

Yield 1.12 g, 75% (white powder).

Transition temperatures ($^{\circ}\text{C}$): Cr 82.5 SmC 115.3 I.

$^1\text{H NMR}$ (400 MHz) δ (CDCl_3): 0.82-0.92 (9 H, m), 0.95 (3 H, d, J 5.9), 1.08-1.20 (2 H, m), 1.22-1.42 (11 H, m), 1.43-1.59 (6 H, m), 1.62-1.72 (1 H, m), 1.84 (2 H, quintet J 4.9), 2.52-2.74 (2 H, m), 4.08 (2 H, t, J 4.9), 6.77-6.87 (1 H, m), 7.08-7.18 (1 H, m), 7.26 (2 H, d), 7.50-7.59 (2 x 2 H, d), 7.65 (2 H, d).

$\nu_{\max}(\text{KCl})$: 2920, 2880, 1630, 1480, 1080, 800 cm^{-1} .

m/z : 534 (M^+), 422, 407, 295, 57.

2,3-Difluoro-4-nonyl-4''-(3,5,5-trimethylhexyl)terphenyl (130)

Quantities: compound 126 (1.00 g, 2.8 mmol) tetrakis(triphenylphosphine)-palladium(0) (0.12 g, 0.12 mmol), and compound 8 (1.00 g, 3.5 mmol).

Yield 1.00 g, 70% (white powder).

Transition temperatures ($^{\circ}\text{C}$): Cr 53.7 SmC 62.7 I.

$^1\text{H NMR}$ (400 MHz) δ (CDCl_3): 0.87-0.94 (12 H, m), 1.00 (3 H, d, J 6.2), 1.08-1.14 (1 H, m), 1.27-1.35 (14 H, m), 1.43-1.59 (4 H, m), 2.57-2.72 (4 H, m), 6.97-7.02 (1 H, m), 7.07-7.17 (1 H, m), 7.27 (2 H, d), 7.53-7.68 (3 x 2 H, d).

$\nu_{\max}(\text{KCl})$: 2980, 2880, 1500, 1460, 1400, 1120, 800 cm^{-1} .

m/z : 518 (M^+), 391 (100%).

4''-(3,7-Dimethyloctyl)-2,3-difluoro-4-nonylterphenyl (131)

Quantities: compound 127 (1.00 g, 2.8 mmol), tetrakis(triphenylphosphine)-palladium(0) (0.12 g, 0.12 mmol), and compound 8 (1.00 g, 3.5 mmol).

Yield 1.10 g, 70% (white powder).

Transition temperatures (°C): Cr 28.2 SmC 75.2 I.

^1H NMR (400 MHz) δ (CDCl_3): 0.86 (9 H, m), 0.94 (3 H, d, J 5.7), 1.09-1.20 (2 H, m), 1.22-1.42 (18 H, m), 1.43-1.58 (2 H, m), 1.62-1.72 (2 H, m), 2.58-2.74 (4 H, m), 6.77-6.87 (1 H, m), 7.08-7.18 (1 H, m), 7.27 (2 H, d), 7.55 (2 H, d), 7.59 (2 H, d), 7.66 (2 H, d).

$\nu_{\text{max}}(\text{KCl})$: 2980, 2880, 1500, 1080, 900, 800 cm^{-1} .

m/z : 532 (M^+), 422, 407, 295, 57.

Scheme 15

4-Bromo-4'-(3-chloropropyl)biphenyl (135)

A solution of compound **125** (3.00 g, 12.8 mmol), aluminium chloride (1.90 g, 0.014 mol) and compound **132** (2.00 g, 0.015 mol), in dry DCM (100 ml) was prepared at room temperature. The stirred reaction mixture was left to react at room temperature until g.l.c. and t.l.c. analyses revealed a complete reaction, the reaction mixture was then treated with triethylsilane (3.60 g, 0.0307 mol) and left stirring overnight. The reaction product was extracted in DCM (2 x 50 ml) and was washed with brine, water and dried (MgSO₄). The product was adsorbed onto silica gel and purified by column chromatography [DCM] and recrystallised from ethanol to give a white powder.

Yield 2.57 g, 65%; mp 87-88 °C.

¹H NMR (270 MHz) δ (CDCl₃): 2.12 (2 H, quintet, J 6.2), 2.84 (2 H, t, J 6.0), 3.55 (2 H, t, J 6.2), 7.26 (2 H, d), 7.40-7.58 (3 x 2 H, d).

ν_{\max} (KCl): 2940, 1480, 1000, 800 cm⁻¹.

m/z: 312/310/308 (M⁺), 250/248, 245 (100%), 165, 139, 82.

Compounds **136** and **137** were prepared following a similar procedure to that described for the preparation of compound **135**.

4-Bromo-4'-(4-chlorobutyl)biphenyl (136)

Quantities: Compound **133** (5.12 g, 0.036 mol), compound **125** (7.00 g, 0.030 mol), aluminium chloride (4.40 g, 0.033 mol), and triethylsilane (8.35 g, 0.072 mol).

Yield 6.29 g, 65%, mp 81-82 °C (white powder).

¹H NMR (270 MHz) δ (CDCl₃): 1.75-1.90 (4 H, m), 2.80 (2 H, t, J 6.0), 3.50-3.60 (2 H, t, J 5.8), 7.25 (2 H, d), 7.40-7.58 (3 x 2 H, d).

ν_{\max} (KCl): 2940, 1480, 1070, 1000, 805, 650 cm⁻¹.

m/z: 326/324/322 (M⁺), 250/248, 245, 165.

4-Bromo-4'-(5-chloropentyl)biphenyl (137)

Quantities: Compound **134** (5.61 g, 0.036 mol), compound **125** (7.00 g, 0.030 mol), aluminium chloride (4.40 g, 0.033 mol), and triethylsilane (8.35 g, 0.072 mol).

Yield 6.56 g, 65% mp 77-78 °C (white powder).

$^1\text{H NMR}$ (270 MHz) δ (CDCl_3): 1.52 (2 H, quintet, J 6.9), 1.68 (2 H, t, J 6.8), 1.82 (2 H, t, J 6.9), 2.82 (2 H, t, J 6.8) 3.54 (2 H, t, J 6.8), 7.25 (2 H, d), 7.38-7.58 (3 x 2 H, d).

ν_{max} (KCl): 2940, 1480, 1070, 1000, 805, 650 cm^{-1} .

m/z : 340/338/336 (M^+), 250/248, 245, 165.

4''-(3-Chloropropyl)-2,3-difluoro-4-octyloxyterphenyl (138)

Compound **135** (0.80 g, 2.6 mmol), an aqueous solution of 2M-sodium carbonate (40 ml) and tetrakis(triphenylphosphine)palladium(0) (0.10 g, 0.10 mmol) were mixed in TBME (60 ml) under dry nitrogen at room temperature and compound **5** (0.92 g, 3.2 mmol) was added. The stirred reaction mixture was heated overnight under reflux under dry nitrogen until g.l.c. and t.l.c. revealed a complete reaction. The product was extracted into DCM (2 x 150 ml) and washed with brine, water and dried (MgSO_4). The solvent was removed under reduced pressure and the residue was purified by column chromatography [DCM-hexane, 1:8] and recrystallised from hexane to give a white powder.

Yield 0.80 g, 65%.

Transition temperatures ($^{\circ}\text{C}$): Cr 102.0 SmA 157.3 I.

$^1\text{H NMR}$ (270 MHz) δ (CDCl_3): 0.89 (3 H, t, J 5.1), 1.23-1.43 (2 H, m), 1.45-1.57 (8 H, m), 1.85 (2 H, quintet, J 7.2), 2.14 (2 H, quintet, J 7.2), 2.89 (2 H, t, J 6.2), 3.57 (2 H, t, J 6.2), 4.09 (2 H, t, J 7.2) 6.78-6.87 (1 H, m), 7.10-7.19 (1 H, m), 7.28-7.31 (2 H, d), 7.55-7.60 (2 x 2 H, d), 7.65 (2 H, d).

ν_{max} (KCl): 2980, 2880, 1640, 1500, 1480, 1300, 1080, 800 cm^{-1} .

m/z : 472/470 (M^+), 358, 295, 266.

Compounds **139** and **140** were prepared following a similar procedure as that described for the preparation of compound **138**.

4''-(4-Chlorobutyl)-2,3-difluoro-4-octyloxyterphenyl (139)

Quantities: compound **136** (0.90 g, 2.8 mmol), tetrakis(triphenylphosphine)-palladium(0) (0.12 g, 0.12 mmol), and compound **5** (1.00 g, 3.5 mmol).

Yield 0.95 g, 70% (white powder).

Transition temperatures ($^{\circ}\text{C}$): Cr 71.0 SmA 151.2 I.

$^1\text{H NMR}$ (270 MHz) δ (CDCl_3): 0.90 (3 H, t, J 5.1), 1.23-1.40 (12 H, m), 1.78-1.91 (4, m), 2.70 (2 H, t, J 6.1), 3.58 (2 H, t, J 6.1), 4.07 (2 H, t, J 7.1), 6.76-6.88 (1 H, m), 7.08-7.20 (1 H, m), 7.25 (2 H, d), 7.55-7.60 (2 x 2 H, d), 7.66 (2 H, d).

ν_{max} (KCl): 2980, 2880, 1640, 1480, 1300, 1200, 1080, 800 cm^{-1} .

m/z : 486/484 (M^+), 372 (100%), 307, 265, 69, 57.

4''-(5-Chloropentyl)-2,3-difluoro-4-octyloxyterphenyl (140)

Quantities: compound 137 (0.90 g, 2.8 mmol), tetrakis(triphenylphosphine)palladium (0) (0.12 g, 0.12 mmol), and compound 5 (0.98 g, 3.4 mmol).

Yield 0.98 g, 70% (white powder).

Transition temperatures ($^{\circ}\text{C}$): Cr 80.2 SmA 154.9 I.

$^1\text{H NMR}$ (400 MHz) δ (CDCl_3): 0.88 (3 H, t, J 5.1), 1.18-1.42 (8 H, m), 1.43-1.59 (4 H, m), 1.68 (2 H, quintet, J 7.2), 1.78-1.92 (4 H, m), 2.68 (2 H, t, J 6.2), 3.55 (2 H, t, J 6.2), 4.08 (2 H, t, J 7.2), 6.78-6.87 (1 H, m), 7.10-7.19 (1 H, m), 7.28 (2 H, d), 7.52-7.60 (2 x 2 H, d), 7.64 (2 H, d).

ν_{max} (KCl): 2980, 2880, 1640, 1500, 1480, 1305, 1080, 800, 720 cm^{-1} .

m/z : 500/498 (M^+), 386 (100%), 295, 69, 57.

Scheme 16

2-Iodoethyl methyl ether (142)

A solution of compound **141** (12.5 g, 0.132 mol) and sodium iodide (22.5 g, 0.150 mol) in acetone (120 ml) was heated under reflux for 15 h. The sodium chloride formed was filtered off and acetone was removed *in vacuo*; the residue was dissolved in DCM (100 ml) and washed with water. The solvent was then removed *in vacuo*. Then residue was fractionally distilled to give a colourless oil.

Yield 11.25 g, 47%, bp 120-123 °C.

$^1\text{H NMR}$ (270 MHz) δ (CDCl_3): 3.25 (2 H, t, J 4.8), 3.40 (3 H, s), 3.66 (2 H, t, J 4.8).

Only the $^1\text{H NMR}$ spectrum of compound **142** was recorded.

Ethyl 2-(4'-bromobiphenyl-4-oxy)propanoate (144)

A solution of triphenylphosphine (28.1 g, 0.100 mol) and DEAD (18.7 g, 0.100 mol) in dry cold THF (200 ml) was added dropwise over fifteen minutes to a solution of compound **12** (24.8 g, 0.100 mol) and compound **143** (11.8 g, 0.100 mol) in dry THF (100 ml) stirring at room temperature. The reaction mixture was left stirring overnight. The reaction product was extracted into diethyl ether (2 x 200 ml), and the combined ethereal solutions were washed with water and dried (MgSO_4). The crude product was adsorbed onto silica gel and purified by column chromatography [DCM-petroleum fraction (bp 40-60 °C), 1:3] and recrystallised from ethanol to yield white crystals.

Yield 26.5 g, 75%, mp 50-51 °C.

$^1\text{H NMR}$ (400 MHz) δ (CDCl_3): 1.26 (3 H, t, J 6.2), 1.63 (3 H, d, J 6.4), 4.23 (2 H, q, J 6.2), 4.76 (1 H, q, J 6.4), 6.94 (2 H, d), 7.36-7.56 (3 x 2 H, d).

ν_{max} (KCl): 3000, 2980, 1750, 1610, 1490, 1280, 1200, 1060, 1180, 820, 500 cm^{-1} .

m/z : 350/348 (M^+), 277/275 (100%), 249/247, 168, 152, 139, 58.

2-(4'-Bromobiphenyl-4-oxy)propan-1-ol (145)

A solution of compound **144** (6.00 g, 0.017 mol) in dry diethyl ether (75 ml) was added dropwise at room temperature to a solution of lithium aluminium hydride (0.50 g, 0.013 mol) in dry diethyl ether (50 ml) in a three necked round bottom flask under dry nitrogen. When the addition was complete the reaction mixture was heated under reflux for 1 h. A mixture of water (5 ml) and THF (15 ml) was added

to the reaction mixture when cooled to room temperature, to decompose any unreacted lithium aluminium hydride. The reaction mixture was then filtered and washed with diethyl ether (2 x 200 ml), and the combined ethereal solutions were washed with water and dried (MgSO₄). The crude product was adsorbed onto silica gel and purified by column chromatography [DCM-petroleum fraction (bp 40-60 °C) 1:1] and recrystallised from ethanol to yield white crystals.

Yield 4.05 g, 75% (mp not recorded).

¹H NMR (270 MHz) δ (CDCl₃): 1.32 (3 H, d, J 6.6), 2.06 (1 H, s), 3.69-3.85 (2 H, m), 4.48-4.62 (1 H, m), 6.95-7.05 (2 H, d), 7.25-7.60 (3 x 2 H, d).

ν_{\max} (KCl): 3400, 3000, 2860, 1610, 1440, 1290, 1200, 1080, 1000, 820, 500 cm⁻¹.

m/z: 308/306 (M⁺), 265, 250/248 (100%), 139.

(R)-(+)-4-Bromo-4'-[2-(2-methoxyethoxy)-1-methylethoxy]biphenyl (146)

A solution of compound **142** (1.30 g, 7.0 mmol) in DMSO (50 ml) was added dropwise to a cooled of solution (-5 °C) compound **145** (2.00 g, 6.5 mmol) and of potassium hydroxide powder (Fluka, 1.03 g, 0.018 mol) in DMSO (100 ml) and stirred using a mechanical stirrer. The reaction mixture was allowed to react at -5 °C for 1 h and removed from the cooling bath to react for 2 h at room temperature. The product was extracted into hexane (200 ml) and washed with water in order to remove all trace of DMSO. Hexane was removed under reduced pressure and the residue was purified by column chromatography [DCM-hexane, 1:8] to yield a white powder.

Yield 1.50 g, 75% (mp not recorded).

¹H NMR (400 MHz) δ (CDCl₃): 1.34 (3 H, d, J 5.6), 3.38 (3 H, s), 3.53-3.61 (3 H, m), 3.67-3.74 (3 H, m), 4.62 (1 H, sextet, J 5.6), 6.98 (2 H, d), 7.41 (2 H, d), 7.47 (2 H, d), 7.53 (2 H, d).

ν_{\max} (KCl): 2940, 1610, 1490, 820, 500 cm⁻¹.

m/z: 366/364 (M⁺), 250/248, 133, 77.

$[\alpha_D]^{20} = 11.7$

(R)-(+)-2,3-Difluoro-4''-[2-(2-methoxyethoxy)-1-methylethoxy]-4-octyloxyterphenyl (147)

Compound **146** (0.80 g, 2.2 mmol) and a 2M-aqueous solution of sodium carbonate (40 ml), were mixed in DME (60 ml), and tetrakis(triphenylphosphine)palladium(0)

(0.12 g, 0.12 mmol) under dry nitrogen and compound **5** (0.88 g, 3.1 mmol) was added to the reaction mixture. The stirred reaction mixture was heated under reflux overnight. The product was extracted into DCM (100 ml) and washed with brine, water and dried (MgSO_4). The solvent was removed under reduced pressure and the residue was purified by column chromatography [DCM-hexane, 1:5] and recrystallised from hexane to give white powder.

Yield 0.57 g, 65%.

Transition temperatures ($^{\circ}\text{C}$): Cr 73.2 SmC* 90.0 N* 109.6 I.

^1H NMR (270 MHz) $\delta(\text{CDCl}_3)$: 0.90 (3 H, t, J 6.0), 1.22-1.55 (13 H, m), 1.84 (2 H, m), 3.40 (3 H, s), 3.52-3.79 (6 H, m), 4.08 (2 H, t, J 5.0), 4.54-4.69 (1 H, m), 6.77-6.87 (1 H, m), 7.02 (2 H, d), 7.08-7.18 (1 H, m), 7.50-7.60 (2 x 2 H, d), 7.60-7.67 (2 H, d).

$\nu_{\text{max}}(\text{KCl})$: 2970, 2880, 1660, 1605, 1605, 1480, 1360, 1115, 1080, 810 cm^{-1} .

m/z : 526 (M^+), 410, 298 (100%), 269, 58.

$[\alpha_{\text{D}}]^{20} = 15.8$

Scheme 17

(R)-(+)-4-Bromo-4'-(2-methoxy-1-methylethoxy)biphenyl (148)

The reaction procedure was as described for the preparation of compound 146

Quantities: compound 145 (1.11 g, 6.0 mmol), methyl iodide (1.00 g, 7.0 mmol), KOH powder (Fluka, 1.34 g, 0.0240 mol). The product was adsorbed onto silica gel and purified by column chromatography [DCM-hexane, 8:1] and recrystallised from ethanol.

Yield 1.54 g, 65% (white powder) (mp not recorded).

$^1\text{H NMR}$ (400 MHz) δ (CDCl_3): 1.36 (3 H, d, J 5.4), 3.38 (3 H, s), 3.37-3.78 (2 H, m), 4.60 (1 H, sextet, J 5.4), 6.96 (2 H, d), 7.39 (2 H, d), 7.45 (2 H, d), 7.51 (2 H, d).

ν_{max} (KCl): 2880, 1605, 1460, 1305, 1080, 840, 500 cm^{-1} .

m/z : 322/320(M^+), 250/248 (100%), 242, 148, 79, 57.

$[\alpha_{\text{D}}]^{20} = 8.7$

(R)-(+)-2,3-Difluoro-4''-(2-methoxy-1-methylethoxy)-4-octyloxyterphenyl (149)

A mixture of compound 148 (0.70 g, 2.2 mmol) in DME (60 ml) with an aqueous solution of sodium carbonate 2M (40 ml) and tetrakis(triphenylphosphine)-palladium(0) (0.12 g, 0.12 mmol) under dry nitrogen was made; to which compound 5 (0.74 g, 2.6 mmol) was added. The stirred reaction mixture was heated under reflux overnight. The product was extracted into DCM (100 ml) and washed with brine and water and dried (MgSO_4). The solvent was removed under reduced pressure and the residue was purified by column chromatography [silica gel; DCM-hexane 1:5] and recrystallised from hexane to give white crystals.

Yield 0.74 g, 70%.

Transition temperatures ($^{\circ}\text{C}$): Cr 84.3 SmC* 90.0 N* 109.6 I.

$^1\text{H NMR}$ (270 MHz) δ (CDCl_3): 0.89 (3 H, t, J 5.8), 1.20-1.33 (8 H, m), 1.37 (3 H, d, J 5.8), 1.42-1.57 (2 H, m), 1.85 (2 H, m), 3.44 (3 H, s), 3.48-3.64 (2 H, m), 4.07 (2 H, t, J 5.8), 4.53-4.64 (1 H, m), 6.76-6.86 (1 H, m), 7.01 (2 H, d), 7.08-7.18 (1 H, m), 7.51-7.58 (2 x 2 H, d), 7.62 (2 H, d).

ν_{max} (KCl): 2980, 2960, 2880, 1500, 1480, 1120, 1080, 810 cm^{-1} .

m/z : 482 (M^+), 410, 298, 73.

$[\alpha_{\text{D}}]^{20} = 10.7$

2.3 Experimental discussion

This chapter discusses the experimental strategy both in term of the chosen synthetic routes and the experimental techniques to obtain the compounds shown in figure 2.1.

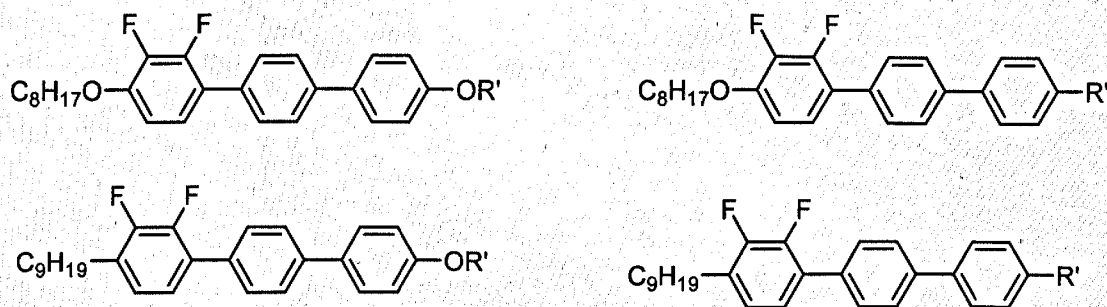


Figure 2.1 General structures of the compounds prepared

The design of the synthesis of these compounds requires a route for a core system and specific ways of preparing the variety of bulky end group R' . The discussion initially deals with the strategies for the synthesis of the cores and then discusses each class of terminal groups separately

2.3.1 Discussion of the general synthesis route

2.3.1.1 Strategies for the synthesis of the cores

The synthesis of 2,3-difluoroterphenyl compounds has been eased by the work of Suzuki and co-workers^{2,4} using the tetrakis(triphenylphosphine)palladium(0)-catalysed coupling of arylboronic acids with aryl halides. The boronic acid can be prepared separately, kept indefinitely and used in coupling reactions under aqueous or non-aqueous conditions. The boronic acid can be prepared safely at low temperature without the risk of forming benzyne.

One viable synthetic route for the 4-alkoxydifluoroterphenyls with any type of targeted end group is shown in figure 2.2 as a disconnection pathway. The route to the 4-alkyldifluoroterphenyls is similar to that shown in figure 2.2, but the route to the 4-alkyl-2,3-difluorobenzeneboronic acid is shown in figure 2.3.

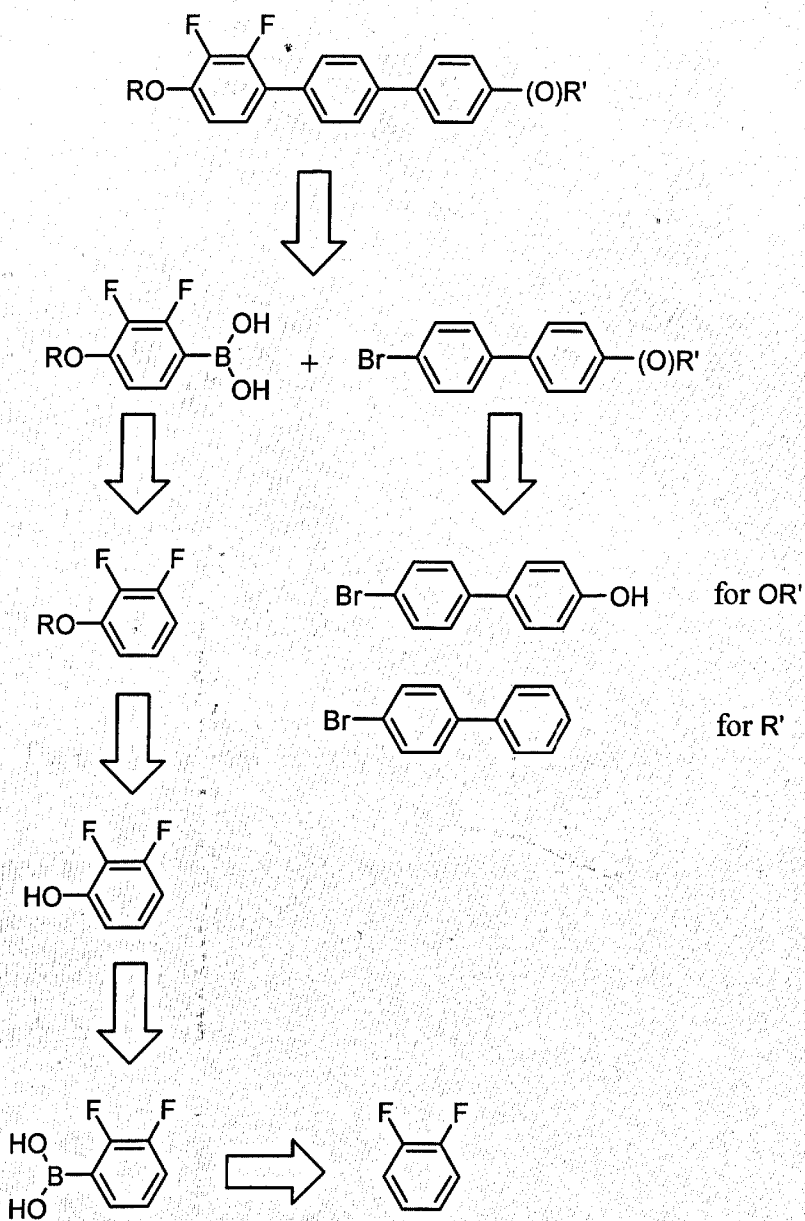


Figure 2.2 Disconnection pathway for the synthesis of 4-alkoxydifluoroterphenyls

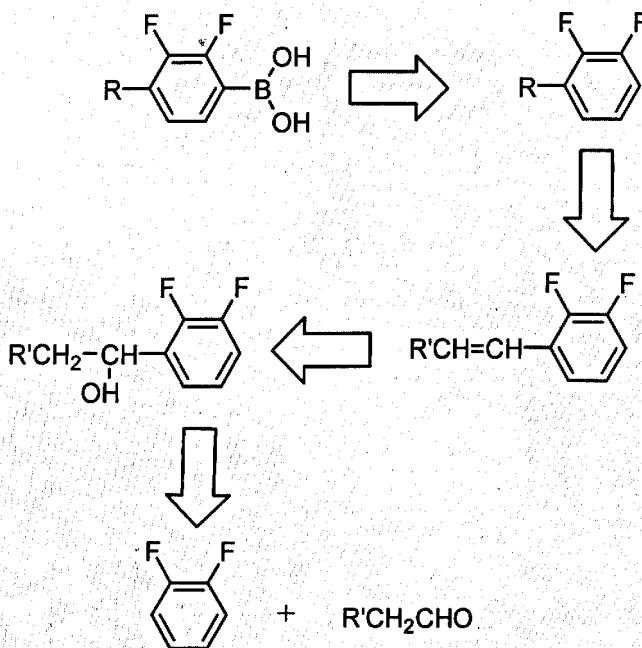


Figure 2.3 The route to 4-alkyl-2,3-difluorobenzeneboronic acid

An alternative pathway using a similar reaction is shown in figure 2.4 for the alkoxy series. The route to the alkyl series, based on the alternative strategy requires the 4-alkyl-2,3-difluorobenzeneboronic acid shown in figure 2.2, but is otherwise identical to the route shown in figure 2.3.

The route shown in figure 2.2 was chosen rather than the alternative route given in figure 2.4 for two reasons:

- (a) the route shown in figure 2.2 has two steps less than the route shown in figure 2.4, namely the lithiation of 4-alkyl/alkoxy-bromobenzenes and the coupling reaction to bromo-4-iodobenzene,
- (b) a further factor arising from the use of the route shown in figure 2.2 is that if the terminal chain at the 4''-position contains functional groups that react with butyllithium, then the route in figure 2.4 would be unacceptable. For example, compounds **138-140** have a chloro substituent in their terminal chain and therefore the targeted compound would not be obtained.

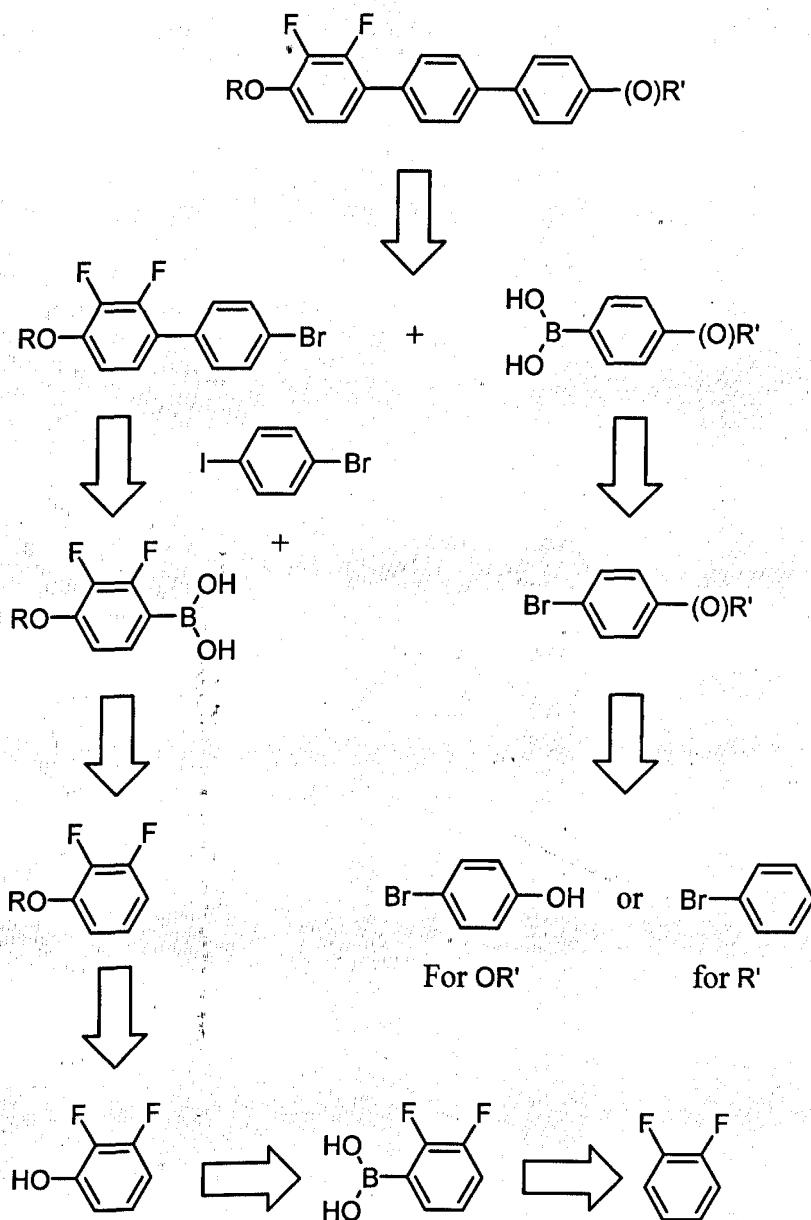


Figure 2.4 An alternative route to the synthesis of 4-alkoxydifluoroterphenyl compounds

A further possible route shown in figure 2.5 for the synthesis of 4-alkoxy-2,3-difluoroterphenyl cores would have improved the efficiency of production of the final products by reducing the number of steps, as compounds Y and Z would only have had to be synthesised once. The synthesis of the 4-alkyl-2,3-difluoroterphenyl cores is similar to the synthesis shown in figure 2.5, except for the synthesis of the 2,3-difluorobenzeneboronic acid shown in figure 2.3.

Therefore the route shown in figure 2.2 was chosen as it provided a viable pathway to the final products and it avoids the problems of the possible route shown in figure 2.4 and 2.5.

An essential reaction in all of these routes to constructing the core unit, is the coupling of aryl units, initiated by Suzuki and co-workers²⁻⁴ and further developed by Gray *et al.*^{7,8} for the synthesis liquid crystals. The palladium-catalysed cross-coupling reaction was either carried out in DME or TBME, as recommended by Gough⁹, but no significant yield difference was found. It was suggested¹⁰ that the palladium catalyst might get oxidised quicker in DME than in TBME and would therefore limit the yield, however no evidence was found to support this hypothesis. The general method used was as described by Gray *et al.*^{7,8}. The substrate containing the leaving group was added to a mixture of the organic solvent and 2M aqueous Na_2CO_3 under a stream of dry nitrogen and then the palladium catalyst was added followed by 15-20% excess of the boronic acid. No investigations were carried out to optimise the yields as they were judged satisfactory at 60-75% after column chromatography and recrystallisation.

The mechanism of the catalytic cycle has been proposed¹¹ to be that shown in figure 2.6.

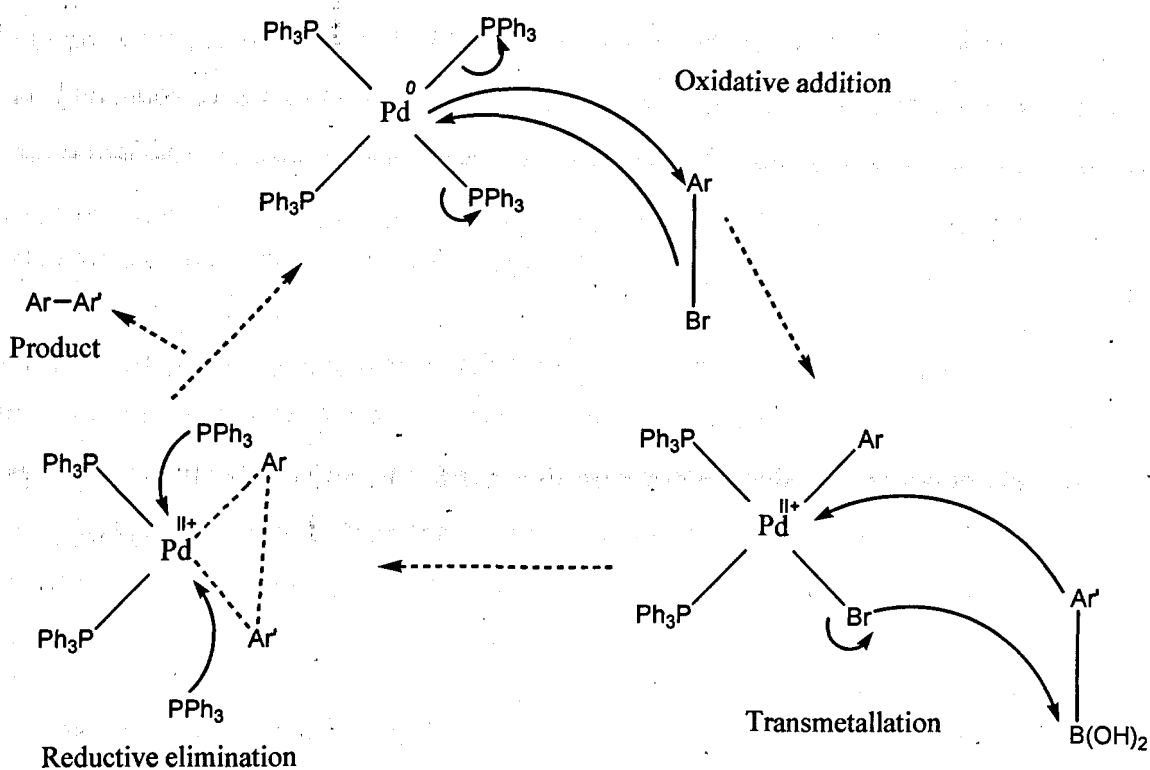


Figure 2.6 Proposed mechanism of the catalytic cycle for the palladium cross-coupling

2.3.2 Specific synthetic strategy for the terminal chains

2.3.2.1 Mitsunobu ether synthesis (Schemes 3 and 7)

Prior to the coupling reaction, a Mitsunobu reaction was carried out which involved the synthesis of a phosphonium complex; triphenylphosphine and DEAD in dry THF were cooled in an ice bath. The solution of the complex was added to a stirred mixture of 4-bromo-4'-hydroxybiphenyl and the alcohol at room temperature. The reaction was always carried out in this fashion and no attempts were made to improve on the yields as they were judged satisfactory at 60-75% after column chromatography and recrystallisation. When the reaction was complete the reaction product was extracted into ether with water and 20% sodium hydroxide to make the sodium salt of any unreacted 4-bromo-4'-hydroxybiphenyl. However, the sodium salt of 4-bromo-4'-hydroxybiphenyl remained water insoluble, therefore this process was not carried out to separate the desired product from its starting material.

The final products were recrystallised from hexane-acetonitrile (8:1) because they could not be recrystallised from ethanol as a gel was formed. Acetonitrile was added to the hexane as required to increase the polarity.

The proposed mechanism for the Mitsunobu⁵ reaction is as follows (figure 2.7):

- 1) Formation of the quaternary phosphonium salt by addition of triphenylphosphine to DEAD.
- 2) Protonation of the quaternary phosphonium salt.
- 3) Formation of an alkoxy-phosphonium salt.
- 4) Nucleophilic substitution (S_N2 type) to give triphenylphosphine oxide and the target ether.

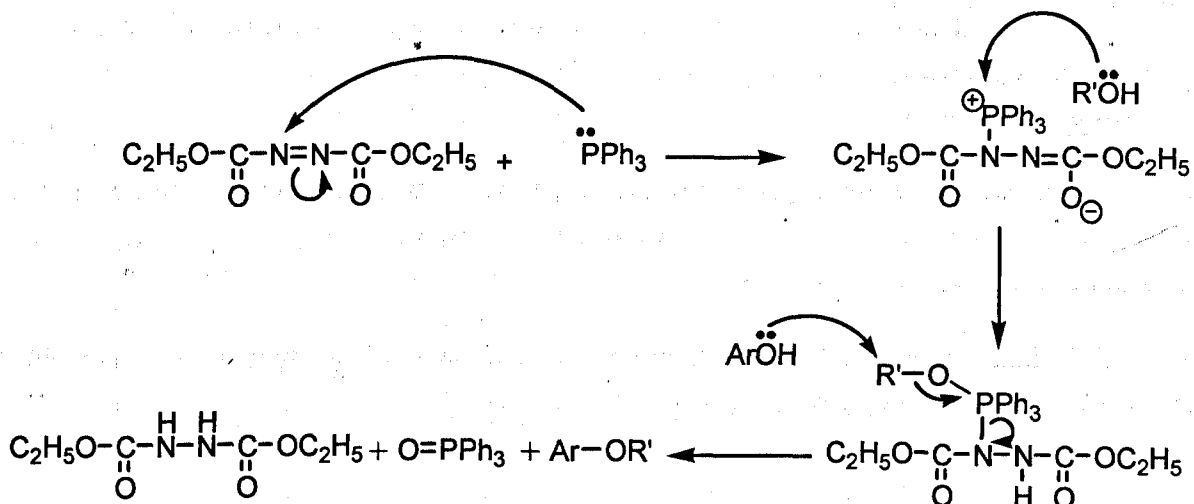


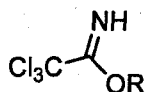
Figure 2.7 Mechanism for the formation of ethers by the Mitsunobu reaction

2.3.2.2 Synthesis of the *tert*-butyloxy end group (Scheme 4)¹²

Compound **29** was synthesised as described by Suk-ku Kang¹³. The reaction was initially carried out in toluene to avoid the use of the carcinogenic solvent benzene, however this attempt was unsuccessful. The reaction was then carried out in benzene and was successful. It appears that benzene is an essential solvent for the success of this reaction and cannot be replaced, as is sometimes the case by toluene.

The yield for compound **31** was poor (30%) and it was the lowest yield by far for the coupling of arylboronic acids with aryl halides. The reason for the low yield may be due to the presence of the hydroxy group on the terminal chain, which in the basic conditions that would give salt formation. The anionic/nucleophilic nature of this group may also interfere with the action of the catalyst.

The final step for the synthesis of compound **32** gave a reasonable yield and illustrates a useful way to synthesise ethers by reaction of a trichloroacetimidate derivative¹⁴ of the form,



which was prepared by addition of a sodium alkoxide to trichloroacetonitrile in the presence of a catalytic amount of boron trifluoride etherate. The trichloroacetimidate reacted with an alcohol to give an ether. However, the reaction may go *via* the

formation of a carbocation, as the reaction is affected by the polarity of the solvent (an apolar solvent is preferred Jackson *et al.*¹⁴). The desired product is only obtained if the carbon atom bonded to the oxygen atom in the acetimidate is a secondary or tertiary carbon. If the carbon atom were primary, a rearrangement would occur to give a more stable secondary or tertiary carbocation.

This route was thought to be a possibility for obtaining the target compounds in scheme 11 and 12, however it was not successful and was therefore abandoned.

2.3.2.3 Synthesis of the trimethylsilyl end group series (Schemes 5 and 6)

Initially the synthesis route for compound 54 was proposed as follows (figure 2.8):

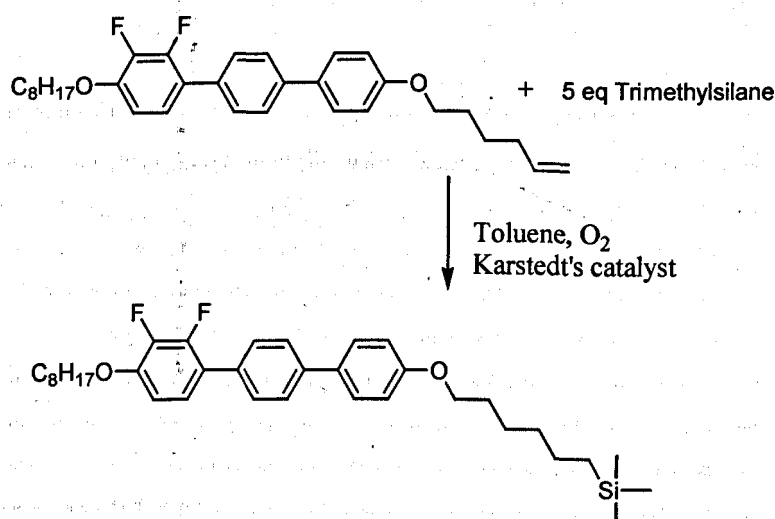
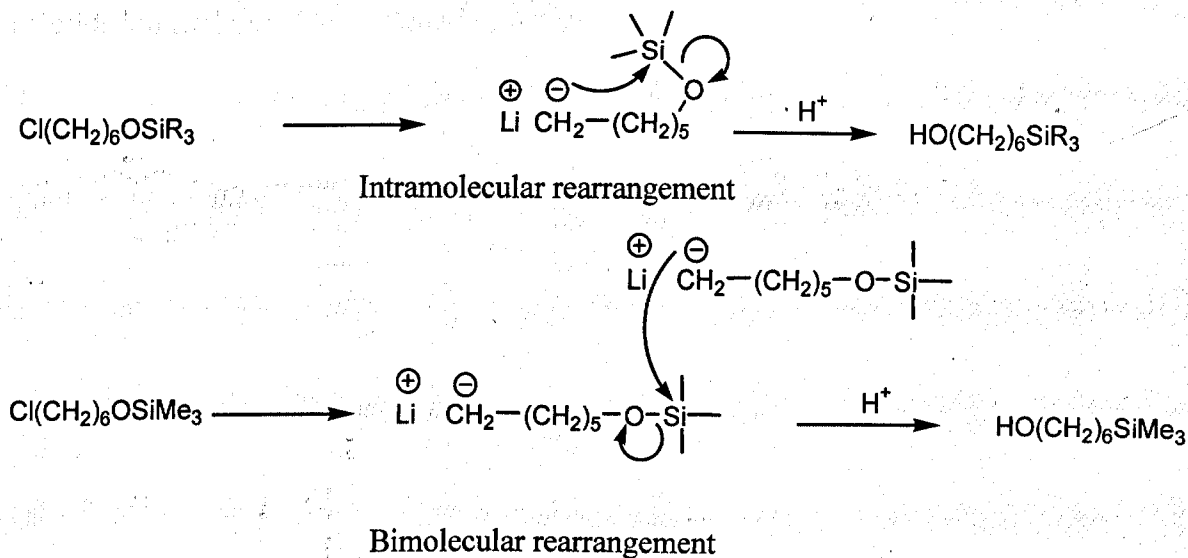


Figure 2.8 Proposed reaction pathway to synthesise compounds 54

However, this reaction was not successful and was therefore abandoned after two attempts.

As 2-trimethylsilylethanol and 3-trimethylsilylpropan-1-ol (compounds 33 and 34) were commercially available from Aldrich, an alternative route to compound 54 could be used if the synthesis of the α,ω -trimethylsilanol with different chain lengths could be achieved. The alcohols could then be linked to the phenol and this would probably be easier and quicker than making several terphenyl alkene ethers. Compounds 36, 37, and 38, when treated as described in scheme 5, gave their corresponding silyl ethers¹⁵. When their silyl ethers are treated with lithium in dry

diethyl ether followed by dry THF, a rearrangement occurs. This molecular rearrangement can occur in two different ways as follows¹⁵,



This reaction was also successful (see scheme 6) and appears to be a good way to synthesise any type of α,ω -trialkylsilanols. The alcohol was connected to the phenol to give the ether link as discussed in section 2.3.2.1.

2.3.2.4 Synthesis of *t*-butyl end group (Scheme 8)

The synthesis of compound **73** involved initially the reaction of an excess of 1,6-dichlorohexane or 1,6-dibromohexane with *tert*-butylmagnesium bromide in the presence or absence of copper(I) bromide as catalyst. This reaction pathway was unsuccessful, but Burns *et al.*¹⁶ proposed a new catalyst $\text{Li}_2\text{CuBr}_2\text{SMe}_2\text{SPh}$ which is prepared from a mixture of equal amounts of $\text{CuBr}\cdot\text{SMe}_2$, LiBr and LiSPh in THF at 0 °C which is used in reaction with tosylates. The catalyst $\text{Li}_2\text{CuBr}_2\text{SMe}_2\text{SPh}$ is reportedly highly efficient at coupling primary, secondary, tertiary, aryl, vinyl, and allylic Grignard reagents to primary tosylates and primary Grignards reagents to secondary tosylates and mesylates. The order of reactivity of Grignard reagents towards tosylates and halides is as follow tosylate > iodo > bromo > chloro >> fluoro. These reactions only require one equivalent of the Grignard reagent, which can improve on the selectivity of Grignard reagents when reacted with molecules containing two different halides or two active sites. As for compound **73**, one equivalent of *t*-butylmagnesium bromide with the catalyst in dry THF did not give a dimeric product containing two *t*-butyl groups. Compound **74** was obtained by

reacting compound **73** with compound **12** in butanone in the presence of 1.5 equivalent of K_2CO_3 as base and KI as catalyst to improve the reactivity of the chloride ion exchanged by iodide (figure 2.9).

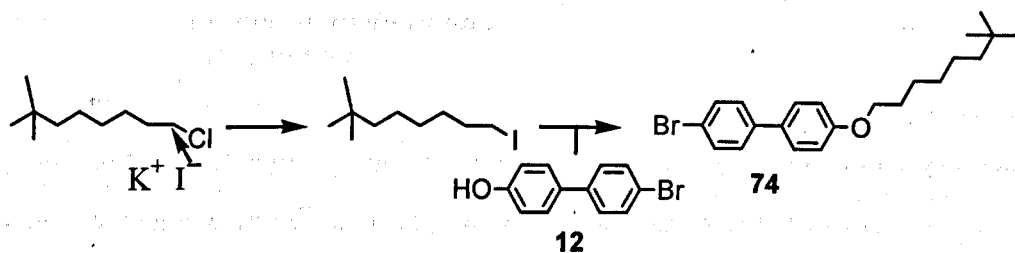
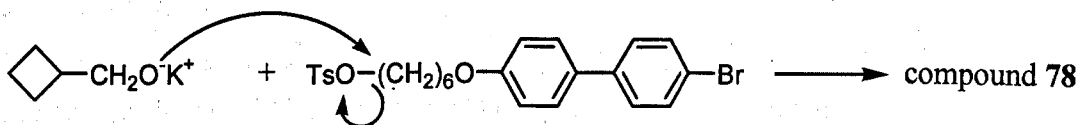


Figure 2.9 Representation of the proposed mechanism

2.3.2.5 Synthesis of the cyclobutyl end group (Scheme 9)

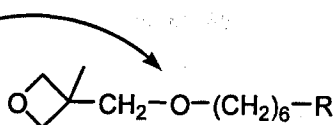
Compound **77** (the tosyl derivative of compound **30**) was made following the method described by Burns *et al.*¹⁶ and compound **78** was synthesised by a modified method detailed by Telfort *et al.*¹⁷ The tosylate is reacted with an alcohol in the very polar solvent DMSO. Cyclobutylmethanol was added to a vigorously mechanically stirred solution of compound **78** mixed with powered potassium hydroxide (from Fluka: water content 15%) in DMSO cooled at $-5\text{ }^\circ\text{C}$. Potassium hydroxide is highly hygroscopic and the reaction yield is reduced by the presence of excessive moisture; a mechanical stirrer was used because DMSO freezes at $18.5\text{ }^\circ\text{C}$. The reaction mixture was a thick paste which became dark brown. The reaction mechanism is as follows:



2.3.2.6 Synthesis of the oxetane end group (Scheme 10)

Compound **82** is a methyl derivative of compound **79**, but the synthesis of compound **82** involved a different synthetic pathway from that used for the synthesis of compound **79**. The synthetic pathway for compound **82** had to be changed because the oxetane ring would have been opened in the presence of a base and therefore the oxetane unit had to be linked to the molecule in the last step of the synthesis¹⁸.

The ether linkage
has to be the last step
to prevent ring-opening
of the oxetane



Compound **29** is bifunctional and was reacted with compound **12** to give compound **80** by a Mitsunobu reaction. Compound **80** was then coupled to the boronic acid compound **5** to give compound **81**. The final step involved the reaction of compound **81** with 3-(hydroxymethyl)-3-methyloxetane in a biphasic medium [50% aq NaOH/hexane (1:1)] with a phase transfer catalyst TBAB under reflux and vigorous mechanical stirring.

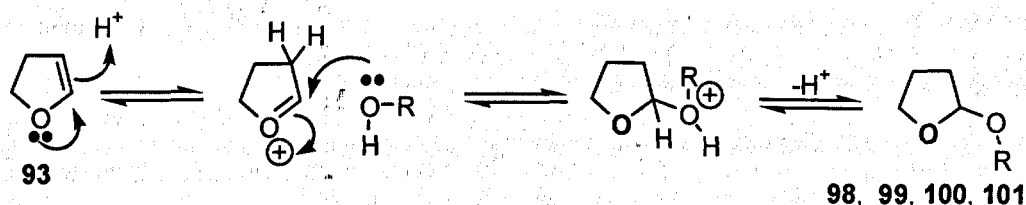
2.3.2.7 Synthesis of the branched end groups (Schemes 11, 12 and 13)

The synthesis of this varied series was challenging because different synthetic strategies had to be devised to synthesise chains with identical length (*i.e.* having the same spacer between the mesogen and the bulky end group) and different steric sizes for the bulky end group.

Several methodologies were used to synthesise this series. Firstly, a methodology similar to the one used to synthesise compound **82** gave compounds **87**, **88** and **89** from the reaction of compound **83** and hydroxy compounds **84**, **85** and **86** respectively (figure 2.10). Compounds **87**, **88** and **89** were obtained in 35-61% yields which are acceptable since all the starting materials are cheap. Compound **83** has two primary bromines which are two sites of equal reactivity and therefore a dimeric product could be obtained, although this was not detected.

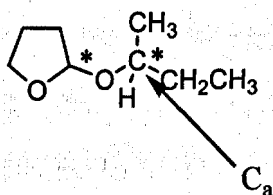
carbon atom forming the ether bridge to the 4-hydroxybutyl ethers needed to be primary, secondary or tertiary.

An efficient synthetic route for compounds of the general formula $\text{HO}(\text{CH}_2)_4\text{OR}'$ involves the reaction of compound **93** (which is commonly used for the protection of alcohols) with an alcohol to make 2-tetrahydrofuranyl ethers. These ethers are ring opened by a lithium aluminium hydride-aluminium chloride complex to give the targeted compounds, irrespective of the nature of the starting alcohol (primary, secondary or tertiary) as demonstrated with compounds **98**, **99**, **100** and **101** as shown below.



The alcohol reacts with compound **93** in the presence of toluene-*p*-sulphonic acid to give compounds **98**, **99**, **100** and **101** via an oxygen-stabilised cation. Compound **98** possesses two chiral centres and therefore gives rise to diastereoisomers. Compound **94** is a racemic mixture and contains a chiral centre, thus a new stereogenic centre is created when compound **98** is formed. This gives a ^1H NMR spectrum where the protons of the methyl group linked directly to the chiral centre, C_a , are split, giving two signals of integration of 1.5 proton as shown below:

Compound **98**:

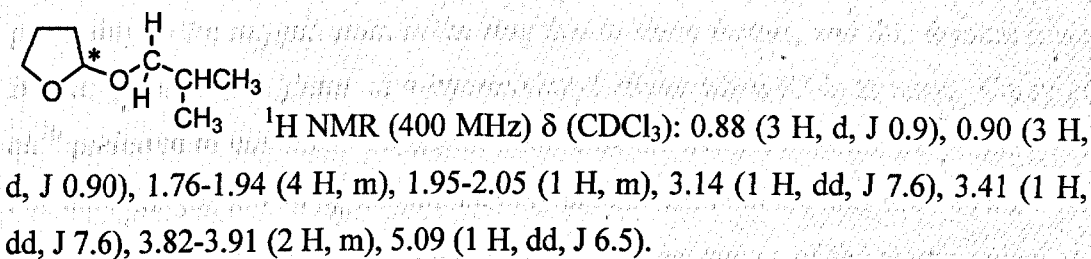


^1H NMR (400 MHz) δ (CDCl_3): 0.85-1.07 (3 H, m), 1.11 (1.5 H, d, J 6.2), 1.17 (1.5 H, d, J 6.2), 1.36-1.58 (2 H, m), 1.77-2.07 (4 H, m), 3.56-3.69 (1 H, m), 3.81-3.95 (2 H, m), 5.19-5.28 (1 H, m).

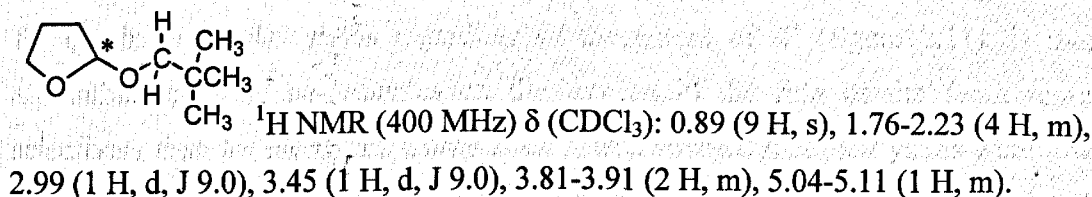
Compounds **99**, **100** and **101** have one chiral centre, and therefore their diastereotopic protons are close to the chiral centre. Compounds **99** and **101** have

some of their diastereotopic protons close enough to the chiral centre for their chemical shifts to be significantly different.

Compound 99:



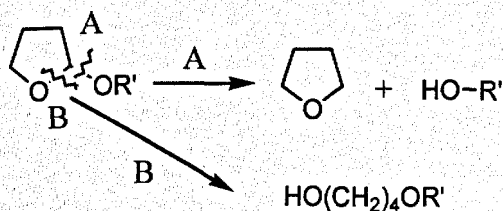
Compound 101:



However the diastereotopic protons of compound **100** in the two methyl groups or the methylene groups are too far from the chiral centre for their chemical shifts to be significantly different.

As stated previously, 2,3-dihydrofuran is used as a derivatising protecting group for alcohols and the 2-tetrahydrofuranyl unit is stable to base, hydrogenation, hydride ions, oxidising agents and is relatively stable to nucleophiles and organometallic reagents¹⁹ However 2-tetrahydrofuranyl ethers are unstable to aqueous acids and Lewis acids²⁰ and they can be reduced with a lithium aluminium hydride-aluminium chloride complex.

There are two possible pathways for cleavage as shown below. Route A has no synthetic value, since it simply regenerates the alcohol and THF, whereas B gives alkoxyalcohols by a ring opening process.



Corey *et al.*²⁰ have given explanations for the direction of the cleavage of tetrahydropyranyl ethers and tetrahydrofuranyl ethers in terms of the electron-donating effect and steric effect of R'. The Lewis acid (AlCl₃) co-ordinates preferably to the oxygen atom in the ring due to steric factors, and this favours route B and gives higher yields of 4-hydroxybutyl ethers when R' is tertiary. Corey *et al.*²⁰ preferred to use boron trifluoride instead of aluminium chloride for primary R'. For the example shown in scheme 12 only aluminium chloride was used as a Lewis acid and all the yields were similar regardless of the nature of the starting alcohol. No evidence was found for steric factors influencing the yield of 4-hydroxybutyl ethers and the R' group had similar electron-donating effects. A possible explanation for obtaining similar yields regardless of the nature of R' (figure 2.11), is that aluminium chloride co-ordinates on the oxygen in the ring of the furan more selectively than for the pyran. Corey *et al.*²⁰ also stressed that their yields were low when R' was primary because of the relative high solubility of the 4-hydroxybutyl ethers in water. The 4-hydroxybutyl ethers prepared in this work were extracted four times (50 ml each) into diethyl ether from the aqueous layer. This synthetic pathway provided an advantageous route to obtain 4-hydroxybutyl ethers irrespective of the nature of R'.

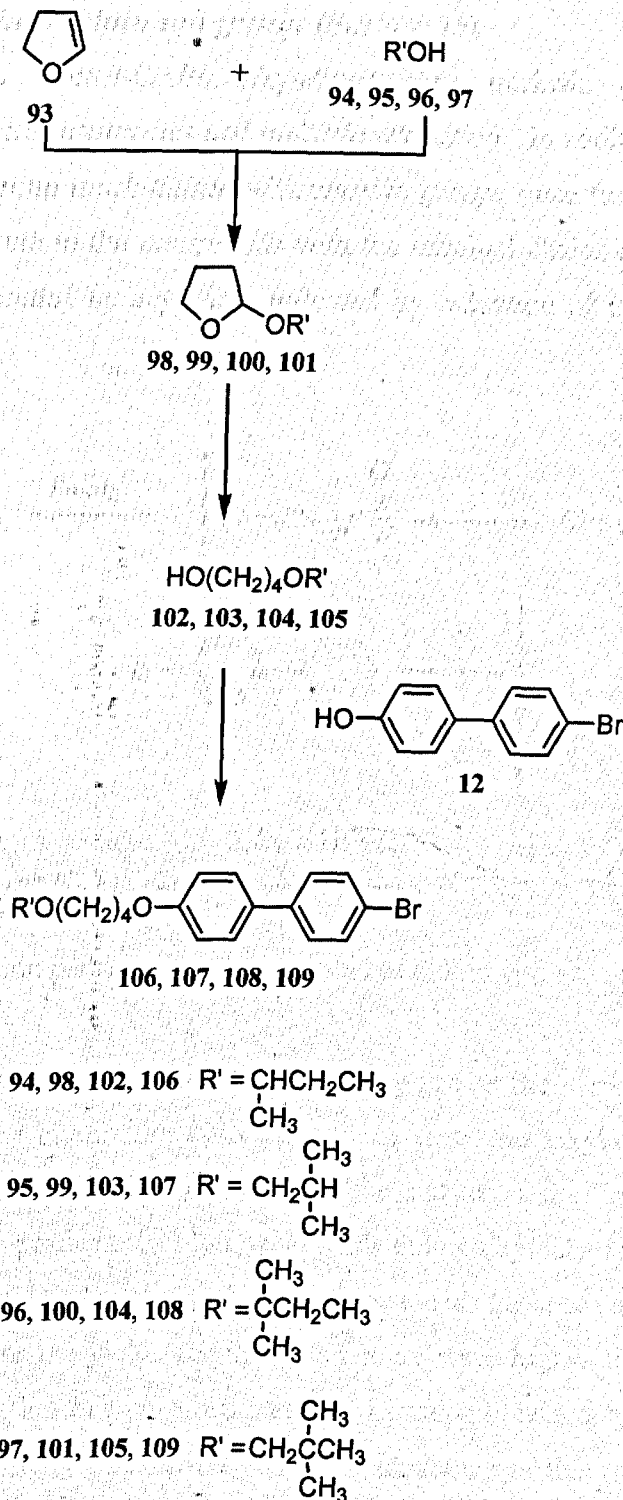


Figure 2.11 Synthetic pathway to obtain 4-hydroxybutyl ethers irrespective of the nature of R'

2.3.2.8 Synthesis of chloro end groups (Scheme 15)

Direct aromatic Friedel-Crafts alkylations have intrinsic problems such as polyalkylations, rearrangements and multiple alkylation. In addition, problems arise when the alkyl group is substituted with reactive groups since further alkylations are possible. The route to the compounds with the terminal chains containing a chloro substituents proceeded by acylation, followed by reduction of the carbonyl group⁶ (figure 2.12).

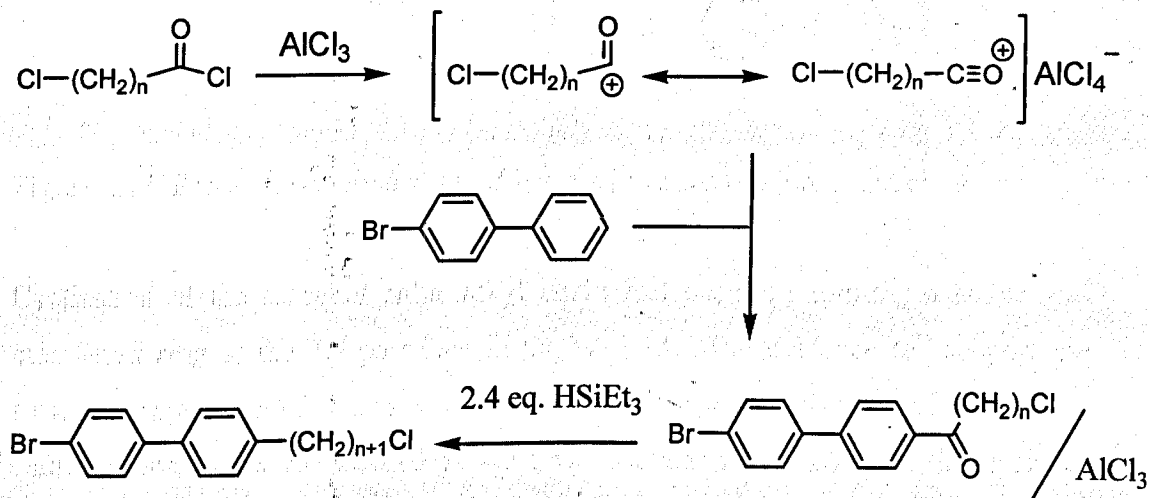


Figure 2.12 Reaction pathway for the synthesis of chloro end group

Triethylsilane is the hydride source used to deoxygenate the carbonyl group which complexes with the aluminium chloride present from the alkylation stage. This method provided an effective process for the acylation and reduction to give alkylated aromatic products in high yield with chloroalkyl chains (> 70%). The chloro substituents in the terminal chain prevented the use of Wolff-Kishner reduction. However the yields for the direct route were higher than those for the acylation and reduction of non-substituted alkyl groups obtained by Friedels Crafts alkylation / Wolff-Kishner reduction. Another advantage of this method is that the reaction is carried out in "one pot" at room temperature and the aryl ketone does not need to be isolated prior to its reduction.

In the first attempt at the synthesis of compound 136, two equivalents of aluminium chloride were used and the product obtained was not the desired substance (figure 2.13).

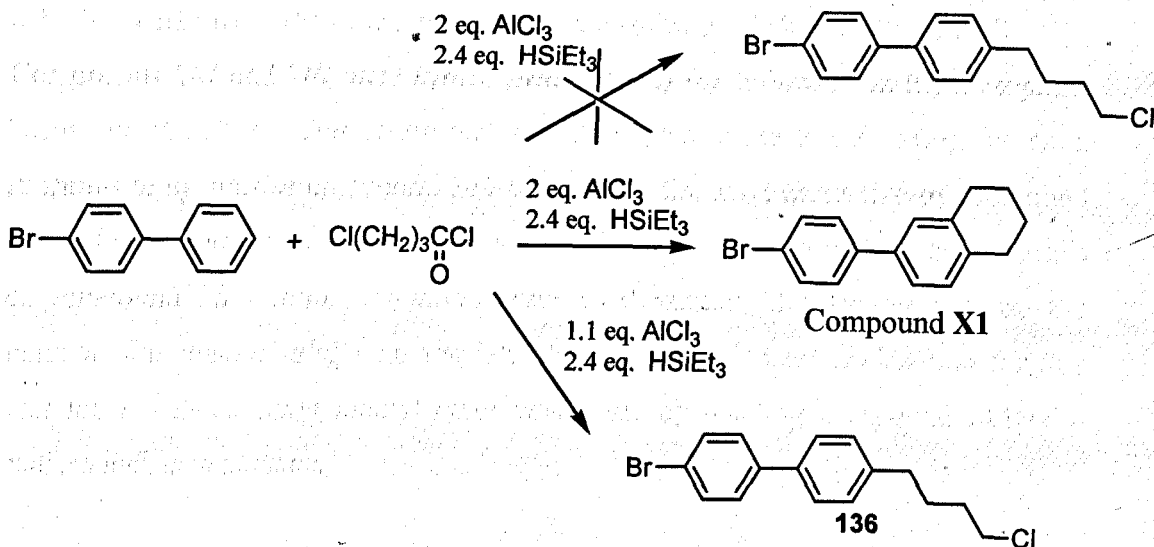


Figure 2.13 Products obtained with different equivalent of aluminium chloride

Cyclisation of the terminal chloroalkyl chain had occurred forming a stable six-membered ring at the 3,4-positions in 65 % yield. The evidence to support the structure of compound X1 is given below. When 1.1 equivalent of aluminium chloride were used, the desired product was obtained as shown by the analyses below.

Analyses of compound X1:

Yield 65%, mp 73-74 °C (white powder).

$^1\text{H NMR}$ (270 MHz) δ (CDCl_3): 1.78-1.87 (4 H; m), 2.75-2.88 (4 H; m), 7.13 (1 H, s), 7.26 (2 H, d), 7.40 (2 H, d), 7.50 (2 H, d).

m/z : 288/286 (M^+ , 100%), 260/258, 165, 152.

Analyses of compound 136

Yield 6.29 g, 65%, mp 81-82 °C (white powder).

$^1\text{H NMR}$ (270 MHz) δ (CDCl_3): 1.75-1.90 (4 H, m), 2.62-2.74 (2 H, t J 6.0), 3.50-3.60 (2 H, t, J 5.8), 7.25 (2 H, d), 7.40-7.58 (3 x 2 H, d).

ν_{max} (KCl): 2940, 1480, 1070, 1000, 805, 650 cm^{-1} .

m/z : 326/324/322 (M^+), 250/248, 245, 165.

2.3.2.9 Synthesis of the chiral ethylenoxy compounds (Schemes 16 and 17)

Compounds **147** and **149** were synthesised to study the influence on the mesophase behaviour of both a chiral centre and a methyl group close to the mesogenic core. Attempts to synthesise compound **146** by reacting the tosyl derivative of compound **145** failed. Compounds **147** and **149** were made *via* a similar route¹⁷ to the synthesis of compound **78**. Iodo derivatives were used instead of tosylates because the reaction was unsuccessful with tosylates (figure 2.14), but no explanation for this was found. 2-Iodoethyl methyl ether was made by reacting compound **141** with sodium iodide in acetone.

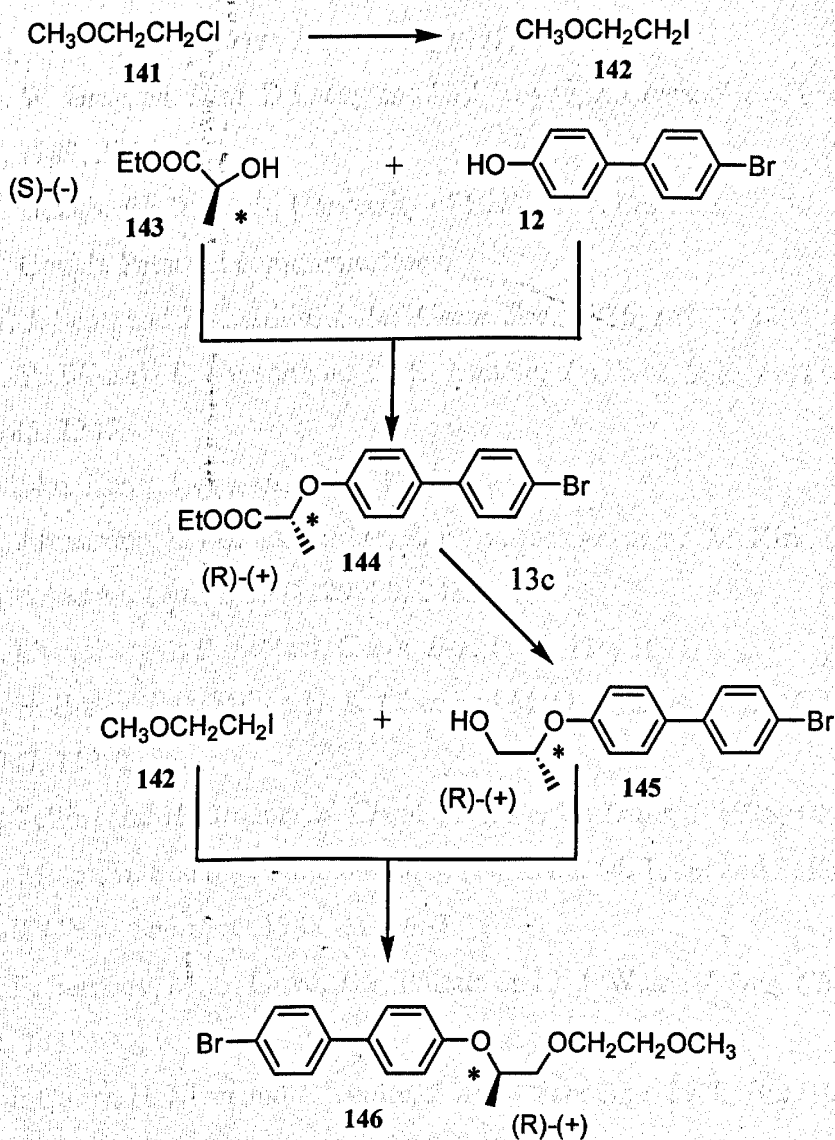


Figure 2.14 Intermediates for the synthesis of compounds **147** and **149**

2.4 Bibliography (Section 2)

- 1 D. R. Coulson, *Inorg. Synth.*, 1972, **13**, 121.
- 2 N. Miyaura, T. Yanagi and A. Suzuki, *Synth Commun.*, 1981, **11**, 513.
- 3 N. Miyaura, K. Yamada, H. Suginome and A. Suzuki, *J. Am. Chem. Soc.*, 1985, **107**, 972.
- 4 N. Miyaura and A. Suzuki, *Chem. Rev.*, 1995, **95**, 2547.
- 5 O. Mitsunobu, *Synthesis*, 1981, 1.
- 6 A. J. Chamiec, V. P. Shah and I Kruse, *J. Chem. Soc., Perkin Trans I*, 1989, 1705.
- 7 G. W. Gray, *Mol. Cryst. Liq. Cryst.*, 1991, **204**, 91.
- 8 G. W. Gray, M. Hird, D Lacey and K. J. Toyne, *J. Chem. Soc., Perkin Trans II*, 1989, 2041.
- 9 N. Gough, *Ph D Thesis*, University of Hull, 1999, England.
- 10 N. Gough, Personal communications.
- 11 W. J. Scott and J. K. Stille, *J. Am. Chem. Soc.*, 1986, **108**, 3033.
- 12 H. P. Wessel, T. Iversen and D. R. Bundle, *J. Chem. Soc., Perkin Trans. I*, 1985, 2247.
- 13 Suk-ku. Kang, *Synthesis*, 1985, 1161.
- 14 A. Armstrong, Ian Brackenridge, R. F. W. Jackson and J. M. Kirk, *Tetrahedron Letters*, 1988, **29**, 20, 2483.
- 15 A. Maercker and R. Stötzel, *Chem. Ber.*, 1987, **120**, 1691.
- 16 D. H. Burns, J. D. Miller, H. K. Chan and M. O. Delaney, *J Am. Chem. Soc.*, 1997, **119**, 2125.
- 17 A. Telfort and H. Brunner, *J. Chem. Soc., Perkin Trans. I*, 1996, 1467.
- 18 M. Motoi, H. Suda, K. Shimamura, S. Nagahara, M. Takei and S. Kanoh, *Bull. Chem. Soc. Jpn.*, 1988, **61**, 1653.
- 19 K. F. Bernady, M. B. Floyd, J. F. Poletto and J. J. Weiss, *J. Org. Chem.* 1979, **44**, 1438.
- 20 E. J. Corey, H. Niwa and J. Knolle, *J. Am. Chem. Soc.* 1978, **100**, 1942.

3.1 Introduction

The first part of the paper reports the results of the first two experiments. In order to investigate the effect of program access on a manual worker's ability to perform his job, the first experiment was designed to measure the effect of program access on the worker's performance. The second experiment was designed to measure the effect of program access on the worker's ability to perform his job.

The second part of the paper reports the results of the third experiment.

Results and Discussion

Section 3

The results of the first two experiments are presented in Table 1. The results of the third experiment are presented in Table 2. The results of the first two experiments show that program access has a significant effect on the worker's performance. The results of the third experiment show that program access has a significant effect on the worker's ability to perform his job.

Table 1. Results of the first two experiments.

Experiment	Program Access	Performance
1	Yes	High
	No	Low
2	Yes	High
	No	Low

The results of the first two experiments are presented in Table 1. The results of the third experiment are presented in Table 2. The results of the first two experiments show that program access has a significant effect on the worker's performance. The results of the third experiment show that program access has a significant effect on the worker's ability to perform his job.

3.0 Results and discussion

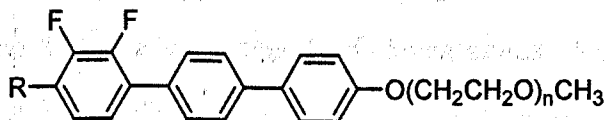
3.1 Mesomorphic studies

3.1.1 The effect of oxygen atoms at various positions along the terminal chain

In order to investigate the effect of oxygen atoms in a terminal chain on melting points and mesophase stabilities¹⁻³, a series of compounds with different chain lengths and different numbers of oxygen atoms was prepared.

3.1.1.1 Non-chiral terminal chains with oxygen substituents

The transition temperatures and mesophase morphologies for the compounds prepared are given in table 3.1. Compounds in table 3.1 contain different numbers of ethyleneoxy units.



16 R = OC₈H₁₇ n = 1

17 R = OC₈H₁₇ n = 2

18 R = OC₈H₁₇ n = 3

19 R = C₉H₁₉ n = 1

20 R = C₉H₁₉ n = 2

21 R = C₉H₁₉ n = 3

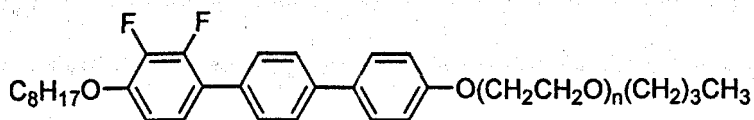
Table 3.1 Transition temperatures (°C) for compounds 16-21 and enthalpies of transitions (J g⁻¹)

Compounds		R	Cr	SmC	SmA	N	I
16	n = 1	C ₈ H ₁₇ O	• 133.8 [16.6]	• 158.5 [0.17]	• 165.3 [0.88]	• 178.9 [3.12]	•
17	n = 2	C ₈ H ₁₇ O	• 120.5 [33.9]	• 130.5 [0.10]	• 135.5 [5.12]	• 140.8 [2.40]	•
18	n = 3	C ₈ H ₁₇ O	• 106.0 [27.82]	• 117.5 [0.12]	• 121.8 [6.56]	• 126.5 [1.71]	•
19	n = 1	C ₉ H ₁₉	• 101.3 [14.1]	• 125.5 [0.10]	• 154.9 [3.17]	• 158.5 [2.91]	•
20	n = 2	C ₉ H ₁₉	• 84.8 [33.7]	• 102.9 [0.40]	• 107.6 [0.14]	• 115.0 [2.66]	•
21	n = 3	C ₉ H ₁₉	• 82.9 [23.4]	• 89.8 [0.17]	—	—	• 92.6 [5.43]

For the dialkoxy series, compounds **16**, **17** and **18** all exhibit a $N \rightarrow \text{SmA} \rightarrow \text{SmC}$ mesophase sequence (table 3.1) and the longer the chain length the lower are the melting points, clearing points and all the phase transitions.

All the mesophases are significantly reduced when the chain length is increased from 5 to 8 atoms and the effects are of a lesser extent when the chain length is increased from 8 to 11 atoms. The smectic phases stabilities usually increase for materials based on a difluoroterphenyl mesogenic core with straight terminal alkyl or alkoxy chain when the chain length is increased. However, compounds in table 3.1 have additional oxygen atoms present in the terminal chain.

Compounds **26** and **27** (see table 3.2) are analogues of compounds **17** and **18** respectively where a methylene group has replaced one atom of oxygen at the 7 and 10 positions along the terminal chain. Compound **26** has a chain length of eight atoms and compound **27** has a chain length of eleven atoms. Compound **26** has a higher melting and clearing point than compound **27** and this relationship is similar to that observed for compounds in table 3.1. Compounds **26** and **27** show only a smectic C phase and have lower melting points than the analogous compounds **17** and **18** (12.5°C and 33.2°C respectively). Compound **26** has a higher clearing point than compound **17** and a lower melting point which shows that the mesophase stability is reduced when the oxygen atom is present at the end of the terminal chain: the introduction of the oxygen atom has depressed the stability of the smectic C phase more than that of the smectic A or nematic phases.



26 $n = 1$
27 $n = 2$

Table 3.2 Transition temperatures ($^\circ\text{C}$) for compounds **26** and **27** and enthalpies of transitions (J g^{-1})

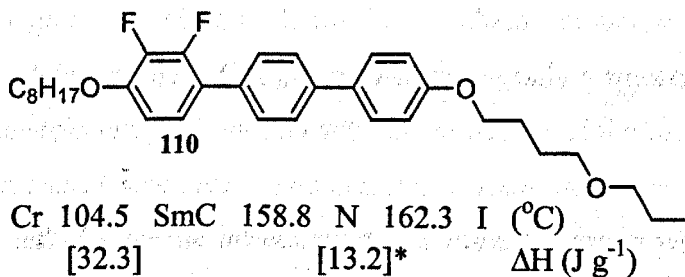
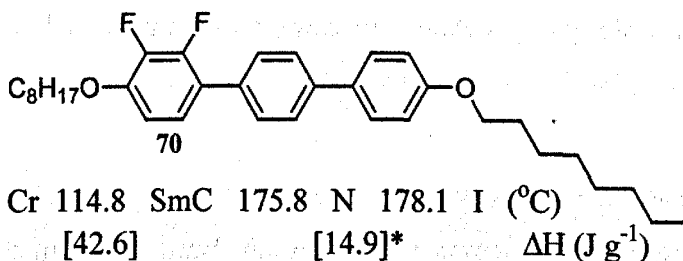
Compounds		Cr	SmC	I
26	$n = 1$	• 108.0 [33.4]	• 146.5 [12.1]	•
27	$n = 2$	• 72.8 [42.4]	• 119.5 [13.1]	•

Compound **27** has a lower melting point and clearing point than compound **18**, and here it can be seen, as for compound **17**, that the oxygen atom present at the end of the terminal chain has revealed a smectic A and nematic phases and indeed, the stabilities of these two phases have been increased. The oxygen atom appears to favour the formation of smectic A and nematic phases, but depresses the stability of the tilted smectic C phase.

Compounds **19**, **20** and **21** are alkyl-alkoxy systems and all have lower melting and clearing points than their respective analogues – compounds **16**, **17** and **18**. These results are consistent with results for difluoroterphenyls containing solely methylene groups within their terminal chains – for which the dialkoxy systems have higher melting points and phase transition temperatures and a greater smectic C phase stability than dialkyl systems. The increased smectic C phase stability of the dialkoxy systems can be explained by the presence of the two oxygen atoms as they increase the polarisability of the core and so give a general increase in the mesogenicity and they increase the dipoles at the end of the core and so give greater molecular tilting⁴.

The alkyl-alkoxy compounds also exhibit the same mesomorphic characteristics as their dialkoxy analogues *i.e.* when the chain length is increased the transition temperatures fall. Compound **21** (eleven atoms in its terminal chain) is the only compound of this series which does not display a smectic A phase. This result is unusual as the smectic A phase is normally absent for short chains and enhanced by longer chains^{5,6}.

Compound **110** is an analogue of compound **70** where a methylene group is replaced by an oxygen atom at the 6 position in the terminal chain.



* ΔH (J g⁻¹) values of I to SmC

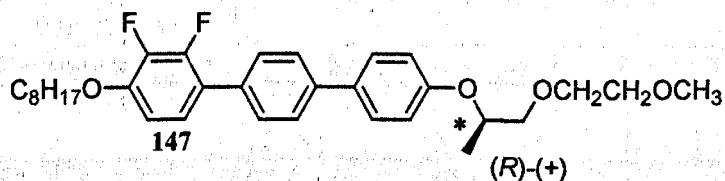
Here the oxygenated derivative compound **110** has a lower melting and clearing point than compound **70** and neither displays a smectic A phase. The results for the melting points of compounds **70** and **110** contrast with the results in table 3.1 and 3.2 where the presence of the oxygen atom near the end of the chain increases the melting points and favours the formation of the smectic A and nematic (compare compounds **26** and **27** with compounds **17** and **18** respectively). For compound **110** the presence of the oxygen atom has decreased the melting point and all phase stabilities.

The main determining factor for the effect of oxygen atoms on the types of mesomorphism and the mesophase stabilities of the compounds is probably *the position* of the oxygen substituent in the terminal chain. For the compounds in table 3.1, an oxygen atom is the penultimate atom in the chain and its presence might significantly affect the inter-digitation and the mixing of the terminal chains of the molecules, and therefore their mesomorphism.

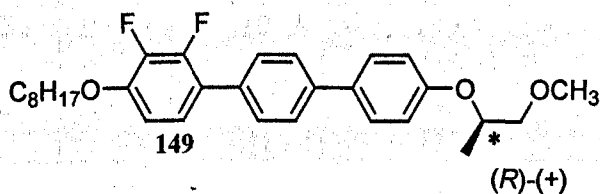
3.1.1.2 Chiral terminal chains with oxygen substituents

Compounds **147** and **149** are chiral derivatives of compounds **17** and **16** respectively and they were synthesised to investigate the effects on the mesomorphism of compounds **16** and **17** of the introduction of a methyl group close to the mesogenic core.

The results in table 3.1 show that the longer the chain the lower the transition temperatures; on the other hand, the results for compounds **147** and **149** show that when a methyl group is introduced, the longer chain compound (see **147**) gives higher transition temperatures. Compound **149** shows only a smectic C phase with a very short mesogenic range. A methyl substituent decreases the mesophase stability especially when close to the core⁷. The mesophase stabilities of compounds **147** and **149** have been reduced by the introduction of the methyl group when compared to those of compounds **17** and **16**, but the mesophase stability of compound **149** has been reduced more than that of compound **147**. This is contrary to the results in table 3.1 which showed that compounds containing shorter the chain have higher transition temperatures than the compounds which contain longer chains.



Cr 84.3 SmC* 90.0 N* 109.6 I (°C)
[38.5] [1.93] [1.82] ΔH (J g⁻¹)



Cr 73.2 SmC* 75.2 I (°C)
[49.4] [1.17] ΔH (J g⁻¹)

3.1.2 Terminal chain with silicon substituents

Compounds were prepared with a bulky trimethylsilyl end group on the terminal chain to study the effect of the group on melting points and on mesophase stabilities. Two series of compounds were considered with silicon-containing alkoxy terminal chains in conjunction with either an octyloxy or a nonyl terminal chain.

3.1.2.1 Dialkoxy systems with silicon substituents

The transition temperatures for the dialkoxy series of compounds **50-54** (see table 3.3) have several features to be noticed. Firstly, only compound **50** exhibits a nematic phase and a smectic C phase. All the other compounds in this dialkoxy series only show a smectic C phase when the number of methylene groups is greater than 2.

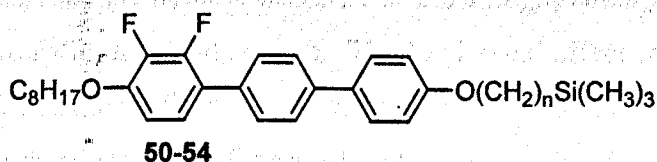


Table 3.3 Transition temperatures ($^{\circ}\text{C}$) for compounds **50-54** and enthalpies of transitions (J g^{-1})

Compounds		Cr	SmC	N	I
50	n = 2	• 72.8 [24.9]	• 119.1 [6.27]	• 130.7 [2.21]	•
51	n = 3	• 95.0 [18.4]	• 149.5 [17.8]	— —	•
52	n = 4	• 80.2 [18.6]	• 143.1 [17.1]	— —	•
53	n = 5	• 106.8 [30.1]	• 159.4 [16.4]	— —	•
54	n = 6	• 93.6 [18.4]	• 156.6 [17.3]	— —	•

There is a clear 'odd-even' effect for both the melting points and the transition temperatures from the smectic C phase. This phenomenon of an alternation in values along an homologous series has been observed for many other systems with straight alkoxy terminal groups (see figure 3.1)⁸.

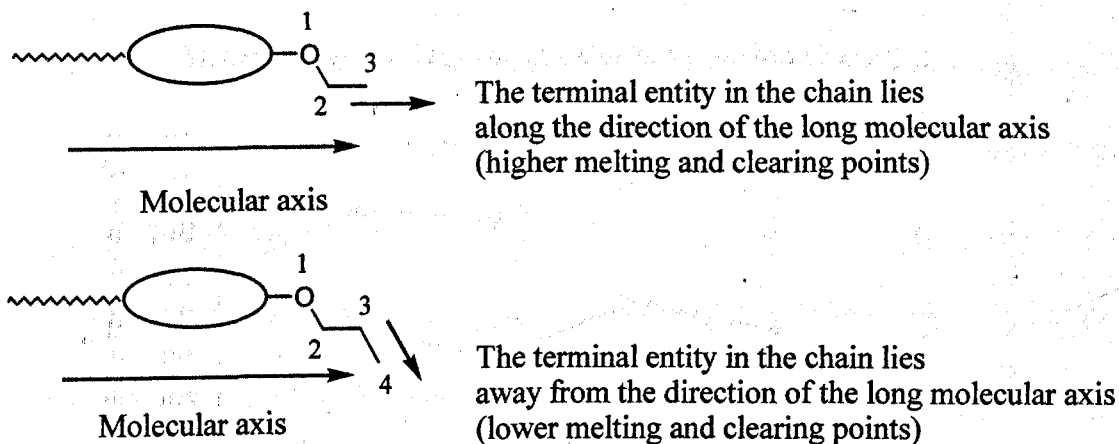


Figure 3.1 Representation of the odd-even effect in an alkoxy system with an unbranched terminal chain

The melting points and clearing points for compounds with unbranched terminal chains are higher when the number of atoms in the straight chain is odd, than when the number of atoms in the chain is even. The 'odd-even' effect is explained by the fact that when the number of atoms is odd the chain lies along the direction of the long molecular axis as shown in figure 3.1. On the other hand, results in table 3.3 show that when the number of oxygen, carbon and silicon atoms in the chain is even, the melting and clearing points are higher than when the number of atoms in the chain is odd, (e.g. for compound 51, $n = 3$, there are six atoms in the chain with dimethyl branching on the penultimate silicon atom in the chain, see figure 3.2). For the compounds which contain a bulky end group, the relationship of the end group to the long axis can explain the 'odd-even' effect, rather than the total number of atoms in the chain as is the case for straight alkoxy chains. When the bulky end group lies along the direction of the long molecular axis (see figure 3.3), the melting and clearing points are higher, even though there is an even number of atoms along the chain.

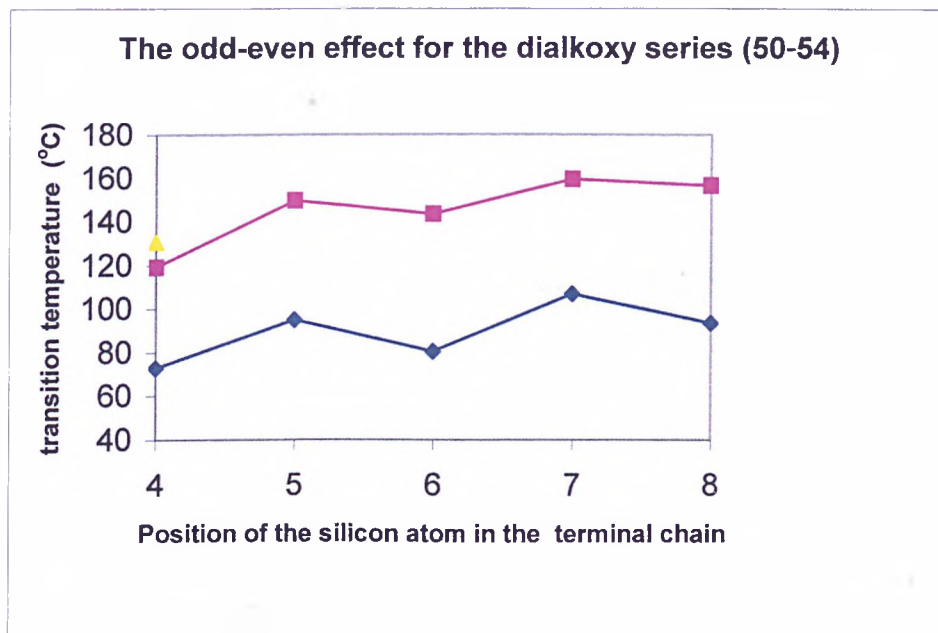


Figure 3.2 Odd-even effect for the dialkoxy series of compounds **50-54**

The structures shown in figure 3.3 were produced using Cerius² (version 1.5), and the preferred conformations were achieved by minimising the energy. The three models for each compounds represent views along the three axes. They show that the trimethylsilyl end group lies along the long molecular axis when the chain has five methylene groups (even series) and away from the axis when the chain has four methylene groups (odd series). When the trimethylsilyl group lies alongside the long molecular axis (see compound **53** in figure 3.3a), the compound has a higher mesophase stability than when the bulky trimethylsilyl end group lies across the molecular long axis (see compound **52** in figure 3.3a and the representation in figure 3.4).

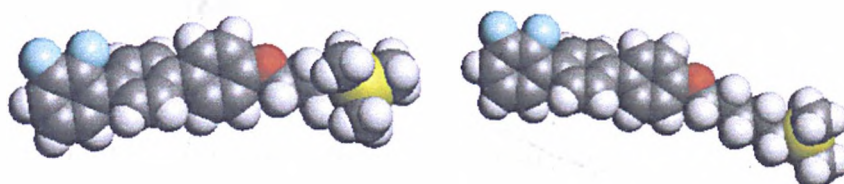
(a)



Compound 52

Compound 53

(b)



Compound 52

Compound 53

(c)



Compound 52

Compound 53

Figure 3.3 (a-c) Representations of preferred conformations for compounds **52** (four methylene groups) and for compound **53** (five methylene groups) where the octyloxy chain is omitted; view (a) with the fluoro-substituted ring horizontal, view (b) with the fluoro-substituted ring vertical and view (c) looking along the terphenyl axis.

In this series, compounds containing trimethylsilyl end groups with an even number of atoms in the alkoxy chain may be better for use in ferroelectric host mixtures because of their higher clearing point (see figure 3.4).

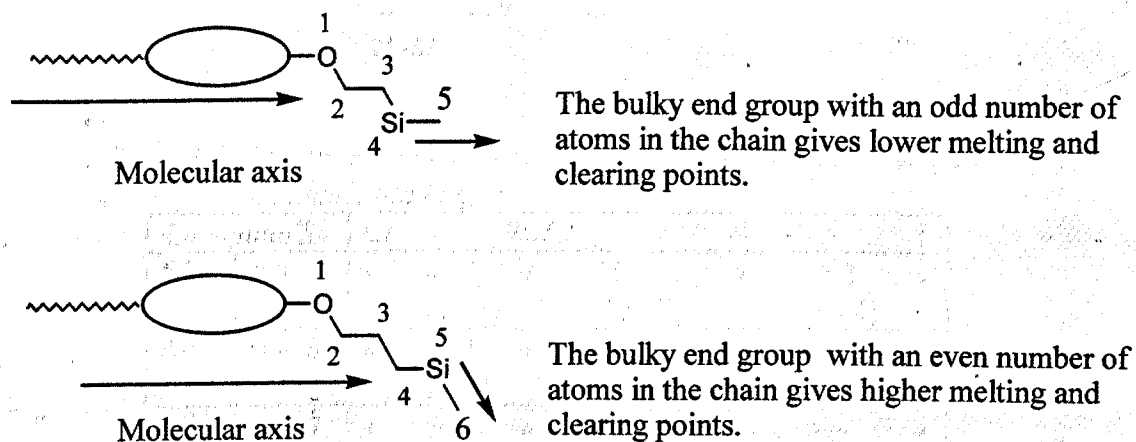


Figure 3.4 Representation of the odd-even effect for the silicon-containing alkoxy system.

3.1.2.2 Alkyl-alkoxy systems with silicon substituents

An alkyl-alkoxy series of compounds analogous to the compounds in table 3.3 was prepared to investigate the differences between alkoxy and alkyl terminal chains on the mesomorphism and transition temperatures of compounds with a bulky end group on their terminal chain (see table 3.4).

As was the case for compounds 50-54, compounds 55-59 show the odd-even effect in melting point and in the transition from the smectic C phase (see figure 3.5). When the number of atoms along the chain is odd, the melting and clearing points are lower. These results are similar to the pattern of alternating temperatures seen for compounds 50-54 and the explanation for its occurrence is similar to that given in section 3.1.2.1. Only compound 55, with the shortest chain, displays the nematic phase as well as the smectic C phase, and this is similar to the results for the dialkoxy analogue, compound 50. Compounds 55-59 all have a lower phase stability than their dialkoxy analogues and this is consistent with work by Hird *et al.*,⁹ which shows that dialkoxy terphenyls have a higher mesophase stability than their alkoxy-alkyl analogues. In the cases of the dialkoxy compounds reported here, the melting

points and their smectic C stabilities are on average 25 and 35 °C higher than for the alkyl-alkoxy compounds.

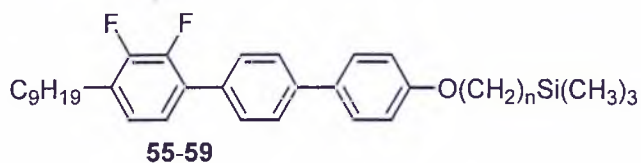


Table 3.4 Transition temperatures (°C) for compounds **55-59** and enthalpies of transitions (J g^{-1})

Compounds		Cr	SmC	N	I
55	n = 2	• 47.2 [25.8]	• 78.6 [7.27]	• 95.3 [3.20]	•
56	n = 3	• 80.1 [19.4]	• 113.3 [16.7]	—	•
57	n = 4	• 54.2 [22.0]	• 107.5 [12.4]	—	•
58	n = 5	• 72.2 [19.5]	• 127.2 [14.0]	—	•
59	n = 6	• 57.6 [15.9]	• 123.0 [12.5]	—	•

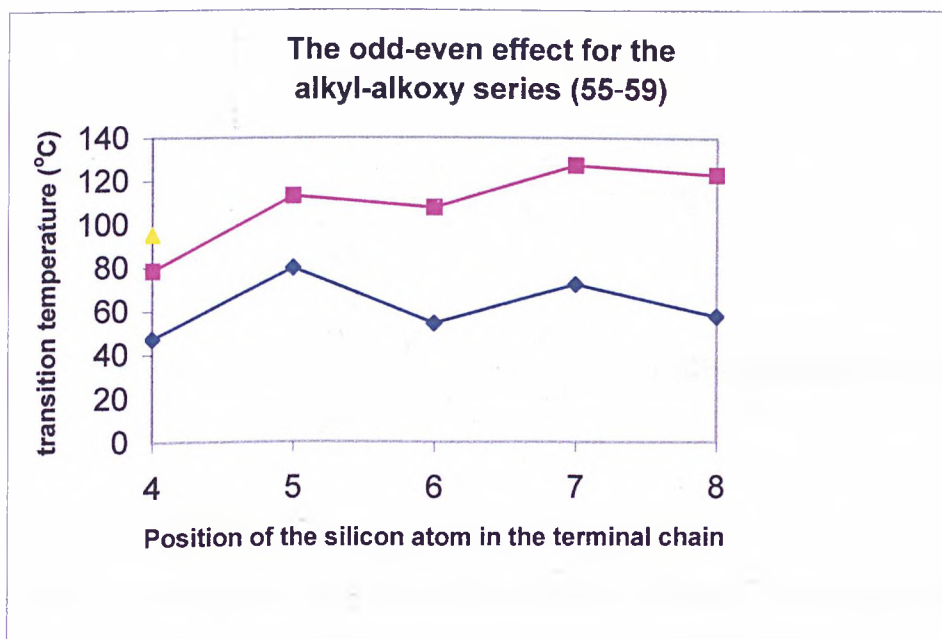
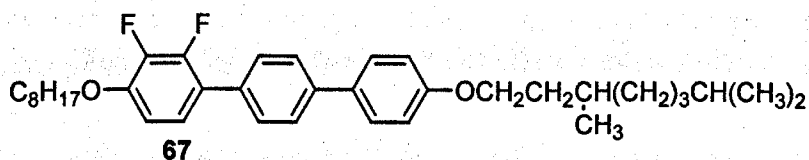
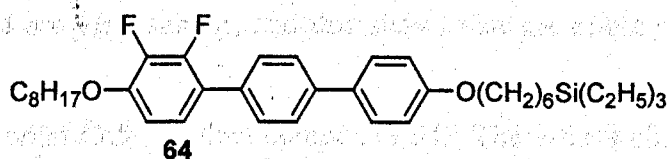
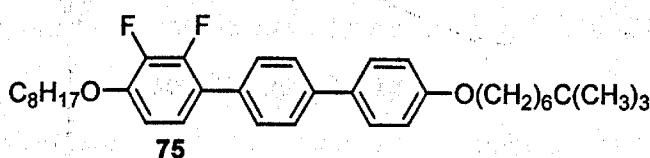
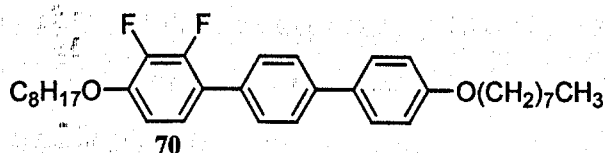


Figure 3.5 Odd-even effect for the alkyl-alkoxy series of compounds **55-59**

3.1.2.3 Dialkoxy systems with nine atom-chains but different end groups

Several compounds related to compound 54 were prepared, which all have a similar chain length but with different end groups.

- ◆ Compound 70 has the same number of atoms along its terminal chain (nine), but no bulky end group (only a straight alkoxy chain).
- ◆ Compound 75 has the same chain length (nine) but the silicon atom present in the terminal chain for compound 54 has been replaced by a carbon atom.
- ◆ Compound 64 possesses a bulkier triethyl unit in place of the trimethyl bulky end group.
- ◆ Compound 67 is related to compound 75 in that it has the same number of carbon atoms in the terminal chain but one methyl group is moved from the end of the chain to the fourth atom.



The transition temperatures of compounds 54, 64, 67, 70 and 75 are given in table 3.5.

Table 3.5 Transition temperatures ($^{\circ}\text{C}$) for compounds **54**, **64**, **67**, **70** and **75** and enthalpies of transitions (J g^{-1})

Compounds	Cr	SmC	N	I
54	• 93.6 [18.4]	• 156.6 [17.3]	— —	•
64	• 54.4 [15.1]	• 125.8 [13.6]	— —	•
67	• 82.5 [33.4]	• 132.2	• 138.0 [10.4]*	•
70	• 114.8 [42.6]	• 175.8	• 178.1 [14.9]*	•
75	• 97.3 [26.1]	• 160.1 [17.9]	— —	•

* ΔH value for the I to SmC transition

The comparison of the values for compound **70** with those for compound **75** which contains a *tert*-butyl end group, shows that the bulky end group has reduced the melting point by 17.5°C and the clearing point by 18.0°C . Compound **75** shows only a smectic C phase; the smectic C phase has been suppressed, but to a lesser extent than for the nematic phase.

As expected, compounds **54** and **75** have lower melting points (21.2 and 17.5°C respectively) and clearing points (21.5 and 18.0°C respectively) than for compound **70** with an unbranched terminal chain. The transition temperatures for compound **75** and compound **54** are very similar, and this shows that the effect of replacing the silicon atom with carbon is very slight; compound **75** has a higher melting point (3.7°C) and clearing point (3.5°C) than compound **54**. The effects observed are only small and do not indicate that there is any appreciable difference between a carbon or silicon unit at the end of a chain.

Compound **64** shows only a smectic C phase and it has a lower melting point and clearing point than compound **54** which is consistent with compound **64** having the bulkiest end group.

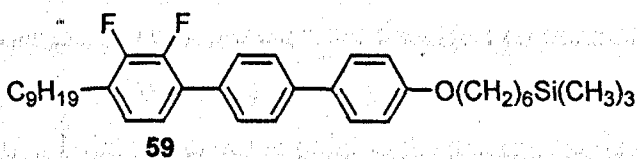
Compound **67** has a lower melting point and a much lower clearing point than compound **75** (14.8 and 22.1°C respectively), showing that the methyl group on the fourth atom has a much greater effect on the depression of the clearing point than a terminal methyl branching. This observation is in agreement with the previously

reported effects of chain branching in straight chain units. The current comparison of compounds **67** and **75** is effectively showing two different positions of methyl substitution in a chain ending in an isopropyl unit. Compound **75** only shows a smectic C phase. The methyl substituent at the fourth atom in the terminal chain gives a compound which allows a nematic phase to exist whereas the bulkier end group in compound **75** is more conducive to the smectic C phase.

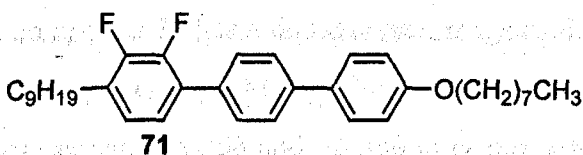
3.1.2.4 Alkyl-alkoxy systems with nine atoms-chains but different end groups

The results for compounds **70** and **75** have been compared with those for compounds **54** (see section 3.1.2.3) and for a similar comparison, analogues of compound **59** were prepared.

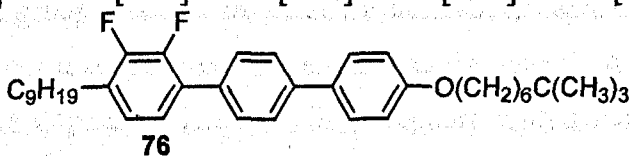
- ◆ Compound **71** has the same number of atoms along its terminal chain (nine), but no bulky end group (only a straight alkoxy chain).
- ◆ Compound **76** has the same chain length (nine) but the silicon atom present in the terminal chain for compound **59** has been replaced by a carbon atom.



Cr 57.6 SmC 123.0 I (°C)
 ΔH [15.9] [12.5] (J g⁻¹)



Cr 63.1 Cryst J 68.9 SmI 79.6 SmC 90.2 SmA 148.9 I (°C)
 ΔH [28.7] [1.34] [15.2] [3.10] [17.0] (J g⁻¹)



Cr 60.4 SmC 126.5 I (°C)
 ΔH [18.7] [16.6] (J g⁻¹)

Compound **71** with two straight chain terminal groups shows a smectic A, a smectic C, a smectic I and a crystal J phase, whereas compounds **59** and **76** show only the SmC phase. Both of the branched chain compounds (**59** and **76**) have a slightly lower melting points (5.5 and 2.7 °C respectively) and rather more greatly depressed

clearing points (25.9 and 22.4 °C respectively) than the straight chain analogue compound 71.

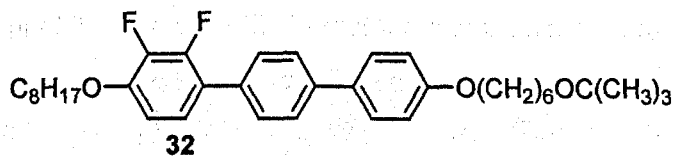
The transition temperatures of compound 76 show that a *tert*-butyl end group gives a slightly higher melting point (2.8 °C) and clearing point (3.5 °C) than the silicon-containing compound 59. The differences between the transition temperatures for the compounds with the *tert*-butyl and trimethylsilyl end groups is similar to that discussed in section 3.1.2.3 for the dialkoxy series.

In conclusion, the bulky end groups in these series of compounds have several effects on the overall mesomorphic properties of the compounds. The effects that have been observed for the dialkoxy and alkyl-alkoxy series are:

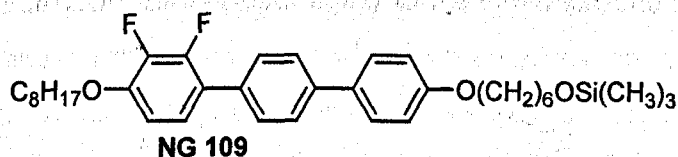
- ◆ The bulky end group reduces the melting and the clearing point and acts to hinder the packing and the molecular association of the molecules.
- ◆ The bulkier the end group the greater the effect on the melting point and on the clearing point. Compound 64 has the bulkiest end group and shows the lowest melting point and clearing point in the dialkoxy series.
- ◆ The liquid crystalline temperature range was not significantly affected by the presence of the bulky end group. Compound 70 has a liquid crystal range of 63.3 °C, compound 75 has a liquid crystal range of 62.8 °C and compound 54 has a liquid crystal range of 63.0 °C
- ◆ Apart from compounds 50 and 55, the only mesophase displayed by the materials reported, is the smectic C phase. This observation suggests that the bulky end group, because of its steric hindrance, depresses the mesophase stabilities but it suppresses the nematic and the smectic A phases more than the smectic C phase. These findings support Wulf's model¹⁰ (see section 1.4.2.1) that the steric hindrance of the non-polar bulky end groups probably causes the molecules to tilt.

3.1.3 *t*-Butyloxy end group

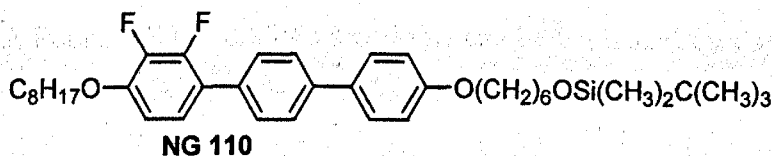
Compound **32** was prepared in order to compare the effect of an ether link to a tertiary carbon with that to a tertiary silyl centre (see compound NG 109, reported by N. Gough⁶). Compound NG 110 (also prepared by N. Gough⁶) has an even longer bulky end group than for compound NG 109. Like most of the materials reported here containing a bulky end group, compound **32** also shows a direct transition from the isotropic liquid to the smectic C phase, but more interestingly, it also shows a smectic C_{alt} phase at 119.8 °C.



Cr 99.1 SmC_{alt} 119.8 SmC 151.8 I (°C)
 ΔH [49.4] [1.17] (J g⁻¹)



Cr 138.5 SmC 161.3 SmA 170.0 N 180.4 I (°C)



Cr 71.0 SmC 137.0 SmA 137.9 N 140.6 I (°C)

Materials synthesised by Coles *et al.*^{13,14} containing a siloxy end group have low melting points, but compound NG 109 has higher melting and clearing points than compound **32**. Compounds NG 109 and NG 110 show nematic and smectic A phases; this is uncharacteristic of the materials with a bulky end group which have been prepared in this work, but the increased bulkiness of NG 110 compared to NG 109 causes lower transition temperatures throughout and this is consistent with previous comments (see section 3.1.2.3). The results for NG 109 are quite exceptional and it is possible that the compound is unstable. The transition

temperatures for the related hydroxy compound (31) are Cr 158.3 SmC 168.9 SmA 179.5 N 185.0 I (°C).

Compounds 54 and 75 (see section 3.1.2.3) showed the same mesomorphism *i.e.* a direct isotropic liquid to smectic C phase transition and compound 75 has higher transition temperatures than 54.

It appears unlikely that the oxygen-to-silicon bond plays an important role in producing low melting materials, as compound NG 109 has a higher melting point than compound 32. It is more likely that the major factor is the size of the end group which causes a reduction in the interchain interactions.

Coles *et al.*^{13,14} found that compounds with a bulky siloxane end group were fast switching materials, as the materials have a low viscosity; the materials also show a direct transition from the isotropic liquid to the chiral smectic C phase. There are several alternative explanations as to why the compounds reported by Coles are fast switching materials. Firstly, Coles *et al.*^{13,14} showed that organosiloxane materials have a low viscosity; by using the current pulse technique, they measured the projection viscosity, γ , ($\tau = \gamma/Ps E$) to be 0.5 Pa s compared to the projection viscosity of the SCE13 mixtures (based on fluoroterphenyls and fluorobiphenol esters, Merck Poole, UK) of 0.85 Pa s and this can be explained by the fact that the oxygen to silicon bond is more flexible than the carbon-carbon bond in alkyl chains; the increased flexibility decreases the gyration radius^{15,16} and so decreases the rotational viscosity. Secondly these organosiloxane liquid crystals contain three distinct parts compared to the usual two (the core and aliphatic regions); Coles *et al.*^{13,14} showed by X-ray studies that the siloxane units agglomerate to create a micro-segregated region giving core, aliphatic, and silyloxy regions. This segregation of the molecules may lead to a lower viscosity and less entanglement and so results in faster switching. Thirdly, because the silicon-oxygen bond has a lower rotational energy barrier (see figure 3.6), it causes a reduction in the interchain interactions, and enables the molecules to switch faster.

In figure 3.6, for (a), the non-bonded interactions between the eclipsing entities destabilises the rotamer in the eclipsed conformation, giving it a higher energy. The

rotation about the bond has an energy barrier to overcome; the same situation exists for (b). For (c) and (d), the rotation about the oxygen-carbon bond and oxygen-silicon bond is easier because the methyl groups on the carbon (c) and silicon (d) are eclipsed by the lone pairs on the oxygen atom, making the rotation energy barrier smaller. Furthermore, the carbon-silicon (b) bond is longer¹⁶ than the carbon-carbon (a), and this probably reduces the energy barrier for the rotation about this bond. In the case of the oxygen-silicon bond (d), a charge transfer occurs from the oxygen lone pair to the silicon atom which shortens the covalent bond and also decreases the linearisation energy barrier¹⁶ and thus reduces the energy barrier about the bond. The relative decreasing ease of rotation for (a)-(d) can reasonably be predicted as follows (d) > (c) > (b) > (a).

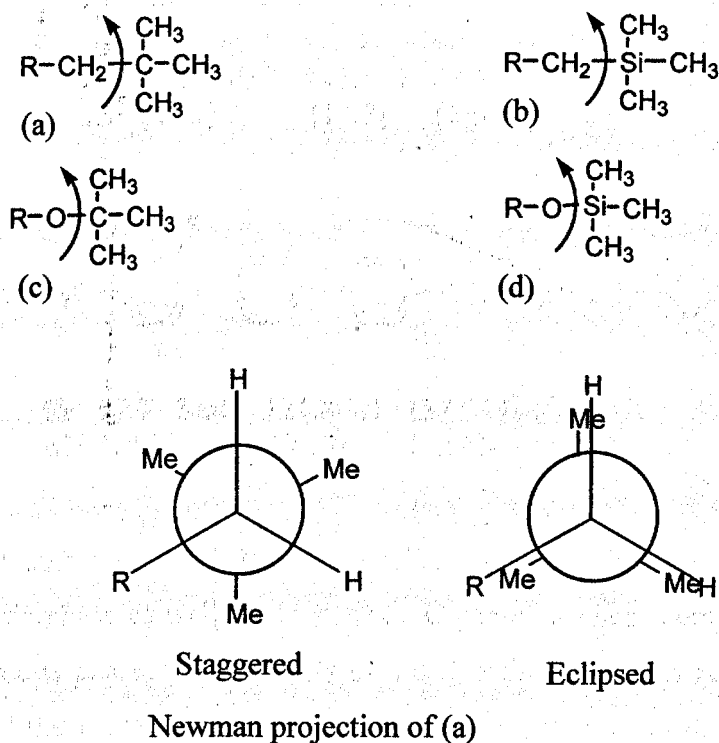
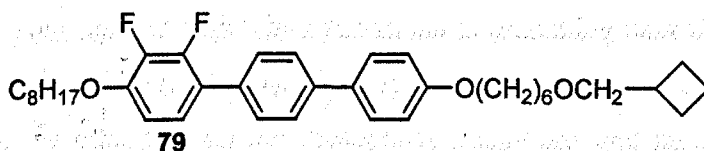


Figure 3.6 Rotation about (a) C-C, (b) C-Si, (c) O-C, (d) O-Si bonds and Newman projection for case (a)

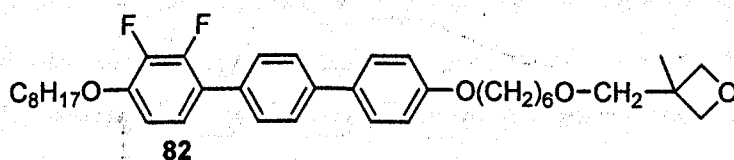
3.1.4 Effects of a four-membered ring end group

Compound **79** was prepared to study the effect of a cyclobutyl end group on the mesomorphism of a difluoroterphenyl core and also to study its miscibility with a standard smectic C material (section 3.2). The cyclobutyl unit is similar to, but less spatially demanding than, an isopropyl end group.

Compound **82** containing a methyl-substituted oxetane ring as an end group was prepared for comparison with compound **79**; the oxetane unit is similar to a *t*-butyl group and has the unusual property of an oxygen atom as the outermost component of the chain.



Cr 92.5 SmC 148.1 I (°C)
 ΔH [24.5] [17.7] (J g⁻¹)



Cr 97.7 SmC 124.8 N 137.8 I (°C)
 ΔH [14.5] [0.13] [0.58] (J g⁻¹)

Compound **82** and compound **79** have similar melting points but compound **82** shows a nematic phase as well as the smectic C phase, whereas compound **79** only shows a smectic C phase. The stability of the smectic C phase in compound **82** is suppressed and the nematic phase is favoured by the presence of the oxygen atom and the methyl substituent. This result was not expected as it was anticipated that the branching substituent would suppress the nematic phase and the polar interactions from the oxygen substituent would favour the formation of the smectic C phase. However, the cyclobutyl end group favours the smectic C phase over the nematic phase and therefore suggests that in this instance the tilted smectic C phase is favoured by steric interactions which force the molecules to tilt as proposed by Wulf's model¹⁰ rather than by dipolar interactions, as proposed by McMillan⁴ (see section 3.1.2.4). Normally, the dipolar interactions which favour the smectic C phase

operate at a point away from the extremity of the molecule, whereas in compound **82** the dipoles are at the very end of the chain.

These comparisons are inevitably incomplete and inconclusive because only one homologue of each series is being compared. Other members of the series may have the terminal ring system of the end group pointing along or across the molecular axis

3.1.5 Terminal chains with constant length but varying size of end groups

Two series of compounds, **110-116** and **117-120** for the octyloxy and nonyl systems respectively, were prepared which had variations in branching near the end of a nine atom chain (see also section 3.1.2.3). End groups of varying size were synthesised to study the effect of bulkiness on the mesophase transitions and melting points (see tables 3.6 and 3.8). Compounds **110-116** and **117-120** differ in the presence and position of various methyl groups in the chain at the 4''-position.

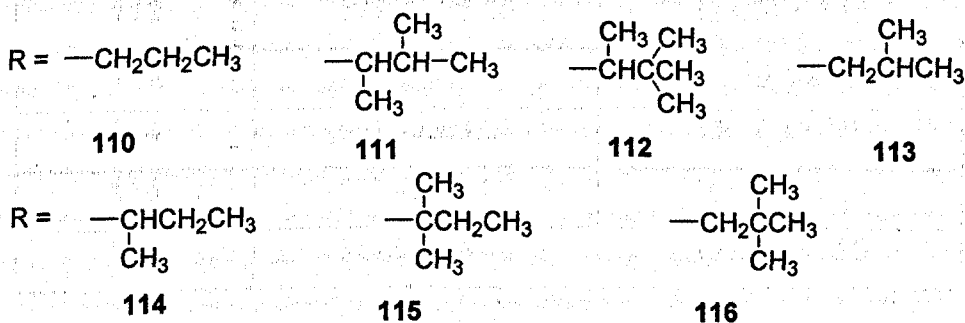
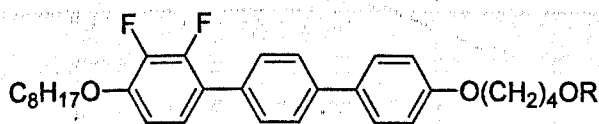


Table 3.6 Transition temperatures for compounds 110-116 (°C) and enthalpies of transitions (J g^{-1})

Compounds	Cr	SmC	N	I
110	• 104.5 [32.3]	• 158.8	• 162.3 [13.2]*	•
111	• 84.5 [16.2]	• 142.8 [14.5]	— —	•
112	• 88.7 [15.4]	• 139.4 [15.6]	— —	•
113	• 99.7 [30.5]	• 155.5 [15.4]	— —	•
114	• 92.0 [14.5]	• 148.7 [13.8]	— —	•
115	• 82.6 [16.3]	• 138.2 [15.3]	— —	•
116	• 87.6 [17.5]	• 148.6 [16.4]	— —	•

* ΔH value for the I to SmC transition

Table 3.7 Molecular volumes and end group volumes of compounds 110-116

Compounds	Molecular volume / \AA^3	End group volume / \AA^3
110	542.50 \pm 5.40	69.15 \pm 3.10
111	583.45 \pm 4.10	106.20 \pm 1.35
112	597.20 \pm 5.20	124.70 \pm 2.15
113	554.10 \pm 3.15	88.10 \pm 1.00
114	561.50 \pm 3.20	88.70 \pm 0.95
115	582.40 \pm 4.80	105.10 \pm 2.80
116	584.95 \pm 4.40	105.15 \pm 1.90

Compound 110 is the straight chain reference compound for this study and is the only material that displays a nematic phase and a smectic C phase. All the other compounds in the series only show the smectic C phase. The mesophase range is retained when bulkiness is varied and branching by methyl groups in the chain occurs at different positions.

The series 110, 113 and 114 shows the effect of moving a methyl substituent from near the end position to a point closer to the mesogenic core. This sequence gives a gradual decrease in clearing and melting points.

Compounds **115** and **116** have two methyl groups attached to the same carbon atom but they differ in the position of attachment along the chain. Compound **116** is a *tert*-butyl end group. Compound **115** has a lower melting point and clearing point than compound **116** (5 and 10.4 °C respectively). This difference conforms to the effects seen for compounds **110**, **113** and **114** on moving the substituent closer to the core.

As with compounds **115** and **116**, compound **111** has two methyl substituents, but the two methyl groups are not at the same position in the chain. Compound **111** has a lower melting point and a lower clearing point than compound **116** (3.1 and 5.8 °C respectively) but has a higher melting point and higher clearing point than compound **115** (1.9 and 4.6 °C respectively); once again these effects are consistent with those noted above.

Compound **112** has three methyl substituents present and is related to compounds **111** and **116**; in these cases the generalities detected for mono- and di-methyl substitution are not maintained. Compound **112** has a higher melting point and a lower clearing point than compound **111** (4.2 and 3.4 °C respectively) and it has a higher melting point and a lower clearing point than compound **116** (1.1 and 9.2 °C respectively).

In general, but with the exception of compound **112**, the more methyl groups that are present and the closer they are to the core, the lower are the melting and clearing points. As seen in this series, introducing bulkiness suppresses the nematic phase and only the straight chain compound **110** shows the nematic phase.

Values of the molecular and end group volumes (see table 3.7) were determined using the Cerius² (version 1.5) software on a silicon graphics workstation. The steric volume of the end group was determined as represented in figure 3.7; the values in table 3.6 and 3.7 show the relationship between the steric volume and the depression of clearing points; the greater the volume, then the higher is the depression of clearing points and melting points, with the exception of the melting point for compound **112**. This is shown by figures 3.8-3.10, the depreciation in the melting and clearing points appears to be linear. The effect is better illustrated by compounds **110**, **112**, **113** and **116** in figures 3.9 and 3.10, in this series the

substitution occurs at the same carbon centre (**110**, **113** and **116**) and compound **112** has the same methyl substitution as compound **116** but one methyl substituent at the 7-position in the chain.



End groups for compounds **110** and **111**

The steric volume was calculated including the oxygen atom

Figure 3.7 Representation of end groups for the calculation of steric volumes

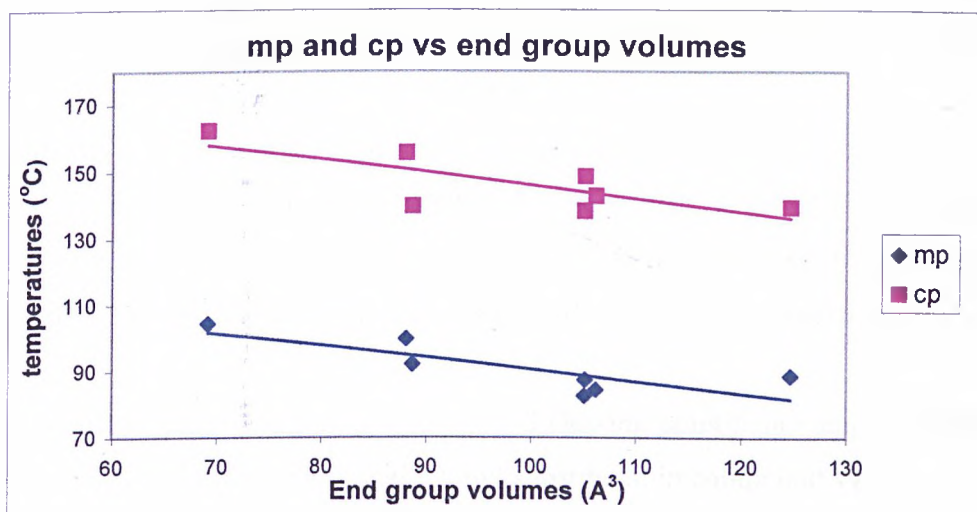


Figure 3.8 Melting and clearing points vs end group volumes for compounds **110-116**

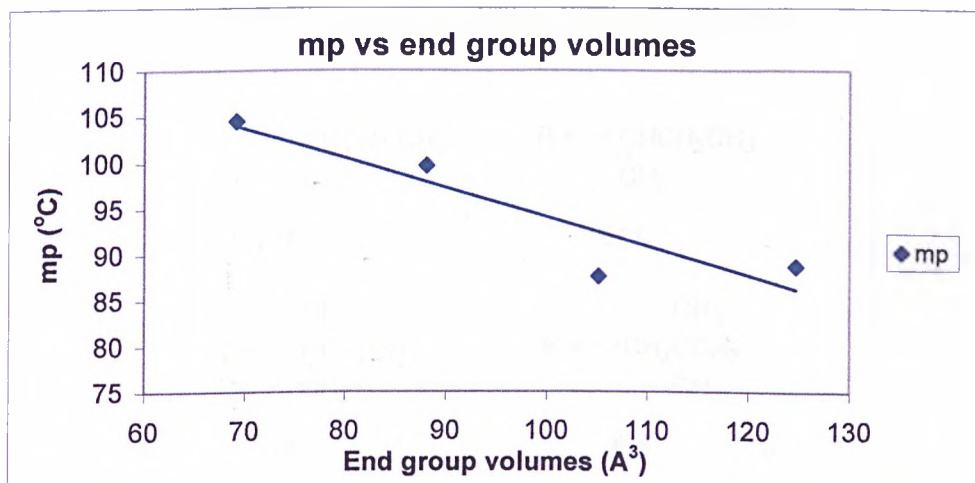


Figure 3.9 Melting points vs end group volumes for compounds **110, 112, 113** and **116**

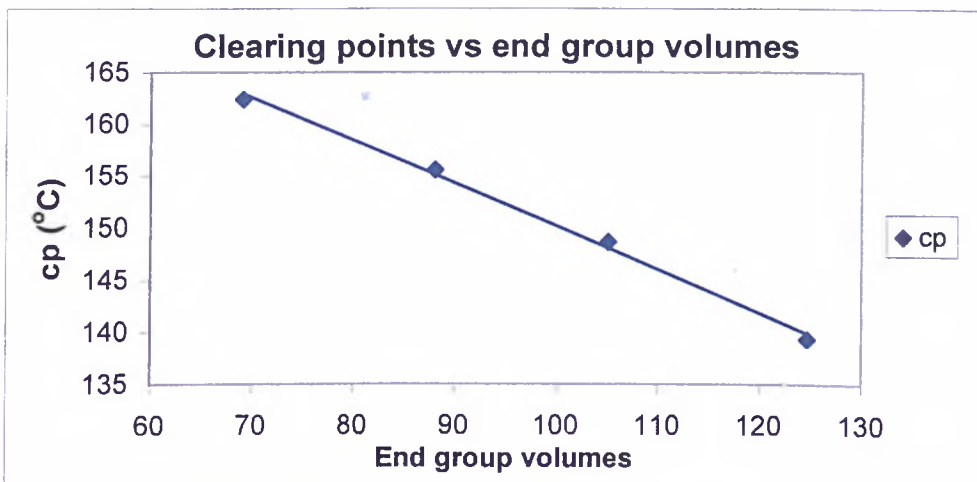
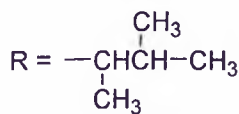
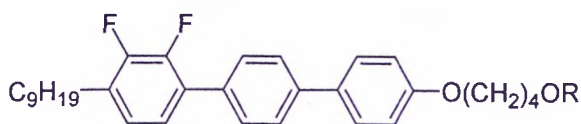


Figure 3.10 Clearing points vs end group volumes for compounds **110**, **112**, **113** and **116**

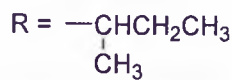
The alkyl-alkoxy compounds in this series (see table 3.8) have lower melting and clearing point than their dialkoxo analogues. They also only show the smectic C phase, as do, their analogues given in table 3.6.

Compounds **119** and **120** have two methyl substituents on the same carbon atom but they differ in the position of substitution in the chain. Both compounds have a similar melting point but compound **119** with the substituents closer to the core has a significantly lower clearing point than compound **120** (10.7 °C respectively).

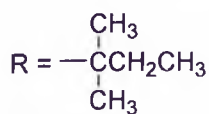
Compound **117** has a lower melting point and clearing point than compound **118** and this is consistent with the additional methyl substituent in compound **117**.



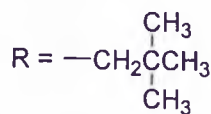
117



118



119



120

Table 3.8 Transition temperatures for compounds 117-120 (°C) and enthalpies of transitions (J g⁻¹)

Compounds	Cr	SmC	I
117	• 55.2 [20.6]	•	114.3 [13.0]
118	• 66.1 [13.4]	•	119.0 [13.8]
119	• 54.7 [31.6]	•	105.7 [20.5]
120	• 54.3 [14.4]	•	116.4 [13.3]

The transition temperatures for these two series of compounds allow the following conclusions to be made.

- ◆ The alkyl-alkoxy series has lower melting and lower clearing points than their dialkoxy analogues.
- ◆ The greater the steric volume the lower the melting and clearing point.
- ◆ The position of the substitution in the chain is important; the clearing point is greater when the branching is closer to the mesogenic core.
- ◆ The bulky end group suppresses the nematic phase.

3.1.6 Branched alkoxy-alkyl and dialkyl terminal chains

Compounds 128-131 were synthesised to investigate the effects of bulky end groups in conjunction with methyl branching in the chain for alkoxy-alkyl compounds (128 and 129) and dialkyl compounds (130 and 131) (see table 3.9).

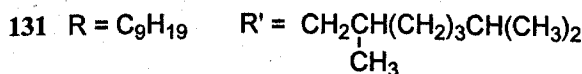
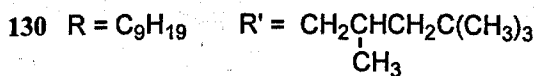
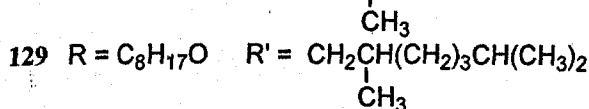
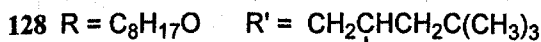
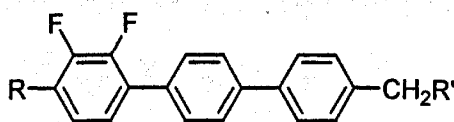


Table 3.9 Transition temperature for compounds **128-131** ($^{\circ}\text{C}$) and enthalpies of transitions (J g^{-1})

Compounds	Cr	SmC	I
128	• 55.4 [15.0]	• 104.5 [11.9]	•
129	• 82.5 [36.9]	• 115.6 [13.5]	•
130	• 53.7 [27.9]	• 62.7 [8.95]	•
131	• 28.2 [13.3]	• 75.2 [10.5]	•

Once again, compounds in this series only show the smectic C phase; all the examples have a methyl substituent at the 3-position in the chain, but compounds **128** and **130** have six atoms along the chain whereas compounds **129** and **131** have eight atoms along the chain. Compound **128** has a lower melting and clearing point than compound **129** (27.1 and 11.1 $^{\circ}\text{C}$ respectively); these results might be explained by the fact that compound **128** possesses the shorter chain and the bulkier end group (*t*-butyl compared to isopropyl for compound **129**).

The compounds shown in table 3.9 have the same relationship of clearing points (compounds **128** and **130** have lower clearing points than compounds **129** and **131** respectively) but compound **130** has a higher melting point than **131**, whereas compound **128** has a lower melting point than **129**. The results for compounds **131** and for compound **129** arise from a combination of two factors and show that a greater smectic C mesophase stability is achieved with longer chains and a less bulky end group.

3.1.7 Chloro end substituents

This alkoxy-alkyl series was prepared to study the influence of a chloro end group on the terminal chain of various lengths. The terminal chain has 3 to 5 methylene groups. The transition temperatures given in table 3.10 show that in this series only the smectic A phase is shown. There appears to be evidence of an odd-even effect where compounds 138 and 140 have higher melting points and clearing points than compound 139. The chloro substituent does not appear to alter the normal 'odd-even' effect relationship.

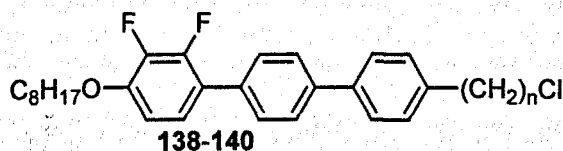
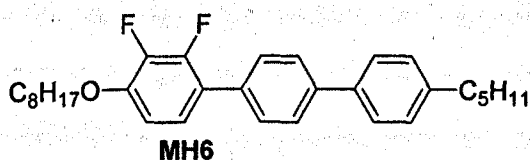
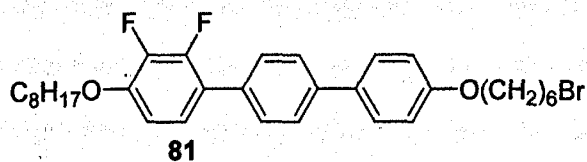


Table 3.10 Transition temperatures ($^{\circ}\text{C}$) for compounds 138-140 and enthalpies of transitions (J g^{-1})

Compounds	Cr	SmA	I
138 $n = 3$	• 102.0 [46.7]	• 157.3 [11.1]	•
139 $n = 4$	• 71.0 [28.5]	• 151.2 [10.2]	•
140 $n = 5$	• 80.2 [33.0]	• 154.9 [11.6]	•



Cr 93.5 SmC 144.0 SmA 148.0 N 159.0 I

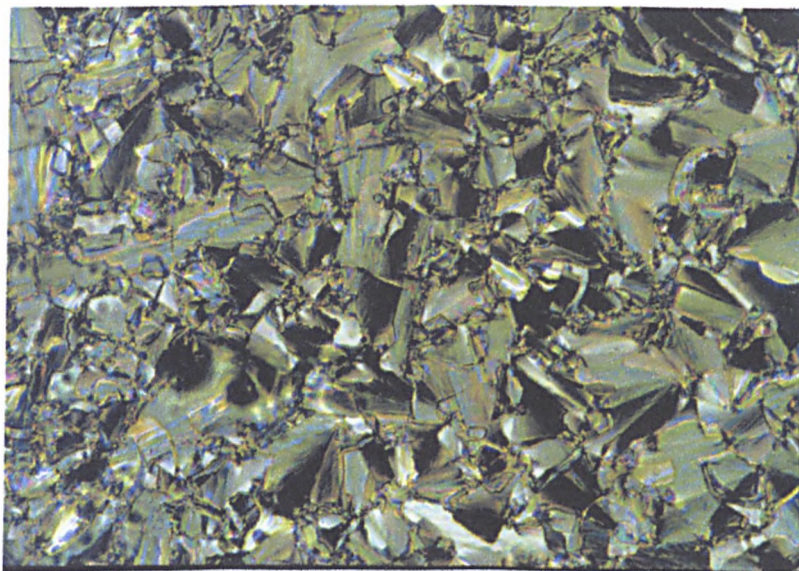


Cr 100.7 SmA 117.8 I

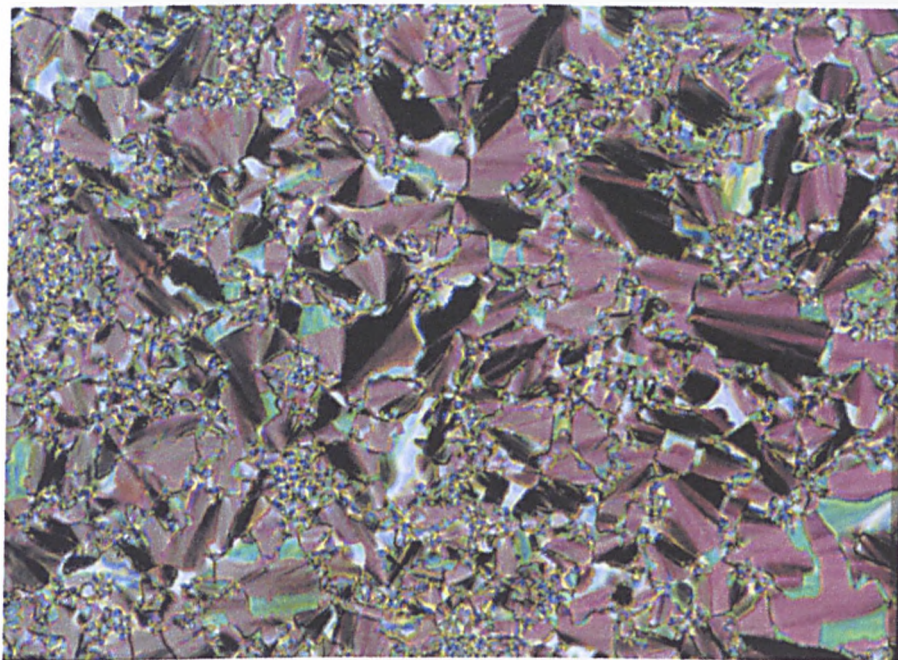
MH6 is analogous¹⁷ to compound **140**, they both have a five-atom chain at the 4''-position, where the chloro substitutes a hydrogen atom. Compound **MH6** exhibits a $N \rightarrow SmA \rightarrow SmC$ cooling phase sequence but the chloro substituent has reduced the melting and clearing points by 13.1 and 4.1 °C respectively, and, more remarkably compound **140** only shows a smectic A phase. The bromo compound **81**, which is similar to compound **140** but has one methylene unit more in its alkoxy chain at the 4''-position. It also only shows a smectic A phase.

The effect of the chloro substituent on the mesophase morphology is significant and appears to encourage an orthogonal arrangement of the molecules in the smectic layers thus suppressing the smectic C and nematic phases. Introducing a chloro or bromo substituent at the end of a terminal chain gives a smectic A phase inducer and therefore such compounds may be used in mixtures when the smectic A phase is required.

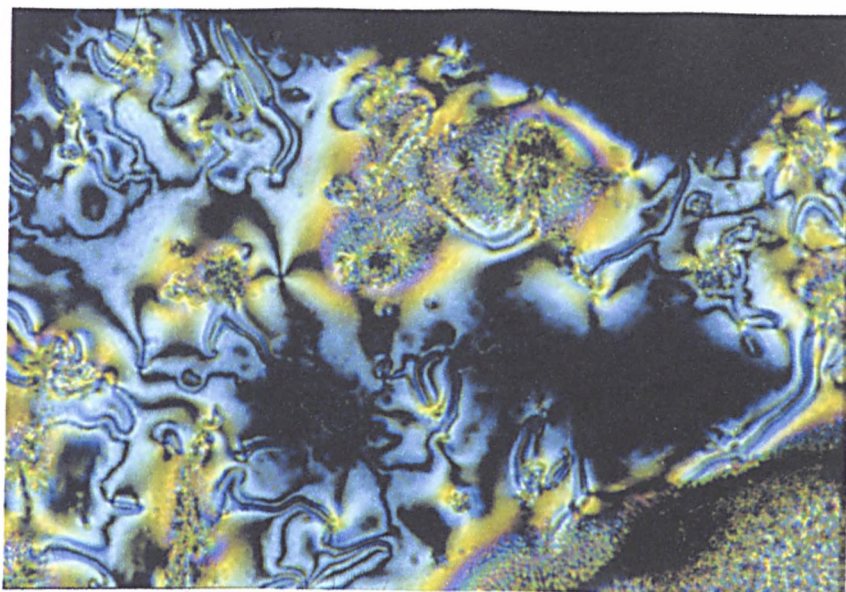
3.1.8 Photomicrographs of the mesophases shown by bulky end group compounds



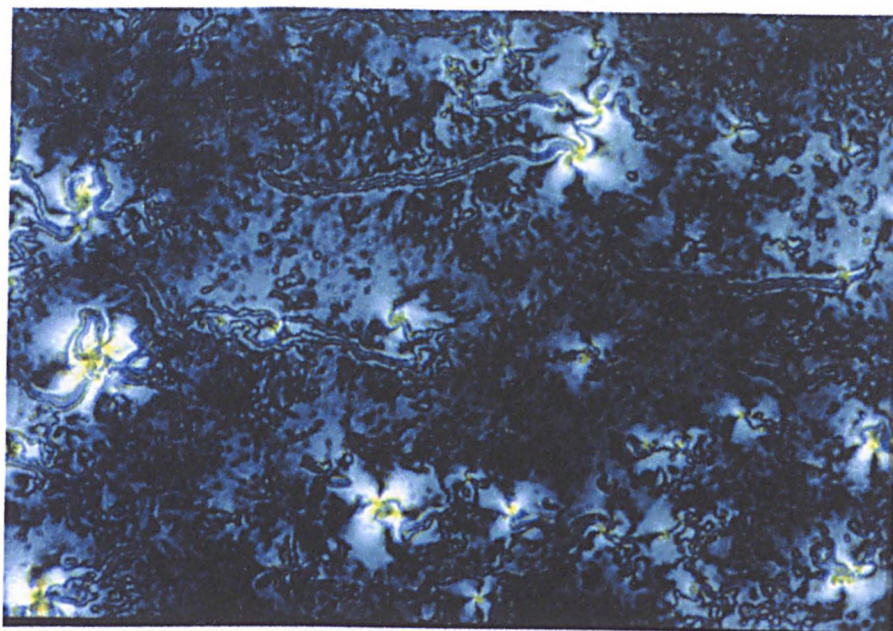
Photograph 3.1 Typical smectic C phase focal-conics (compound 54).



Photograph 3.2 Focal-conics, smectic C phase compound 75.

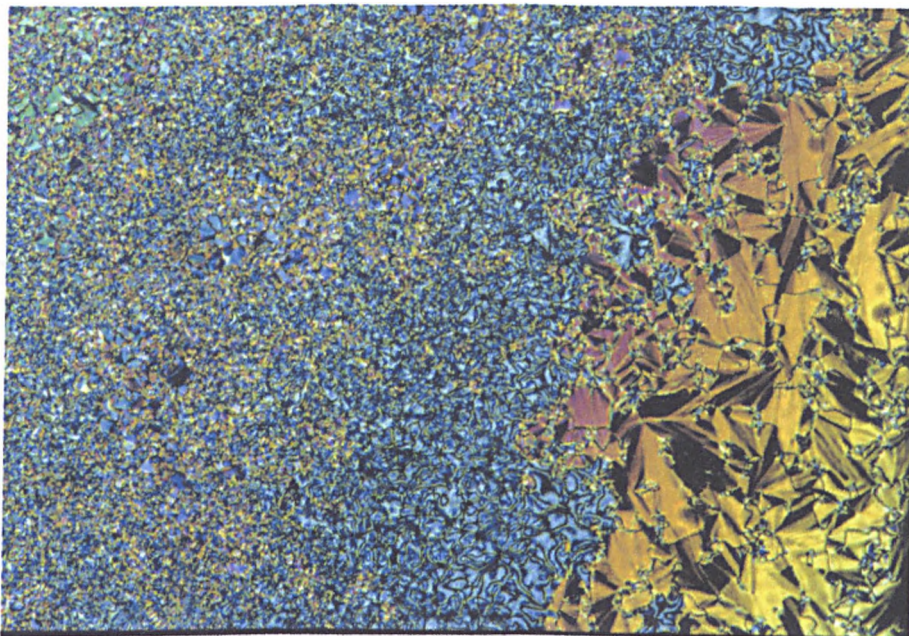


Photograph 3.3



Photograph 3.4

Photographs 3.3 and 3.4 show a typical schlieren 4-brush texture of the smectic C phase (compound 53 and 57).



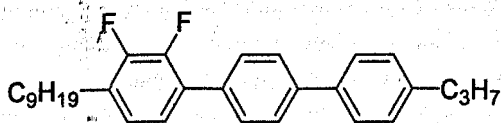
Photograph 3.5 Focal-conics region (right) and schlieren texture (left) compound 58.

The texture of the smectic C phase formed on cooling from the isotropic liquid was, for most compounds, as batonnets blending into conic fans.

All the DSC traces of the compounds discussed in section 3.1.1-3.1.7 showed first order transitions from I to SmC, I to SmA, SmA to SmC or N to SmA.

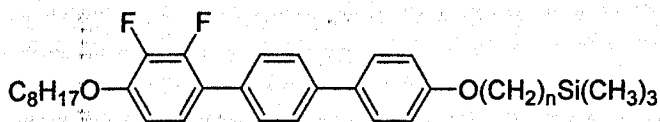
3.2 Mixture studies on compounds containing a bulky end group

Two assessments of the miscibility of compounds with bulky end groups were carried out. Firstly, a series of mixtures were prepared to assess whether compounds containing bulky end groups are miscible with compounds with straight alkyl chains; the mesophases and the transition temperatures produced in these mixtures are given in tables 3.11-3.13 for accurate compositions which are close to 20% by weight of each compound in the host. The host compound chosen for the mixture work was **MH 198**, which is typical of components in the difluoroterphenyl ferroelectric host systems produced at DERA (Malvern). All the compounds were found to be miscible with **MH 198** which suggests that they are probably miscible with other similar straight alkyl chain terphenyls.



MH 198

Cr 80.0 SmC 84.5 SmA 117.0 N 131.5 I (°C)



50-54

Table 3.11 Transition temperatures (°C) for mixtures of compounds **50-54** in **MH 198** (the change in transition temperatures from the value for the host is given in parenthesis)

Compound % in MH198	Cr	SmC	SmA	N	I
(n = 2) 50 18%	• 49.3 (-30.7)	• 96.9 (+12.4)	• 115.7 (-1.3)	• 130.7 (-0.8)	•
(n = 3) 51 19%	• 52.9 (-27.1)	• 95.2 (+10.7)	• 125.7 (+8.7)	• 132.3 (+0.8)	•
(n = 4) 52 25%	• 53.7 (-26.3)	• 102.5 (+18.0)	• 126.5 (+9.5)	• 133.7 (+2.2)	•
(n = 5) 53 25%	• 55.7 (-24.3)	• 110.5 (+26.0)	• 130.5 (+13.5)	• 135.1 (+3.6)	•
(n = 6) 54 33%	• 53.7 (-26.3)	• 109.0 (+24.5)	• 134.8 (+17.8)	• 138.3 (+6.8)	•

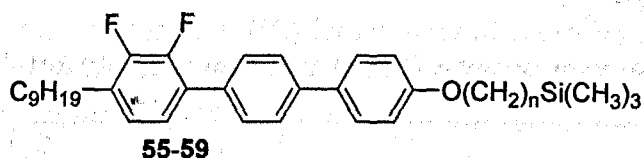


Table 3.12 Transition temperatures ($^{\circ}\text{C}$) for mixtures of compounds 55-59 in MH 198 (the change in each transition temperature from the value for the host is given in parenthesis)

Compound % in MH198	Cr	SmC	SmA	N	I
(n=2) 55 19%	• 47.9 (-32.1)	• 90.0 (+5.5)	• 115.2 (-1.8)	• 126.9 (-4.6)	•
(n=3) 56 20%	• 54.7 (-25.3)	• 92.3 (+7.8)	• 123.3 (+6.3)	• 128.6 (-2.9)	•
(n=4) 57 16%	• 53.2 (-26.8)	• 91.0 (+6.5)	• 119.8 (+2.8)	• 129.1 (-2.4)	•
(n=5) 58 19%	• 53.9 (-26.1)	• 89.9 (+5.4)	• 126.9 (+9.9)	• 130.7 (-0.8)	•
(n=6) 59 20%	• 54.9 (-25.1)	• 90.6 (+6.1)	• 126.0 (+9.0)	• 130.0 (-1.5)	•

Tables 3.11-3.13 show that the melting points are down as expected in a mixture. The transition temperatures of smectic C and A phases are nearly always increased and the transition temperatures of the nematic to isotropic are unchanged.

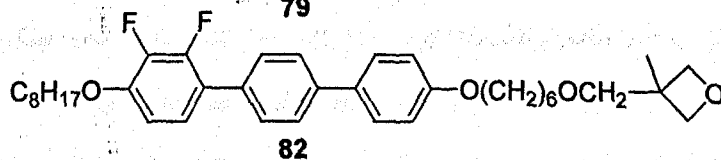
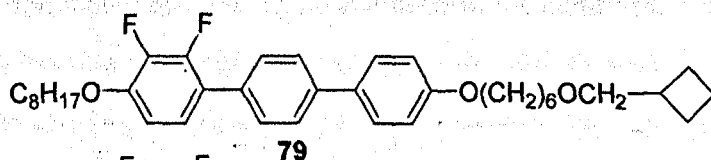
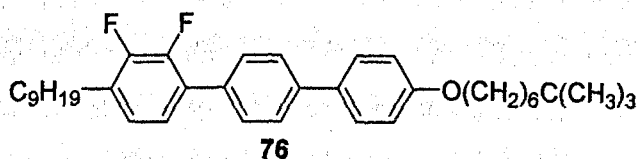
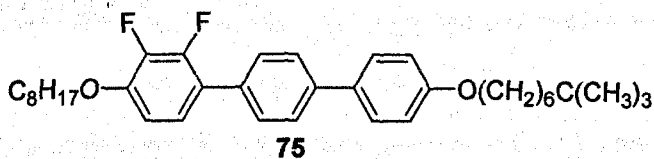


Table 3.13 Transition temperatures ($^{\circ}\text{C}$) for mixtures of compounds **75**, **76**, **79**, **82** in **MH198** (the change in each transition temperature from the value for the host is given in parenthesis)

Compound % in MH198	Cr	SmC	SmA	N	I
75 19%	• 53.3 (-26.7)	• 98.8 (+14.3)	• 132.2 (+15.2)	• 135.5 (+4.0)	•
76 20%	• 54.2 (-25.8)	• 87.0 (+2.5)	• 127.6 (+10.6)	• 130.5 (-1.0)	•
79 20%	• 55.6 (-24.4)	• 97.8 (+13.3)	• 123.9 (-6.9)	• 134.0 (+2.5)	•
82 19%	• 54.1 (-25.9)	• 89.7 (+5.2)	• 117.8 (+0.8)	• 131.1 (-0.4)	•

In the second assessment of miscibility, compounds **79** and **58** (with an octyloxy and nonyl chain respectively) were mixed with compound **MH 198** in all proportions, and the transition temperatures are given in tables 3.14 and 3.15. The binary miscibility diagrams are shown in figure 3.11 and 3.12 and these do not show any discontinuity across the phase diagram. These compounds containing bulky end groups in their terminal chains are miscible with similar compounds containing straight terminal chains, and this suggests that the compounds with the bulky end groups do not microsegregate on mixing with the straight chain analogues. This result is different from that reported by Coles and co-workers¹¹⁻¹⁴ for siloxane end groups which give microsegregated regions.

Although compounds **58** and **79** do not possess either a smectic A or a nematic phase, the miscibility diagrams show that these compounds are quite supportive of the smectic A and of the nematic phases in mixtures. The smectic A and the nematic phase transitions do not drop to lower values but are maintained across the diagram until they are dominated by the smectic character of the additives.

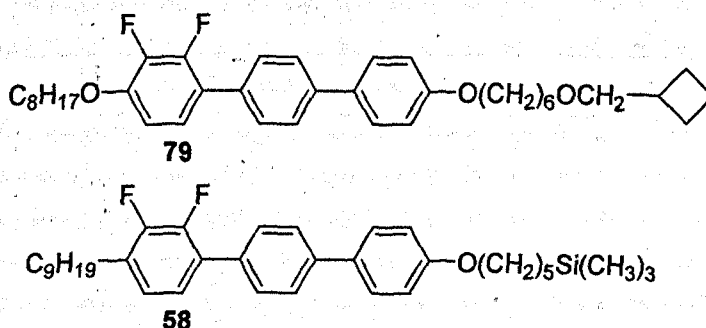


Table 3.14 Transition temperatures (°C) for mixtures of compound 79 and MH 198

% of 79 in MH 198	Cr	SmC	SmA	N	I
10	• 53.3	• 91.5	• 119.4	• 131.8	•
20	• 52.6	• 97.8	• 123.9	• 134.0	•
30	• 53.9	• 104.5	• 126.1	• 135.2	•
40	• 52.9	• 114.3	• 130.7	• 137.5	•
50	• 53.6	• 121.4	• 133.2	• 139.2	•
60	• 59.5	• 130.7	• 136.5	• 141.6	•
70	• 65.0	• 136.7	• 138.6	• 142.6	•
80	• 79.9	• 141.3	— —	• 144.6	•
90	• 89.5	• 145.1	— —	• 146.2	•
100	• 92.5	• 148.1	— —	— —	•

Table 3.15 Transition temperatures (°C) for mixtures of compound 58 and MH 198

% of 58 in MH 198	Cr	SmC	SmA	N	I
10	• 58.2	• 87.8	• 124.4	• 131.1	•
20	• 53.9	• 89.9	• 126.9	• 130.9	•
30	• 56.0	• 100.6	• 130.6	— —	•
40	• 58.8	• 107.5	• 130.4	— —	•
50	• 62.8	• 122.3	• 132.0	— —	•
60	• 64.2	• 126.2	• 132.4	— —	•
70	• 66.8	• 131.8	— —	— —	•
80	• 68.0	• 130.6	— —	— —	•
90	• 66.8	• 129.8	— —	— —	•
100	• 72.2	• 127.2	— —	— —	•

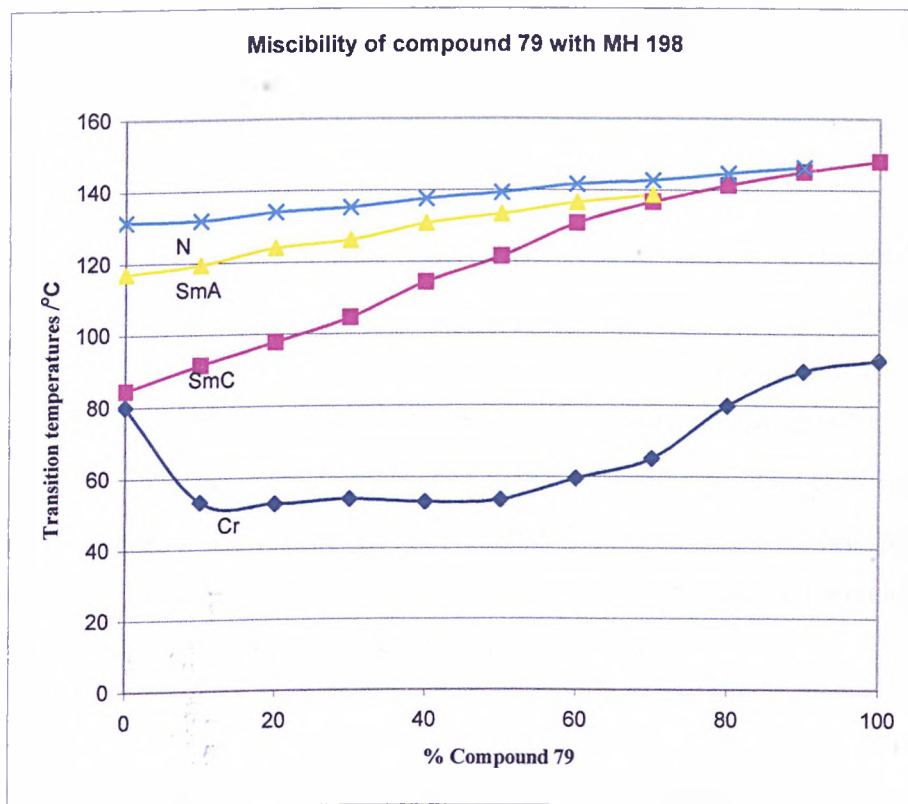


Figure 3.11 Binary phase diagram for mixtures of 79 and MH 198

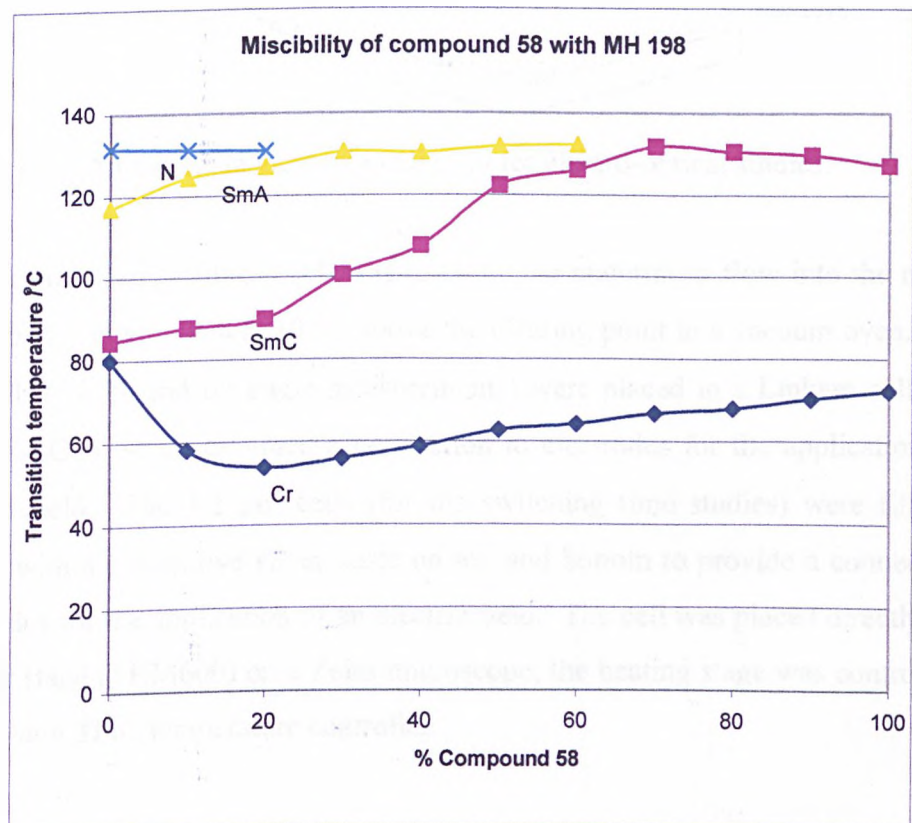


Figure 3.12 Binary phase diagram for mixtures of 58 and MH 198

3.3 Electro-optical studies of bulky end groups in a standard mixture

3.3.1 Experimental techniques

Several of the compounds prepared were mixed in a standard ferroelectric mixture used at DERA (Malvern) to determine the magnitude of their P_s , their tilt angle and the switching times as a function of temperature. The P_s and tilt angle measurements were carried out in $5\ \mu\text{m}$ cells filled by capillary action as described below, and the switching time measurements were carried out in $1.2\ \mu\text{m}$ cells. The cells used were provided by DERA Malvern and were coated with a parallel-rubbed polyimide alignment layer. Figure 3.13 shows an exploded view of a typical cell which consists of three parts – ITO electrodes, glass substrates and spacers.

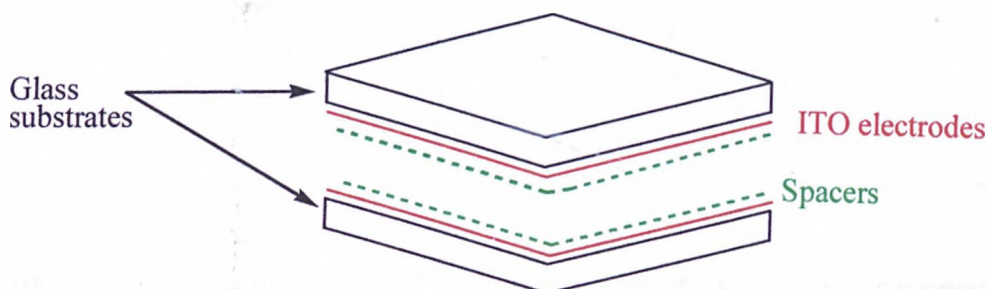


Figure 3.13 An exploded view of a cell used for electro-optical studies.

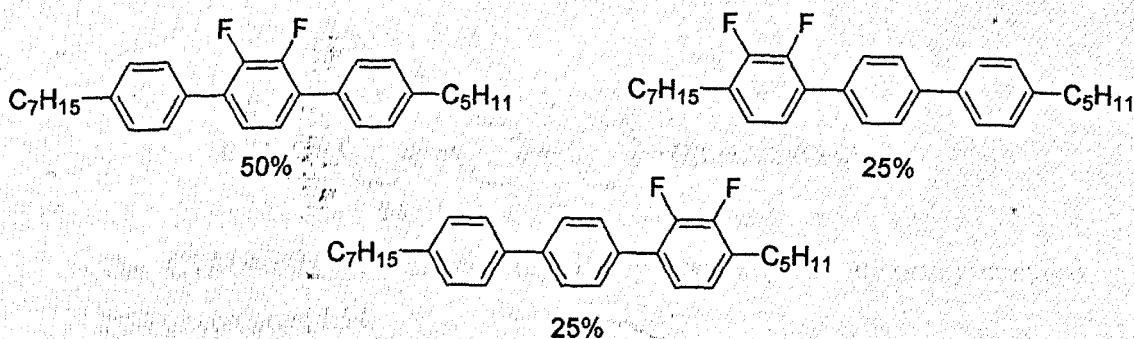
The method used to fill the cell was to allow the material to flow into the cell at a temperature approximately $10\ ^\circ\text{C}$ above the clearing point in a vacuum oven. The $5\ \mu\text{m}$ cells (for P_s and tilt angle measurements) were placed in a Linkam cell holder (THMS/LCC) which provided a connection to electrodes for the application of an electric field. The $1.2\ \mu\text{m}$ cells (for the switching time studies) were filled and coated with a conductive silver paste on top and bottom to provide a connection to electrodes for the application of an electric field. The cell was placed directly in the heating stage (THM600) on a Zeiss microscope; the heating stage was controlled by the Linkam TP61 temperature controller.

In order to align the materials homogeneously, the liquid crystal sample was cooled from the isotropic liquid into the SmC^* phase *via* the N^* and SmA^* phases. Several conditions were tried to obtain optimum alignment in the cells and the best procedure

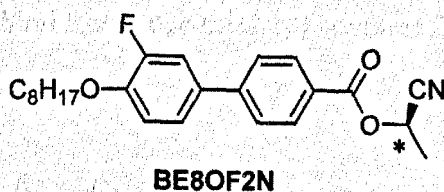
was as follows, a frequency of 200 Hz was applied and a voltage of ± 10 V (2 V μm^{-1} for the 5 μm cells and ± 8.5 V μm^{-1} for the 1.2 cells) with a cooling rate of 0.2 $^{\circ}\text{C}$ min^{-1} .

Most of the compounds prepared did not display the desired cooling sequence to obtain good homogeneous alignment, and when the host was doped with the chiral dopant only the SmC^* phase was displayed. For this reason, a standard host mixture was used to provide the desired cooling sequence and the bulky end group ferroelectric host compounds were added in the proportion shown below.

The DFT1 mixture is composed of the following compounds (% by weight):



CSmix (Chiral Standard mixture) DFT1 mixture with 2% by weight of **BE8OF2N** dopant was prepared, to which 25% by weight of a bulky end group compound was added. The chiral dopant **BE8OF2N** was supplied by DERA (Malvern).

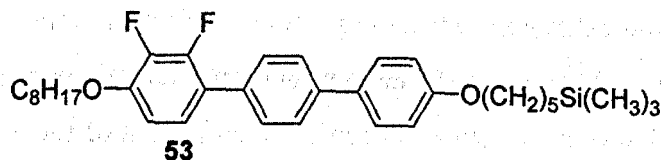


The aim of the electro-optic study was to compare the effect of a bulky end group on the switching time of the standard **CSmix** mixture. Each mixture tested contains 25% of a bulky end group material, but only a few materials were tested due to the great difficulty in aligning the sample in the cells. The materials chosen for this study are as follows,

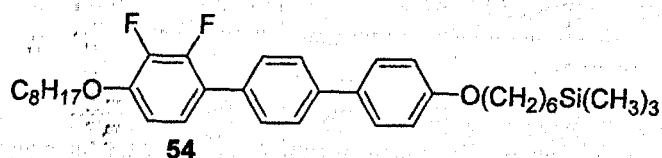
- ◆ Compound **53** which contains a bulky trimethylsilyl end group.
- ◆ Compound **54** which contains a bulky trimethylsilyl end group but with

one more methylene group in the chain than compound 53.

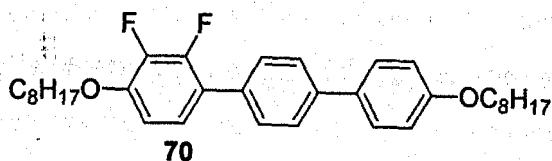
- ◆ Compound 70 is the reference compound and has a straight alkoxy chain.
- ◆ Compound 75 is related to compound 54 but contains a carbon atom in place of a silicon atom.



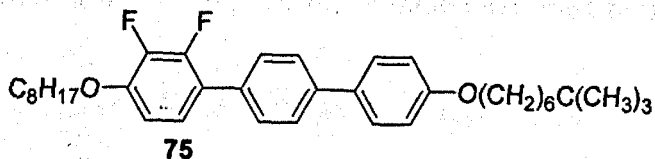
The **CTMS5mix** (Chiral trimethylsilyl pentamethylene mixture) contains 25% of compound 53.



The **CTMS6mix** (Chiral trimethylsilyl pentamethylene mixture) contains 25% of compound 54.



The **CRefmix** (Chiral Reference mixture) contains 25% of compound 70.



The **CTBu6mix** (Chiral *tert*-butyl hexamethylene mixture) contains 25% of compound 75.

3.3.2 Procedures for P_s measurements - Triangular Wave Studies¹⁸

The P_s value was measured by the application of an AC driving voltage using a triangular waveform to an aligned SmC^* sample; this method is also known as current reversal. Since the dipoles in the medium tend to align perpendicular to the plane of the glass plates, it is possible to directly couple the P_s of the medium to the applied electric field. In a ferroelectric phase, the molecules will rapidly reorient themselves from one aligned state into another aligned state by switching around a cone and so give rise to a brief pulse of current which is detected as a single peak. This is shown in greater detail in figure 3.14

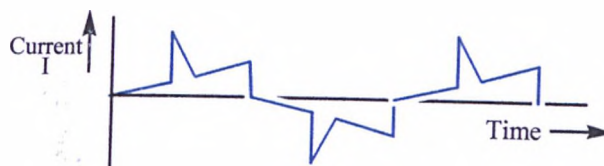


Figure 3.14 Response to an applied triangular waveform driving voltage for ferroelectric liquid crystals.

The total response observed from the triangular wave (current reversal) method is not solely based on the rapid reorientation of the molecules, but the capacitance of the cell and its resistance (due to ions within the cell) also contribute. The overall response that is usually observed is a result of these elements, although the triangular wave experiment decreases the influence of the capacitance (see figure 3.15). It must also be noted that the area underneath the peak in the triangular wave measurement is equivalent to twice the value of the P_s and in order to determine the value of P_s , it is necessary to determine the area under the peak. For the purposes of this research, this was carried out using a computer programme developed by M. Watson¹⁹, " *P_s and Optical Response*".

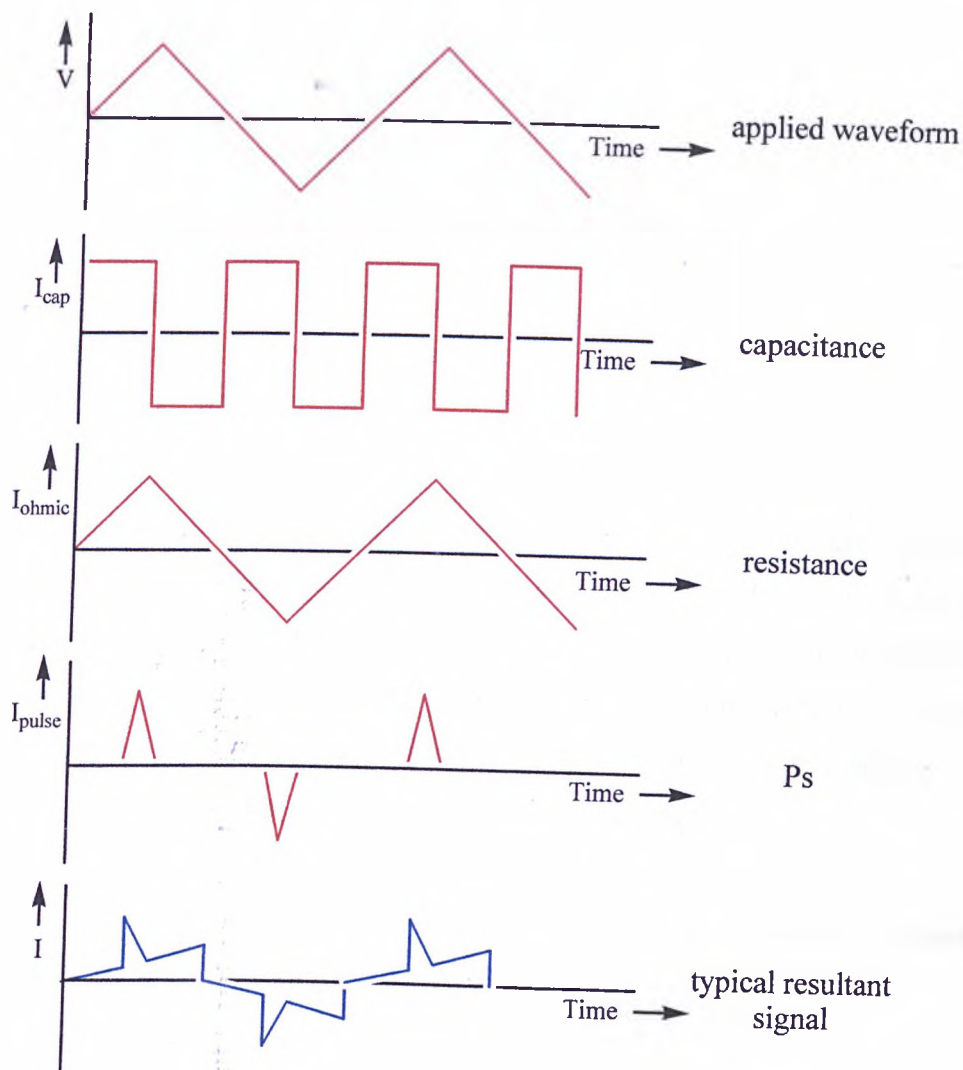


Figure 3.15 Components of the triangular waveform elements²⁰.

3.3.3 Procedure for measuring P_s values²¹

The cell was placed in the Linkam cell holder, and the cell holder was connected to the electronic wave generator and inserted into the THM600 Linkam heating stage on a Zeiss microscope. An AC driving voltage using a triangular waveform was applied so that when the electrical field started to rise in the cell, at a certain point the dipoles would align with the field and the aligned sample would switch. An oscilloscope measured the resulting current, I , from the cell and showed a peak (current pulse) which represents the spontaneous polarisation. The signal for the peak was sent to a computer via an RS232 port, and by using the computer programme, "*Ps and Optical Response*", the spontaneous polarisation was calculated¹⁸. The spontaneous polarisation reported is in nC cm^{-2} . The typical field

applied across the cell was ± 50 V at a frequency of 20 Hz, this was so that it was possible to observe the sample switching.

The Ps values for all the samples were 2.0 ± 0.2 nC cm⁻² when fully saturated and did not vary for different materials. The presence or nature of the bulky end group did not seem to affect the Ps of the ferroelectric mixture.

3.3.4 Tilt angle measurements

The tilt angles of the aligned samples were measured by applying a driving voltage using a square waveform across the cell at the same voltage as for the Ps measurements but at a much lower frequency, (typically 10 mHz) to determine the point of extinction. Once the switching had occurred, the sample was rotated through the minimum angle in order to obtain optical extinction again. This measurement gave the cone angle 2θ , where θ is the tilt angle.

As was the case for the Ps measurements, the tilt angles for all the mixtures at various temperatures were similar 22.5-23.5°.

3.3.5 Response time measurements²¹

The mixture was placed in a 2 μ m cell and the voltage applied was 10 V peak-to-peak at a frequency of 100 Hz. A photodiode (RS303-674; 1 cm² active area, high speed >50 ns) in an apparatus designed at DERA, Malvern, detected the difference in the transmission of light through the cell as the molecules changed their orientation in response to the applied electric field. A green eye response filter (Coherent-Ealing, 26-7617-000, 1" diameter, transmittance 400-700 nm, maximum transmittance 539.5 nm) was used to remove any UV and IR radiations that may have affected the results. The photodiode was linked to the oscilloscope and a signal which represented the delayed switching of the molecules within the cell was produced. It was possible to measure the response time in both directions and this is reported as the rise time (0-90% transmission) and the fall time (100-10% transmission). The switching times were reported in μ s.

The rise times and fall times of **CTMS6mix**, **CRefmix**, **CTBu6mix** and **CTMS5mix** were obtained by the method described above to study the effect of a bulky end group on the switching times of the **CSmix** mixture (see table 3.16 and 3.17 and figures 3.16 and 3.17).

CRefmix is the mixture of compound **70** which does not have a bulky terminal group chain and **CTMS6mix** which contains a trimethylsilyl end group.

The **CRefmix** mixture switches slower than **CTMS6mix** down to 30 °C into the smectic C phase but is faster below that temperature. The rise and fall times run parallel to each other for **CTMS6mix**, but for **CRefmix** the fall time is faster when more than 25 °C into the smectic C phase.

CTBu6mix contains a bulky end group where the silicon atom has been replaced by a carbon atom. **CTBu6mix** is faster than both **CTMS6mix** and **CRefmix** and its rise and fall times run parallel down to 30 °C into the smectic C phase and then is faster than its rise time.

CTMS5mix contains compound **53**, with its terminal chain one methylene group shorter than for compound **54**. This mixture is faster than **CTMS6mix** but is slower than **CTBu6mix**; its fall time and rise times run parallel to each other as for **CTMS6mix**.

Bulky end groups, (as judged from these 25% mixtures) seem to give faster switching in **TMS6mix**, **CTBu6mix** and **CTMS5mix**; all of these mixtures are at least for some temperatures, faster switching than **CRefmix** (see tables 3.16-3.19 and figures 3.16-3.19).

Table 3.16 Rise time and fall time values for CTMS6mix

Reduced Temperature* / °C	Rise Time / μs	Fall Time / μs
5	420	440
10	448	492
15	504	556
20	572	664
25	692	810
30	860	960
35	1030	1310
40	1520	1770
45	2000	2520
50	2880	3490
55	4100	4600
60	5800	6200

*($T_c - T$)

Table 3.17 Rise time and fall time values for CRefmix

Reduced Temperature* / °C	Rise Time / μs	Fall Time / μs
5	444	448
10	520	532
15	590	596
20	694	690
25	790	720
30	870	750
35	920	780
40	1020	740
45	1080	790
50	1210	820
55	1230	1000
60	1290	1030

*($T_c - T$)

Table 3.18 Rise time and fall time values for CTBu6mix

Reduced Temperature* / °C	Rise Time / μs	Fall Time / μs
5	424	416
10	480	460
15	500	480
20	560	520
25	612	560
30	660	660
35	750	680
40	840	704
45	940	820
50	1100	870
55	1130	890

*($T_c - T$)

Table 3.19 Rise time and fall time values for CTMS5mix

Reduced Temperature* / °C	Rise Time / μs	Fall Time / μs
5	380	380
10	420	480
15	520	580
20	600	660
25	680	760
30	740	840
35	780	880
40	880	940
45	940	980
50	1020	1040
55	1040	1080

*($T_c - T$)

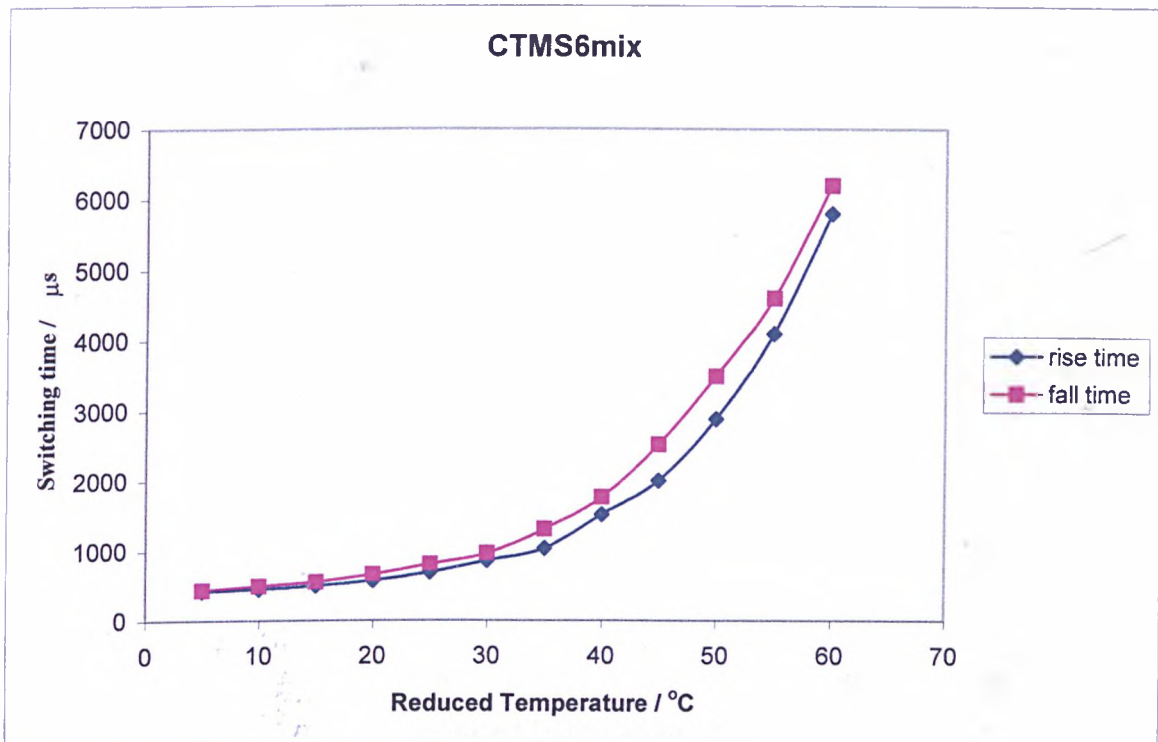


Figure 3.16 Switching times for **CTMS6mix**

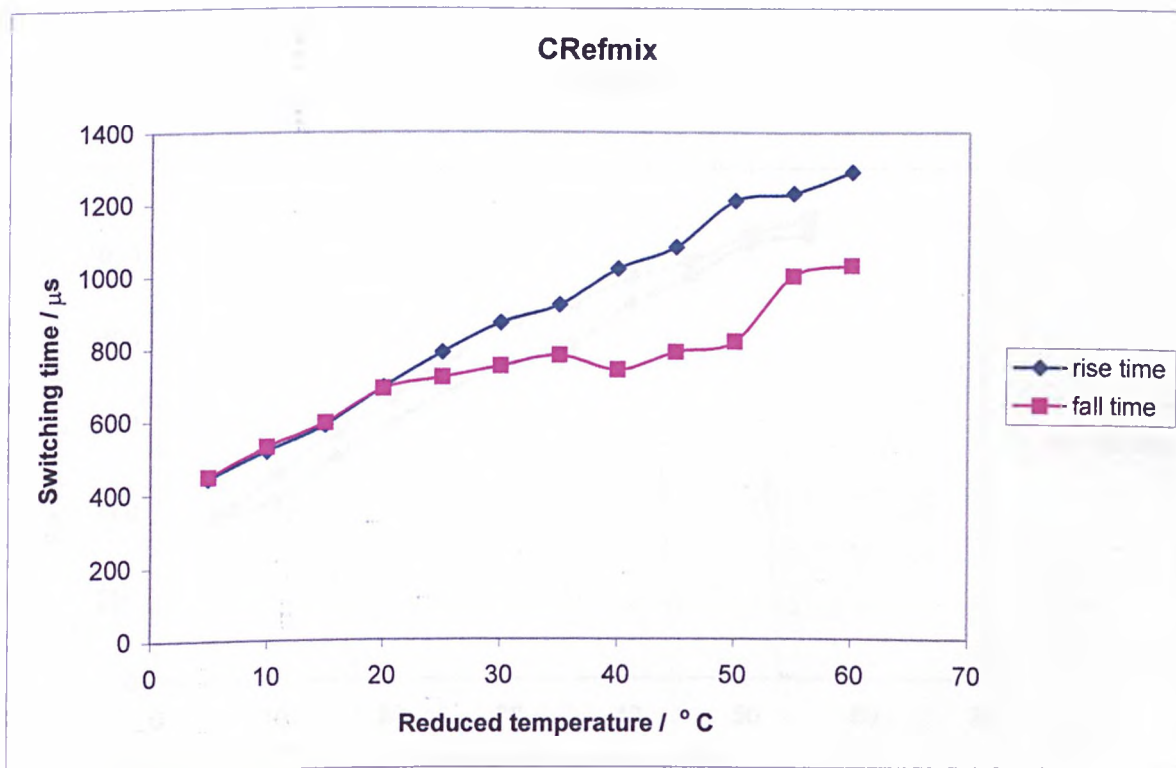


Figure 3.17 Switching times for **CRefmix**

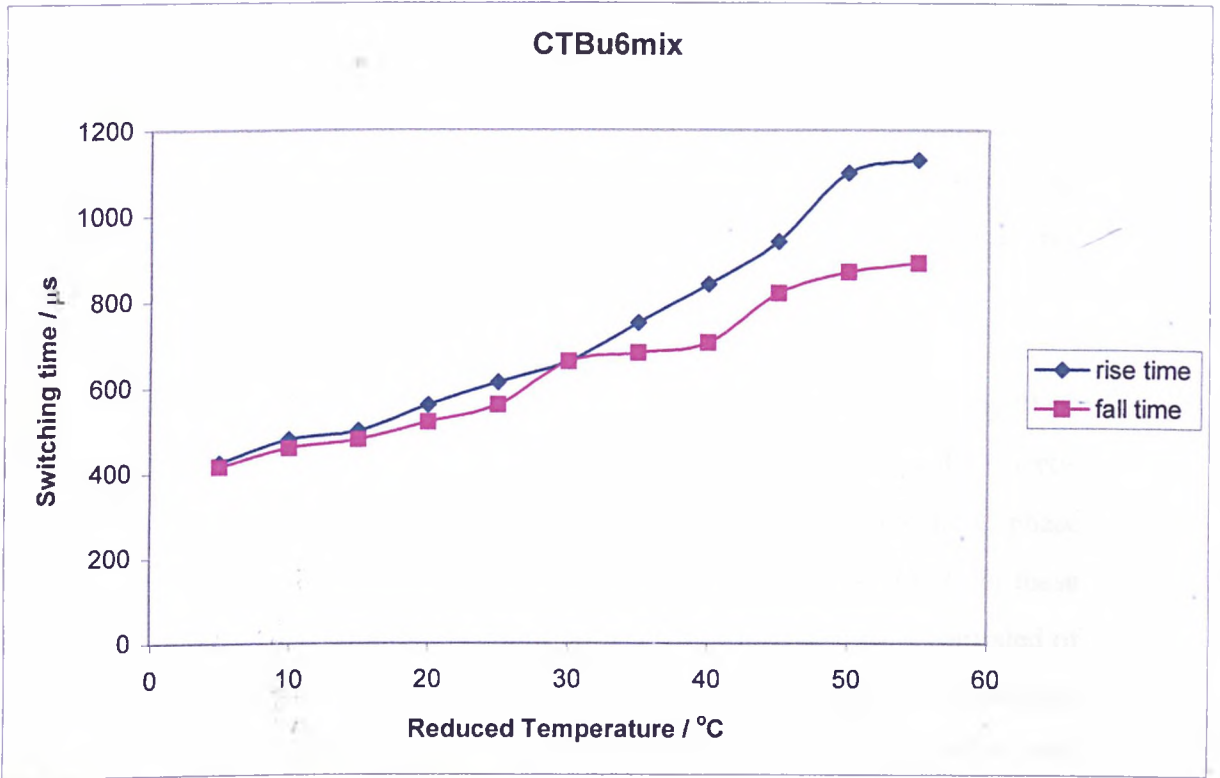


Figure 3.18 Switching times for **CTBu6mix**

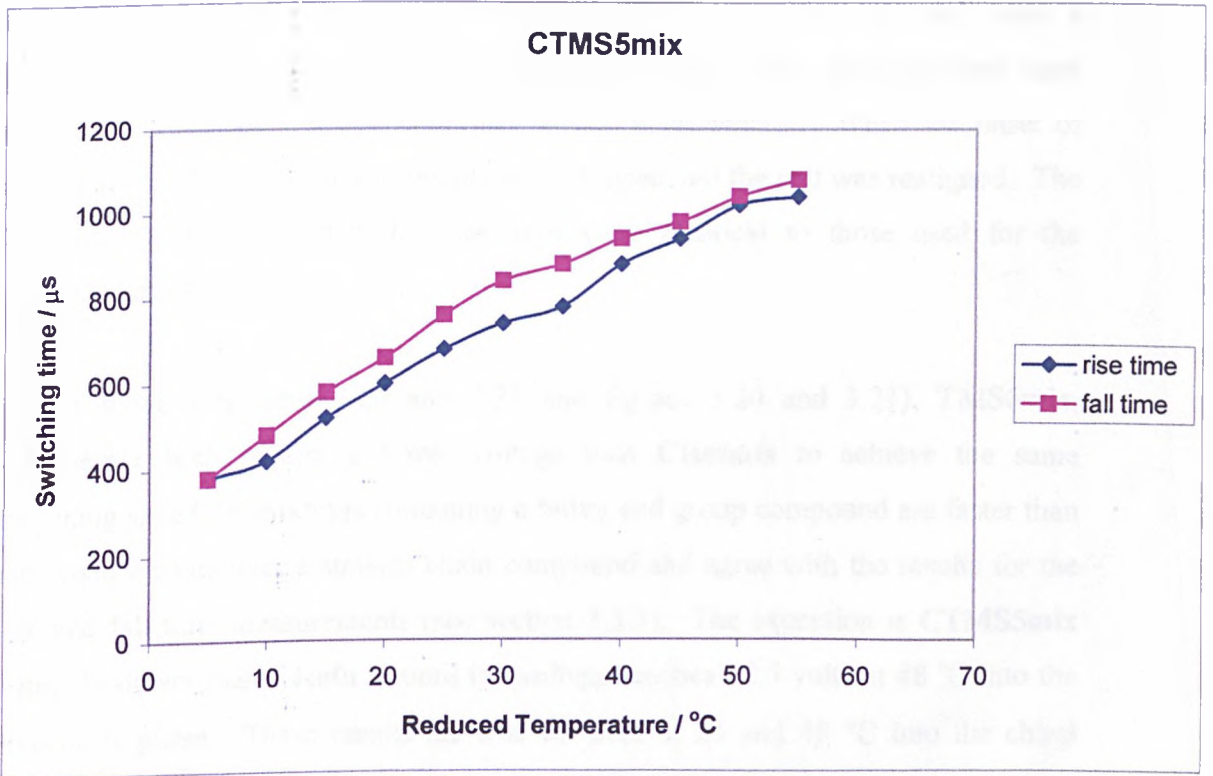


Figure 3.19 Switching times for **CTMS5mix**

3.3.6 τ/V_{\min} measurements

In order to improve the full bistability and eliminate crosstalk in conventional FLC displays which subsequently reduce contrast, an AC field of high frequency can be applied (see section 1.7.3.1) as it will couple to the dielectric tensor without coupling to the P_s vector to maintain the transmission in the maximum or minimum desired states.

The τ/V_{\min} measurements were carried out at DERA²² (Malvern) using their standard technique at the two different temperatures of 25 and 48 °C into the smectic C phase. Usually measurements are carried out at 25 °C into the smectic C phase and at 25 °C, but it was not possible to make the measurements at 25 °C in these cases as the mixtures recrystallised at about 30 °C. The equipment used consisted of a Nikon Optiphot polarising microscope, Mettler FP82 heating stage in conjunction with a FP80HT temperature controller, a feedback function generator F6601A, and an in-house built photodiode assembly and an amplifier (x 10) wave form generator (Wavetek Generator 395) and a Gould oscilloscope model 4072A. The measurements were taken in a 1:100 duty cycle multiplexing waveform applied from the arbitrary function generator, and the τ/V curves were obtained with a superimposed square wave AC of 50 kHz frequency. The measurements were started at a RMS of 5 V and continued at 2.5 V increments. When the onset of defects was noticed, the measurements were stopped and the cell was realigned. The cells used and alignment techniques used were identical to those used for the switching studies.

In this mode (see table 3.20 and 3.21 and figures 3.20 and 3.21), **TMS6mix**, **CTBu6mix** both require a lower voltage than **CRefmix** to achieve the same switching speed *i.e.* mixtures containing a bulky end group compound are faster than the mixture containing a straight chain compound and agree with the results for the rise and fall time measurements (see section 3.3.5). The exception is **CTMS5mix** which is slower than **CRefmix** until the voltage reaches 12.5 volts at 48 °C into the smectic C phase. These results are true for both at 25 and 48 °C into the chiral smectic C phase. **CTBu6mix** is faster than **TMS6mix** which suggests the silicon atom does not play a vital role in the faster switching of **TMS6mix**, **CTBu6mix** and

CTMS5mix mixtures. The τ/V_{min} measurements for **CTMS5mix** show that it is not faster than **TMS6mix** and **CTBu6mix**, unlike the results of the switching studies in section 3.3.5.

Table 3.20 Times (μs) for the switching vs voltage for **TMS6mix**, **Crefmix**, **CTBu6mix** and **CTMS5mix** at 25 °C into the Smectic C* phase.

Volt	TMS6mix	CRefmix	CTBu6mix	CTMS5mix
5	67	132	114	155
7.5	39	59	51	51
10	24	43	32	35
12.5	16	29	24	30
15	12	23	19	20
17.5	11	19	14	14
20	9	17	9	12
22.5	9	15	9	10
25	9	12	7	9

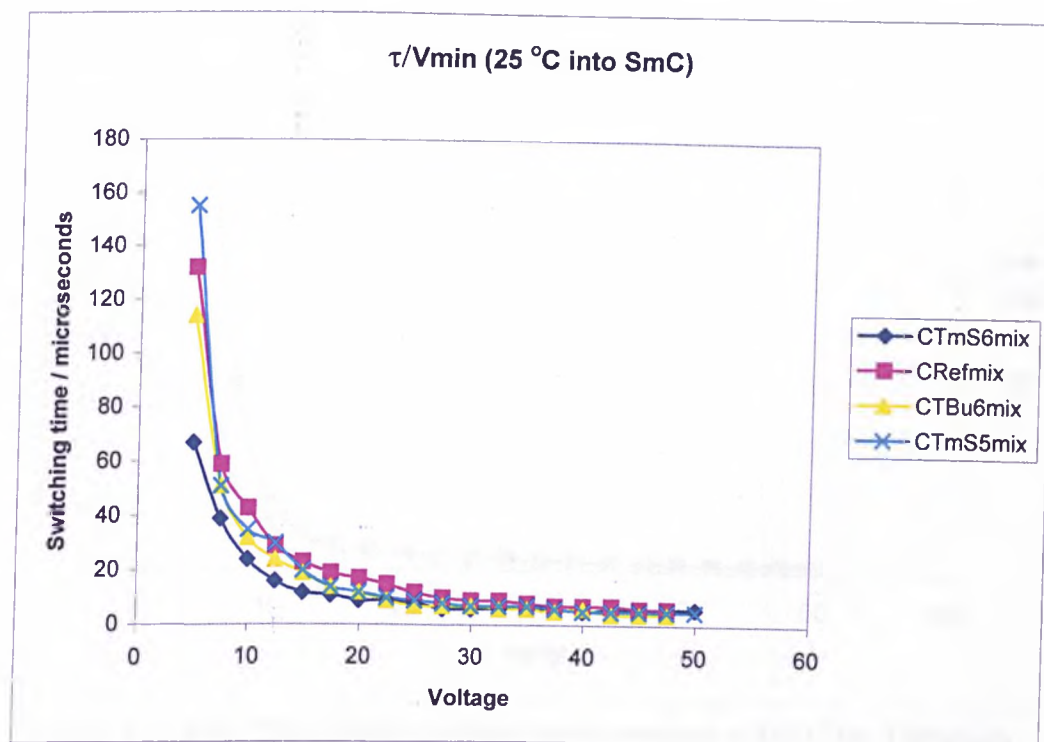


Figure 3.20 Switching vs voltage measurements for **TMS6mix**, **Crefmix**, **CTBu6mix** and **CTMS5mix** at 25 °C into the Smectic C* phase.

Table 3.21 Times (μs) for the switching vs voltage (V) for **TMS6mix**, **Crefmix**, **CTBu6mix** and **CTMS5mix** 48 °C into the smectic C* phase

Volt	CTmS6mix	CRefmix	CTBu6mix	CTmS5mix
5	437	798	407	*
7.5	135	323	230	*
10	78	130	140	91
12.5	51	65	52	63
15	37	44	37	45
17.5	32	36	30	36
20	27	28	25	30
22.5	23	24	21	25
25	21	22	19	22

* Could not be determined

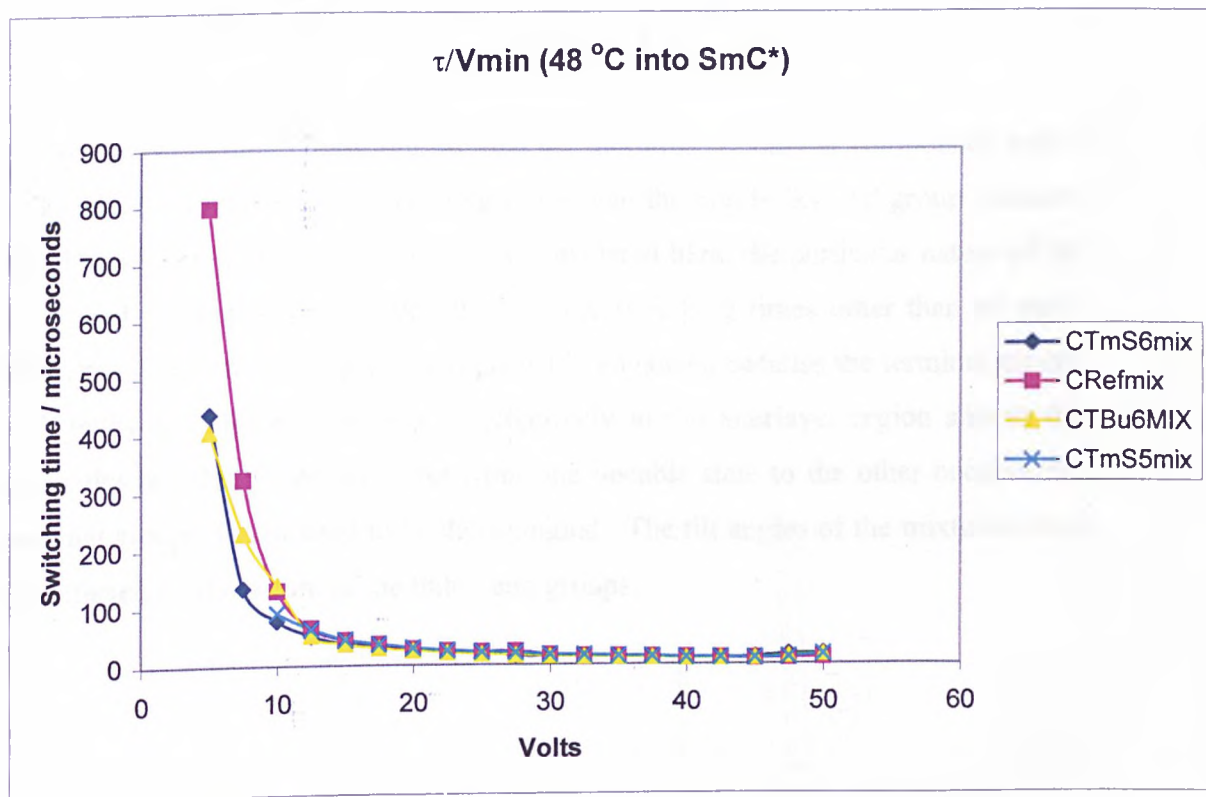


Figure 3.21 Switching times vs voltage measurements at 48 °C for **TMS6mix**, **CRefmix**, **CTBu6mix** and **CTMS5mix** into the Smectic C phase.

A turn around is not detected in figures 3.20 and 3.21 but the switching times appear to have reached a minimum value.

All the measurements reported above, were not obtained for neat materials, but only for materials as a mixture in a host, and so the results should only be regarded qualitatively. However, a conclusion that can be drawn from these results is that a bulky end group clearly affects the switching times to give faster switching times than for materials without a bulky group (see CRefmix). The reason for the faster switching probably arises more from the steric effects on the interlayer mixing process than from the intrinsic nature of the bulky end groups. Coles and co-workers found that the siloxane tails aggregate to form micro-regions and the organosiloxane materials have a low rotational viscosity (320 mPa s compared to 510 mPa s for the SCE13 mixtures based on fluoroterphenyls and fluorobiphenyl esters, Merk Poole, UK) giving short switching times (optical response of 16 μs at 25 °C with 20 V μm^{-1}). Coles and co-workers¹¹⁻¹⁴ proposed that the flexibility may be the reason for the low viscosity of their materials and consequently the reason for their short switching times. Their materials have also high tilt angles which do not vary with temperature (36°C).

All the results in this section suggest that the mixtures containing compounds with a bulky end group have faster switching times than the non-bulky end group mixtures and that, within the range of end groups considered here, the particular nature of the bulky end group has no specific effect on the switching times other than its steric hindrance. The switching process is probably enhanced because the terminal groups with bulky ends do not intermix as effectively in the interlayer region and so the molecules are able to switch faster from one bistable state to the other because the terminal groups do not need to be disentangled. The tilt angles of the mixtures were not affected by the nature of the bulky end groups.

3.4 Conclusions

Several series of compounds based on a 2,3-difluoroterphenyl mesogenic core with a straight nine-atom chain at the 4-position (alkoxy and/or alkyl chain), and with an atypical alkoxy or alkyl chain at the 4''-position were synthesised to study how the unusual terminal groups influence the mesomorphology of the compounds. The effects of the bulky end groups on the switching times of a standard ferroelectric mixtures were also investigated.

When the chain contained a bulky end group, it was found to depress the clearing and melting points; the nematic and smectic A phases were depressed to the greatest extent but the stability of the smectic C phase was less affected, and most of the compounds only displayed the smectic C phase. The direct isotropic to smectic C phase usually gives high tilt angle but the tilt angle of the materials synthesised in this work were not measured as they were difficult to align. These findings suggest that the smectic C phase, in these compounds, is favoured by steric interactions at the interlayer regions which encourage the molecules to tilt, as proposed by Wulf¹⁰, rather than by dipolar interactions as proposed by McMillan⁴. Bulky end groups can therefore be used to favour the formation of the smectic C phase by a mesogenic core.

Compounds containing a halogen atom as the end group only displayed a smectic A phase which suggests that dipolar interactions at the interlayer regions favour the straightening of the smectic layers thus suppressing the smectic C and nematic phases. Thus, introducing a chloro or bromo substituent at the end of a terminal chain gives a smectic A inducer.

Mixture studies were carried out to test the miscibility of the compounds containing bulky end groups, and these measurements showed that the materials are miscible with parent difluoroterphenyls systems containing straight terminal chains. The complete miscibility of the straight and bulky chains indicates that there is no evidence of any microsegregation caused by the bulky end groups. Coles et al.¹¹⁻¹⁴ found evidence of microsegregation, however it might be caused by the nature of the siloxy end group rather than its sheer bulkiness. The electro-optical measurements

carried out in this work showed that mixtures containing compounds with bulky end groups switch faster than the straight chain parent compound; this suggests that the steric hindrance at the end of the chain minimises the entanglement of the molecules in the interlayer regions and therefore the molecules switch faster from one bistable state to the other. The faster switch is not caused by microsegregation as suggested by Coles et al.¹¹⁻¹⁴ but by the bulkiness of the end group.

3.4 Bibliography (Section 3)

- 1 M. J. Goulding and S. Greenfield, *Liquid Crystals*, 1993, **13**, 345.
- 2 T. Kitamura, A. Mukoh and S. Era, *Mol. Cryst. Liq. Cryst.*, 1984, **110**, 319.
- 3 T. Kitamura and A. Mukoh, *Mol. Cryst. Liq. Cryst.*, 1984, **108**, 257-262.
- 4 W. L. McMillan, *Physical Review A*, 1973, **8**, 1921.
- 5 D. M. Walba, S. C. Slater, W. N. Thurmes, N. A. Clark, M. A. Handsby and F. Supon, *J. Am. Chem. Soc.*, 1986, **108**, 5210.
- 6 N. Gough, *PhD Thesis*, University of Hull, 1999, England.
- 7 D. Coates, *Liquid Crystals*, 1987, **2**, 63.
- 8 G. W. Gray, *Advances in Liquid Crystals*, **2**, 1976, Academic Press, Inc. (New York, San Francisco, London).
- 9 G. W. Gray, M. Hird, D. Lacey and K. J. Toyne, *J. Chem. Soc., Perkin Trans II*, 1989, 2041.
- 10 A. Wulf, *Physical Review A*, 1975, **11**, 365.
- 11 J. Newton, H. J. Coles and H. Owen, *Ferroelectrics*, 1993, **148**, 379.
- 12 J. Newton, H. J. Coles and H. Owen, *Liquid Crystals*, 1993, **15**, No 5, 739.
- 13 M. Ibn-Elhaj, H. J. Coles, D. Guillon and A. Skoulios, *J. Phys. II France*, 1993, **3**, 1807.
- 14 M. Ibn-Elhaj, A. Skoulios, D. Guillon, J. Newton, P. Hodge and H. J. Coles, *J. Phys. II France*, 1996, **6**, 271.
- 15 S. Kazuyuki, K. Takatoh and M. Sakamoto, *Liquid Crystals*, 1993, **13**, 283.
- 16 S. Grigoras and T. Lane, *Advances in Chemistry Series*, 1990, **224**, 125.
- 17 M. Hird, *PhD Thesis*, University of Hull, 1991, England.
- 18 K. Miyasto, S. Abe, H. Takezoe, A. Fukuda and E. Kuze, *Jpn. J. Appl. Phys.*, 1983, **22**, L661.
- 19 M. Watson, *PhD Thesis*, University of Hull, 1994, England.
- 20 S. J. Cowling, *PhD Thesis*, University of Hull, 1999, England.
- 21 S. J. Cowling, Personal communication.
- 22 K. Leymer, DERA (Malvern), Personal communication.